UTS UNIVERSITY OF TECHNOLOGY SYDNEY

Development of semi-quantitative earthquake risk assessment models using machine learning, multi-criteria decision-making, and GIS

by Ratiranjan Jena

Thesis submitted in fulfilment of the requirements for the degree of

Doctor of Philosophy

under the supervision of Distinguished Professor Biswajeet Pradhan and Professor Ghassan Beydoun

University of Technology Sydney
Faculty of engineering and IT

April 2021

CERTIFICATE OF AUTHORSHIP/ORIGINALITY

I, Ratiranjan Jena declare that this thesis, is submitted in fulfilment of the requirements for the award of Doctoral of Philosophy, in the FEIT at the University of Technology Sydney.
This thesis is wholly my own work unless otherwise reference or acknowledged. In addition, I certify that all information sources and literature used are indicated in the thesis.
This document has not been submitted for qualifications at any other academic institution.
This research is supported by the Australian Government Research Training Program.

Signature: Production Note: Signature removed prior to publication.

Ratiranjan Jena

Date: 27/04/2020

COPYRIGHT

DEDICATION

This thesis is dedicated to my Parents.

ACKNOWLEDGEMENT

Praise belongs to God, the Lord of the world who inspires me everywhere.

There are a number of people without whom this thesis might not have been written, and to whom I am greatly indebted. I express my deep and sincere sense of indebtedness to my Supervisor Distinguished Professor Dr. Biswajeet Pradhan, at School of Information, Systems and Modelling, Faculty of Engineering and IT for his invaluable guidance, painstaking effort, constant encouragement and inspiration during each and every step of my project work throughout the Ph.D. period. Despite his extremely busy schedule, I have always found him accessible for suggestions and discussions.

I would like to thank Prof. Ghassan Beydoun for providing me the academic facilities and constant motivation. I am also grateful to Dr. Nagesh Shukla and all candidature assessment panel members for their discussions and suggestions.

Further, I am very much thankful to the office staff of the department for their help in administrative matters.

I wish to convey my heartiest thanks to my lab mate Abolfazl Abdollahi and all my friends in the lab for their encouragement and moral support during the course of my thesis work.

Last but not least, I am grateful to my parents and my brother for their consistent moral support and inspiration.

LIST OF PAPERS/PUBLICATIONS

Published journal articles

1. Jena, R., Pradhan, B., Beydoun, G., Sofyan, H. & Affan, M. 2020, 'Integrated model for earthquake risk assessment using neural network and analytic hierarchy process: Aceh province, Indonesia', *Geoscience Frontiers*, vol. 11, no. 2, pp. 613-34. https://doi.org/10.1016/j.gsf.2019.07.006 (IF. 4.202)

2. Jena, R., Pradhan, B., Beydoun, G., Alamri, A.M. & Sofyan, H. 2020, 'Earthquake hazard and risk assessment using machine learning approaches at Palu, Indonesia', *Science of The Total Environment*, p. 141582. https://doi.org/10.1016/j.scitotenv.2020.141582 (IF. 6.551)
3. Jena, R., Pradhan, B. & Beydoun, G. 2020, 'Earthquake vulnerability assessment in Northern Sumatra province by using a multi-criteria decision-making model', *International Journal of Disaster Risk Reduction*, vol. 46, p. 101518. https://doi.org/10.1016/j.ijdrr.2020.101518 (IF. 2.896)

4. Jena, R. & Pradhan, B. 2020, 'Integrated ANN-cross-validation and AHP-TOPSIS model to improve earthquake risk assessment', *International Journal of Disaster Risk Reduction*, vol. 50, p. 101723. https://doi.org/10.1016/j.ijdrr.2020.101723 (IF. 2.896)

5. Jena, R., Pradhan, B., Beydoun, G., Al-Amri, A. & Sofyan, H. 2020, 'Seismic hazard and risk assessment: a review of state-of-the-art traditional and GIS models', *Arabian Journal of Geosciences*, vol. 13, no. 2, p. 50. https://doi.org/10.1007/s12517-019-5012-x (IF. 1.327)

Published conference papers

1. Jena, R. & Pradhan, B. 2019, 'Earthquake Vulnerability Assessment using Expert-based Approach in GIS', 2019 6th International Conference on Space Science and Communication (IconSpace), IEEE, pp. 53-6. IEEE. 10.1109/IconSpace.2019.8905929.

2. Jena, R. Pradhan, B., & Beydoun, G. 2019, Structural vulnerability assessment using an artificial neural network for earthquake hazard in Banda Aceh city, Aceh Province, Indonesia, IAG Conference 2019, Hobart, Tasmania. *(Published abstract only)*

3. Jena, R. & Pradhan, B. 2020, 'Earthquake Risk Assessment Using Integrated Influence Diagram–AHP Approach', IOP Conference Series: Earth and Environmental Science, vol. 540, IOP Publishing, p. 012078. https://doi.org/10.1088/1755-1315/540/1/012078.

4. Jena, R. & Pradhan, B. 2020, 'Earthquake Social Vulnerability Assessment Using Entropy Method', IOP Conference Series: Earth and Environmental Science, vol. 540, IOP Publishing, p. 012079. https://doi.org/10.1088/1755-1315/540/1/012079.

All the aforementioned papers have been published during my Ph.D. candidature.

Abstract of thesis presented to the Senate of University of Technology Sydney in fulfilment of the requirement for the degree of Doctor of Philosophy

PUBLICATIONS INCLUDED IN THIS THESIS

Publication citation – incorporated within chapters in a conventional form.

Jena, R., Pradhan, B., Beydoun, G., Alamri, A.M. & Sofyan, H. 2020, 'Earthquake hazard and risk assessment using machine learning approaches at Palu, Indonesia', Science of The Total Environment, p. 141582. https://doi.org/10.1016/j.scitotenv.2020.141582 (IF. 6.551)

Jena, R., Pradhan, B., Beydoun, G., Sofyan, H. & Affan, M. 2020, 'Integrated model for earthquake risk assessment using neural network and analytic hierarchy process: Aceh province, Indonesia', Geoscience Frontiers, vol. 11, no. 2, pp. 613-34. https://doi.org/10.1016/j.gsf.2019.07.006 (IF. 4.202)

Contributor	Statement of contribution	Thesis chapters
Ratiranjan Jena	Literature review and analysis (100%) Research direction and manuscript writing (75%)	Chapter 3, 4 and 5
Biswajeet Pradhan	Research direction and manuscript review (15%)	
Ghassan Beydoun	Research direction and manuscript review (5%)	
Other authors	Research direction and manuscript review (5%)	

Jena, R., Pradhan, B. & Beydoun, G. 2020, 'Earthquake vulnerability assessment in Northern Sumatra province by using a multi-criteria decision-making model', International Journal of Disaster Risk Reduction, vol. 46, p. 101518. https://doi.org/10.1016/j.ijdrr.2020.101518 (IF. 2.896)

Contributor	Statement of contribution	Thesis chapters
Ratiranjan Jena	Literature review and analysis (100%) Research direction and manuscript writing (75%)	Chapter 3, 4 and 5
Biswajeet Pradhan	Research direction and manuscript review (20%)	
Ghassan Beydoun	Research direction and manuscript review (5%)	

Jena, R. & Pradhan, B. 2020, 'Integrated ANN-cross-validation and AHP-TOPSIS model to improve earthquake risk assessment', International Journal of Disaster Risk Reduction, vol. 50, p. 101723. https://doi.org/10.1016/j.ijdrr.2020.101723 (IF. 2.896)

Contributor	Statement of contribution	Thesis chapters
Ratiranjan Jena	Literature review and analysis (100%) Research direction and manuscript writing (75%)	Chapter 3, 4 and 5
Biswajeet Pradhan	Research direction and manuscript review (25%)	

Jena, R., Pradhan, B., Beydoun, G., Al-Amri, A. & Sofyan, H. 2020, 'Seismic hazard and risk assessment: a review of state-of-the-art traditional and GIS models', Arabian Journal of Geosciences, vol. 13, no. 2, p. 50. https://doi.org/10.1007/s12517-019-5012-x (IF. 1.327)

Contributor	Statement of contribution	Thesis chapters
Ratiranjan Jena	Literature review and analysis (100%) Research direction and manuscript writing (75%)	Chapter 1 and 2
Biswajeet Pradhan	Research direction and manuscript review (15%)	
Ghassan Beydoun	Research direction and manuscript review (5%)	
Other authors	Research direction and manuscript review (5%)	

TABLE OF CONTENTS

LIST OF TABLES

LIST OF FIGURES

LIST OF ABBREVIATIONS

AHP	Analytic Hierarchy Process
ANN	Artificial Neural Network
ANN-CV	Artificial Neural Network-Cross Validation
AUC	Area Under the Curve
CR	Consistency Ratio
DEM	Digital Elevation Model
ERA	Earthquake Risk Assessment
EVA	Earthquake Vulnerability Assessment
EHA	Earthquake Hazard Assessment
GIS	Geospatial Information System
HCA	Hierachical clustering Analysis
LiDAR	Light Detection and Ranging
LULC	Land Use / Land Cover
MCDM	Multi-criteria Decision Making
MLP	Multi-Layer Perceptron
MMI	Modified Mercalli Intensity
MSL	Mean Sea Level
PGA	Peak Ground Acceleration
PLC	Pure Locational Clustering
RI	Random Index
ROC	Receiver Operating Curves
SVM	Support Vector Machine
TOPSIS	Technique of Order Preference Similarity to the Ideal Solution
VIKOR	VIseKriterijumska Optimizacija I Kompromisno Resenje (Multi-criteria Optimization and Compromise Solution)
WGS	World Geodetic System

DEVELOPMENT OF SEMI-QUANTITATIVE EARTHQUAKE RISK ASSESSMENT MODELS USING MACHINE LEARNING, MULTI-CRITERIA DECISION-MAKING, AND GIS

By

RATIRANJAN JENA

October 2020

Supervisor: Professor Biswajeet Pradhan,

Abstract

Catastrophic natural hazards, such as earthquakes, pose serious threats to properties and human lives in urban areas. Earthquake risk assessment (ERA) is specifically required for areas with complicated tectonics because of the catastrophic nature of mega-events that result in a massive death toll. Therefore, ERA is indispensable in disaster management. The prerequisite for earthquake risk estimation is probability, hazard and vulnerability assessment. Several research gaps such as failure to establish comprehensive GIS-based models, not much work on ERA has been done in city scale using integrated geospatial information system (GIS) techniques, use of limited conditioning factors, and little research on optimization of factors are specified in literature. Therefore, this study aims to develop models and estimate risk in city scale that is necessary to reduce future fatalities. The study evaluates the earthquake vulnerability by using the multi-criteria decision-making approach through a novel integrated analytical hierarchy process and VIseKriterijumska Optimizacija I Kompromisno Resenje method using a geographical information system in the first objective. This research develops an integrated model by using the artificial neural network–analytic hierarchy process for constructing the ERA map in the second objective. The third objective presents a novel combination of artificial neural network cross-validation (fourfold ANN-CV) with a hybrid analytic hierarchy process-Technique for Order of Preference by Similarity to Ideal Solution (AHP-TOPSIS) method to improve the ERA and applied to Aceh, Indonesia to test.

Firstly, in the objective 1, several factors were used to produce social vulnerability, structural vulnerability, and geotechnical vulnerability indices. Subsequently, the adopted approaches were integrated and applied to estimate the criteria weight, priority ranking,

and alternatives of criterion by applying the pair-wise comparison at all levels. Finally, vulnerability layers were superimposed to estimate the earthquake vulnerability index and produce the vulnerability map. The proposed method for earthquake vulnerability assessment (EVA) provides useful information that could assist in earthquake disaster mitigation.

Secondly, in the objective 2, the aim of the ERA was to quantify urban population risk that may be caused by impending earthquakes. The ANN is used for probability mapping, whereas AHP is used to assess urban vulnerability after the hazard map is created with the aid of earthquake intensity variation thematic layering. The risk map is subsequently created by combining the probability, hazard, and vulnerability maps. Then, the risk levels of various zones are obtained. The validation process reveals that the proposed model can map the earthquake probability based on historical events with an accuracy of 84%. The model is applied to the city of Banda Aceh in Indonesia, a seismically active zone of Aceh province frequently affected by devastating earthquakes. The findings of this research are useful for government agencies and decision-makers, particularly in estimating risk dimensions in urban areas and for future studies to project the preparedness strategies for Banda Aceh.

Thirdly, in the objective 3, this study explored and specified the major indicators needed to improve the predictive accuracy in probability mapping. Previous studies have suggested that neural networks improve the probability mapping on a city scale. The network architecture design with the probability index remains unexplored in case of an earthquake-based probability study. First, probability mapping was conducted and used for hazard assessment in the next step. Second, a vulnerability map was created based on social and structural factors. Finally, hazard and vulnerability indices were multiplied to produce the ERA, and the population and areas under risk were calculated. The proposed model achieved an improve accuracy of 85.4%. The model's performance changes based on the input parameters, indicating the selection and importance of input layers on network architecture selection. The proposed model was found to generalize better results than traditional and some existing probabilistic models.

The proposed models are transferable to other regions by localizing the input parameters

that contribute to earthquake risk mitigation and prevention planning. Therefore, as a case study, the third model was implemented to estimate the earthquake risk based on probability and hazard in Palu region along with cross-correlation among the derived parameters, Silhouette clustering (SC), pure locational clustering (PLC) based on hierarchical clustering analysis (HCA). There is no specific or simple way of identifying risks as the definition of risk varies with time and space. The main aim of this study was to conduct the clustering analysis to identify the earthquake prone areas, to estimate probability based on ANN-CV technique, and to assess earthquake risk. Using ANN-CV model the probability assessment was conducted while SC and PLC were implemented to understand the spatial clustering, Euclidean distance among clusters, spatial relationship and cross-correlation among the estimated Mw, PGA and intensity including events depth. Finally, AHP was implemented for the vulnerability assessment. To this end, earthquake probability assessment (EPA) and earthquake vulnerability assessment (EVA) results were employed to generate risk. These results obtained from this research have important implications for future large-scale risk assessment, land use planning and hazard mitigation.

The current research designs novel combination of multi-criteria decision making (MCDM), machine learning and GIS to develop models such as AHP-VIKOR, neural network-AHP and k-fold neural network cross-validation (Fourfold ANN-CV) with a hybrid AHP-TOPSIS method for probability, hazard, vulnerability, risk estimation and the ERA improvement in a city scale.

Keywords: Earthquake, probability, hazard, vulnerability, risk, machine learning, multi-criteria decision making, integrated models development

CHAPTER 1

INTRODUCTION

This chapter reflects a general introduction, research background along with geotectonic setting, and earthquakes in Indonesia.This chapter also reveals the main context of the study, structure, problem statement, specified objectives, research goal, research plan, specific research questions, motivation, research limitation, and thesis organization. It addresses the earthquake impacts and provides the importance and significance of earthquake risk assessment.

1.1. General introduction

Natural hazards, such as earthquakes, landslides, floods, and fires are the major types that increase casualties, damage, and loss of property. These hazards significantly affect the social community, infrastructures, and local environment. Earthquake is a natural phenomenon that is characterized by a short period, but its impacts on valuable infrastructures and buildings or bridges, persist for years. Therefore, a study on earthquake is a major research field to investigate and analyze the effective contribution of geospatial information system (GIS) and remote sensing techniques for the detection of potential areas of earthquakes. By definition, a hazard is a potential threat to a particular place (Brooks 2003). The conditions determined by various factors, which can increase the susceptibility of the impact of hazard to any community is called vulnerability and the risk is the probability of harmful consequences or expected losses as a product of hazard, vulnerability and coping capacity (McGuire 1978, 1995; Yohe & Tol 2002). For the analysis of susceptibility to seismic amplification, conditions of local site effects play an important role. So large earthquakes can cause damages in which ground shaking is a

primary effect and the collateral secondary effects are liquefaction, landslides, and tsunami (Bui, Ho, et al. 2016; Bui, Tuan, et al. 2016; Karimzadeh et al. 2013; Shaw et al. 2006).

Many studies on probabilistic seismic hazard assessment are conducted globally (Brinkman et al. 2015; Hagiwara 1974; Hardebeck 2004; Krinitzsky 1993; Parsons 2005; Shapiro, Dinske & Kummerow 2007; Shcherbakov et al. 2019). Krinitzsky (1993) implemented the Gutenberg-Richter magnitude and recurrence relationship and estimated the probabilistic earthquake ground motions. Hardebeck (2004) included stress triggering and fault interaction that is necessary for the earthquake probability assessment quantitatively. Hagiwara (1974) conducted the earthquake probability in a large-scale geodetically using the crustal strain in an earthquake location. Shcherbakov et al. (2019) demonstrated that earthquakes are unexpected that could trigger successive events which can lead to strong earthquakes.

Several studies have been conducted on the 2004 event in northern Sumatra, which was originated in the Indian Ocean creating a 9.2 Mw earthquake (Stein & Okal 2007, 2011). However, mostly all studies have interacted with the tsunami propagation models. Therefore, the works conducted by Consultant (2009); Roy, Karim & Ismail (2007); Jaffe & Gelfenbuam (2007); Koh et al. (2009) and Wijetunge (2009) are highly appreciated. Some of the studies such as Paris et al. (2007); Srinivasalu et al. (2007) and Paris et al. (2009) were focused on tsunami based geomorphological changes. Violette, Boulicot & Gorelick (2009) described in their study about how environments get affected by the tsunami and the mechanism of ecological protection for damage. Kaplan, Renaud & Lüchters (2009) explained that the 2004 tsunami in the Indian Ocean was one of the

deadliest disasters during the last decade. Aceh Province in Indonesia experienced the highest death of 163,978 people and many more injured. Sinaga et al. (2011) presented the tsunami vulnerability mapping using GIS, where they employed the Jembrana Regency in Bali as a case study. Rusydy et al. (2020) have aimed to predict the earthquake effects in Banda Aceh city by estimating injuries, casualties, and expected damage ratio based on the event intensity. Sengara et al. (2008) explained in their case study pointing the probabilistic seismic hazard and tsunami analysis. They analyzed the hazard by using the collected data of shear wave velocity from the spectral analysis of surface wave and geotechnical subsurface exploration. Rusydy et al. (2020) estimated the damage in their study pinpointing to several scenarios of the earthquake intensity model for the sub-district of Kuta Alam in Banda Aceh. Therefore, pre-disaster assessment are required for the land-use planning, construction, or design of buildings (Clinton 2005; da Silva & Batchelor 2010; Bappenas & Community 2005). In this study, three models were developed as described in the objectives and novelty section. It can be seen that all the developed models have performed well in terms of data modelling, processing time, accuracy, and results than several traditional models presented in the literature review.

1.2. Research background

Geo-tectonic setting

The destructive power of earthquakes in Indonesia is very strong, has a wide-range effect, and endangers the safety of human lives and properties (Xu, Dai & Xu 2010). Indonesia is one of the highly seismically active countries in the world with severe damage rates (Sørensen & Atakan 2008). The country has experienced a number of destructive earthquakes in the last two decades. Indonesia was experienced a massive number of

events with magnitudes ranging from 2 to 9.3 in a Richter scale associated with crustal faults and subduction zone are known to occur before 1600 to date.

Indonesia consists of several thousands of small islands situated along the continental oceanic plate boundary of the Eurasian plate and Indo–Australian plate in the central part of the Alpine–Himalayan seismic belt (Petersen et al. 2004; Granger et al. 1999). Trends on plate tectonics reveal the Indian plate to be part of the large Indo–Australian plate underlying Bengal Bay and the Indian Ocean. The plate motion is towards the northeastern direction with an average speed of six centimeters annually (Sørensen & Atakan 2008). The plate subducts beneath the microplate (Burma plate) of the large Eurasian plate at the region of the Sunda trench (Sørensen & Atakan 2008). This subduction process creates thrust faults and volcanic activities, the two major reasons for earthquakes in Indonesia (Bellier et al. 1997).

Although the motion of the Sundaland block is currently known in the global context relatively well, the differential movements along the fault lines have not been charted consistently. The campaign by the Indonesian government and private agencies were conducted for the purpose of studying the tectonic behavior of the area by determining the magnitudes and directions of the movement of active faults. The network comprises several seismic stations and global positioning system (GPS) stations located in different parts of Indonesia. The study is based on the station coordinates changes between three epochs.

Indonesia is located on a relatively stable Sundaland block that forms the southern edge of the Eurasian plate (Figure 1.1). Sundaland block is affected by the continental collision between the Indian subcontinent and the Eurasian plate (Socquet et al. 2006). This block includes not only Vietnam, Thailand, and Malaysia but also the Sunda shelf, Borneo, Sumatra, and Java of particular interest is the triple junction area where the convergence of Eurasia and Australian continental plates with the Philippine Sea/Caroline/Pacific oceanic plates occurs. Aceh is located in the north of the Sumatra.

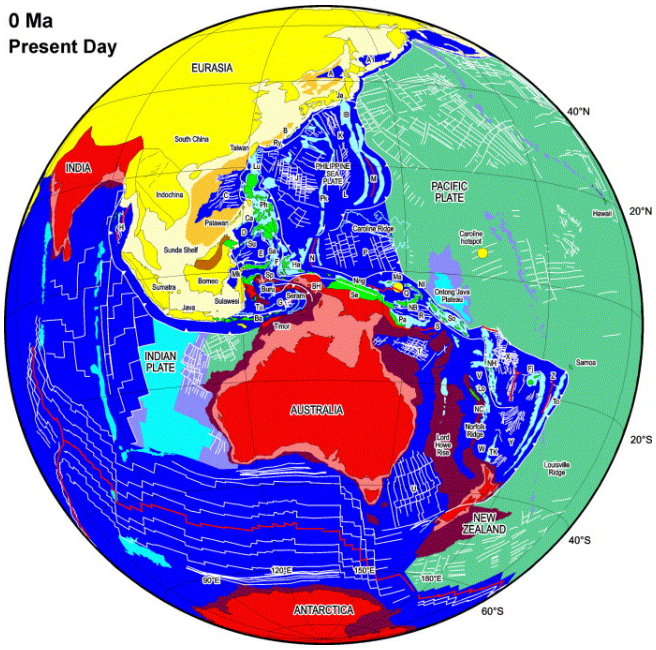

Figure 1.1: Sundaland block of Eurasian Plate and tectonics (*Source:* Adopted from *Hall 2002*).

Great Sumatran Fault is the largest crustal fault that passes through the Banda Aceh city (Barber, Crow & Milsom 2005). Banda Aceh has its unique features of land cover, geographical structure and characterized by quaternary sedimentary rocks. Earthquake inventory data reveals that severe ground shaking has been observed in the city. Probabilistic study reveals that strong events might be struck the city near the seismic gap

within the city. Figure 1.2 presents the probabilistic and deterministic methodology used for hazard assessment.

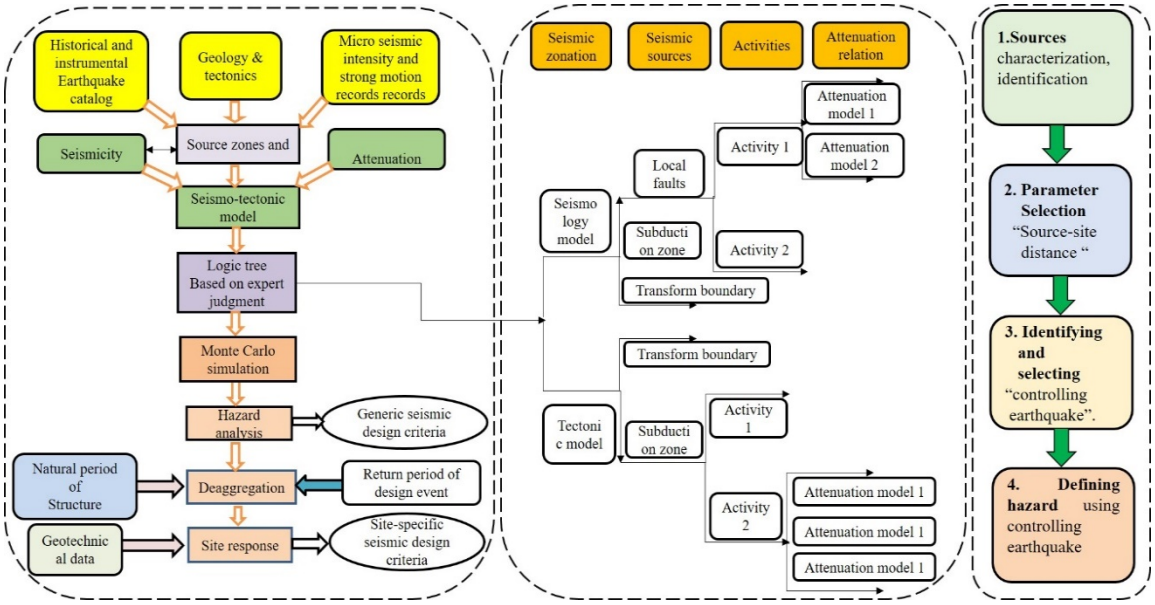

Figure 1.2: The traditional methodologies for seismic hazard assessment.

1.3. Earthquakes in Indonesia

During the last decade, total death and injuries were observed in Indonesia is around 0.8 million (Table 1.1). This explains that the situation in Indonesia is critical and it is the region with complicated tectonics where the study area is coming under the extremely high probable zone.

Table 1.1: Total death and injuries in Indonesia due to earthquakes.

No	Year	Region	Fatalities	Injuries	Remarks	Sources
1	2018	Sulawesi, Java, Sulawesi Lombok, Sumatra	2828	12566	Landslides, Tsunami, Aftershock,	NGDC, NOAA, USGS

					Foreshock, Building damage, widespread fatalities	
2	2017	Java, Ambon	5	36		
3	2016	Sumatra	104	1,273	Heavy damage in Aceh region.	NOAA
4	2015	Papua	1		Buildings damaged or destroyed.	NOAA
5	2013	Sumatra	43	276		USGS
6	2012	Wharton Basin	12	12	Doublet & building damage	
7	2011	Sumatra	10			
8	2010	Sumatra, Papua	425	62	Tsunami (local), hundreds missing.	
9	2009	Sumatra, Java, Talaud, West Papua	1201	4266	Severe damage, Local tsunami, doublet	NGDC
10	2008	Sulawesi, Simeulue	7	59		USGS
11	2007	Sumatra, Molucca Sea	95	548		USGS
12	2006	Sumatra, Java, Seram	6428	47867	Tsunami (Local & regional), Extreme damage	
13	2005	Sumatra	1,314	1,146		USGS
14	2004	Sumatra–Andaman, Papua, Alor, Western New Guinea, Bali	228,002	629	Tsunami (basin-wide), severe damage, doublet, several thousand buildings damaged	NGDC
15	2003	Halmahera	1		Extensive damage	

16	2002	Sumatra, Western new guinea	11	65	Tsunami & damage	
17	2000	Sumatra, Sulawesi	149	2438	Tsunami & destruction	NGDC
18	1996	Biak, Sulawesi	174	423	Local tsunami	
19	1995	Sumatra	84	1868	Extreme damage	NGDC
20	1994	Java, Sumatra	457	2,000+	Tsunami	NGDC
21	1992	Flores	2,500	500	Severe damage (Tsunami)	
22	1989	West Papua	120	125		
23	1984	Sumatra		1		
24	1982	Flores	15	390		
25	1981	Papua	305		Thousands missing	
26	1979	Bali	30	200+		
27	1977	Sumba	180	1,100	Tsunami(local)	
28	1976	Bali, Papua	995	4,750	Landslides, thousands missing	USGS, NGDC
29	1968	Sulawesi	213			
30	1965	Sanana	73			
31	1943	Sumatra, Java	213	2,096	Extensive damage	NGDC
32	1938	Banda Sea			Local tsunami	
33	1935	Sumatra			Local tsunami	
34	1917	Bali	1,500		Landslides	
35	1899	Seram	3,864		Destructive	
36	1867	Java	8		Extensive damage	NGDC
37	1861	Sumatra	2,000+			
38	1852	Banda Sea			Severe damage	NGDC
39	1833	Sumatra	1000+		Tsunami (local)	
40	1815	Bali	10,253		Tsunami	NGDC
41	1797	Sumatra	1000+		Tsunami(local)	USGS
42	1699	Batavia (Jakarta)	30		Building collapsed	

43	1674	Ambon Serem	89	135	Tsunami & building damage	NGDC
44	1629	Banda sea			Regional tsunami	

Due to this fact of historical evidence, there has been a growing trend in risk assessment for various natural hazards in Indonesia. Research on earthquake engineering provides options for risk assessment (Dilley et al. 2005). Although several researchers have conducted studies that are natural for damages results from earthquakes within a distance of 100-200 km radius. Nevertheless, a high-intensity earthquake can create an impact up to a range of 700 km, as experienced in Mexico 1985 (Megawati, Pan & Koketsu 2005). Since Indonesia is known to be underlain by a tectonically stable crust and active seismic zone as a part of "Ring of Fire" surrounding the country, hence, we can raise the point that Indonesia is seismically active towards high risk indicating that Indonesia is forever immune to seismic risk. Thus, necessitating the need for this research, which is aimed at estimation of seismic risk in Aceh and Palu cities in Indonesia by an integrated GIS technique.

1.4. Problem statement

Mega-earthquakes mostly experienced in areas with complicated fault tectonics (Bletery et al. 2016). However, the densely populated cities in India, Nepal, Indonesia, Japan, and America are extensively catastrophic due to earthquakes that trigger landslides, destroy buildings and results in fatalities, injuries, and death tolls (Spence & So 2009). Population growth, old and poor planned infrastructure creating a critical condition for several countries. As the focus is specifically on city level risk assessment therefore, it can be observed that the cities over the world are expanding each year based on the

developmental planning in a proper way. However, most of the cities have been critically affected by natural disasters unlike earthquakes, floods, landslides, etc. Therefore, recognition and reduction of the vulnerability of population and buildings with respect to earthquakes are required (Cannon 1994). Buildings up-gradation against earthquakes is important for the reduction of loss of properties and lives.

Very poor implementation of some pre-existing methodology and poor results from the traditional methods having uncertainty. Because, the understanding of the fault geometry, geographical location and tectonic structures by using the current knowledge of ongoing research is essential and difficult (Stead, Eberhardt & Coggan 2006). Choose of important factors, well articulated information and proper implementation following the exact process is still not well established. Poor understanding of the complex mechanism of fault movement and internal structure of the study location is another problem in current times that could lead to poor results and uncertainity (Bray et al. 1994). The collection of complete data is another issue in solving the major seismic hazard and risks in local areas.

Failure to establish a comprehensive GIS-based model including all effective parameters for the seismic probability analysis of earthquake-prone areas (Dou et al. 2019; Zhou et al. 2003). However, the detail literature review as explained in chapter 2 suggests that the risk areas assessment and urban population risk estimation is necessary to minimize the consequences and severity. To date, there is still an inability to implement a suitable methodology for a country like Indonesia. Adopting the global risk assessment models designed by developed countries, the tremendous effect of earthquakes can be reduced scientifically (Crowley et al. 2013). It is required to develop risk assessment models to evaluate earthquake risk from the major earthquake scenario for the risk reduction, future

strategy, and improvement of systematic inventory (Peduzzi et al. 2009). The applicability of these models in the Indonesian environment needs to analyze to identify the shortcomings. To fill the identified gaps in the literature and to understand the strength of the model, the evaluation of complete parameters is needed.

Unfortunately, no major study has been conducted in the city-level through which an accurate and comprehensive assessment of probability, hazard, vulnerability, and risk can be performed using novel integrated GIS based models (Davidson & Shah 1997; Lindell & Perry 2000; Mohsen et al. 2018). Indonesia was choosen as the case study region in the northern Sumatra region that is falling under a very high seismic zone always affected by major earthquakes. Banda Aceh is falling under the seismic gap of the Great Sumatran Fault. Banda Aceh is coming under the high-risk zones for future seismic events because of its unique geographical location, geostructural features, and quaternary sedimentary rocks. Death-toll is increasing from the last decade and the record of fatalities and injuries reveals the importance of earthquake risk assessment. The growing population in Banda Aceh city in Indonesia can acute a big problem. Therefore, it is important to assess the risk of future seismic events (Delescluse et al. 2012; McCloskey, Nalbant & Steacy 2005). Historical analysis and events explained that the city has experienced severe ground shaking due to devastating events (McCloskey, Nalbant & Steacy 2005). Based on the probabilistic and deterministic approaches, seismologists and geologists believe that strong events might hit the city in the near future because of the release of the accumulated stress in the seismic gap. From the view explained in motivation, it can be considered that there is a necessity to propose further studies to estimate population risk and generate risk models at a level of city scale.

1.5. Research gap

The earth's internal structure is complicated; however, understanding the whole tectonics of the study region is difficult (Stead, Eberhardt & Coggan 2006). Earthquake prediction is important but the result may not satisfy seismologists in terms of expected accuracy. Therefore, working more on the probability, hazard, vulnerability, risk analysis, and mitigation is important (Greiving, Fleischhauer & Lückenkötter 2006). Various thematic layers can be generated via remote sensing and GIS to create a probability map for seismic amplification due to local site effects. Moreover, GIS is used to evaluate seismic hazards by using a suitable ranking scheme and for data integration techniques. There are many studies have been performed regarding the probabilistic and deterministic seismic hazard assessment and limited machine learning methods for earthquake risk assessment (Scawthorn & Chen 2002; Ram and Wang 2013; McGuire 1978, 1995). However, there are some limitations associated with the implementation of these studies. Therefore, in this section, we highlight the main research gaps obtained from an extensive literature review are:

1. Failure to establish a comprehensive GIS-based model, including all effective parameters, for the seismic probability analysis of earthquake-prone areas. Implementing a suitable methodology remains difficult for many developing countries, such as Indonesia and Malaysia.
2. Not much work has been done, especially on earthquakes, using integrated GIS techniques with historical earthquake catalog in underdeveloped countries. Moreover, no feasible and effective way exists for the comprehensive risk assessment and evaluation of parameters for mapping using open-access databases without focusing on the management and loss estimation strategy.

3. Many researchers have implemented a single machine learning algorithm for earthquake vulnerability and damage assessment; nevertheless, they did not test integrated machine learning and GIS-based models, and very limited hybrid models were developed that can produce better accuracy and consistency. No study has been conducted on earthquake probability assessment using machine learning techniques.
4. Most of the works done on GIS-based earthquake probability assessment have limited conditioning factors as earthquake phenomenon controlled by several conditioning factors. Besides, very fewer researchers conducted optimization of factors specified in the field of earthquake/seismology.
5. Improving old and developing new models that could inform risk is still a huge research gap (Greiving, Fleischhauer & Lückenkötter 2006). This is required for all seismic prone urban areas, while this could introduce new parameters, factors, methodologies based on local tectonic conditions and applicability.

1.6. Scope of study

Earthquake generally occurs in plate boundaries and the locations with complicated tectonics. Study on history of earthquake events and determining the earthquake probability, hazard, vulnerability, and risk is on demand. Complexity nature of earth's tectonic boundaries, catastrophic consequences results due to earthquake forces established a research environment. The earthquake prediction, probability assessment in earthquake research that has evolved for urban planning and development through tectonic analysis, simulation, modeling, mapping and monitoring of earthquakes are the major scopes.

Thus, the scope of this research deals with:

1. The earthquake prediction and probability assessment.

2. Estimation of earthquake vulnerability, risk, and microzonation maps (Figure A1,A2).
3. Earthquake ground motions and peak ground acceleration study.
4. Hybrid and integrated decision-making models formulation.
5. Seismic- modelling approaches or models development.
6. The methods to integrate the coping capacity with the earthquake risk.
7. In the past decade, the use of digital elevation model (DEM) has become quite popular. High resolution LiDAR data can surpass widely and can be used for earthquake probability analysis.
8. The scope of this study may lead to early warning system development and improvement in earthquake monitoring.
9. The USGS current projects also include earthquake hazard and risk assessment for future land use planning.

In this thesis, DEM data was collected from the national agency named Statistics Indonesia applied to generate some thematic conditioning factors for probability assessment. The scope is more towards the current technology of LiDAR to implement in geohazard applications (Fanos & Pradhan 2019). The earthquake probability assessment is a key element in risk assessment. Therefore, in this research, a semi-quantitative earthquake risk assessment model was developed based on artificial intelligence techniques along with decision-making models within a GIS environment for risk mapping. The model was based on Artificial Neural Network (ANN), Analytical Hierarchy Process, the Technique for Order of Preference by Similarity to Ideal Solution (TOPSIS), VIseKriterijumska Optimizacija I Kompromisno Resenje (VIKOR), Locational Clustering Techniques, Matrix Plotting, and Excel-based analysis. The

probability assessment was performed in the thesis that could be the evolved trend in prediction analysis and could be a path for future probability and prediction modeling.

The achievement of the whole Ph.D. thesis includes the development of a semi-quantitative ERA model that efficiently handles various parameters and performs the risk analysis on a city scale. The model was applied in two case studies such as Banda Aceh and Palu city in Indonesia. Firstly, a detailed vulnerability assessment was conducted and then the model was developed for the probability and hazard analysis and integrated approach of both employed in ERA. In a later stage, the model was modified in terms of parameters and combined approaches. The final parameters required for the probability analysis, such as slope angle, elevation, fault density, lithology with amplification factor, depth density, proximity to the epicenter, epicenter density, magnitude density, and peak ground acceleration (PGA) density. The vulnerability factors that were considered in this research are household density, building surface area, building quality, building heights, proximity to the road, building types, proximity to buildings, building density, and population density.

1.7. Research aim and objectives

The aim of the study is to develop semi-quantitative earthquake risk assessment models using machine learning, multi-criteria decision-making, and GIS techniques.

The current research developed three models that fulfill the research gap in the literature. The proposed models are complicated and comprehensive. This study developed three integrated models and continuously improved the models for different purposes. The developed models applied for the Banda Aceh city in Indonesia to estimate the population risk and area under risk. The main objectives of the present research are as follows;

1. To **develop a novel integrated model** AHP-VIKOR (Analytical hierarchy process-VIseKriterijumska Optimizacija I Kompromisno Resenje) technique for earthquake vulnerability estimation through structural, geotechnical, and social information.
2. To **develop an integrated model** of neural network and AHP for earthquake risk mapping in a city-scale.
3. To **develop a fourfold ANN CV-hybrid AHP-TOPSIS** (Artificial Neural Network-Cross Validation- Hybrid Analytical Hierarchy Process- The Technique for Order of Preference by Similarity to Ideal Solution) model to improve the risk assessment.

1.7.1. Objective 1

The first objective of the designed approach is to develop an innovative intuition for earthquake vulnerability assessment (EVA) that deals with the understanding of geometry and interrelationship of faults, and seismo-tectonic setting, building characteristics, social characteristics, and geotechnical characteristics. The input databases that are needed for the vulnerability analysis are building information, population density including other attributes. The routine of the model starts with vulnerable layers preparation that were derived from satellite images or the geological map or the collected shapefiles. The use of these data genuinely needed for fault and lineament density, geology, elevation, slope analysis by following the steps presented in the first objective. The model provides the novel idea of introducing the ViKOR method coupled with AHP for EVA. It is possible to understand the output results at this stage presented through maps that will help in the next stage to apply it directly.

1.7.2. Objective 2

This stage of the research involves earthquake risk assessment using a developed ANN-

AHP model. It will allow us to find out the population and area under risk at a city level. Various parameters derived from the collected data to achieve the expected result. However, this model was developed based on the proposed integrated models. Therefore, the parameters were chosen carefully through the ANN technique to achieve acceptable accuracy. The applicability of all the parameters was assessed and the probability, hazard, vulnerability, and risk maps were produced for Banda Aceh city. Identifications of parameters and their influence on the earthquake scenario is important for the risk assessment in the next stage.

1.7.3. Objective 3

This stage develops a new integrated fourfold ANN CV-AHP-TOPSIS model to improve the earthquake risk assessment. To do this inventory data was divided into training and testing randomly and run the ANN model four times. Firstly, the earthquake probability assessment was conducted and then hazard analysis based on the earthquake intensity was performed. In the second step, vulnerability assessment was conducted based on the important parameters by employing a hybrid AHP-TOPSIS approach. The third step involves the risk assessment by multiplying the hazard and vulnerability. Finally, the risk model can be done based on all the described steps that provide the expected result pinpointing the number of people and the areas are under risk in the study area. Then the cross-validation reveals the output is accurate.

Moreover, the overall designed model has novelty and prepared based on analyzing various older and recent models for earthquake vulnerability and risk assessment on a city scale. However, the models developed in the current research includes various parameters making it comprehensive and accurate. The limitations and the drawbacks of the model

can be understood from the conclusion section.

1.8. Research questions

1.8.1. Questions pertaining to objective 1

In this study, some specific research questions that were addressed on vulnerability estimation such as;

(i) Is it possible that MCDM methods can be applied for risk assessment by understanding the lack of current knowledge?;

(ii) Can we propose novel ideas into the factors applied for EVA?; and

(iii) How can we assess the MCDM model for EVA in an urban environment with useful information?

By considering the above research questions, the main objectives of this research were set to estimate EVA in Banda Aceh by (1) presenting an innovative intuition into the dominant criteria; and (2) disclosing the prerequisite and effectiveness of applying MCDM methods for EVA. Accurate EVA is always hard and challenging, especially at large scales. Some computational models can reduce their impacts by assessing vulnerability to threats. Unfortunately, these models are data-dependent with plenty of uncertainty; It needs to understand them to use them reliably.

1.8.2. Questions pertaining to objective 2

In the second objective, the main research questions that were addressed are;

(i) Is the accuracy of neural network models are good to estimate the earthquake risk in the city scale?;

(ii) Can this study develop any well-performed integrated model for earthquake risk assessment?;

(iii) Is it possible to achieve more accuracy on the modification of the developed model? To achieve this goal, this study contains three objectives such as; (1) Develops an integrated model combining ANN and AHP methods to produce an earthquake risk map; (2) Applies and assesses the dimensions of earthquake probability, hazard, and vulnerability for Banda Aceh City; (3) Estimates the urban population risk quantitatively and qualitatively.

1.8.3. Questions pertaining to objective 3

The third objective of this research obtains three main research questions, which are necessary to address such as;

(i) how the improved model for the earthquake risk assessment can be better than the previous model described in objective 2?;

(ii) Is it possible to modify the current improved model to improve further to achieve more accurate results?;

(iii) What are the main factors in the current model for better accuracy? To achieve this goal, the present study; (1) developed a fourfold ANN CV-AHP-TOPSIS model to estimate risk; (2) Applied the model for the Banda Aceh city and assess the population risk; and (3) evaluated the accuracy between the previously developed model and the current model.

1.9. Motivation behind this research

In the current period, natural hazards are quite common all over the world. The importance of the issues raised from natural hazards for environmental, social, and structural safety is increasing with the increase of natural catastrophes. Complicated tectonics, geological structure, rock types, active faults, and historical mega-events are expected to raise the probability of earthquakes. Earthquakes are disastrous in some

counties like Indonesia, Japan, United States of America, and India. Therefore, the focus of the government is continuous monitoring of natural hazards through mapping, modeling, and mitigation plan (Kussul, Shelestov & Skakun 2008; Schilderman 2004). These processes are complicated to implement as the earth's internal structure is not simple. Humans are incapable to control and predict earthquakes. The influence of natural catastrophes could depend on the magnitude, intensity, and coverage region. Therefore, probability, vulnerability, hazard and risk assessments are quite important to study before moving to the post-disaster analysis for which development of novel models are necessary.

The motivation of this thesis indicates that Aceh is a seismic-prone province on Sumatra with devastating seismic events that resulted in severe casualties and damages (Petersen et al. 2004; Yücemen, Özcebe & Pay 2004). The seismic prone area of Banda Aceh City provides many opportunities for numerous research. Banda Aceh is considered as a high-risk zone for future seismic events because of its unique geographical location, geostructural features, and quaternary sedimentary rocks (Siemon, Ploethner & Pielawa 2006; Irwansyah 2010). Many surveys and other investigations have been conducted to understand the tectonics and to improve the reconstruction of buildings in this location. The majority of conducted studies have focused on the rebuilding of structures, rebuilding houses, community rehabilitation, and livelihoods. Several studies have been conducted on tsunami evacuation planning (Løvholt et al. 2014; Synolakis & Kong 2006). Historical analysis shows that the city has experienced severe ground shaking due to devastating events (Irwansyah 2010). Therefore, very few researches could be found on the predictive analysis, vulnerability, and risk assessment based on the properties and population. On the basis of the probabilistic and deterministic approach, seismologists and geologists

believe that strong events may hit the city in the near future because of the release of the accumulated stress in the seismic gap. Thus, proposing further studies to generate risk assessment models at the city-scale is necessary. Unfortunately, much fewer studies are conducted at the city level by which an accurate assessment of probability, hazard, and risk can be conducted (e.g., Consultant 2009; Johar et al. 2013; Kafle 2006). Second, no comprehensive model has been developed for Banda Aceh for a detailed ERA. However, a literature review suggests that risk assessment and urban population risk estimation is necessary to minimize the consequences and severity (Zebardast 2013; Chaulagain et al. 2015; Ram & Wang 2013; Blaikie et al. 2014).

This thesis attempts to propose a semi-quantitative earthquake risk assessment model to map the earthquake probability, vulnerability, hazard, and risk combining the coping capacity for the Banda Aceh city in Indonesia. This research provides key motivation to use the developed maps to avoid more urbanization in seismic zones and to create a sustainable environment. In order to reduce the earthquake damages, injuries, fatalities, this study would help to identify the probable and vulnerable areas. Governments and planners could make use of the developed map and the quantitative results obtained by this study to determine the safe regions for residents, support fast emergencies response, can state infrastructure construction plans and update the strategies for city planning and development. Information released from this study could decrease the necessity to conduct an in-situ investigation by government and local surveying departments.

1.10. Novelty and main contribution of the research

In this study, three integrated models are developed for earthquake risk assessment. The purpose of this study is to address the lack of comprehensive GIS based models for risk

mapping. As a main contribution the novel combination of several machine learning techniques, MCDM approaches and GIS are conducted to overcome the uncertainties associated with traditional methods. Therefore, the detail mapping of probability, hazard, vulnerability and risk was conducted to update the old maps.

The current research is designed as a novel combination of AHP-VIKOR, neural network-AHP and N-fold neural network cross-validation (Fourfold ANN-CV) with a hybrid AHP-TOPSIS method to develop models for vulnerability, estimate the risk and improve the ERA in a city scale. These models are implemented in Aceh, Indonesia to test. The study developed and applied all three models for the first time in ERA and in Banda Aceh city. The study developed some new equations as described in the sub-sections "3.2.1.3 Integration of AHP-VIKOR" and "3.7.1 Objective 1". The detail description of implementation of developed models are described in the section "3.7 Implementation of the methodology" for all objectives. All the models are integrated models, which has not been applied in ERA that provides them as geographically consistent and long-term assessments. This study estimates the population under risk for the Banda Aceh city and finally evaluates the usefulness and limitations of the developed models. This study do not assume that earthquakes occur randomly through space and time and faults with their branched lineaments as one. In this study, geological, topographical, structural information and historical events were integrated to GIS with the aim to estimate and to map the future risk areas.

1.11. Thesis organization

The thesis consists of five chapters. The detail of contents carried out by the chapters were pointed out below.

Chapter 1 reveals the introduction to the topic and research background, earthquakes in indonesia, research problem, research gap, aim of the research, objectives and questions, the scope of the study, motivation behind this research, novelty and main contribution of the research and thesis organization in detail.

Chapter 2 demonstrates the literature on seismic hazard and risk assessment. The first part of the chapter mainly discusses about the basic principles, data, and the methodology of various models used for seismic hazard and risk assessment. In the second part, comparative analysis in terms of the limitations and strengths of the models, as well as application variability is presented. Furthermore, the paper includes the descriptions of software, data resources, and major conclusions.

Chapter 3 in the thesis discusses the methodology and the proposed models. This chapter demonstrates and discusses the data acquisition, study area, overall methodology, and implementation of the developed models for risk analysis. This chapter also describes the following: digital elevation model (DEM), vector datasets, modeling approaches for spatial analysis to generate risk maps.

Chapter 4 describes the results of earthquake probability, hazard, vulnerability, and risk assessment in terms of maps, identified risk locations, expected population under risk.

Chapter 5 concludes the study with detail description of research limitations, main findings, and future directions.

All the published papers mentioned in the “LIST OF PAPERS/PUBLICATIONS” page were included in this thesis with proper citation as per the requirement of all the chapters.

CHAPTER 2

LITERATURE REVIEW

This chapter provides an extensive review of several traditional and GIS-based models for earthquake hazard and risk assessment. This chapter introduces some globally used seismic hazard- assessment models. The traditional models are discussed by highlighting the involvement of some supporting models, uncertainties, and accuracy. Similarly, review and discussion on GIS, machine learning, and AHP-based models are described. A section that discusses the findings, software and data for the modeling. Two sections provide a review of current issues and the brief summary. Finally, the last section draws ideas for future research. In general, this chapter reflects a general view of the use of several models for earthquake risk assessment.

2.1. Introduction

In literature, many models and tools have been widely employed for the earthquake probability and hazard analysis (Bommer & Abrahamson 2006; Scherbaum, Delavaud & Riggelsen 2009). In principle, these models rely on the high ability to perform a trustable result in seismic hazard and risk assessment. Nowadays, researchers are working on active tectonic faults and structural geology using both GIS and remote sensing techniques (Barreca, Bonforte & Neri 2013). In general, seismic hazard and risk assessment use fault specific analysis where the sources of seismic activities are geologically strained active faults (Deligiannakis, Papanikolaou & Roberts 2018). Fault specific based methods can be assessed quantitatively because they usually measure slip rates of faults from fault and geological data, which provides a more reliable estimation of the seismic hazard than that of historical records of seismicity (Michetti & Marco

2005). For the planning of land-use and assessment of critical facilities or the purpose of risk evaluation, the desirability of high-quality spatial resolution is also important (Deligiannakis, Papanikolaou & Roberts 2018). It is also possible to extract the recurrence interval information of associated major earthquakes and neo-tectonic movements (Papanikolaou et al. 2015).

GIS-based models for seismic hazard and risk assessment are quite popular and most recommended by researchers (Sarker 2011). New models are being developed by researchers by keeping GIS technology as a base (Bommer & Abrahamson 2006). Geotechnical information system (GTIS) is one of them and has been used for the estimation of the local site effects which is associated with the ground motion amplification, earthquake micro-zonation and the mean shear wave velocity (Chang & King 2005). The ground surface generally consists of alluvial deposits, while in some other cases dominance of layers of weak stones such as siltstone, claystone, and conglomerate (Karimzadeh et al. 2017). Some researchers are focusing on the traditional based models such as probabilistic and deterministic seismic hazard assessment (Klügel 2008). Seismic hazard, risk analysis and the simulation of ground motion have been traditionally treated as an important section of the probabilistic seismic hazard assessment (PSHA) (Theilen-Willige 2010). During earthquakes, the pore-water pressure inside the aquifer can easily describe the mechanism and triggering factors of liquefaction (Hannich, Hötzl & Cudmani 2006). Damage potential will be high in wetlands during large earthquakes if vibrations are high, lasting for a long period (Theilen-Willige 2010). Therefore, decomposition of the PSHA has been done into smaller components, which are probabilistically designed such as seismicity rate, attenuation model of waves, and source-site distance calculation, site attenuation model, stress drop, shear wave velocity,

etc., are used in simulation methods. Most of the literature revealed that these traditional methods are limited to major drawbacks in terms of completeness of data, data quality, time consumed, accuracy and validation. Apart from this, not much work has been reported on the comprehensive seismic hazard and risk analysis in the growing field of GIS, which can reveal a comparative analysis of methodology, validation, strength, and limitations of various models. Therefore, in this study, we conducted a thorough analysis of kinds of literature, with an aim; (1) to investigate various models of seismic hazard and risk analysis for the understanding of suitability, core principles, and performances; (2) to make a comparative investigation based on strength and limitations; and (3) to motivate readers for the further research and progression. The focus is limited to the probability, hazard, vulnerability and risk assessment; therefore, management strategies are not discussed or analyzed.

2.2. Seismic hazard and risk assessment models

The hazard-damage assessment model shows that models use various parameters and mathematical formulation and can be categorized into two main groups: (1) worldwide models and (2) local (case-based) models (Karimzadeh et al. 2014). An overview of seismic hazard analysis is described below in Figure 2.1. PAGER (Prompt Assessment of Global Earthquakes for Response) and HAZUS (National Institute of Building Sciences 1999, 2004) (Hazards US) are different worldwide platforms used for different purposes. GEM (Global Earthquake Model) aims at creating tools, platforms, and models to assess seismic hazard and risk globally. CAPRA (Comprehensive Approach to Probabilistic Risk Assessment) is a global tool designed for Central America.

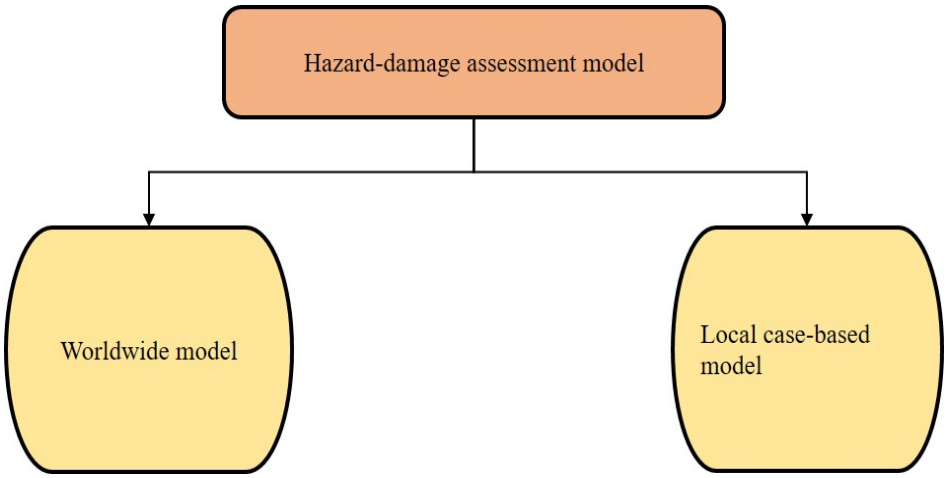

Figure 2.1: Classification of hazard assessment models.

Various global and local risk models:

Other models rather than the ones described below exist, such as models for hazard, risk analysis, damage and loss estimation, including risk reduction. The European seismic hazard model (ESHM13) (Woessner et al. 2015), Earthquake Model of the Middle East (EMME14) (Danciu, Kale & Akkar 2018), Earthquake Model of Central Asia, and all other hazard models worldwide can be found in (https://hazardwiki.openquake.org/models). Apart from these, other models have been developed by different international and local agencies, but are not popularly used as a basis for earthquake risk assessment. Earthquake hazard and susceptibility analysis using GIS technology will provide new ideas for research and development. All the models that are listed in (Table 2.1 and 2.2) are highly useful for earthquake risk and damage analysis.

Table 2.1: Various local and global programs used for earthquake hazard, risk analysis, and loss estimation purpose.

Criteria	HAZUS	PAGER	RADIUS	GEM	CAPRA	SELENA
Launched By	USA	USA	USA	Italy	Nicaragua	Norway
Developed by	National Institute of Building Science (NIBS)	US Geological Survey under the Advanced national seismic system(ANSS)	Geo-hazard International	Stakeholders worldwide	GFDRR is supporting the countries of Central America	The International Centre for Geo-hazards ICG, through NORSAR
Input data	Buildings, Critical Facilities, Transportation and Demographic data	Population, Buildings, Seismic Intensity, Fault and ground motion, Soil amplification	Building Population Ground shaking lifeline	Population, Global land cover, building data, global GDP data.	Population, Building inventory data, PGA, and Infrastructure	Building Demographical data and Seismic data, different Soil class
Methodology	1-Prepare shake map 2-building vulnerability assessment map 3-Estimation of damage and	1. Preparation of shake map. 2. Addition of fault geometry, attenuation of the regional shake	1-Prepare earthquake risk map 2-Prepare building vulnerability map 3-Estimate damage and casualty.	1-seismic risk Evaluation 2-Use of analytical and empirical methods for vulnerability	1- seismic hazard evaluation 2-Identifying inventory, 3-Application of vulnerability functions, 4-Estimation	1-Prepare seismic risk map 2-Produce building vulnerability map 3-Estimate damage and casualty.

	casualty 4- Estimate loss	map. 3.seismic intensity map 4.economic loss and casualty estimation 5. Determination of alert level.		analysis 3- socioeconomic impact and losses estimation.	of losses	
Output	1. Loss estimates for utilities and lifelines, 2.Estimation of vulnerability and casualties, 3.Estimation of economic and social loss.	1. Estimation of loss and fatalities	1. Seismic intensity calculation, 2.Estimation of Building damage and Casualty	1. Loss of life and Property, 2.damage estimation, 3. Social and economic changes due to disruption.	1. Physical and economic losses approximated per property, 2. Probable % of loss, 3. Annually expected economic losses.	1. Physical damage estimation, 2. Estimation of total economic loss, 3. Damage and casualty.
Accessibility	Open source	Open source	Open source		Open source	Open source

Table 2.2: Continuation of models used for earthquake hazard, risk analysis, and loss estimation purpose.

Criteria	EQRM	INFORM	RQE
Launched by	Australia	Inter-agency standing committee task team for preparedness and resilience and the European Commission	Used for Global Catastrophe Modeling.
Developed by	Geoscience Australia	International organizations and government with JRC	EQECAT
Input data	1.Active fault types 2.Event scenario 3.Attenuation 4.Threshold Distance 5.Amplification 6.Building Classification	1.Earthquake events 2. Conflict Intensity 3.Socio-economic layers 4.Uprooted people 5.DRR 6.Governance 7.Communication 8.Infrastructures	1. Seismo-tectonic conditions 2.Active faults 3.Intensity of shaking 4.Stability of soils
Methodology	1. Generation of Synthetic earthquake catalog 2.preparation of Attenuation relation 3. Account of interaction between geology and seismic waves 4.Preparing probability of every earthquake and hazard 5. Using buildings and population risk analysis can be done	1. Hazard analysis and exposure caused by both natural and human-induced. 2. Vulnerability map preparation such as Socioeconomic and Vulnerable groups 3.Lack of coping capacity analysis using both institutional and Infrastructure	1. Hazard model preparation 2. Vulnerability analysis 3.Risk analysis 4.Damage estimation
Output	1.Probability estimation 2.Level of damage estimation 3.Financial loss 4.Computation of risk	1 Risk reduction 2. Geospatial Information and Risk Analysis 3. Estimation of statistics	1.Hazard estimation 2.Damage and loss estimation

Accessibility	Open access	Open access	Open access

2.3. Traditional approaches

2.3.1. Probabilistic seismic hazard assessment

A probabilistic model for hazard uses an extensive process of collecting and harmonizing relevant datasets (e.g. catalogues, active faults, geodetic, GPS measurements, and ground motions) to build seismogenic source models to forecast future seismicity and its effects (ground motions) (Azeez et al. 2019). Given the entire process, inherent uncertainties are associated with the data and methods used. Probabilistic Seismic Hazard Analysis (PSHA) has been widely used for almost 50 years by researchers and experts as a traditional seismic hazard assessment tool. PSHA is widely used for deciding safety and security criteria for nuclear power plants, making case-based local and official national hazard maps, development of required building codes, and determination of earthquake probability rates (Solomos, Pinto & Dimova 2008; Hanks et al. 2009). Hence, PSHA is widely used for designing and building critical structures.

PSHA is the most widely used approach for the determination of seismic loads for infrastructures and to understand the effects of these loads on the environment. However, using a model of probabilistic seismic hazard assessment creates uncertainties in terms of magnitude, location, and recurrence rate of earthquakes (McGuire 1978, 1995). Explicitly, the variation of ground motion behaviors with the earthquake magnitude and location is important and considered for the estimation of seismic hazard. In addition, PSHA provides a model network in which various uncertainties are quantified and combined to make qualitative and quantitative pictures of the seismic hazard. Equations (2.1) and (2.2) show the process to calculate the level of shaking using PSHA in a

simplified manner, and mathematically it is the level of shaking;

$$log\ (IM|M,R,SF,SE,NS)\ =\ f1\ (M)\ +\ f2\ (R)\ +\ f3\ \ +\ f4\ (SE)\ +\ f5\ (NS)\ +\ \varepsilon!\tag{2.1}$$

And synthetic signal in the frequency domain;

$$FFT\ (y|M,R)\ =\ g1\ (\text{Source})\ \times\ g2\ (\text{Path and Site})!\tag{2.2}$$

where $FFT\ (y|M,R)$ = intensity measure, M = magnitude, R = distance, *SF* = style of faulting, *SE* = local site soil effects, *NS* = near source effect, and $\varepsilon!$ = random error and $f1$ to $f5$ is considered as functions and FFT is the fast Fourier transform $g1$, $g2$ are representing ground motion (spectral acceleration) and y is yielding and $y|M,R$ represents to PGA/spectral acceleration.

This analysis is simple and allows the systematic investigation of a highly complicated process. The internal processes that generate seismic ground motions and affect the propagation of seismic waves are complicated (Corral 2004; Stein & Liu 2009). The overall methodology of PSHA is presented in Figure 2.2, as well as the core principles and applications of this model for seismic hazard and risk analysis. Some models that support the PSHA are discussed below individually. The regional recurrence model is a specific model that comes from the framework of PSHA. A maximum magnitude of the earthquake exists at a particular seismic zone that cannot be exceeded in the upcoming period. However, the primary objective of this model is to ascertain the chances of recurrence of an earthquake with the same or different magnitude (Cornel 1968).

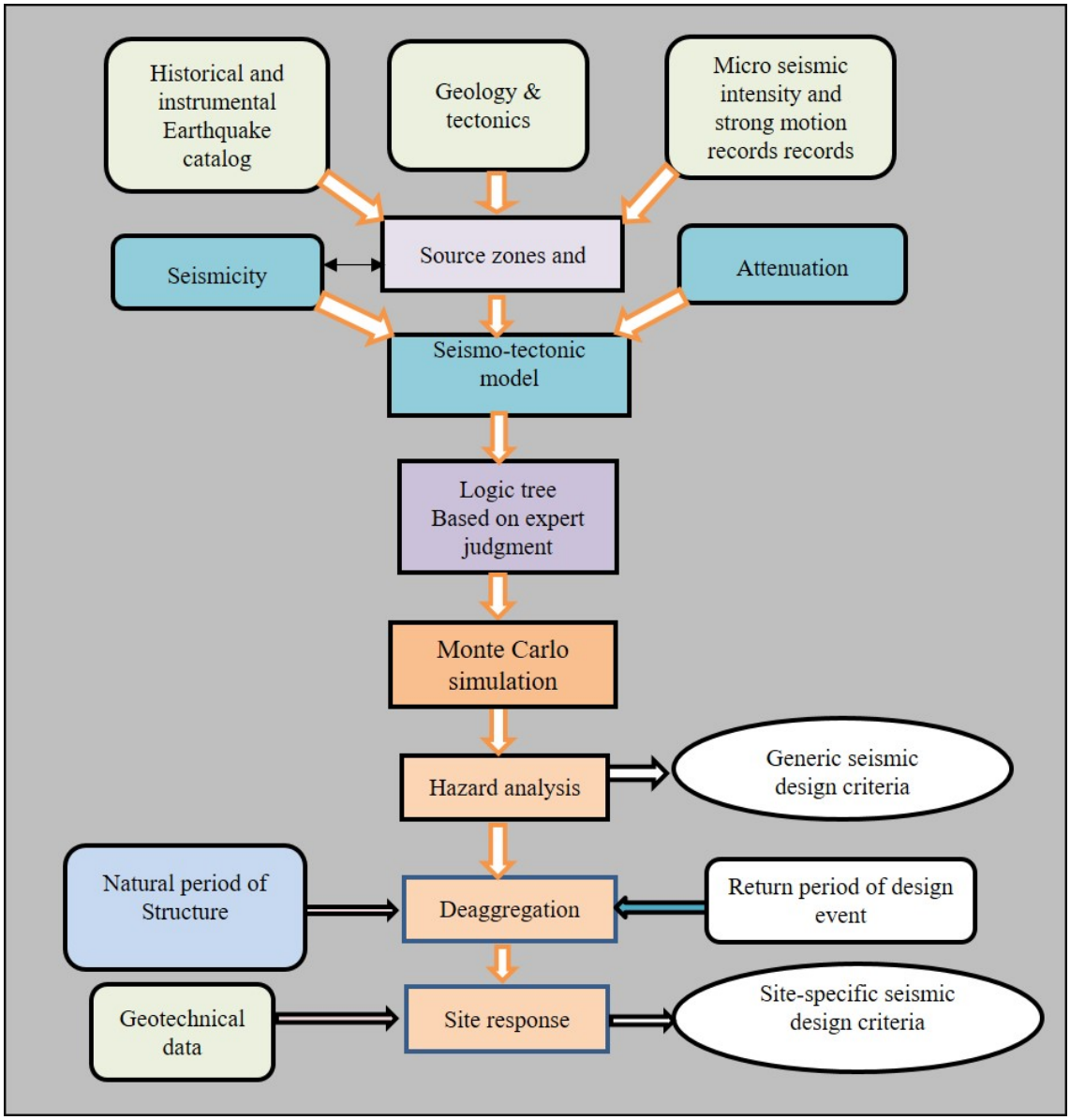

Figure 2.2: Overall model for probabilistic seismic hazard assessment. (This is an adaptation form FIGURE 8.1 of Chapter 8, Earthquake Engineering Handbook W.F. Chen and Charles Scawthorn).

In PSHA, for each seismic source, the low magnitude should be considered as 4.0 to 5.0 magnitude, because a magnitude lower than 4.0 cannot significantly damage constructions and important engineering infrastructures. Nevertheless, the incompleteness of lower magnitude earthquakes needs to be considered for PSHA (Lee

& Brillinger 1979; Tinti & Mulargia 1985; Rydelek & Sacks 1989). The large earthquake magnitudes can be easily estimated by considering the seismo-tectonics of the whole region and historical earthquake catalog. The magnitude recurrence model depends on the frequencies of various sizes of event magnitudes annually. In general, for any seismic source region, the seismic parameters can be determined by using the Gutenberg-Richter (G-R) magnitude-frequency relationship (Gutenberg & Richter 1944). Each fault has a capacity to produce earthquakes with magnitudes in the range of m^0 to m^u, which can be calculated by using the exponential recurrence model introduced and developed by Cornel and Vanmarcke (1969), and can be presented by the following mathematical expression;

$$\mathrm{N\ (m)} = \mathrm{Ni}\ (m_0)\ \{\beta e\hat{}(-\beta\ (m - m^0))/1 - e\hat{}(-\beta\ (m^u - m^0))\} \tag{2.3}$$

For $m^0 < m < m^u$, where β = bln(10) and Ni (m_0) is weightage factor based on the deaggregation for a specific source and m_0 is the seismic moment, m^u are magnitudes and b value could be calculated from the known measured slip rate. The purpose of this model is to provide information on the recurrence of earthquakes. Details of principles and methodology of this model can be found in (Cornel and Vanmarcke 1969; Utsu 1984; Weichert 1980).

2.3.2. Uniform hazard spectrum (UHS)

The uniform hazard spectrum (UHS) is a highly important aspect and can be evaluated from the (PSHA) (Atkinson 2009). In the first step, seismicity, geo-tectonic, and fault geometry information are used to analyze seismo-tectonic zones (Atkinson 2009). For each seismic source zone, the historical earthquake data are used to analyze the recurrence

relationship of magnitude and uncertainty; the recurrence relationship states that the frequency of occurrence of earthquakes is a simple function of magnitudes (Cornell 1968). Ground shaking relations are well-defined and provide an interlink between the occurrence of earthquake events and the ground motions, and this interlink results to a particular location in the seismo-tectonic zone (Kanai 1961). Ground shaking relationship can be understood as PGA or peak ground velocity (PGV). The final and most important step of hazard analysis is the integration of all magnitudes, distances, and their contributions to the probability of ground motion exceedance at the study area. Uniform hazard spectrum can be defined by repeating this process of analysis for a number of vibration periods, which is a spectrum with a specified probability of exceedance (Sen 2006). The uniform hazard spectrum is a valuable composition of major earthquakes that strongly contribute to the seismic hazard at a level of specified probability. In general, the spectrum of ground motion and the spectrum of response are dependent strongly on magnitudes of earthquakes and distance. Ground shaking for short period of time generally can be attributed to small-to-moderate earthquake events at a short distance, whereas large earthquake events at a longer distance create strong ground motions for long time periods. Details of this model can be found in (Cornell 1968; McGuire 1976; Campbell & Bozorgnia 2003; Sen 2006).

2.3.3. Hazard curves and maps

Hazard curves can be calculated for a specific site and are located by using lat-long and by interpolating data at surrounding four-grid points (Stirling & Petersen 2006). Seismic hazard curves can be represented by using Mean Annual Rate of Exceedance with peak ground acceleration or spectral accelerations (Stirling & Petersen 2006). A response spectrum can be created by plotting the parameters of magnitudes versus periods from

seismic hazard curves. The data used for the hazard curves must be tabulated along with the plot. The maps were generally designed by computing such hazard curves at each grid point within the particular mapping region (Frankel 1995). Details of this model can be found in (Cornell 1968; McGuire 1976).

2.3.4. Deaggregation

The PSHA methodology allows mean calculation of the annual exceedance rate at a specific region based on the combined risk resulted from potential earthquakes of various magnitudes. This is the method in a probabilistic analysis that can provide necessary information about the return period of events (Cornell & Vanmarcke 1969). The exceedance derived by PSHA is not due to any specified earthquake magnitude or distance from the source to site (Harmsen, Perkins & Frankel 1999). Sometimes, estimating any particular earthquake magnitude and the most appropriate distance from the source to site is important. Basically, the model is used for the response analysis by selecting the historical ground motion acceleration records. This process is called deaggregation and it can be expressed by the function of magnitude and distance (Halchuk & Adams 2004). Details of this model can be found in (Cornell & Vanmarcke 1969; McGuire 1976; Campbell & Bozorgnia 2003; Halchuk & Adams 2004).

2.3.5. Logic tree

The logic tree model is designed as a prominent and potential network for the treatment of the uncertainty (Delavaud et al. 2012). However, the best choice of elements for seismic hazard models remains unclear (Delavaud et al. 2012). In some applications of PSHA, which always seeks to combine all the probable options into a ‘‘logic tree,” setting more or less subjectively assigning a weight to each branch and it can create a wide variety

of scenarios (Bommer et al. 2005). The sum of all possibilities from all the branches of a logic tree in a given node must not exceed 1. Such techniques have their origin in the Delphi method (Dalkey & Helmer 1963), which is used to assimilate expert opinions on possible outcomes. The logic tree method allows the uncertainty for the model selection for attenuation equation and distribution of magnitude (Bommer et al. 2005). In the logic tree method, attenuation equation that was derived by the authors (Campbell & Bozorgnia 1994) should be considered equally and are valuable; hence, each equation should be assigned by a relative weight. In the next level of the logic tree model, the Gutenberg-Richter magnitude distribution should be considered over earthquake distribution, and finally, different relative likelihoods need to be assigned to the maximum magnitude. Therefore, Campbell and Bozorgnia (1994) calculated the branches of the logic tree, as follows:

$$\text{Total no of branches} = (\text{No. of attenuation equation} \times \text{no. of magnitude distributions} \times \text{no. of maximum magnitudes}) \quad (2.4)$$

The logic tree model can be used in a seismic hazard analysis, in which the composition of models is based on the interpretation of alternative datasets, assumptions, and expert elicitation and/or parameters are associated with every branch of the model. The result can be taken as the sum of the individual results. Cornell's (1968) approach is essential to separate the tasks of the seismologist and engineer. The job of the researcher is to provide "best estimates of the average activity levels of various potential sources of earthquakes". Details of this model can be found in (Cornell 1968; Dalkey & Helmer 1963; Bommer et al. 2005).

2.3.6. Uncertainty and accuracy of PSHA

Uncertainties in earthquake magnitude, location, recurrence, and effects in ground shaking in PSHA are to be effectively considered in the seismic hazard estimation. PSHA requires the quantification of all those uncertainties. Moreover, the accuracy of the probabilistic analysis based on the uncertainties can be characterized. Different models and procedures are available and can be used to quantify the uncertainty of all the parameters. Therefore, uncertainties may result because of the manner of data collection in a geologically short time period (Scawthorn & Chen 2002). For accuracy, technological knowledge and ideal judgment based on engineering decision-making models should be used wisely for the valuable interpretation of the PSHA model. A logic tree model is helpful enough for the uncertainties to be incorporated into the probabilistic model (Scawthorn & Chen 2002). A logic tree is an effective model and allows for the use of alternative models for improved understanding and analysis. The weight factors are important to be assigned in a logic tree and often use expert opinion, which can provide improved results.

2.4. Deterministic seismic hazard assessment

Deterministic Seismic Hazard Analysis (DSHA), is generally used for ground motion characteristics by applying the assumed or a real set of earthquake events in a specific region (Shah et al. 2012). The main contribution of DSHA depends on the understanding of the complexity of the seismo-tectonic zone (Ambraseys & Melville 1995). In the DSHA approach, the model identifies the major seismic sources near the study region can affect the region in a vibrant manner (Shah et al. 2012). Understanding the historical seismic records and geo-tectonic data regarding the characteristics of various destructive events that make the ground motion is important as well.

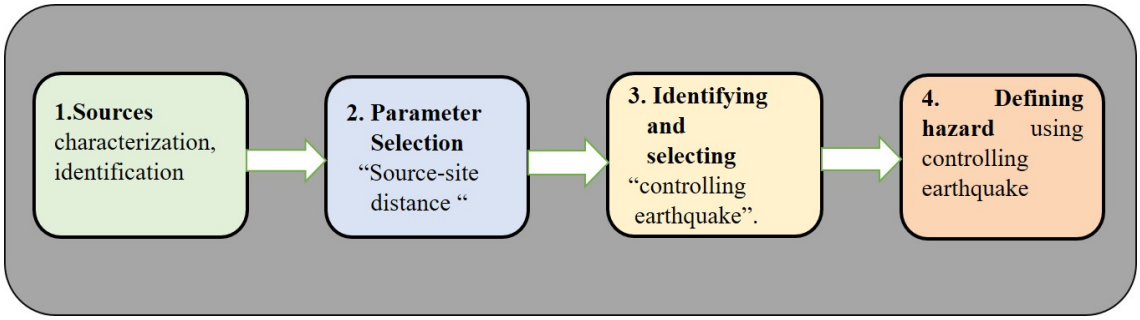

Figure 2.3: Overall model for deterministic seismic hazard assessment.

In general, one or more earthquakes are highly dangerous in terms of magnitude and location, which can be called controlling earthquakes (Deif et al. 2012). The ground shaking of the region can be estimated deterministically because the analysis requires the magnitude, source-site distance, and condition of the study region. Details of the principles and methodology of this model can be found in (Campbell & Bozorgnia 2003; Shah et al. 2012; Deif et al. 2012) (See Figure 2.3). DSHA can be used for the hazard estimation in four important steps, namely,

2.4.1. Uncertainty of DSHA

DSHA is a traditional method that involves some scenario assumption, which can create uncertainty (Shah et al. 2012). The occurrence of a specified earthquake of a particular magnitude at a site for which ground shaking characteristics can be evaluated. The most important benefit comes from this approach when it provides a straight framework for the worst ground shakings. Catastrophic consequences may occur because of failure of nuclear power plants, large bridges, and dams, and DSHA is applied in these consequences. Therefore, DHSA is useful for creating an improved model.

2.4.2. Accuracy of DSHA

DHSA does not provide any information on the likelihood of recurrence of the controlling earthquake. A controlling earthquake is assumed to occur in the region in which the expected ground shaking level can be understood during a limited time period. The uncertainties in different parts of the study are important to compute, and the accuracy depends on the uncertainty type.

2.5. GIS-based models

Nowadays researchers mostly use GIS-based models for seismic hazard and risk assessment (Frigerio et al. 2016). This review examined the core principles of many GIS-based models with their applications. Moreover, the review discussed some of the models with methodology and their successful results. All the models have strengths and limitations, which are discussed in (Table 3).

2.5.1. GTIS (Geotechnical Information System)

Geotechnical information system (GTIS) is a modified technique to manage and use the geotechnical spatial information efficiently for the ground surface and sub-surface. It is derived by using GIS technology as a synthetic tool, and the main objective of GTIS is to make proper planning for multiple hazards analysis (Chang & King 2005; Erden & Karaman 2012; Karaman & Erden 2014; Williams et al. 2002). GTISs were developed based on GIS technology, thus Williams et al. (2002) called this system the geotechnical geographic information system (GEOGIS). The developed GTIS model can be applied to evaluate the site characteristics in seismic hazard analysis. As part of the model for site characterization, surface wave velocity (V_S) values and geotechnical information need to be predicted to build a well-designed model of GTIS. GTIS has been developed using

new ideas of an extended research and geotechnical knowledge with an established procedure. First, important parameters need to be identified those are useful to solve geotechnical and earthquake engineering problems. Next, the step is to prepare the parameters for the micro-zonation mapping of the study region (Gong 1996). In a way forward, it is important to make response analyzes, and seismic micro-zoning maps (Kramer 1996). Seismic zonation mapping can verify the importance of the GTIS model. A large dataset is needed for building a GTIS model, which has the capacity to analyze and manage effectively. It is applicable in any environment as a globally developed model. Details of the principles, parameters, methodology, and accuracy of the output of this model can be found in (Williams et al. 2002; Chang & King 2005; Kramer 1996).

2.5.2. Fault-specific GIS-based seismic hazard analysis

A fault-specific seismic hazard assessment model has been developed and modified by several authors (Youngs & Coppersmith 1985). This method of seismic hazard mapping from geological fault throw-rate data was first presented by Papanikolaou (2003) and Roberts et al. (2004). The main objective of this model is to prepare fault-specific seismic hazard map that shows the recurrence of earthquakes with expected intensities (Deligiannakis, Papanikolaou & Roberts 2018; Giardini et al. 2018). This system requires a large dataset, which can be used for understanding current tectonic conditions and tectonic activity rates.

The dataset and analysis include aerial photographs, satellite data, interferometry data, strain rate, GPS data, quaternary formations mapping and analysis, pedological, sedimentological, geological, geomorphological, and geophysical studies for the identification and characterization of the structure (Michetti & Marco 2005). The

resulting hazard map may have uncertainties because of the consideration of many poorly affected parameters (Stein, Geller & Liu 2012). By doing proper scientific analysis of the active faults and geological conditions, the chances of uncertainties can be reduced. Some assumptions and errors that need to be considered in this analysis. Some assumption can be made for the delineation of the database of the fault geometry. The error parameters that can create a major problem in the study can be clearly understood from the research articles of; (Benedetti et al. 2003; Ganas, Pavlides & Karastathis 2005; Papanikolaou & Royden 2007; Sakellariou et al. 2007; Roberts et al. 2009; Grützner et al. 2014; Grützner et al. 2016; Deligiannakis, Papanikolaou & Roberts 2018). It can be applied for the seismic assessment of any seismically active zone. Therefore, the following four processes as described in the Figure 2.4 can represent the model.

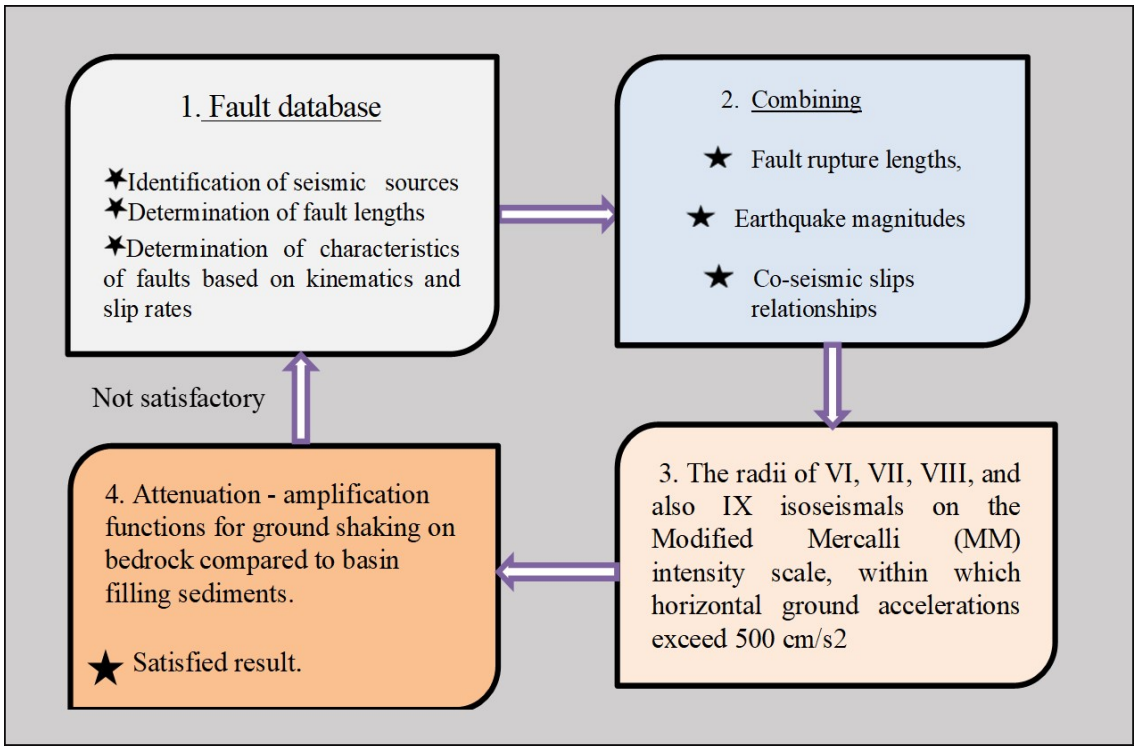

Figure 2.4: Methodology for fault-specific GIS-based seismic hazard analysis.

2.5.3. Intelligent simulation system using artificial intelligence

Intelligent simulation is an effective system, which can be used simulating earthquakes, seismic hazards, damage, and losses. The main objectives of the model are to identify the weakness of the structures before an earthquake, and make an intelligent emergency response after an earthquake (Tao et al. 1996; Tang & Wen 2009). The structure of the system is clear, and has three steps: hazard simulation, risk analysis, and emergency response simulation, as shown in (Figure 2.5). The intelligent simulation method is helpful to identify aseismic weak structures and to accomplish quick damage assessment. The types of data needed for this simulation analysis are: (1) geographical location; (2) coverage of seismic monitoring network; (3) destructive earthquakes based on inventory; (4) coverage of recorded earthquake by instruments; coverage of active fault systems; (6) seismo-tectonic province; (7) coverage of the whole seismic zone (Tang & Wen 2009). The information sub-system is designed for analyzing various data quickly and efficiently. It is a platform for easy communication among all the sub-systems, and has a user-friendly interface for various users at different levels.

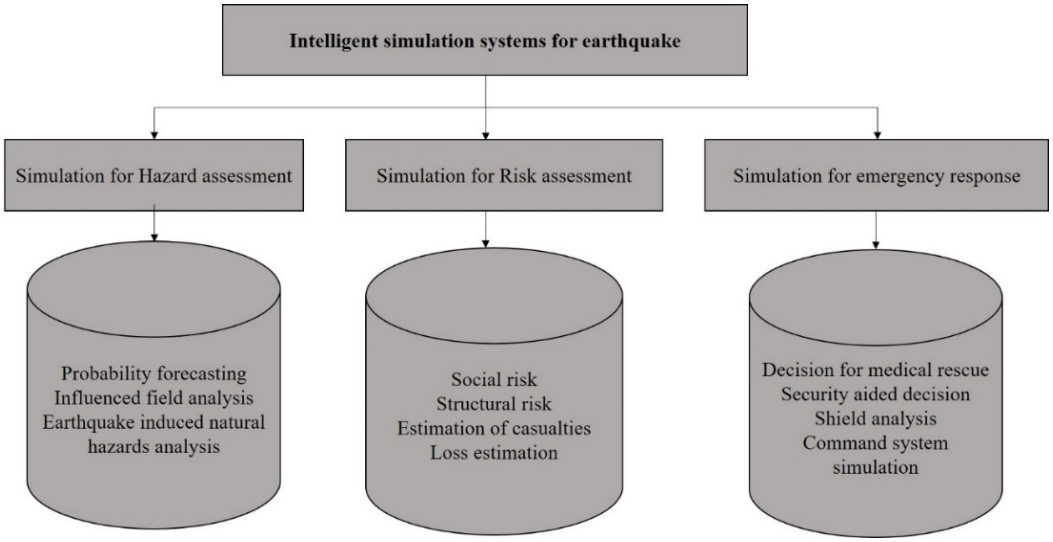

Figure 2.5: Steps for the simulation based on GIS and artificial intelligence.

A worldwide model of this system has been designed and is used in various environments. Details of methodology, errors, and accuracy of this model can be found in (Tao et al. 1996; Tang & Wen 2009).

2.5.4. Vulnerability mapping using the FEMA-RVS method

FEMA-RVS method is developed by Federal Emergency Management Agency for the vulnerability mapping for moderate seismicity. Another method of RVS was developed by Turkey, and is only applicable for reinforced concrete buildings (Rahman, Ansary & Islam 2015; Tas, Cosgun & Tas 2007). The main objective of this method is to evaluate composite vulnerability (Rahman, Ansary & Islam 2015). In this method, the score obtained is from a high to a low value, and a high value means low vulnerability and a low value means high vulnerability (Rahman, Ansary & Islam 2015). In this method, vulnerability assessment can be done using all parameters and can be done for multi-hazard purposes (Gentile et al. 2019). A composite score of vulnerability can be estimated by combining the vulnerability of all hazards. This method can provide a complex scenario of vulnerability analysis. This integrated analysis of vulnerability model can be a relevant tool for disaster risk assessment. Moreover, it can provide an ideal methodology wherein the researchers can prioritize the hotspot areas for vulnerability assessment. The parameters required for the vulnerability assessment depends on the proper documentation of building identification information, such as the use of buildings, size, area, photograph, building plan sketch, elevation and its relation to seismic performance, vulnerability score, and the numerical value of seismic hazard (Jahan et al. 2011). Details of methodology and analysis of this method can be found in some articles (Rahman, Ansary & Islam 2015; Jahan et al. 2011) (See Figure 2.6).

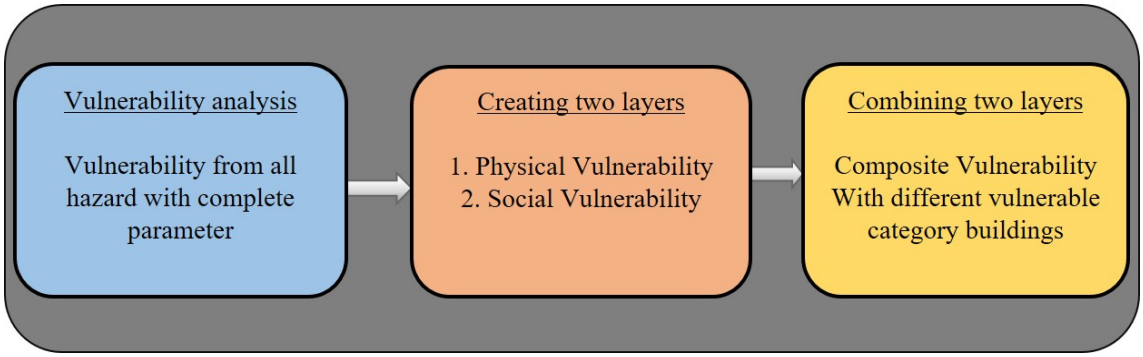

Figure 2.6: Methodology of RVS FEMA for vulnerability analysis.

2.5.5. GIS-based risk assessment

The primary objective of this model is to integrate various relevant data with the concepts of risk assessment by considering the characteristics and sources of the earthquake (Tsai & Chen 2010). The method is one of the most popular methods in seismic risk assessment. Evaluating the potential ratio of disaster occurrence and ultimate loss or damage caused by that disaster is necessary.

$$R = H \times V \times E \tag{2.5}$$

where R: risk

H: a ratio of disaster occurrence

E: exposure to the disaster

V: level of damage

The earthquake risk needs to be calculated using three elements, namely, hazard source, damage level to objects, and threat (Varazanashvili et al. 2012). The level of risk calculation is impossible to ascertain if any of these three elements is missing. In next step, an earthquake risk manager can only analyze the risk sources and scope of all the effects that may occur by using this risk assessment system (Tsai & Chen 2010). This leaves the responsibility of strategizing the assessment to the decision maker. Prevention training and organizational plans are necessary to create a proper risk assessment.

This method is efficient and quite feasible. The details of the principles and methodology can be found in (Smith 2003). Figure 2.7 shows the steps needed for risk assessment.

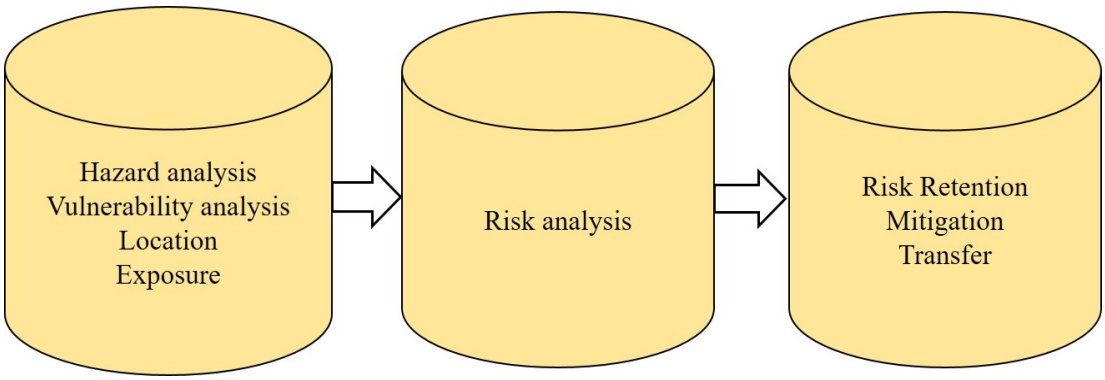

Figure 2.7: Methodology for earthquake risk assessment.

2.5.6. Integrated model for seismic vulnerability assessment

Various methods have been developed to calculate seismic vulnerability (Varazanashvili et al. 2012). However, developing and improving a seismic vulnerability map using an integrated model is the most efficient method for seismically active areas (Ilanlu et al. 2013; Oliveira 2003). The purpose of this method is for risk mitigation and risk reduction. The main objective of this method to estimate seismic vulnerability, including all parameters, by using an integrated technique. A weighted overlay technique is used for vulnerability mapping by using analytic hierarchy process to make the logical decision on the weight of the parameters (Bahadori, Hasheminezhad & Karimi 2017). A spatial map of city structures can be created and used as a basis for collecting information.

The survey can be done based on various factors, which can be utilized for the investigation and for the evaluation of seismic damage (See Figure 2.8).

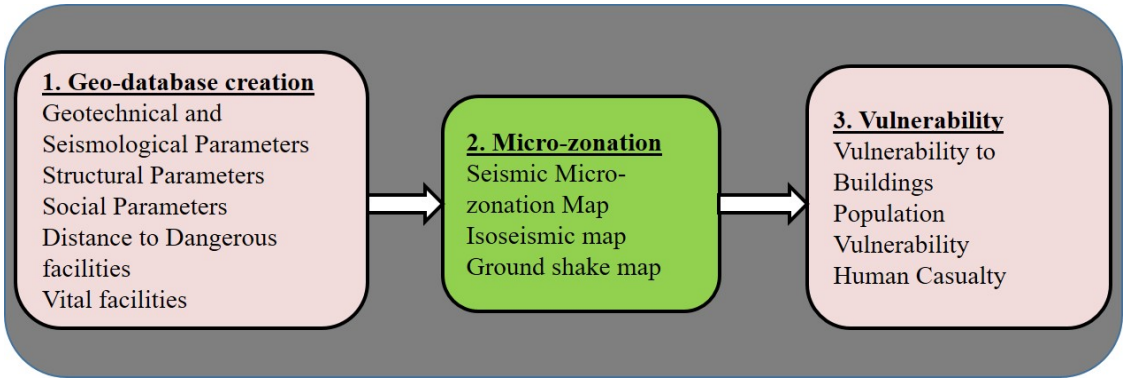

Figure 2.8: Steps for the integrated seismic vulnerability assessment.

The model can be applied to all countries with the same conditions by making some modifications in the parameters and weight factors (Bahadori, Hasheminezhad & Karimi 2017). This model can be a significant tool for the crisis resulting from the strong earthquakes (Bahadori, Hasheminezhad & Karimi 2017; Papoulia, Stavrakakis & Papanikolaou 2001). Details of this method can be found in (Ilanlu et al. 2013; Bahadori, Hasheminezhad & Karimi 2017).

2.5.7. Soil liquefaction potential analysis

Soil liquefaction due to the earthquake is one of the major challenges at this current time (Jefferies & Been 2015). Soil liquefaction depends on the soil properties and seismo-tectonic behavior of the site. According to seismologists, active faults can be identified by using the geological feature known as Panvel flexure (Subrahmanyan 2001; Mhaske & Choudhury 2010). Detailed soil data is needed to ascertain the soil characteristics and for soil liquefaction analysis, and some more factors need to be considered for safety analysis. A simple method has been designed by (Youd 1995; Mhaske & Choudhury 2010) for safety factor analysis, and can be used for estimating liquefaction potential. First, the undisturbed soil data should be collected for the evaluation of liquefaction

potential (Stokoe 2001). In next step, the safety factors of liquefaction for earthquakes of different magnitudes are derived. Then, the liquefaction of soil is classified by using the values from the previous step involving safety factors. Finally, a potential to soil liquefaction map can be prepared by using the soil liquefaction susceptibility method in GIS. The required soil data for the susceptibility analysis are depth of water table, depth of collected soil sample, dry density, saturated density and soil friction angle, among others (Murthy 2007). Three types of liquefaction maps exist: liquefaction susceptibility, liquefaction potential, and liquefaction-induced ground failure maps. The liquefaction susceptibility map indicates the susceptibility of soils to liquefaction, the potential map indicates the susceptibility of soil and earthquake potential, and the liquefaction-induced ground failure map indicates ground displacement associated with liquefaction. Details of the methodology of these methods can be found in (Murthy 2007; Youd 1995; Mhaske & Choudhury 2010).

2.5.8. Seismic micro-zonation analysis

Previously, micro-zonation was applied as one of the traditional methods. Nowadays, GIS-based micro-zonation model is commonly used by many researchers (Sekac et al. 2016). The GIS-based micro-zonation model is generally used for earthquake risk analysis purposes (Pitilakis et al. 2005**)**. The main objective of this model is to prepare a micro-zonation map that can be used to update the historical map and for risk assessment (Cox et al. 2011). Nevertheless, the completeness of parameters is highly important in micro-zonation mapping. In general, for preparing a micro-zonation map, various kinds of input data are required, such as local site effects, wave propagation, landslide hazard, liquefaction, and fault rupture. Ground shaking and site effects for the different scenario can be derived and used in this model for a proper analysis with precision and accuracy

(Louie 2001). Details of principles and applications of this model can be found in (Louie 2001; Cox et al. 2011).

2.5.9. Seismic amplification susceptibility analysis

The main objective of this method is to ascertain the potential areas of accumulation of unconsolidated sediments and to prepare a seismic amplification susceptibility map with spatial variation (Dhar, Rai & Nayak 2017). To prepare the susceptibility map of seismic amplification, important input data layers need to be considered, such as soil amplification factor, lithology, unconsolidated sediment, slope, height level, curvature, and flow accumulation (Theilen-Willige 2010). Weighted overlay technique can be an effective tool for preparing the soil amplification map in seismic hazard assessment (Theilen-Willige 2010). This model will help decide how the region is going to be affected by seismic waves. Because of loose sediment deposits, the seismic amplification increases. Seismic amplification analysis can help to create the seismic micro-zonation in the next stage. This model is feasible and useful for seismic hazard and risk analysis. The details of this model can be found in (Theilen-Willige 2010; Sekac et al. 2016).

2.5.10. Unified risk assessment

It summarizes the global hazard model HAZUS with various small modules and their interconnection (Pitilakis et al. 2005). The main objective of this method is to prepare a risk map and quantify the risk level (Pitilakis et al. 2006). This risk assessment method is useful for every lifeline, including population and buildings. In this assessment, the weak zones, such as seismic amplification, micro-zonation, and inventory of whole lifelines, are needed to identify the hazard analysis. For a feasible analysis of earthquake risk, a effective scenario should be developed. This system can be described as a multi-hazard

model for risk assessment by using the GIS tool (Pitilakis et al. 2006). The main ideal processing steps are global value estimation and impact on economic damages and losses. For improved results of risk assessment, the inventory data should be accurate and detailed with seismic hazard data. In this unified risk assessment model, several steps are needed for an effective analysis. Details of this risk assessment model can be found in (Werner et al. 2000; Pachakis & Kiremidjian 2004).

2.5.11. Holistic model for seismic risk analysis

This model can be applied to any seismic-prone region. Parameters of this model can be determined on the basis of local site conditions. Public and private sectors can utilize the risk assessment criteria developed in this model. An integrated earthquake safety index has been used for evaluating the level of safety (Mili, Hosseini & Izadkhah 2018). Many types of software are relevant for risk estimation, such as SAFER, Risk –UE, KOERILOSS, and DBELA (Pitilakis et al. 2006). A relative seismic risk index needs to be calculated based on vulnerability, damage, casualty, and social characteristics, and is the best method to address risk. In this model, the risk analysis is done based on required data. First, EHI (Equivalent Hazard Index) is to be calculated, and then EVI (Equivalent Vulnerability Index), and finally, the evaluation of (Response Capacity Index) RC; all these factors are important to reduce risk. This model is popular and recommended by many researchers. Details of principles, methodology, and efficiency of this method can be found in (Mili, Hosseini & Izadkhah 2018).

2.5.12. Arithmetic and weighted overlay approach to seismic hazard assessments

Integrated data analysis is used for the detection, visualization, mapping, and analysis of factors related directly or indirectly to earthquake occurrence (Kaliraj, Chandrasekar &

Magesh 2015). The main objective of this method is to produce an earthquake potential map by using all the parameters with relevant factors (Theilen-Willige 2010). Factors can be extracted using the input data for the detection of local site conditions. Thematic layers are generally used to evaluate numeric data layers that are applicable for arithmetic overlay analysis. Casual factors are important for the analysis of potential to earthquake areas (Theilen-Willige 2010). Based on weighted value, data integration can be done for earthquake potential analysis.

Validation is important to validate the resulting map from the analysis, and can be done by using the historic map of seismic hazard. The weight value assigned to all the factors are attributed to the information, which depends on the thematic data layers for the integration of data and geospatial analysis in the GIS system (Ahmad, Singh & Adris 2017; Pradhan & Jena 2016).

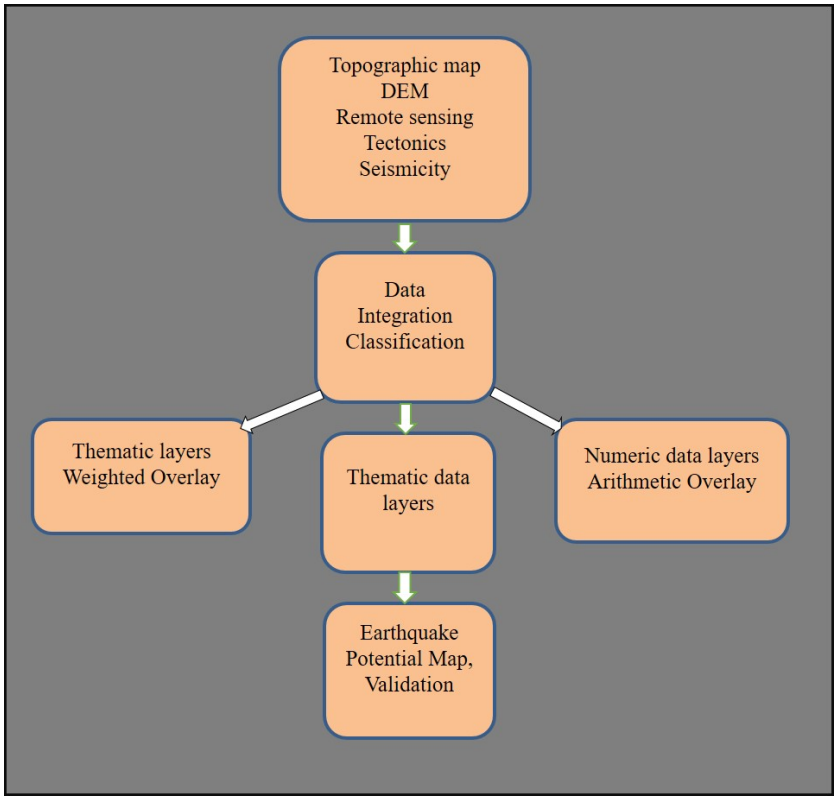

Figure 2.9: Weighted overlay technique for the earthquake potential analysis.

The layers of input data must be multiplied by their corresponding ranks and should be added to obtain an Earthquake Potential Index (EPI) needed for earthquake hazard evaluation.

The EPI can be calculated by using the following formula:

$$\text{EPI} = 0.1 \times \text{DEM (ij)} + 0.1 \times \text{Slope (ij)} + 0.15 \times \text{DenF (ij)} + 0.15 \times \text{DenEv (ij)} + 0.2 \times \text{ML (ij)} + 0.15 \times \text{DisF (ij)} + 0.15 \times \text{Disepiev (ij)} \quad (2.6)$$

$$EPI = \sum_{i=1}^{10}(Ri \times Wij) \quad (2.7)$$

where Ri is the rank for factor (i) ,Wij is the weight of the class (j) of factor (i) and DEM (Digital Elevation Model), DenF (fault density) and DenEV (event density), ML(local magnitude), DisF (fault distance) and Disepiev (distance from epicenter of an event). The method is popular and highly recommended by researchers for earthquake potential analysis. Details of this method can be found in (Theilen-Willige 2010; Ahmad, Singh & Adris 2017) (See Figure 2.9).

2.6. Machine learning techniques in predicting earthquakes

Data mining is one of the most popular processes for analyzing and discovering hidden parts in data (Fayyad, Piatetsky-Shapiro & Smyth 1996). Machine learning is a part of data mining and considered as the process of automatic data-pattern recognition based on the collected training data (Fayyad, Piatetsky-Shapiro & Smyth 1996). In recent years, numerous studies have been performed on machine learning techniques. Most of the recent studies focuses on analyzing which machine learning techniques are most suitable and able to predict the earthquake with good accuracy (Rouet-Leduc et al. 2017; Ruano et al. 2014; Idowu et al. 2016). Extensive research has been done on earthquakes (Asim

et al. 2017; Rouet-Leduc et al. 2017). Machine learning techniques have recently become effective and prominent in the field of the seismology for earthquake prediction. Machine learning is well described by categorizing the machine learning algorithms into supervised and unsupervised learning, as mentioned by Idowu et al. (2016). In supervised learning input and target, an output is given to train and run a function. In unsupervised learning, no label is given in the sampled data. For the prediction of earthquakes, almost seven techniques are considered: Linear Regression (LR), Polynomial Regression (PR), Local Polynomial Regression (LPR), Vector Linear Regression (VLR), Gaussian Process, Support Vector Machine (SVM), and Neural Networks (Fayyad, Piatetsky-Shapiro & Smyth 1996). Holdout method is the one, which is used for evaluation. This method is simple and compatible with cross-validation, as described by Muñoz et al. (2015). Furthermore, the latitudes that the models are using in linear regression provide minimum errors. Polynomial regression and Gaussian process models cannot efficiently define the longitude. SVM is the best method for magnitude prediction (Ikram & Qamar 2015), and neural networks produce enhanced results in depth prediction. The most popular methods, such as SVM, ANN, and CNN are used for earthquake prediction and present with good accuracy. The details of all other methods for earthquake prediction can be found in (Asencio-Cortés et al. 2016; Atkinson & Tatnall 1997; Uyeda 2015; Florido et al. 2015; Dutta et al. 2016; Idowu et al. 2016).

2.6.1. Support Vector Machine (SVM): a method of seismic detector

In the last decade, the most applied technology used for various problems in the field of seismology is computational intelligence (CI). One of the major challenges in seismology is earthquake prediction, wherein research is conducted by many global organizations by analyzing and developing different models and parameters (Ruano et al. 2014; Yeats &

Prentice 1996). SVM is widely applied for various problems, including seismic detection. Moreover, SVM is one of the best methods for detecting earthquakes at an almost equal level to those detected by seismic stations. The least square support vector machine (LSSVM) is a better model for the prediction of seismic attenuation and is used to compute error bars as well. Nevertheless, SVM method provides excellent earthquake detection in terms of specificity. The drawback of this model is it takes too long for detecting earthquakes. Studies have stated that this technique is best for earthquake magnitude prediction (Panakkat & Adeli 2007, 2009).

Furthermore, according to studies, this model provides good results when the data collected from the seismic stations are used in the SVM detector (Ruano et al. 2014). A general methodology was presented in the (Figure 2.10).

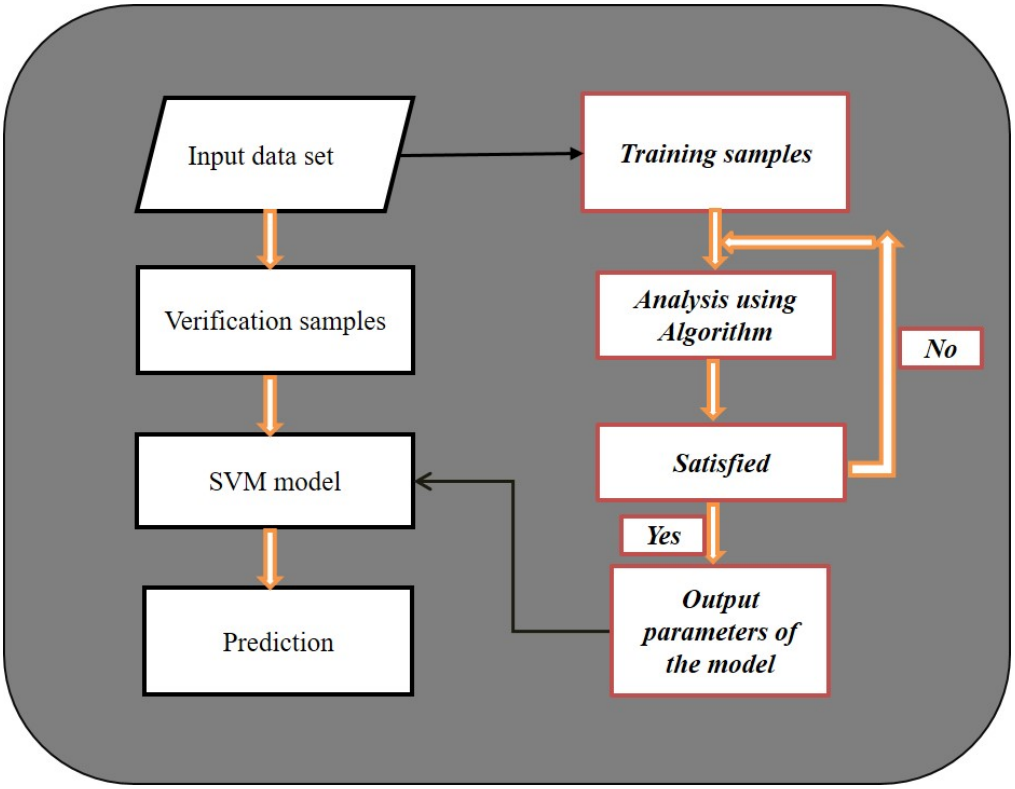

Figure 2.10: A general SVM methodology for the earthquake prediction.

2.6.2. Artificial Neural Network for earthquake prediction

In a scientific manner, predicting an earthquake is possible, but the prediction might have low accuracy (Wilson 1985). An artificial neural network is one of the technologies for that is better at predicting earthquakes compared with other traditional methods (Al-arifi et al. 2013; Alizadeh, Alizadeh, et al. 2018; Beale, Demuth & Hagan 1996; Nedic et al. 2014). The prediction accuracy will be more prominent and correct if the input parameters are complete and comprehensive (Abraham 2005). A three-layer Levenberg Marquardt feed-forward learning algorithm generally seems to be used for earthquake prediction (Jena et al. 2019). Therefore, ANN accepts the strategy of individual training with a perfect weight leading to estimations (Sietsma & Dow 1991; Alizadeh, Alizadeh, et al. 2018). Seismicity rhythm can be recognized using an ANN approach. The seismicity cycle can be represented by energy accumulation, that is, increasing release in energy, intense release, and the remnant release of seismic energy. It is a successfully operated application that realizes the seismic hazard evaluation (Figure 2.11b).

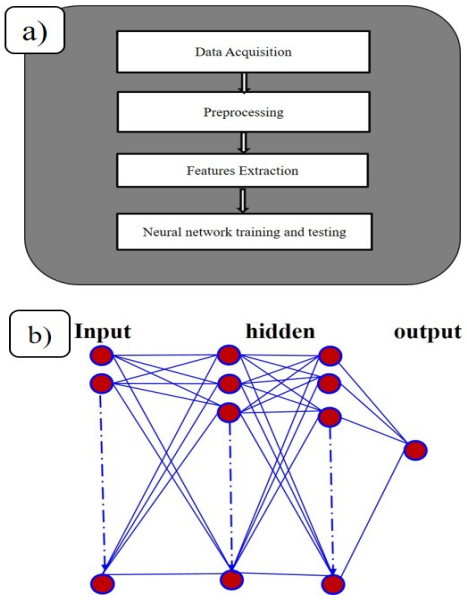

Figure 2.11: (a) The phases of a neural network for earthquake prediction, (b) the general model of neural network adopted from (Jena et al. 2019).

Moreover, it is one of the complex mathematical expressions that may be an alternative to other models, and can predict improved results with accuracy. A model of neural network is presented below to show the complexity of the structure in (Figure 2.11b).

2.6.3. Deep learning techniques

Advancement of the deep learning that has been serving the artificial intelligence community from last few decades. It is very good to uncover the complex patterns in high-dimensional data. Therefore, deep learning is used in several areas of science and engineering. Several applications such as image recognition (Farabet et al. 2012; Krizhevsky, Sutskever & Hinton 2012; Szegedy et al. 2015; Tompson et al. 2014) and speech recognition (Mohamed & Hinton 2013; Hinton et al. 2012; Mikolov et al. 2011), it has beaten other techniques at predicting the seismic activity, brain circuits recreation (Helmstaedter et al. 2013), and predicting the disease, mutation and gene expression and many implemented in many medical science platforms (Leung et al. 2014). Deep learning has generated promising results in several fields (Collobert et al. 2011), specifically in classification, prediction, translation of language and other aspects (Abdollahi et al. 2020).

The recent advancement has been recorded in artificial intelligence and Conv-Net-Quake, a highly scalable and developed convolutional neural network that is designed for earthquake location detection from a single waveform analysis (Perol, Gharbi & Denolle 2018). The research is being conducted by researchers on models to modify the methodology. However, various types of neural network models are being used, and among these, a deep convolutional neural network is highly suited for earthquake depth prediction (Perol, Gharbi & Denolle 2018).Deep convolutional neural network takes input

data as a 3-channel waveform data and predicts the label, such as noise and event. The parameters of the neural network model are highly optimized to either minimize or eliminate the discrepancy between the predicted result and the true labels on the training dataset. The detection accuracy depends on the percentage of windows, which is correctly classified as earthquake or noise. In general, the algorithm can detect all the events cataloged from any source successfully. This method is efficient for depth prediction.

2.7. AHP-based Seismic analysis

Seismic hazard and risk assessment based on analytical hierarchy process are among the popular techniques used by researchers. Usually, AHP is one of the best methods in decision making studies. Complex and complicated decisions can be analyzed by using the analytical hierarchy method, the criteria that is quantified and tangible (Saaty 1988, 1990a, 1990b, 2008). AHP is one of the best methods, and it creates a hierarchy for the enhanced decision for parameter ranking and it is a highly popular method for creating a matrix to compare the pairs so that the weight of each element can be assigned consistently (Saaty 1988, 2008; Estoque 2012).

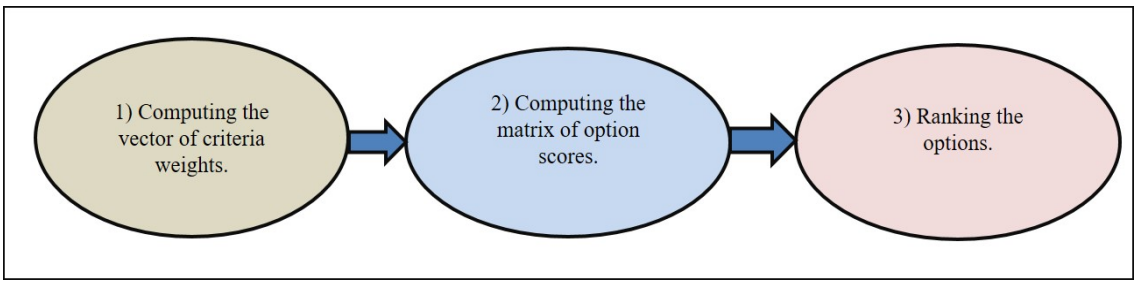

Figure 2.12: Processes for making the decision in AHP.

This is one of the latest decision-making models for successfully mapping seismic hazards worldwide by assigning the perfect weight to each factor (Malczewski 1999;

Mohanty & Walling 2008). AHP divides the problem into primary and secondary parts of the objectives. The whole agenda of processing is mathematically joined, making an effective and favorable statement for each element or group. The principal eigenvalue (λmax) needs to be calculated to check the consistency of the created matrix, where n is the good measure of consistency. To define the consistency degree, a consistency index (CI) can be computed as (Saaty 1988, 1990a):

$$\mathrm{CI} = (\lambda_{max} - \mathrm{n})/(n-1) \tag{2.8}$$

A high consistency index (CI) points towards a matrix of low consistency. The consistency ratio is important for determining a satisfactory consistency level (Saaty 1988, 1990a, 1990b, 2008), therefore:

$$\mathrm{CR} = CI/RI \tag{2.9}$$

The average consistency (RI) index can be created by using a random matrix that depends on the order of the matrix. A matrix with a satisfactory consistency level must yield a CR value of less than 0.10; thus, the calculated weight value for each factor is acceptable (Saaty 2008). AHP combines the weights of the criteria and the scores from the options in order to determine a global score and ranking evaluation. The global score is a weighted sum of the scores derived from all the criteria. The AHP simply can be implemented in three major and consecutive processes (See Figure 2.12).

2.8. Previous works on earthquake prediction and probability, vulnerability, and risk assessment

We divide this section into three subsections. The first subsection discusses about

earthquake probability mapping and forecasting. The second subsection provides a brief description of vulnerability, and the third section provides the overview of risk assessment using various methods.

2.8.1. Prediction and probability assessment

Avoiding earthquakes may be impossible, but accurate predictions and early warning can reduce the effect of the damage and consequences (Ikram & Qamar 2015). Research shows that natural hazards, such as earthquakes, are measured by probabilities, which explain the identification of potential zones for earthquakes in a semi quantitative analysis (Wang et al. 2006). Hazard is the probability of an earthquake in a specific geographic position within a period, and the intensity of ground shaking crosses a given threshold. Artificial neural network (ANN) has a wide range of applications, ranging from civil engineering (Karunanithi et al. 1994) to image processing (McIlraith & Card 1997**)** and to geology and seismology (Zhao & Takano 1999). ANN has been used in earthquake prediction and probability by calculating the importance of seismicity indicators for small and large events (Panakkat & Adeli 2007, 2009). Researchers have used different ANN architectures for earthquake prediction. A recurrent neural network was developed by Panakkat & Adeli (2009) for the prediction of earthquake time and location by using eight seismicity indicators (e.g., T (time), a (latitude), and μ (days)). Moreover, they analyzed several sets of events and computed the latitude and longitude of the location of epicenter, as well as the occurrence time for the same events. Pradhan and Lee (2009, 2010) used ANN model for the landslide hazard and risk assessment using remote sensing and GIS. Turmov et al. (2000) developed earthquake-induced tsunami prediction models using the measurement of electromagnetic and elastic waves simultaneously. Shimizu, Sugisaki & Ohmori (2008) studied earthquake forecasting using the technique of sample-

entropy based on the VAN method. Stefánsson (2020) used historical inventory and sensor data to conduct a probabilistic analysis and identify earthquake nucleation. They aimed to find the governing factors of impending earthquakes through nucleation monitoring. They conducted extrapolation to identify the fault size, hypocenter, earthquake impact, and time. They predicted frequent medium-sized events and discussed how significant events could trigger possible events at other locations. Xu et al. (2018) structured a weighted earthquake network using the maximum magnitude and event influence number. They predicted earthquakes by considering the minimum edge weight. Their results showed that the prediction accuracy is improved using the two networks. Asencio-Cortés et al. (2016) explained the use of ensemble learning along with regression algorithms subject to big data context. They used 1 GB catalogue data to predict the magnitude of events within a short period. They reported promising results using Amazon cloud infrastructure, Apache Spark framework, and R language. A recent study by Dias et al. (2019) described the influence of incomplete datasets on earthquake probability assessment based on spatial and temporal distributions. The data were collected from California from 2003 to 2016, with different magnitude thresholds and depths. They implemented nonextensive statistical mechanics and obtained the sequence forms caused by the increase in a jump between events. Martínez-Garzó et al. (2019) conducted a comparative assessment of the mainshocks, foreshocks, and aftershocks in the Sea of Marmara. Cluster statistics was used to identify particular locations where repeated events occur. Susceptibility analysis suggested that the western high region and Cinarcik have high probability where events may trigger. Uchida et al. (2019) identified the repeating earthquake events in the North Anatolian Fault areas. Past repeated events are located near the rupture borders. They observed that the creep rates are similar to relative plate motion, which is approximately 10–20 km depth. Several pieces of work on earthquake

induced landslide susceptibility assessment was proposed by (Aghdam, Varzandeh & Pradhan 2016; Bai et al. 2012; Cao et al. 2019; Pradhan et al. 2014; Tehrany, Pradhan & Jebur 2014; Umar et al. 2014; Youssef, Al-Kathery & Pradhan 2015; Wistuba et al. 2018; Zare et al. 2013).

2.8.2. Vulnerability assessment

The concept of vulnerability is associated with exposure to disaster, which is a prerequisite for risk mapping. Structural design, geological conditions, social behavior, and poverty are found to be the major key factors in understanding earthquake vulnerability assessment (EVA). Social vulnerabilities can be identified by considering gender, age, education level, population, households, and ethnicity (Jena et al. 2019). Zahran et al. (2008) argued on the situations for disaster depending on capacities of personal, socio-economic conditions, and infrastructure. Ruddock (2007) argued that women are disproportionately more vulnerable than men to disasters because of pre-existing norms and practices. Innumerable techniques have been recommended by researchers to assess structural vulnerability on a city scale. Therefore, EVA is crucial in the urban environment (Yakut et al. 2003). Based on predefined relations, some approaches are relevant for a particular study area. In recent years, many studies have been implemented by using observation approach models or vulnerability indices under the Spatial Decision Support Systems framework (Aghataher et al. 2008; Choi, Engel & Farnsworth 2005; Wang, Peng & Wang 2018; Wang et al. 2020). However, to this end, researchers have not paid enough attention to the EVA method implementation in specific areas due to restricted data availability (Rashed & Weeks 2003). The lack of building inventory data and the statistics of destruction experienced due to past earthquakes can be seen in some highly susceptible urban areas. Owing to data limitation and prerequisite

to estimate structural, social, and geotechnical vulnerability, some efficiently applicable approach has been proposed in EVA for urban areas (Rashed & Weeks 2003). In this regard, researchers have implemented AHP and ANP methods using geographical information system and multi-criteria decision-making approach (MCDM) (Alizadeh, Hashim, et al. 2018). Some inherent uncertainties associated with EVA that come through the MCDM approach could substantially influence the results (Jena, Pradhan & Beydoun 2020).

Some works have examined and inscribed the integrated unreliability. For the uncertainty evaluation that is associated with MCDM procedures, fuzzy logic has been applied, which was accepted for the seismic vulnerability assessment (SVA) (Alizadeh et al. 2018). Maps of human loss were prepared for Tehran City using a fuzzy logic approach based on sensitivity analysis. Several studies have used the granular computing technique for SVA in Tehran by applying the derived decision. An ordered weighted averaging operator was applied to assess the vulnerability in Tabriz city (Alizadeh, Alizadeh, et al. 2018). Through these approaches, experts have inscribed all the statistical units of the vulnerability, and they ranked the selected sample units. Alizadeh et al. (2018) performed an urban EVA of Tabriz City by using a hybrid technique of the Analytic Network Process and Artificial Neural Network. Alizadeh, Hashim, et al. (2018) developed a new model for the earthquake urban vulnerability and tested it for the Tabriz City of Iran. They observed reasonably good results due to the use of hybrid ANN and analytic hierarchy process approach. They achieved an accuracy of 90%. Alizadeh et al. (2018) and Panahi, Rezaie & Meshkani (2014) proposed a model for the seismic vulnerability assessment of the urban buildings in Tabriz City of Iran by using the Multi Criteria Decision Making (MCDM) approach. Vulnerability and behavior of residential and industrial buildings

associated with earthquakes are a prime concept in hazard assessment. These considerations have recognized the essential indicators in earthquake hazard estimation and applied various techniques for constructing a seismic hazard map. Recognition and reduction of the earthquake vulnerability of population and buildings with respect to earthquakes are required. The upgradation of buildings against earthquakes is important for the reduction of loss of properties and lives (Mehta & Burrows 2001).

More recently, Zebardast (2013) proposed the hybrid factor analysis approach and analytic network process model for projecting a composite social vulnerability index by aggregating the vulnerability indicators. The main objective in this research was to develop a hybrid FA and ANP (F'ANP) model for the assessment of social vulnerability and to apply in county scale. Gulkan and Sozen (1999) developed a model for seismic vulnerability of concrete and masonry buildings. They explained their methods through the ratios of column and walls using graphical representation. Pay (2001) proposed a novel method for the seismic vulnerability assessment of buildings using the discriminant technique analysis in Turkey. The success rate achieved by Pay was approximately 71.1%. Yakut et al. (2003) proposed another model for the earthquake vulnerability assessment of the reinforced concrete buildings. The method was similar to that of Pay. However, statistical analysis was included in their model. They achieved an accuracy of 80.3% for the highly damaged buildings. Bahadori, Hasheminezhad & Karimi (2017) developed an integrated model best suited for the assessment of seismic vulnerability of buildings in Mahabad City in Iran. The methodology is an integration of five parameters, such as geotechnical, social, seismological, distance to dangerous facilities, and access to vital facilities along with the sub-parameters. Zhang, Xu & Chen (2017) described the construction of an evaluation model for the most significant assessment of social

vulnerability using a rough set up based on catastrophe progression.

Karimzadeh et al. (2017) prepared a Vs30 map by applying an indirect approach using geological and topographical data in Iran. Sarmah & Das (2018) produced a hazard map of a city through vulnerability mapping using hazard microzonation and ward-level hazard maps. Tall buildings and high population density were observed in five out of 31 wards, which were considered the most vulnerable areas and selected in their study. Torres et al. (2019) presented a process for seismic vulnerability assessment that combines aerial images with light detection and ranging (LIDAR) data collected from the Spanish National Plan of Aerial Orthophotography. Their results indicated that machine learning (ML) techniques could exhibit good performance with an accuracy of 77%–80% using SVM classification techniques. Thiri (2017) examined the interconnection between social vulnerability and environmental migration for 30 municipalities caused by the 2011 Japan earthquake. Analysis revealed a 33.3% increase in out-migration is attributed to earthquake events. The evidence of linkage between the indicators of social vulnerability with environmental migration can be observed to understand the natural migration (Martins, e Silva & Cabral 2012). Very limited studies on earthquake vulnerability have been conducted in Banda Aceh City in Indonesia (Johar et al. 2013; Kafle 2006; Culshaw, Duncan & Sutarto 1979).

2.8.3. Risk assessment

Zhihuan & Junjing (1990) applied fuzzy logic in their research on damage and risk assessment. Mili, Hosseini & Izadkhah (2018) proposed a holistic model for earthquake risk assessment and determine the risk reduction and management priorities in urban areas. Chaulagain et al. (2015) presented the estimation of structural vulnerability and

successfully analyzed the risk and the expected economic losses for future earthquakes in Nepal. They used the Open Quake-engine for earthquake hazard and risk in Nepal. Ram and Wang (2013) explained the seismic ground motion that has been estimated by a probabilistic approach in Nepal. They also calculated the PGAs using seismic source information and probabilistic parameters in their study. Khan et al. (2018) estimated the earthquake risk for developing countries using the modern ERA methods in their article. They analyzed Pakistan as a case study. They successfully estimated the earthquake risk using a practical event-based PSHA method. The proposed model is applicable for any earthquake-prone urban areas, and its parameters depend on the local conditions. (Battarra, Balcik & Xu 2018) focused on the prepositioning of emergency supplies during the preparation period. They proposed a new method to calculate the likelihood of events and affected people. (Abdollahzadeh & Faghihmaleki 2017) assessed the risk using a probabilistic approach of engineering structure against earthquake and earthquake-induced natural hazards. They compared the two phase-based risk and revealed the near-field earthquake risk. They observed that the risk of near-field earthquake is higher than that of far-fault earthquake with an extended return period. Schnebele et al. (2019) developed methods to quantify (i) the earthquake hazard and mineral production coincidence and (ii) the annual disruption of mineral supply on the basis of expected annual disruption (EAD) from earthquakes.

Table 2.3: Comparative analysis of strength and limitations of traditional methods.

Criteria	Models	Strength	Limitations
Traditional models	PSHA	Generally used to evaluate the seismic design load for the important engineering structures capability to solve some issues,	Data scarcity, Invalid physical model and mathematical formulation (Scawthorn & Chen 2002),

		Method is innovative, Provides a feasible methodology.	Can't find how crustal properties affect attenuation, Conflicts with seism physics (Mulgaria et al. 2017), Failure of PSHA results (1988 Spitak, Armenia, event and the 2011 Tohoku, Japan, event (Mulgaria et al. 2017)), PSHA is highly limited Poor quantification of uncertainties.
	DSHA	Very easy methodology, Calculations are relatively simple, Can apply to assumed earthquake.	No strong solid physics roots, Low-quality model, Lack of consideration of uncertainties, Highly limited, Poor result (Campbell & Bozorgnia 2003; Shah et al. 2012; Deif et al. 2012).

They calculated EAD based on the production, hazard, and vulnerability of the facility. Chaulagain et al. (2015) presented the structural vulnerability estimation in Nepal and carefully estimated the risk along with the expected losses for future events. They used the OpenQuake Engine for hazard and ERA.

2.9. Strength and limitations of models

Many models have been developed for seismic analysis. Each model has strengths and limitations. All the models are in Table 2.3 and 2.4 and are comparatively analyzed based on their strengths and limitations.

Table 2.4: Comparative analysis of strength and limitations of various GIS-based models/modules/platforms.

Criteria	Models	Strength	Limitations
GIS-based models	GTIS (Geotechnical Information System)	A lot of geotechnical data can be stored and managed, Integrated technology can solve problems in global scale, Convenient and cost-effective, An effective tool to promote accessibility, efficient distribution, Administration and cross-platform flexibility of geotechnical information, Data exchange and improvement is easy	Impossible to manage easily without adopting the facilities in information system (Williams et al. 2002; Chang & King 2005), Some information needs to be stored in images, Scanning of images with resolution, scale inconsistency, file size etc.
	Fault specific seismic hazard model	Can be applied to any seismically active zone (Deligiannakis, Papanikolaou & Roberts 2018) Use to address the problems of the incompleteness of historical records, Method is efficient, Provide very effective result with proper scientific analysis,	May provide uncertainties because of poorly affected parameters, Large dataset needed, Some assumption can be made for the delineation of the database (Benedetti et al. 2003; Ganas, Pavlides & Karastathis 2005; Papanikolaou & Royden 2007; Sakellariou et al. 2007), Error parameters can create a problem (Papanikolaou 2003).
	Intelligent simulation system using Artificial Intelligence	Designed for analysis various kind of data in a quick mode and it is efficient (Tao et al. 1996; Tang & Wen 2009), Useful for post-earthquake analysis, Provides successful results,	Complex coding, Data should be in a specific format,
	Vulnerability mapping using the FEMA-	Provides a complete picture of existing vulnerability, Helpful to relocate the people living in vulnerable buildings	Applicable to a small portion of the study area.

	RVS method	(Rahman, Ansary & Islam 2015), The method is efficient and developed.	
	Integrated model for seismic vulnerability assessment	Significant tool for confronting crisis resulting from future earthquakes, Results have important implications for risk reduction, Can be applied to other countries easily by modifying the parameters, sub-parameters, and their weights (Ilanlu et al. 2013).	A requirement of multiple parameters, Efficiency depends on practicability and applicability parameters (Bahadori, Hasheminezhad & Karimi 2017).
	Soil liquefaction susceptibility analysis	Identified and displayed the susceptible area to liquefaction using the analyzes and the classification techniques of GIS (Subrahmanyan 2001; Mhaske & Choudhury 2010), Updating hazard map, Extend the liquefaction hazard maps to areas that lack geotechnical information using interpolation.	Lack of information can't provide a logical result (Youd et al. 1995; Mhaske & Choudhury 2010).
	Micro-zonation model	Simple methodology, Can handle a large dataset, Can provide four different level of micro-zonation (Pitilakis et al. 2005), Efficient method.	Need large dataset 3rd level of micro-zonation based on complex coding(Louie 2001; Cox et al. 2011).
	Seismic amplification analysis	Easily mapping can be done for susceptible areas, Over a large area in a short duration and are used for performing a reconnaissance study (Theilen-Willige 2010; Sekac et al. 2016), Efficient method.	Accuracy depends on the quality of data and amount of input layers, The weight of layers can choose both manually and decision making methods, Not useful for small areas (Theilen-Willige 2010; Sekac et al. 2016).
	Unified risk assessment	It highlights various modules and their interconnections, Enhance the reliability of the systems and improve mitigation policies (Werner et al. 2000;	Different aspects of uncertainty (Pitilakis et al. 2005), Large dataset needed.

		Pachakis & Kiremidjian 2004), Provides sophisticated assessments, Aiming to create mitigation strategy and minimize losses,	
	A holistic model for risk analysis	Applicable for all seismic prone, Can be used to reduce earthquake damage and casualties (Mili, Hosseini & Izadkhah 2018), Appropriate for estimation of safety level, Applicable for countries with similar conditions.	Parameters should be determined based on local conditions, A need for large dataset.
	Arithmetic and weighted overlay approach to hazard assessments	Can cover a large area, Efficient method, Can apply to low-resolution data (Ahmad et. al. 2017).	A weight of layers can't choose manually, Very poor accuracy, with lack of parameters (Theilen-Willige 2010).
Machine learning	Support vector machine (SVM)	Regularisation parameters, High dimensional input space, Sparse document vectors, Produce excellent results, Produced several successful applications (Ruano et al. 2014), Better at computation speed, It's feasible and efficient.	The time taken for achieving the detection is too large, Can't handle a large dataset (Akhoondzadeh et al. 2018).
	Neural Network (NN)	Perform better than a linear program, It can continue without any problem if any element of it fails, It learns and doesn't need to be programmed again (Sietsma & Dow 1991; Alizadeh et al. 2018), Can be implemented in any application without any problem.	Needs the training to operate, Architecture is different from microprocessors, therefore, needs to be emulated Requires high processing time for the large neural network (Alarifi, Alarifi & Al-Humidan 2012; Alizadeh et al. 2018).
AHP based models		It allows multicriteria decision making, It is applicable when it is formulated criteria evaluations, It allows qualitative evaluation	Hidden assumptions like consistency, Difficult to use when no of criteria is high, Difficult to add a new

		Applicable for group decision-making environment (Saaty 1988, 1990a, 1990b, 2008; Estoque 2012).	criterion or alternative, Difficult to take out existing criteria (Malczewski 1999; Mohanty & Walling 2008).
Remarks: GIS based models and Machine-learning models (Table 4) are better than all the traditional models described above in Table (3), which is concluded based on their strengths and limitations.			

2.10. Data required for the models

Collection of a well-organized dataset is mandatory for earthquake hazard analysis. To improve the understanding of hazard analysis, the data of geology, geomorphology, soil, PGA, earthquake intensity, slope of the study area, digital elevation model, and topography and other factors need to have good quality (Moustafa 2015). Clearly, the completeness of important parameters can improve the accuracy of the resulting model. Therefore, data organization should be reliable and well-collected or digitized with all the effective parameters. The data can be collected from various sources for a relevant analysis.

Bedrock and surficial geological data either collected from field survey or scanned from various maps should be rasterized. The data can be digitized for spatial accuracy via geo-referencing. Images should be geometrically corrected as per the coordinate system WGS84 datum as layers within the GIS system (Moustafa 2015). A valuable database is necessary, wherein points, lines, and polygons correspond to a record in the GIS system. Attributes in GIS include the place name, rock type, rock age, lineament type, and recorded magnitude. Table 2.5 does not explain the minimum requirements for the seismic study, but these are the base data needed for seismic analysis. The completeness of data can enhance the result that can be utilized for correlations and validation.

Table 2.5: Data required for the seismic risk analysis.

Category	Data	Scale	Type
Base data	Digital contour lines Digital elevation model Digital topographic map Air photos Satellite images Quick bird	1:25000	Contour (Segment map) Aster DEM(Raster map) Topo map(Raster map) Landsat (7,8) Raster images
Hazard data	Earthquake catalog Earthquake Intensity map(MMI) Geological map City center Faults and lineament Borehole Locations Landslides Depth to water table Soil or Overburden Thickness Geo soil	1:2000 1:100 000 1:100 000 1:25000	Point map and table Raster map Geological Units(Polygon map) Point map Segment map Point map Segment map Segment map Raster map Polygon map
Elements at risk	Population Land use and land cover Social and structural characteristics Roads Cities Villages	1:2000 1:2000 1:2000 1:25000 1:25000	polygon map polygon map polygon map Segment map polygon map

2.11. Software used for the hazard and risk analysis

We need some software for seismic hazard analysis. We described the software needed for the hazard and risk assessment. In Table 2.6, we discuss some important and most commonly used software and Matlab codes and their applications, along with their developers.

Table 2.6: Applications of various GIS, hazard, and risk software.

Criteria	Softwares	Applications	Developers
GIS software	ArcGIS	Susceptibility and vulnerability analysis for hazard and risk assessment	ESRI, (Geographic information system company)
	QGIS	Susceptibility and vulnerability analysis for hazard and risk assessment	QGIS Development Team
	gVSIG		Development team
	Whitebox GAT		
	SAGA GIS		
	GRASS GIS		
	DIVAGIS		
	ILWIS		
Hazard and risk software	GRAM++	Used for earthquake hazard analysis.	CSRE, IIT Bombay, India
	CU-PSHA	Used to analyze probabilistic earthquake hazards.	MATLAB based software
	OpenSHA	OpenSHA used to develop object-oriented, web- & GUI-enabled, open-source, and freely available code for conducting Seismic Hazard Analyzes (SHA). Applied for earthquake rupture forecast, ground motion and response model	US Department of the Interior
	EZ FRISK FRISK EQRISK	When performing seismic source characterization and the integration methods, the main difference can be found.	(McGuire 1978, 1995)
	SEISRISK II & III Crisis	Applied for seismic hazard and risk analysis, spectral matching and site response analysis, slope stability, liquefaction, site-specific PSHA.	(Bender & Perkins 1987) (Ordaz, Aguilar & Arboleda 2001)
	PRISK	Used for uncertainties	LLNL-NRC

	PSHC	quantification and sensibility analyzes through logic tree methodology	Principia Mathematica Ltd.
	KERFRACT	A program, which assumes a fractal geometry for the seismicity that, is represented by Kernel statistics.	Woo, G., (1996)
	SAFER Risk-UE KOERILOSS DBELA	Used for seismic risk estimation.	KOERI, (2002) developed the KOERILOSS.
	Open quake	An open source software used for hazard and risk modeling	GEM team

2.12. Current challenges in earthquake research

1. Implementation of a suitable comprehensive methodology remains difficult for many developing countries.
2. Few integrated GIS techniques with historical earthquake catalogue in underdeveloped countries have been used.
3. Understanding of the fault geometry by using the current knowledge of ongoing research is essential and difficult.
4. Fault mechanism study from fault data to understand the complex mechanism of fault movement is the main issue in current times.
5. Most of the developed models are data dependent. Very few bespoke model development study has been conducted on earthquake study.
6. The collection of complete data is another issue in solving the major seismic hazard and risks problems in local areas.

2.13. Summary

Collecting and integrating various data from different sources for creating an effective scenario for hazard and risk assessment is not highly feasible, but the availability of some free data can fulfill some requirements. Evaluation and analysis of seismic hazard and

risk to lifelines have been serious and sensitive issues as of current time. Today many well-established models have been developed that can be used for the seismic hazard, risk assessment, and damage estimation. Seismic analysis creates several steps towards urban development. Moreover, several proposed approaches are discussed in this review for hazard, vulnerability and risk assessment, and loss estimation for lifelines. In this study, we found that the attention of most researchers is towards the robust models to reduce limitations.

1. All the models were applied for different environments using various data, and the paper gathered valuable conclusions, as follows;
2. The capabilities of GIS-based and data mining approaches are more efficient than those of traditional models, as described and analyzed in (Table 2.3 and 2.4).
3. A high seismicity concentration increases the chance of risk, depending on several factors.
4. The suitability of a model for hazard and risk assessment depends on various factors, such as data, source, parameters, and expected results.
5. Poor performance of models depends on the framework of methodology and quality of data and computational requirements as described in the limitations of various models.
6. Modification of models regularly enhances the state of the research.
7. More research is needed to establish comprehensive models with accuracy.
8. More models for seismic hazard and risk assessment will provide more options to the research community.

Using a decision-making process, the weight value for different factors can be established to derive accurate results. The development of research on various models and technology leads to more efficient and holistic mitigation strategies. Therefore, this review describes

the traditional seismic hazard models and GIS-based models for the hazard and risk analysis, and introduces some early and recently developed methodologies. Therefore, research on various proposed approaches are relatively growing with an advanced methodology for hazard, risk analysis, and mitigation plans. Introducing some novel models regarding seismic hazard analysis is important.

One of the major findings of this review is that seismic analysis creates several steps to enrich research and establish new ideal models. In seismic analysis, every field of hazard, risk, and loss estimation should be considered as important. This study can provide knowledge for the future research and development. In general, there are many more GIS-based models developed for qualitative and quantitative seismic hazard and risk assessment. There are many traditional models, which are not realistic but still used for seismic analysis (Mulargia, Stark & Geller 2017). Therefore, researchers must be concerned about their own models, which should be accurate and useful in society. First, researchers should prepare realistic and comprehensive models for the accurate results. Second, we need to acknowledge that "prediction of earthquake" is possible but might not be highly accurate. Therefore, disaster risk analysis and reduction are more important than prediction. Fault mechanism analysis using various methods are needed to understand the complexity of earth's internal mechanism, and it might help risk reduction. A new state-of-the art models will be helpful for model developers, seismic researchers, scientists, academicians, and research scholars to understand the models and applications. The most accurate analysis needs to be presented to the public to be prepared for future earthquakes.

CHAPTER 3

MATERIALS AND METHODOLOGY

3.1. Introduction

This chapter illustrates several methods applied in this study. Overall methodology, implementation of the detailed methodology and performance evaluation are described. Location and study area characteristics are reported. The data and materials used have been described in detail. Conditioning factors of probability and vulnerability factors and hazard factors are presented. An integrated AHP-VIKOR (Analytical Hierarchy Process-VIseKriterijumska Optimizacija I Kompromisno Resenje) model was introduced to demonstrate earthquake vulnerable areas on a city scale. An integrated ANN-AHP (Artificial Neural Network-Analytical Hierarchy Process) model was developed for earthquake risk mapping and the population under risk associated with them has been explored. An integrated ANN-CV and AHP-TOPSIS (Analytical Hierarchy Process- The Technique for Order of Preference by Similarity to Ideal Solution) raster modeling was conducted using geostatistical techniques to improve the spatial risk mapping with better accuracy. Software used for the implementation of different models were also described. The chosen areas for spatial risk mapping as case studies are Banda Aceh and Palu city in Indonesia. Several mitigation processes are suggested in this chapter by analyzing the results.

3.2. Multi-criteria decision-making model

Multi-criteria decision-making is a potential tool that analyzes real complex problems to judge different alternatives on the basis of some aspects for a suitable alternative selection (Armaş 2012; Malczewski & Liu 2014). MCDM allows storing, modifying, analyzing,

and visualizing data for decision-makers, whereas GIS provides a platform to analyze and realize the desirability of alternatives (Sánchez-Lozano et al. 2013). To understand the desirability relationships, an expert's opinion is obligatory. In general, uncertainty can be found among experts' opinion in decision-making problems (Jankowski & Nyerges 2001; Ouma & Tateishi 2014; Meng & Malczewski 2015). The MCDM approaches were implemented in this research such as AHP, VIKOR, and TOPSIS for the vulnerability assessment.

3.2.1. Integrated AHP-VIKOR approach

In this research, the MCDM approaches, such as AHP and VIKOR methods, were applied to solve the current problem (Saaty 2008). AHP is the most used decision-making method in both academia and industries (Liu et al. 2008). Assessors believe in the results obtained by AHP than other decision-making methods on estimating the priority. VIKOR method is something, which is applied in other studies but not in earthquake research (Mardani et al. 2016). This research applied VIKOR to evaluate the ranking and weights of social, structural, and geotechnical vulnerability layers as very fewer studies have been conducted and limited experts opinion on ranking and prioritizing of all the described layers (Shaw et al. 2006). AHP and VIKOR methods were integrated to develop a new MCDM model for earthquake vulnerability assessment. The details of the new integrated model is presented below.

3.2.1.1. AHP approach

AHP can be used in developing a robust method like MCDM approaches that consider a selection of the best suitable alternatives for specific problems (Figure 15) (Ouma & Tateishi 2014). Owing to its user-friendliness, AHP is a popular approach among spatial

scientists (Nyimbili, Erden & Karaman 2018). AHP can be applied to manage complex problems. Sensitivity analyzes need to be applied to explore the changing effect of the priority of several indicators on different alternative ranking systems (Panahi, Rezaie & Meshkani 2014).

Steps involved in the application of the AHP method in spatial decision-making are:

Step 1: Criteria score calculation. To obtain the scores, a pair-wise comparison should be performed in which each alternative can be compared with a specific criterion (x1,. . .xn) of alternatives. The eigenvectors can be calculated once the normalizing process of judgmental matrices is completed (Panahi, Rezaie & Meshkani 2014).

Step 2: Criteria weights estimation. Saaty (2008) described the use of the lambda max technique to calculate the weights through pair-wise comparison. A comparison between alternatives and criterion should be in a pair-wise manner to calculate weights (wi. . .wn). For each matrix, there is a set of eigenvalues and the corresponding eigenvector can be found for every eigenvalue. In Saaty's technique of lambda max, a normalized eigenvector is the vector of weights where the largest Eigenvalue is λ max.

Step 3: Priorities and consistency estimation. Once the matrix through criteria comparisons is developed according to the goal, the priorities and consistency of criteria and judgments can be determined, respectively. Saaty (1990) also introduced the scale for the pair-wise comparison, which is presented in Table 4.7. The priorities could be calculated through eigenvector *w* of matrix A using equation 3.1.

$$\mathrm{AW} = \lambda_{max}\omega\,. \tag{3.1}$$

Once the vector normalization is obtained, the vector of priorities of the criteria resulted according to the goal. However, λ_{max} is the largest eigenvalue of the obtained matrix A, and *w* is the corresponding eigenvector that only considers positive values. The consistency ratio can provide the consistency of the judgmental matrix which is defined

as:

$$CR = CI/RI\ , \tag{3.2}$$

where RI is known as a random index and CI is the consistency index that provides a value of deviation from consistency. Therefore, consistency index can be calculated as:

$$C\ I = (\lambda_{max} - n)n - 1, \tag{3.3}$$

where the largest eigenvalue is λ_{max} of matrix A, and n is the criteria number. If the matrix has a high CR value, it indicates that the judgmental inputs are not well approved and not reliable. However, a 0.10 or less CR value is acceptable. If CR crosses 0.1 toward high values, then the judgments are not reliable and again need to be elicited.

In this study, the AHP technique was adopted to assess earthquake vulnerability using spatial information for Banda Aceh City. The weight results computed are considered satisfactory if the obtained consistency ratio values are reasonable. Figure 2 shows the methodology adopted in this research. The individual weighted pixels in the vulnerability map were calculated using Equation 4:

$$Wi = \sum j X_{ij} W_j, \tag{3.4}$$

where terms X_{ij} shows the rank of the *i*th class on the basis of *j*th layer. W_j is the normalized weight for *j*th layer. By increasing the normalized weighted, the absolute weight can be achieved for each layer in a consistent rank.

3.2.1.2. VIKOR method

The VIKOR approach was first proposed as one pertinent technique to be executed within MCDM problems and as a multi-attribute decision-making approach (Shen & Wang 2018). This method emphasizes ranking and alternatives selection and regulates the compromise solution for conflicting criteria that can assist decision-makers to achieve an ultimate solution (Shen & Wang 2018; Wang et al. 2018; San Cristóbal 2011). The multi-

criteria approach for ranking evolved from the aggregating function of LP-metric used through a compromise programming method (Baja, Chapman & Dragovich 2007). The detailed steps of the VIKOR method are described by Mardani et al. (2016).

Step 1: Calculation of X_i^* and $\overline{Xi}$.

$$X_i^* = max\left[(X_{ij})|j = 1,2,\ldots.m\right]. \tag{3.5}$$

$$\overline{Xi} = min\left[(X_{ij})|j = 1,2,\ldots.m\right]. \tag{3.6}$$

Here, X_i^* and $\overline{Xi}$ are the maximum and minimum value of X_{ij}. X_{ij} is the matrix value and X_i is the alternative of *i*th criterion function.

Step 2: Calculation of the Sj and Rj values.

$$S_j = \sum_{i=1}^{n} W_i \frac{X_i^* - X_{ij}}{X_i^* - \overline{Xi}}. \tag{3.7}$$

$$Rj = Max\left[W_i\left(\frac{X_i^* - X_{ij}}{\overline{Xi} - X_{ij}}\right)\right]. \tag{3.8}$$

And i =1, 2,….n

Here, S_j and R_j represent the utility measure and regret the measure for $X_j$as an alternative. Moreover, W_i is the assigned criterion weight.

Step 3: Estimation of S^* and R^*.

$$S^* = min(S_j), \bar{S} = max(S_j),\ \ J = 1,2,\ldots.m. \tag{3.9}$$

$$R^* = min(R_j), \bar{R} = max(R_j),\ \ J = 1,2,\ldots.m. \tag{3.10}$$

Here, S^* represents the minimum of utility measure while $R^*$is the minimum of regret measure. Accordingly, $\bar{S}$ and $\bar{R}$ are the maximum value of utility and regret measure.

Step 4: Estimation of the value of Q_j for j =1, 2…., m, and using the Q_j values, alternatives can be ranked.

$$Q_j = v\left(\frac{S_j - S^*}{\bar{S} - S^*}\right) + (1 - v)\left(\frac{R_j - R^*}{\bar{R} - R^*}\right), \tag{3.11}$$

where *v* is the strategy weight of maximum group utility and the individual regret weight

is $1 - v$. In general, v=0.5, but if v>0.5, then rank can be expressed as Q_j index that will tend toward majority agreement. However, when v<0.5, the Q_j index will indicate the majority negative attitude.

VIKOR is a powerful tool for solving multi-criteria problems, specifically in a condition where the decision-maker is unable or unaware of the system design at the beginning. It provides a maximum "group utility" and a minimum of the "individual regret" (represented by min *S* and *R*, respectively) of the "opponent" (Mardani et al. 2016).

3.2.1.3. Integration of AHP-VIKOR

Here, once the Q_j value achieved, the ranks could be calculated. The lowest Q_j value will have the highest rank while the highest Q_j value will have the lowest rank. Then the final weights W_f of all the layers can be calculated by using the developed formula;

$$W_f = \frac{Q_j}{\sum_{j=1}^{n} Q_j}. \tag{3.12}$$

Where in W_f for f =1, 2…., n and the ranks of the weights could be calculated. Here, the ranks of the weights can be estimated based on the AHP approach. The highest weight will achieve highest rank while the lowest weight will achieve lowest rank.

In the next step, the interchanging of the weights based on the Q_j rank will be conducted. Here, the highest Q_j rank will achieve lowest weight (L_w) while the lowest rank will achieve highest weight (H_w).

Finally, the normalization of weights will be conducted. In this process, all the weight values will be considered up to two levels after the decimal point. Then the lowest weight L_w can be achieved using the formula written below.

$$L_w = 1 - \sum W_f. \tag{3.13}$$

The details of implementation was described in the implementation of methodology

section in “3.7.1 Objective 1”.

3.3. Hybrid AHP-TOPSIS model

Based on the experts' opinion and literature review criteria and alternatives could be considered to formulate the AHP-TOPSIS model (Nyimbili, Erden & Karaman 2018). AHP approach was implemented to make a pair-wise comparison matrix and to obtain the priority weights for criteria. The reliability of this matrix can be understood by using important consistency measures such as maximum eigenvalue, consistency index, and consistency ratio. After the confirmation of the consistency of the matrix through the computed consistency ratio, using the Saaty’s rule weights could be applied in TOPSIS to make a hybrid approach. For the alternatives assessment, the TOPSIS approach was used as a reliable MCDM approach. A decision matrix for alternatives need to be developed with respect to criteria and then normalized decision matrix is determined. Accordingly, a weighted normalized decision matrix could be calculated to obtain the final ranks of alternatives. The details of AHP and TOPSIS algorithms were presented below with the flowchart presenting the hybrid relationship (Figure 3.1).

3.3.1. AHP algorithm

AHP is a well-established multicriteria decision-making (MCDM) approach developed by (Satty, 1990). It deals with the measurement of intangible and quantifiable criteria and has been applied to various fields, such as conflict resolution and decision making. The procedure of AHP is described as follows:

In the first step, a pairwise comparison matrix need to be constructed for the criteria with scale 1 to 9, as directed by Saaty (2008). The criteria can be presented by 1 when they have the same priority, providing a square matrix where Criteria =N and matrix is A_{NXN}.

a_{ij} represents the relative importance of I concerning to j. Normalized weight can be obtained in a comparison matrix by applying the geometric mean of rows. GM_j can be presented as:

$$GM_j = \left[\prod_{j=1}^{n} a_{ij}\right]^{1/N} \text{and} \quad W_j = \frac{GM_j}{\sum_{j=1}^{N} GM_j}. \tag{3.14}$$

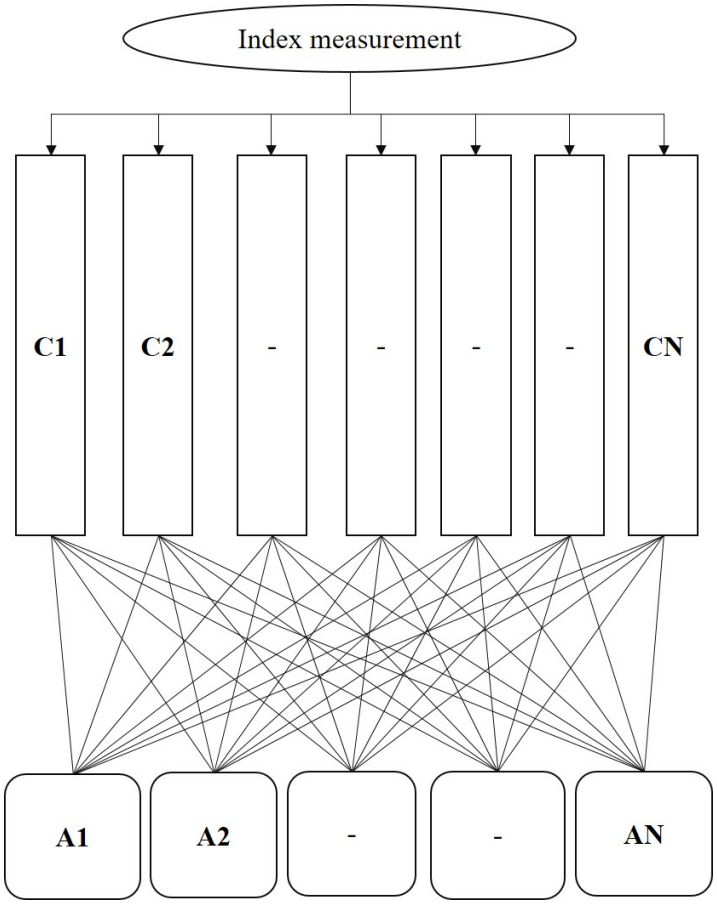

Figure 3.1: Architecture of hybrid AHP-TOPSIS approach.

Matrices A3 and A4 are calculated as:

$$A3 = A1 * A2 \; and \; A4 = A3/A2, \tag{3.15}$$

where

$$A2 = [W1, W2 \ldots, WJ]^T, \tag{3.16}$$

The maximum Eigenvalue can be calculated by averaging matrix A4.

Therefore, the consistency index can be calculated as:

$$\mathrm{CI} = (\lambda \max - \mathrm{n})/(n-1). \tag{3.17}$$

Accurate results can be indicated by lower C.I. value that shows a smaller deviation from the consistency level.

The consistency ratio can be determined as:

$$\mathrm{CR} = \frac{CI}{RI}. \tag{3.18}$$

In a pairwise comparison, the value CR ≤ 0.1 is acceptable according to (Satty, 2008). Here, RI represents the random index associated with the matrix size. The RI value is suggested as 1.41 for the matrix size of 8.

3.3.2. TOPSIS algorithm

TOPSIS belongs to the MCDM models used for ranking the alternatives in several applications. In general, this model could be performed in seven steps (García-Cascales & Lamata 2012).

Step 1: Develop a decision matrix.

Criteria weights were calculated using the abovementioned AHP approach, and a decision matrix was constructed (García-Cascales & Lamata 2012).

Step 2: Normalized decision matrix construction.

Two attributes, such as cost and benefit attributes, are involved in the MCDM problem. Normalization is needed to transform attribute unit dimensions into non-dimensional attributes, and internal comparisons are conducted using a standardized equation (Cheng et al. 2006). The frequently used method for normalization is described below.

$$R = \left(R_{ij}\right)_{m\times n} = \begin{matrix} A1 \\ A2 \\ \cdot \\ \cdot \\ A_m \end{matrix} \begin{pmatrix} u_1 \ldots\ldots u_2 \ldots\ldots u_n \\ u_{11} \ldots\ldots u_{12} \ldots\ldots u_{1n} \\ u_{21} \ldots\ldots u_{22} \ldots\ldots u_{2n} \\ \vdots \qquad\qquad \vdots \qquad\qquad \vdots \\ r_{m1} \ldots\ldots r_{m2} \ldots r_{mn} \end{pmatrix}, \tag{3.19}$$

where R_{ij} is the normalized value, attribute value x_{ij}, and matrix $X = (X_{ij})\ m \times n$

$$r_{ij} = x_{ij}/\sqrt{\sum_{i=1}^{m}(x_{ij})^2}. \tag{3.20}$$

For benefit attribute $x_{ij}, i \in M, j \in N$

$$r_{ij} = 1 - (x_{ij}/\sqrt{\sum_{i=1}^{m}(x_{ij})^2}\,). \tag{3.21}$$

For cost attribute $x_{ij}, i \in M, j \in N$.

All the GIS-based layers, including building density, building surface area, building quality, building heights, proximity to the road, building types, proximity to buildings, household density, and population density, were transformed into non-dimensional attributes using Eqs. 18 and 19.

Step 3: Construction of the weighted normalized decision matrix.

Here, the weighted normalized value v_{ij} is estimated as:

$$v_{ij} = w_{j\times} r_{ij}, \tag{3.22}$$

where w_j is the normalized decision matrix, and $w_j = w_{j/\sum_{j=1}^{n} w_j}$. Thus, $\sum_{j=1}^{n} w_j = 1$, where W_j is the assigned original weight, r_{ij} is the normalized weight, $i = 1, \ldots, m; j = 1, \ldots, n$, and n and m are the number of criteria and number of attributes, respectively.

Step 4: Determination of positive and negative ideal solutions.

The cost criteria minimized by positive ideal solutions maximize the benefit criteria, whereas the cost criteria maximized by negative ideal solutions minimize the benefit criteria.

Positive and negative ideal solutions can be expressed as:

$$A^+ = [v^+, \ldots, v^+, \ldots, v_n{}^+]. \tag{3.23}$$

$$A^- = [v^-, \ldots, v^-, \ldots, v_n^-]. \quad (3.24)$$

Therefore,

$$\begin{cases} v_j^+ = \max\limits_i \{v_{ij}\}\, i = 1, 2, \ldots, m \\ v_j^- = \min\limits_i \{v_{ij}\}\, i = 1, 2, \ldots, m \end{cases}, \quad \text{If the jth criterion is a beneficial criterion} \quad (3.25)$$

$$\begin{cases} v_j^+ = \min\limits_i \{v_{ij}\}\, i = 1, 2, \ldots, m \\ v_j^- = \min\limits_i \{v_{ij}\}\, i = 1, 2, \ldots, m \end{cases}, \quad \text{If the jth criterion is a cost criterion} \quad (3.26)$$

where v_{ij} indicates the cell attribute values for the jth layer.

Step 5: Estimation of the alternative separation from the positive and negative ideal solutions.

In this step, the separation of each alternative was calculated, and GIS layers, such as S + i and S – I, were created.

The equations for each alternative can be expressed as:

$$S_i^+ = \sum_{j=1}^n \left| v_{ij} - v_j^+ \right| = \sum_{j=1}^n D_{ij}^+, \quad (3.27)$$

$$S_i^- = \sum_{j=1}^n \left| v_{ij} - v_j^- \right| = \sum_{j=1}^n D_{ij}^-, \quad (3.28)$$

Step 6: Relative closeness calculation to the positive ideal solution

The relative closeness for an ith alternative based on the positive ideal solution is given as:

$$C_i^- = \frac{(S_i^-)}{(S_i^+ + S_i^-)}, \quad (3.29)$$

where $0 \leq C + i \leq 1, i = 1, 2, \ldots, m.$

Step 7: Alternative rank determination based on relative closeness.

"The relative closeness to the positive ideal solution" layer was created. The set of sites was observed to rank the value of C + i in descending order of. The higher the C + i value is, the best the sites will be. They are preferable and must be chosen when they are close

to the positive ideal solution.

3.4 ANN architecture

The ANN architecture imitates the performance of the human brain interconnected by many nodes, as presented in Figure 16 (Ghorbanzadeh et al. 2018; Bui et al., 2016). The ANN model operates in two parts, namely, learning the information and knowledge through training, and storing the synaptic info weights (Haykin 2009). A connection is found between weighted interconnections and interconnected neural networks (Figure 3.2). An ANN can discover multiple nonlinear issues, such as predictions and probability analysis, and find the patterns between the indicators and responses. Various neural network architectures were proposed for several purposes. We applied the multilayer perceptron (MLP) architecture (for prediction classification) and backpropagation algorithm (to optimize parameters and update weights) in the current study for probability assessment. Neurons within the same hidden layer are connected to the neurons of the next layer rather than interconnected. Given that the number and size of hidden layers can be changed based on the requirements, some fixed values for the specific application are obtained (Safi & Bouroumi 2013).

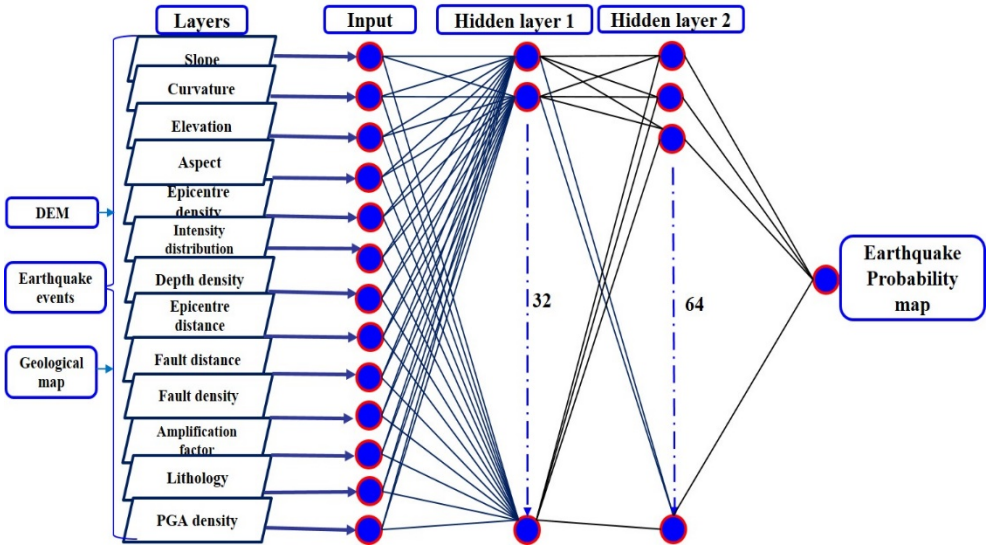

Figure 3.2: **Network architecture for probability assessment.**

Randomly chosen weightings of input nodes are updated based on backpropagation to minimize the errors (Paola & Schowengerdt 1995; Park et al. 2013).

MLP and backpropagation learning:

The used data are composed of $N_v$training patterns $(X_{p,}T_p)$, where p can be considered as the pattern number (Haykin 2009). For the absence of difficulty of analysis and notation, an augmented vector $X_p(N+1)$ that can handle the threshold on hidden and output units are assigned. Therefore, X_p is consistent with the input vector of N-dimension of the Pth training pattern, whereas Y_p is consistent with the output vector of M-dimension for the Pth pattern from the training pattern (Haykin 2009). The details of MLP algorithms can be found in (Haykin 2009; Nazzal, El-Emary & Najim 2008; Park et al. 2015). The output and input units have rectified linear unit activations. Jth hidden unit input, netP (j) can be presented as:

$$net_p(j) = \sum_{k=1}^{n+1} W_{hi}(j,k)X_p(K) \quad 1 \le j \le N_h. \tag{3.30}$$

For the Pth training pattern, the output activation can be presented as Op (j), which is expressed as:

$$O_p(j) = f\left(net_p\,(j)\right). \tag{3.31}$$

The chosen sigmoid function is typically a nonlinear activation, which can be expressed as:

$$f\left(net_p\,(j)\right) = \frac{1}{1+e^{-net_p\,(j)}}, \tag{3.32}$$

where K is the index, which represents input N, and W_{hi} (J, K) represents the connecting weight to the K*th* input unit to J*th* hidden unit. The performance of the MLP was measured

based on root-mean-square-error.

MSE can be represented as:

$$E = 1/N \sum_{p=1}^{Nv} E_p = 1/N \sum_{p=1}^{Nv} \sum_{i=1}^{M} \left[T_P(i) - Y_p(i)\right]^2, \quad (3.33)$$

and

$$E_p = \sum_{i=0}^{M} \left[T_P(i) - Y_p(i)\right]^2, \quad (3.34)$$

where E_p is the Pth pattern error, and T_p is the required output for the Pth pattern. The mapping error calculation for the ith output unit can be represented as:

$$E_i = 1/N_v \sum_{p=1}^{M} \left[T_P(i) - Y_p(i)\right]^2. \quad (3.35)$$

The Pth training pattern with the ith output can be written as;

$$Y_p(i) = \sum_{k=1}^{N+1} W_{0i}(i,k) X_p(k) + \sum_{j=1}^{N_h} W_{0i}(i,k).\, O_p(j), \quad (3.36)$$

Where $W_{0i}\ (i,k)$ explains the input nodes' weight to the output nodes, and $W_{0i}\ (i,k)$can be considered as the weights of the hidden nodes to the output nodes.

3.5. PGA, source to site distance and intensity calculation

Historical earthquake catalogue was implemented to estimate PGA along with the actual distance from the epicenter to the proposed study area, the intensity variation, magnitude, and tectonic sources. Several attenuation equations proposed in the current methodology, however, this study inclusively used the equation developed by (Joyner & Boore 1981). For PGA calculations, the distance (D) should be estimated using the degree to km calculation. Therefore, D value can be estimated by the formula;

$$\mathrm{D} = \ (E\text{^}2 + 7.3\text{^}2)\ \text{^}0.5. \quad (3.37)$$

Where E = Epicentral distance

According to Joyner & Boore (1981) the PGA can be calculated as,

$$10\text{^}(0.249 * M - \mathrm{Log}(D) - 0.00255 * D - 1.02,\ \mathrm{D} = (\mathrm{E}\text{^}2 + 7.3\text{^}2)\text{^}0.5 \quad (3.38)$$

Similarly, according to Campbell (1981),

$$0.0185 * \mathrm{EXP}(1.28 * \mathrm{M}) * \mathrm{D}\hat{}(-1.75), \mathrm{D} = E + 0.147 * \mathrm{EXP}(0.732 * M) \quad (3.39)$$

And according to Fukushima & Tanaka (1990),

$$(10\hat{}(0.41 * M - \mathrm{LOG10}(R + 0.032 * 10\hat{}(0.41 * M)) - 0.0034 * R + 1.30))/980 \quad (3.40)$$

Several authors developed many attenuation relationships, which have been implemented in several probabilistic earthquake hazard analysis research (Boore and Joyner 1982; Campbell 1985; Fukushima and Tanaka 1990). Out of them, the general equation of regression by Boore and Joyner (1982) is most popular and applied in several regional and worldwide datasets. Therefore, MMI (Modified Mercalli Intensity) could be calculated by implementing the formula,

$$MMI = 1/0.3 * (log10\ (PGA * 980) - 0.014 \quad (3.41)$$

Where the PGA unit is G (Gal).

It is feasible to understand the resulted MMI and applied in GIS to generate thematic layer as well as several other layers from the same dataset. Firstly, the detailed investigation of various attributes of earthquakes is the requirement to start the process. Secondly, PGA and MMI were estimated using the attenuation laws and implemented in all three objectives. PGA density map and Intensity variation layers were implemented in earthquake probability mapping and hazard estimation. Several lithological units were extracted from the geological map and assigned amplification factor values to each unit to generate another thematic layer.

3.6. Overall methodology of the proposed research

The overall methodological flowchart is presented in Figure 3.3 that briefly describes

three objectives: Earthquake vulnerability assessment using an integrated AHP-VIKOR approach, earthquake risk assessment using integrated ANN-AHP model, and the spatial improvement of earthquake risk using developed ANN-CV-AHP-TOPSIS model. All the objectives used integrated models that provide a novel combination of python developed models with MCDM models for better earthquake risk assessment with good accuracy.

In the first stage, all the vulnerability layers were prepared using the raster and vectors data collected from Indonesia. AHP and VIKOR methods were integrated to make a new approach to implement in the field of earthquake for the first time to generate an earthquake risk map. The second stage dealt with the pre-processing of the input data, model development, processing, and then post-processing integrated with MCDM results. The inventory data was preprocessed subjected to removing missing values and modifying the data points, creating a geospatial database, georeferencing (placing a digital photo in real world scenario), converting the data into a single format. The projection system of UTM WGS84 was applied to DEM, inventories, and the GIS database. ANN model was implemented for the probability assessment. Several conditioning factors were applied to map the probabilities. AHP was implemented for vulnerability assessment using several factors and the risk was calculated for the Banda Aceh city. The population under risk was estimated.

The third stage deals with the improvement of the proposed method in the second objective, which consists of ANN-CV and hybrid AHP-TOPSIS models. The proposed model is developed to estimate the population at risk at Banda Aceh city with better accuracy than the integrated ANN-AHP model.

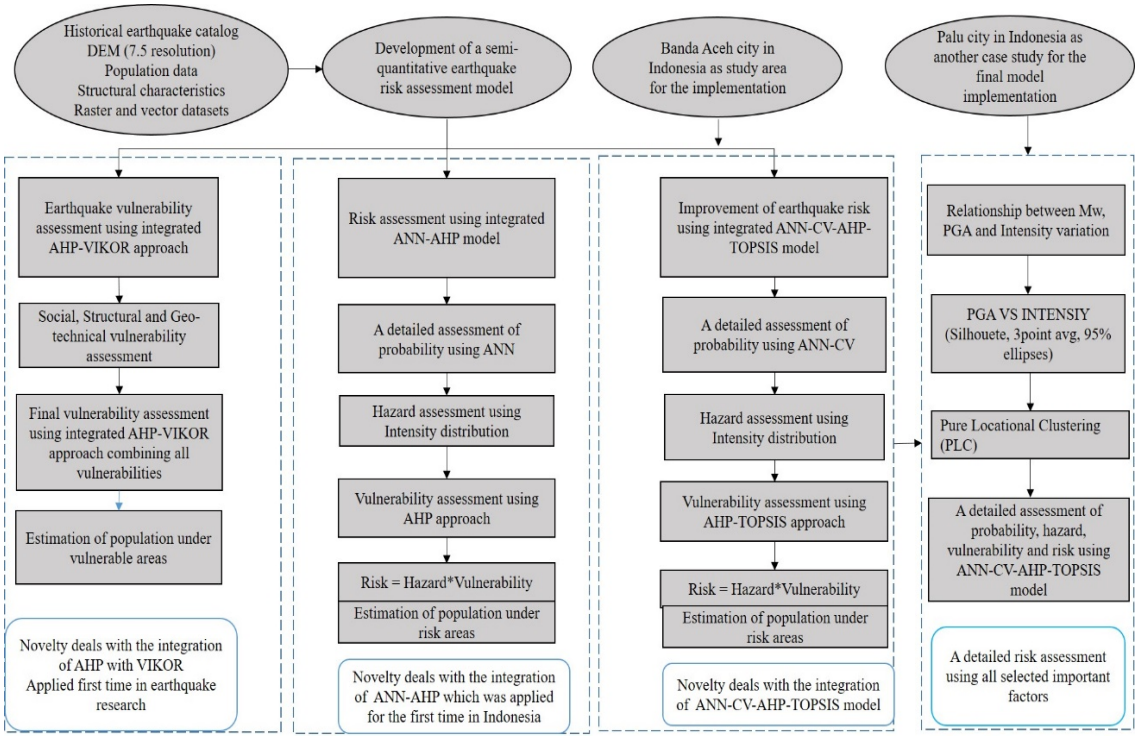

Figure 3.3: Overall methodological flowchart for earthquake risk assessment.

The factors used here were considered based on the accuracy of the results and error and trial method. The ANN-CV model was trained and tested four times by randomly selecting the data points derived from all raster layers. The cross-validation approach describes the accuracy of the result in each test. The hyperparameters of the model were chosen via iterative search and previously developed models for earthquakes or any other natural hazards. The proposed ANN-CV model was implemented to generate an earthquake probability map. A hazard map was developed in the next stage by using the probability and the intensity variation. Then the hybrid AHP-TOPSIS model was applied to produce earthquake vulnerability. The chosen layers for the vulnerability assessment fully focused on social and structural characteristics. However, very carefully all the vulnerable layers were chosen to develop a vulnerability map with better accuracy than the previous study. Finally, the risk was calculated by using both hazard and vulnerability

results. In the fourth stage, another case study was conducted using the same ANN-CV-AHP-TOPSIS model with the additional Silhouette clustering, Pure Locational Clustering (PLC) approach, and dendrogram to understand the locations prone to earthquakes. Consistency ratio, Receiver Operating Characteristics curves, Cross-validation, and overall accuracy were used to obtain the best model. The details of the implementation of all the three objectives were described below.

3.7. Implementation of the methodology

3.7.1. Objective 1

In the current study, a multi-criteria evaluation model is developed by using the integrated approach of the AHP and the VIKOR method (Figure 3.4). First, 20 criteria are selected to produce three different vulnerability indices. Cultural beliefs, Population, Poverty, Livelihoods, Gender, Equity, Social groups are the major factors of vulnerability estimation. However, all the described factors are not always needed for all-natural hazards vulnerability or risk estimation. This study classified the factors into three vulnerability types based on the requirements of earthquake vulnerability assessment (Alizadeh et al., 2018; Jena et al. 2019). Therefore, several other factors are chosen based on the different vulnerability categories to achieve the total vulnerability for Banda Aceh focusing on the location, active tectonics, population, building, etc. Then by using the expert's opinion, this work produced the geotechnical, structural, and social vulnerability maps against earthquakes by using the AHP approach. Based on the relative importance according to Satty's intensity scale, two criteria are evaluated in a pairwise comparison. In general, Index values ranging from 1 to 9 were applied. If the criteria have exactly equal importance then the pair receives a value of 1. If one criterion has the highest importance than the other then the value will be 9. All criteria will be graded in a possible

way with values between 1 to 9. Criteria standardization is the major issue for decision-making models. For standardization, the classification of the map is the simplest way. Therefore, the layers were classified as suitable conditions (2 classes), unsuitable domains (2 classes), and medium domain (1 class). The scaling code of 1 to 5 was implemented for social, structural, and geotechnical layers on the basis of strength and value of the structure. Then, the VIKOR approach is employed as described in section 3.2.1.2 to produce the final vulnerability map by ranking the three vulnerability layers. VIKOR is then applied to determine the degree of vulnerability for area and population in Banda Aceh City. Weighted sum technique was applied to all the layers with weight values and rank. Finally, the total vulnerability was estimated.

The digital environment of GIS was involved to predict the final vulnerability map by using all the three vulnerable layers. The final vulnerability map was then classified into five classes, such as very high, high, moderate, low, and very low. No specific research available on the total vulnerability mapping using all the three described layers in earthquake vulnerability mapping that can help in ranking the layers and calculating the weights. Therefore, this method is not exactly a hybrid method but an integration of AHP and VIKOR, where the results of AHP were applied to produce the final map using VIKOR. Here, we can write it as,

Final vulnerability = Weighted sum (Layers resulted by AHP)

$$V = \sum_{i=1}^{n} L(AHP) \tag{3.42}$$

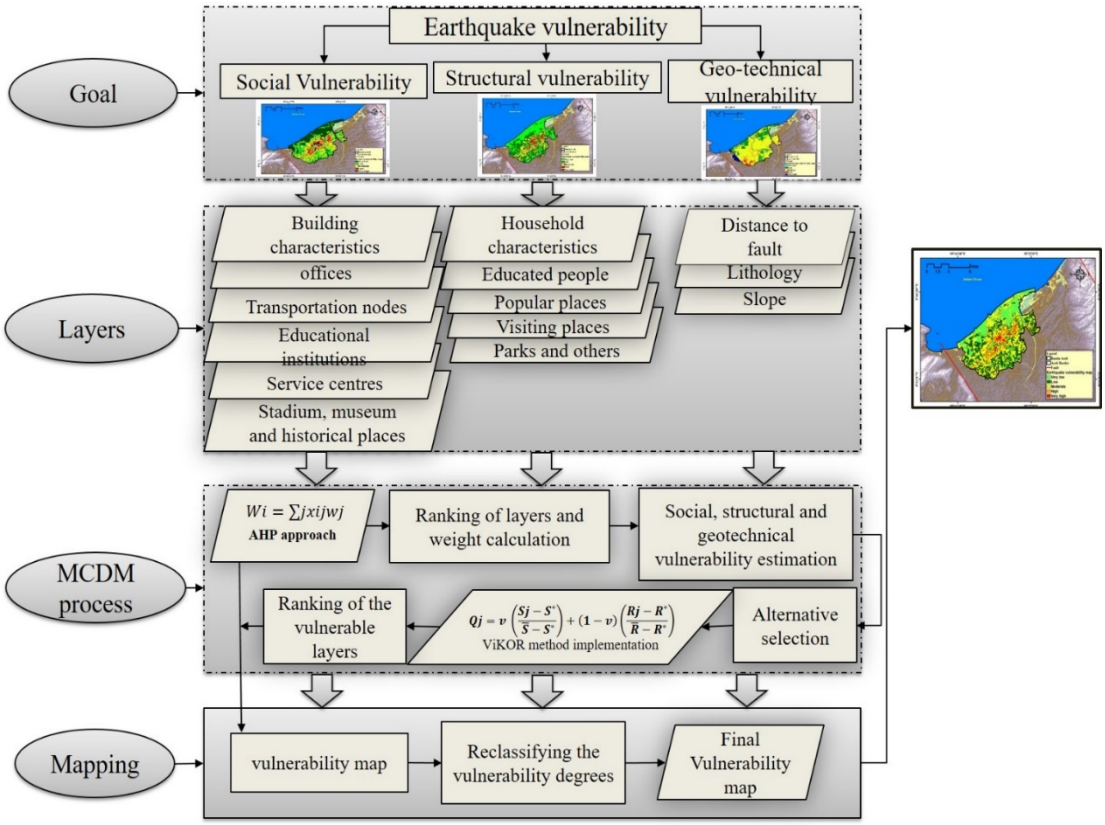

Figure 3.4: Methodological flowchart of the MCDM model for objective 1.

Where, V is considered as final vulnerability, $L(AHP)$ is the layers obtained by AHP. Rank and weights of layers were obtained by VIKOR method and i is the number of layers up to n.

3.7.2. Objective 2

In this current analysis, an ANN–AHP model was developed, implemented and presented in Figure 3.5. A feed-forward ANN with a three-layered structure was applied, and we trained the large area of Aceh province with a set of earthquake data points and an applied backpropagation algorithm for root mean square error calculation. Feed-forward ANN clearly describes the interconnection between the neurons in different layers. Then, the

small area of Banda Aceh was applied to test and to map the probability. First, the input data layers were converted into multiple data point values. In the first step, the model was loaded by some external libraries to conduct modeling; these libraries include operation systems, data management, numerical analysis, and neural network. Next step was performed to measure the error rate of a model and for plotting purposes. In the next step, a neural network was built using the MLP classifiers. Then, the study applied normalization to all the layers. In the next step, the neural network was trained for probability mapping. The parameters applied for developing the model include input specifications, network topology, training parameters, and stopping criteria (Table 3.1). We measured the accuracy of the trained model. Then, the pixel values were predicted for the study area of Banda Aceh. The final map of probability was the result, which we analyzed on the basis of the literature review and expert experience. The final probability map was characterized by a high to a low probability of earthquake occurrence in Banda Aceh. Consequently, this work produced a hazard map by considering the earthquake intensity distribution. Then, the hazard map was classified into five different zones. The ANN model works significantly with good accuracy. The AHP methodology was implemented for vulnerability mapping based on the steps described above in AHP methodology architecture.

Table 3.1: Parameters and stopping criteria for the ANN model.

Criteria	Parameters	Values
Input specifications	Total training points Total earthquake events	1546 623
Network topology	Hidden layers Hidden layer sizes Input layer nodes Output layer nodes	2 (32,64) 13 1

Training parameters	Activation Solver Batch size, Learning rate initialization Shuffle Random state Momentum Nesterovs momentum early stopping validation fraction	 relu sgd 2 0.01 True 0 0.9 True True 0.05
Stopping criteria	RMSE Accuracy rate	0.3 84

Layers for analysis were chosen correctly and referred to some current literature. In addition, the quality of the results was analyzed on the basis of the achieved CR (0.04), which yielded good results. Finally, we multiplied both the hazard and vulnerability map to produce the earthquake risk map.

3.7.2.1. Performance evaluation

This section is important for understanding the obtained results. Several metrics are available that are used as benchmarks to analyze the performance of our projected neural network model, such as space, time, and model accuracy. Although time and space are highly important for the training of a model and may create an obstacle; therefore, we applied RMSE to evaluate the performance of applied ANN inside the ANN–AHP model. Several researchers have applied and understood the best performance obtained by the metric RMSE, which was selected on the basis of the problem nature and the expected results (Alarifi, Alarifi & Al-Humidan 2012). The results of our ANN model and the AHP method are presented in the section of results and discussion. The presented results are

easy to understand and facilitate decision-making.

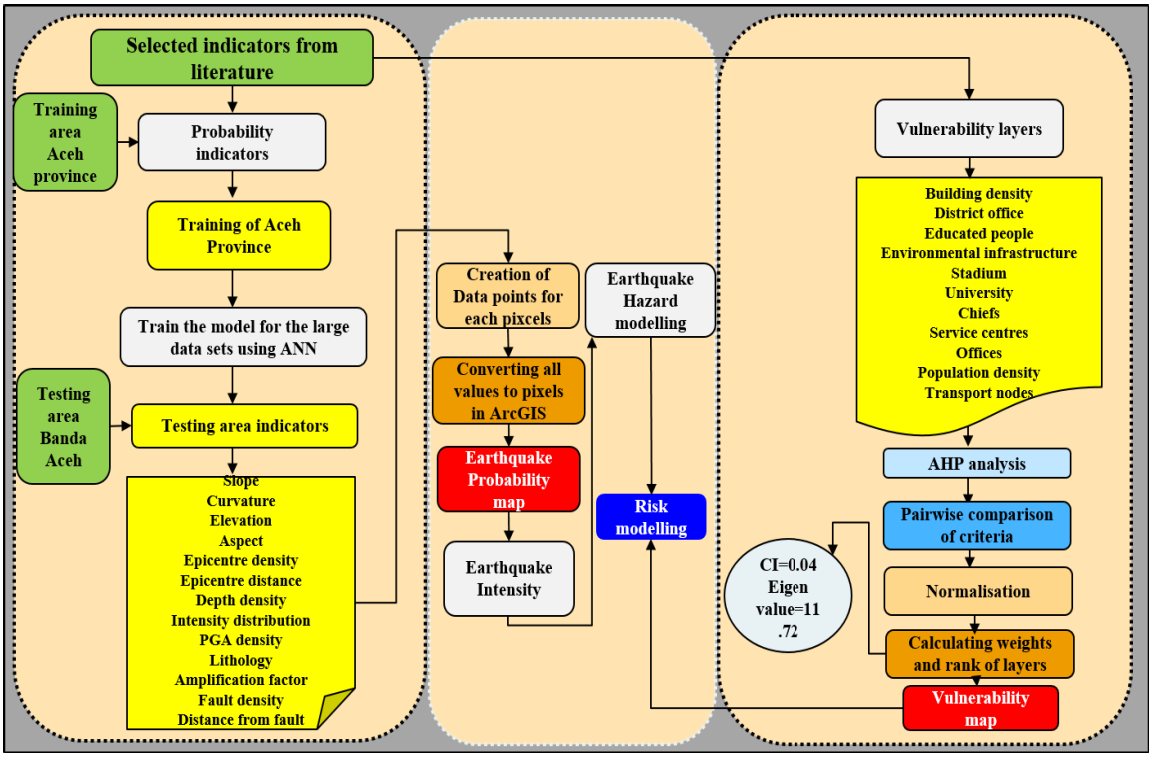

Figure 3.5: Methodological flowchart of the developed model for objective 2.

3.7.2.2. Performance metrics

Mean absolute error (MAE):

MAE is a quantity used to measure how close predictions are to the target outcomes. The mean absolute error is defined as follows (Chai & Draxler 2014):

$$\mathrm{MAE} = 1/n \sum_{i=1}^{n} |error_i| \tag{3.43}$$

Root mean square error (RMSE):

RMSE estimates the average error based on a quadratic scoring rule. RMSE is the square root of the average of squared differences between prediction and actual observation

(Chai & Draxler 2014). It provides the average prediction error of a network. The values of RMSE ranges from zero to infinity. However, the lower values expressed by the RMSE gives a better result. RMSE is better than the mean absolute error (MAE), whereas large errors are unacceptable. Therefore, RMSE is more appropriate for error measurement (Alarifi, Alarifi & Al-Humidan 2012).

$$\text{RMSE} = \sqrt{1/n \sum_{j=1}^{n} \left(y_j - \hat{y}_j\right)^2} \tag{3.44}$$

The RMSE values $\hat{y}_j$ that are predicted for times j of a variable of regression's dependent y_j with y different predictions for observed variables over T times are computed as the RMSE. The RMSE value for this study is 0.3 based on the training site of Aceh province with an accuracy value of 0.84. An accuracy curve was developed and described in the results and discussion part of the paper.

3.7.3. Objective 3

In this subsection, the newly developed hybrid fourfold ANN CV-AHP-TOPSIS model is used to improve the ERA. The inventory data were divided, and the fourfold CV was implemented to organize them into training and testing datasets. In this approach, the earthquake dataset applied K-folds of $E1, E2 \ldots Ek,$ where $\forall_n$ and $m \in t$, and size E_n =size E_m. The proposed model was run for K times, where time $t \leq K$. The randomly prepared inventory dataset was divided into fourfolds, 70% of earthquake events were considered in model training, and 30% were applied for CV purposes (Ghorbanzadeh et al. 2019). The details of the ANN model parameters are described in Table 3.2. The number of folds was created based on several factors, such as problem complexity,

inventory data volume, and implemented methodology. The CV approach was used to optimize the randomness effects on the results of ANN-based earthquake probability mapping. First, earthquake probability assessment was conducted, and hazard analysis was performed based on earthquake intensity (Figure 3.6). Table 3.2 describes all the criteria used in this research. Second, vulnerability assessment was conducted based on the important parameters by using the hybrid AHP-TOPSIS approach presented in Table 3.5 and Figure 3.13. Third, risk assessment was conducted by multiplying the hazard and vulnerability.

Table 3.2: Accuracy assessment and the parameters of the k-fold ANN model.

ML	AUC-Fold1	AUC-Fold2	AUC-Fold3	AUC-Fold4	Cross validation
ANN	81	85.4	81.3	83	84.8
Criteria	Parameters				Value
Input training and testing	Training points Testing points Earthquake events				70% randomly out of 1810 30% randomly out of 1810 1210
Network architecture	Hidden layers Size of hidden layers Total input nodes Output node				3 (64, 32, 16) 9 1
ANN training parameters	K-fold training Dynamic learning Batch size Solver Activation Momentum				Yes Yes 100 SGD Relu 0.9
Stopping criteria	RMSE Iterations Best accuracy				0.183 50000 85.4

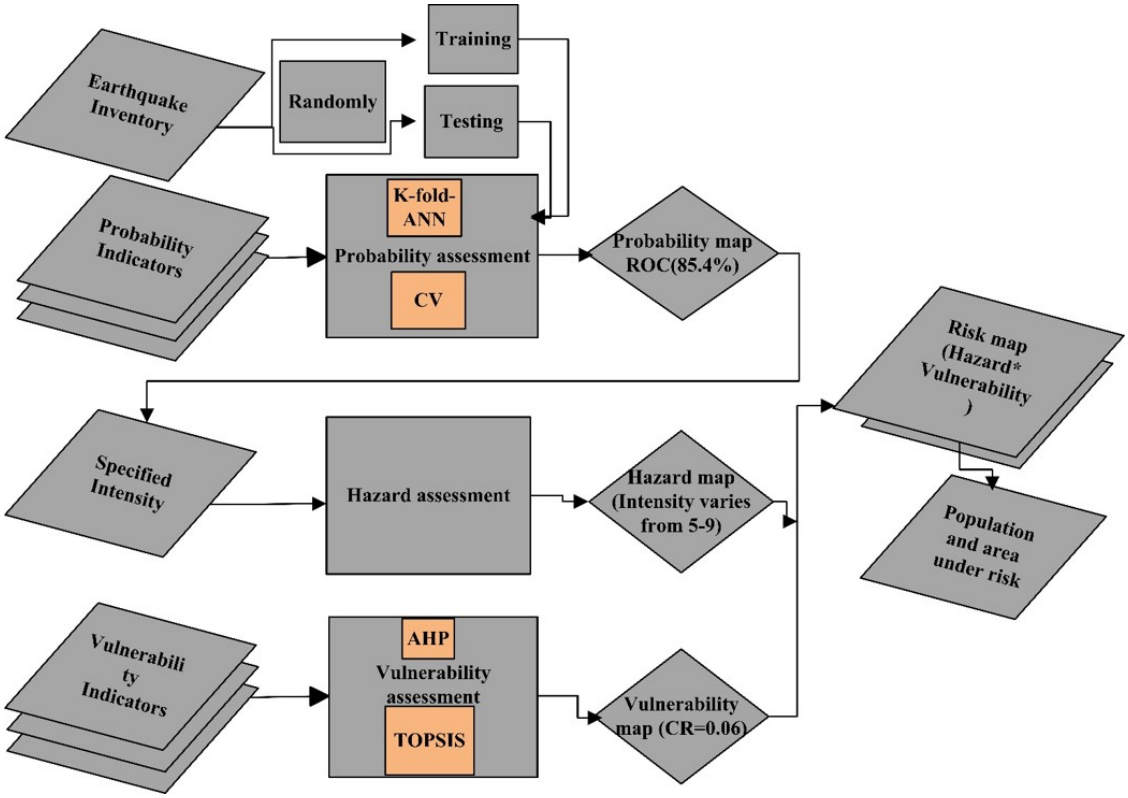

Figure 3.6: Methodological flowchart of the improved model for objective 3.

Finally, risk modeling was performed based on the described steps to provide the expected result of the number of people and the areas under risk in the study area. CV revealed that the output is accurate. The proposed novel model was prepared by analyzing various previous and recent models for earthquake vulnerability and risk assessment on a city scale. The proposed model included various parameters, making it comprehensive, accurate, and cost-effective. The limitations of the model are provided in the conclusion section. The details of the workflow are presented in Figure 3.6.

3.8. Study area

The meeting of the tectonic plates produces a reverse fault system governed by regional geology and active volcanos. According to worldwide earthquake databases, 150 or more

high magnitude earthquakes (Mw>5.5) were experienced from 1900 to 2017. Total fatalities exceeded 266,270 in the last 400 years in different regions of Indonesia. Some high deformation rates have triggered many large earthquake events (≥ 8.0), such as the 1861 Nias event, 2004 event in the Indian Ocean, and the Simeulue event in 2005. The Sumatra–Andaman megathrust earthquake in 2004 is the second-largest magnitude earthquake recorded to date (Bilham & Ambraseys 2005). The earthquake created a rupture of 1300 km (length) characterized by seven separate segments from the northwest to the Andaman Islands at more than 1600 km (Bilham & Ambraseys 2005). The earthquake duration is the longest event period recorded at approximately 600 sec. Lin & Lee (2008) explained that the inter-tectonic subduction of the plate was associated with the event and bedrock movement. In Indonesia, the recorded human toll in Aceh province and North Sumatra due to the 2004 earthquake was approximately 110,229 deaths, 12,123 missing, and 703,518 displaced (Siemon, Ploethner & Pielawa 2006). The details of fatalities and injuries are presented in Table 1.1. Infrastructure damage due to the dominant disastrous earthquakes may be due to the use of poor construction materials. Damage to buildings was caused by the earthquake magnitudes (i.e., ≥ 8.0) that used to frequently occur in Aceh province, thus continuously affecting the city of Banda Aceh (Irwansyah 2010). The total damage estimated for the buildings accounted for 35% of all buildings (Siemon, Ploethner & Pielawa 2006).

Banda Aceh is the capital city of Aceh province that is exposed potentially to a significant earthquake vulnerability and risk along the major fault of the Great Sumatran Fault (GSF) (Figure 3.7). The west, north, and southern borders of Banda Aceh are close to the Indian Ocean, Malacca Strait, and Aceh Besar District, respectively. Banda Aceh is close to the Sunda Arc characterized by furious events and vulnerable to earthquakes because of its

unique geographical location and active tectonics. GSF is a right-lateral strike-slip fault that has not experienced any large earthquake in the northern part of the fault particularly in Banda Aceh from the last 200 years. This tranquil part of the fault is considerably recognized as a seismic gap in Aceh province. An accumulation of increased stress along the GSF may be observed due to the collision between plates. Petersen et al. (2004) mentioned the capability of GSF for producing up to M=7.9 event, as the history explained the capability of M=7.7 that has occurred along this fault. This earthquake occurred in 1892 near the city of Sibolga (approximately ±570 km at the southeast of Banda Aceh) (Petersen et al. 2004; Siemon, Ploethner & Pielawa 2006). Back marshes commonly found behind the sand dunes form the Banda Aceh coastline. Buildings or houses that are present at a distance of 3 to 5 km inland from the coastline were affected by the 2004 tsunami. The tsunami height in Banda Aceh was between 5 to 30 m (Natawidjaja & Triyoso 2007, Johar et al. 2013).

The city is predominantly developed on soft soil, characterized by large reinforced concrete structures, such as public and private infrastructures, shopping malls, hotels, restaurants, and hospitals (Culshaw, Duncan & Sutarto 1979). The buildings are quite old and damaged because of strong ground motion. Building damage varies from total collapsed to minor damage depending on ground conditions, foundation type, and ground motion variation. The soft ground condition was the main factor for the damage of buildings in coastal and hilly areas of Banda Aceh. However, the site amplification probability is extremely high in the thick alluvium (Brebbia 1996; Setiawan 2017; Setiawan et al. 2018). Therefore, estimation of the seismic site amplification of Banda Aceh is required by recognizing the probability of future earthquakes because the city is surrounded by several earthquake events (Lin & Lee 2008; Yunita et al. 2018). The city

has experienced ground shaking due to some major earthquakes in recent years. Moreover, understanding Banda Aceh's vulnerability and risk due to earthquakes are essential and significant for urban planning (Zhang & Jia 2010; Zhang et al. 2017). The probability, hazard, and social vulnerability analysis can be applied in future risk mapping and decision management by considering the risk reduction, prevention, and mitigation (Setiawan et al. 2020; Birkmann 2007; Adger et al. 2005; Adger & Kelly 1999; Rygel, O'sullivan & Yarnal 2006; Blaikie et al. 2014; Turner et al. 2003; Davidson & Shah 1997; Davidson & Freudenburg 1996). In the current analysis, the hazards and vulnerability resulting in high ability and stand on socially operated attributes and contexts, for a large population, are unsheltered.

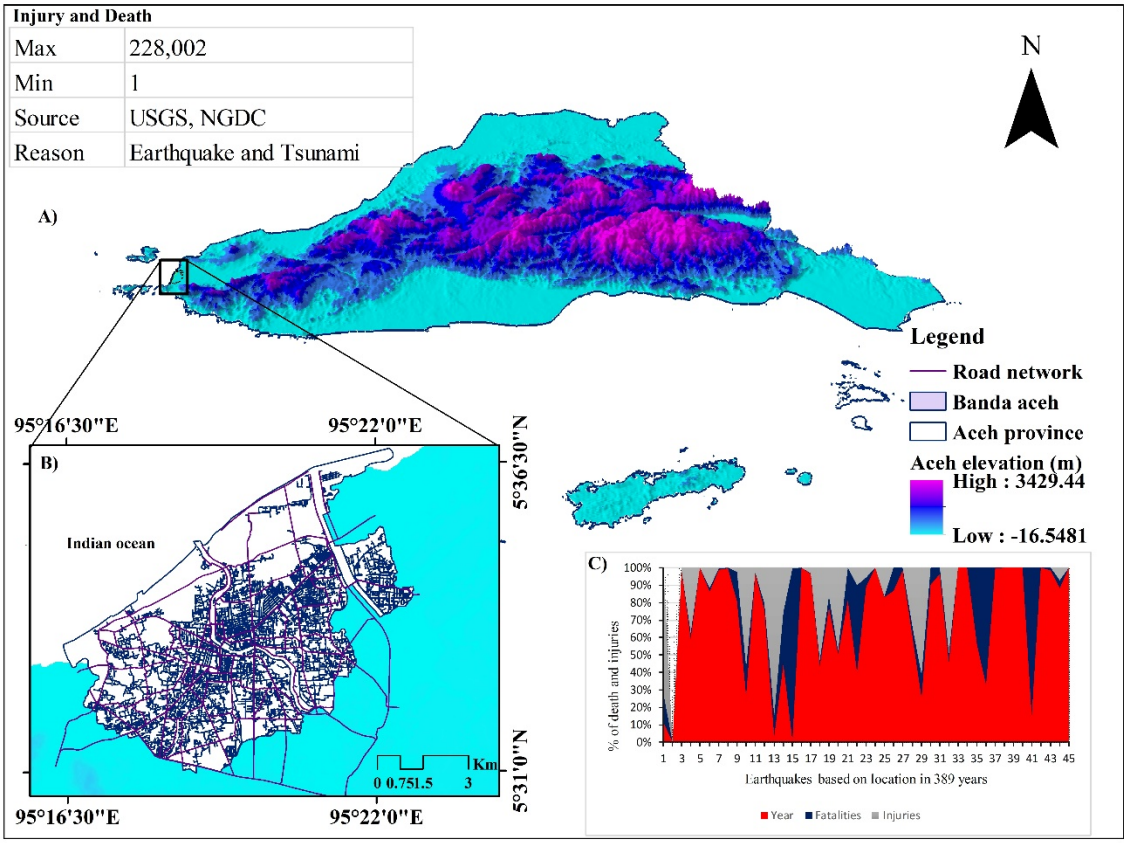

Figure 3.7: Location of Banda Aceh.

Research scholars and scientists have divergent definitions for the notion of vulnerability and risk because of the complexity behavior (Adger et al. 2005; Adger & Kelly 1999; Cutter 1996; Cutter, Mitchell & Scott 2000; Khan 2012; Tierney 2006; Hosseini et al. 2014; Beccari 2016). Therefore, it's a requirement for researchers to develop models, breakthrough techniques to implement and work on earthquake probability, hazard, vulnerability, and risk assessment.

3.9. Characteristics of the Banda Aceh city

The study area is located at 5°33′0″ N and 95°19′0″ E. The city is located at an elevation of approximately 35m m.s.l. Banda Aceh is divided into nine subdistricts, in which four of them, namely, Kuta Raja, Meuraxa, Syiah Kuala, and Kuta Alam, share their boundaries with the Indian Ocean. The city extends approximately 20 km in an east-to-west direction and 10 km in a north-to-south direction. The coastline shared by Banda Aceh is around 12 km. Topographic elevation in the city varies from 0–10 m. The city covers an area of approximately 61.4 km^2 based on the 2010 census; the city is populated with 219,070 and 250,227 people based on the 2010 and 2015 census (Johar et al. 2013; Yuzal et al. 2017). Moreover, 10 ethnic groups can be found in the city, of whom the Acehnese is the largest group that comprises approximately 80% to 90% of the total population (Yuzal et al. 2017). The most noticeable Aceh fault is the measured structural discontinuity that passes through Banda Aceh. The Aceh fault is active; however, no events are experienced historically inside Banda Aceh. Banda Aceh was affected by a 7.7 magnitude earthquake near the city in the NE region. After the 2004 tsunami event, the city experienced massive morphological changes, and the Indonesian government conducted developmental and recovery work. The building density in Banda Aceh city is highly concentrated in the central part than in coastal regions. The 2004 earthquake and

tsunami destroyed 0.2 million lives because of the lack of earthquake knowledge for land use planning (Telford & Cosgrave 2006). The study area is presented in Figure 3.7.

3.10. Geology of the study area

The relatively flat topography of Banda Aceh is characterized as quaternary sedimentary rocks, sands, and clay deposits (Switzer et al. 2012). Banda Aceh is situated on thick sedimentary alluvium deposits (Siemon, Ploethner & Pielawa 2006). However, loose sedimentary deposits in Banda Aceh make the city vulnerable to ground shaking caused by devastating events (Jena et al. 2019). The geology of Banda Aceh is composed of limestone, phyllite, and slate (Culshaw, Duncan & Sutarto 1979). Furthermore, the city is located at a low-lying area underlain by deposits of the Holocene age characterized by fluvial deposits and estuarine deposits (Figure 3.8). Its geology is classified as surface and subsurface types primarily as silt and clay deposits, and sand deposits can be found on the right bank of Aceh River close to the coastline (Culshaw, Duncan & Sutarto 1979).

These rocks in the Cretaceous age in the geological timescale and the morphology indicates the mountainous structure at the end of the northern Barisan range in Sumatra (Culshaw, Duncan & Sutarto 1979). Massive and moderately weathered limestones are specifically found in this range. In the western part of the Indrapuri, mixed lithic conglomerates can be found at the outcrops. The wedges of conglomeratic outcrops are placed between the limestone and the Quaternary deposits and are believed to be of the Palaeogene age (Culshaw, Duncan & Sutarto 1979). Fossiliferous sandstone deposits can be found in the upper valley of Pliocene or early Pleistocene.

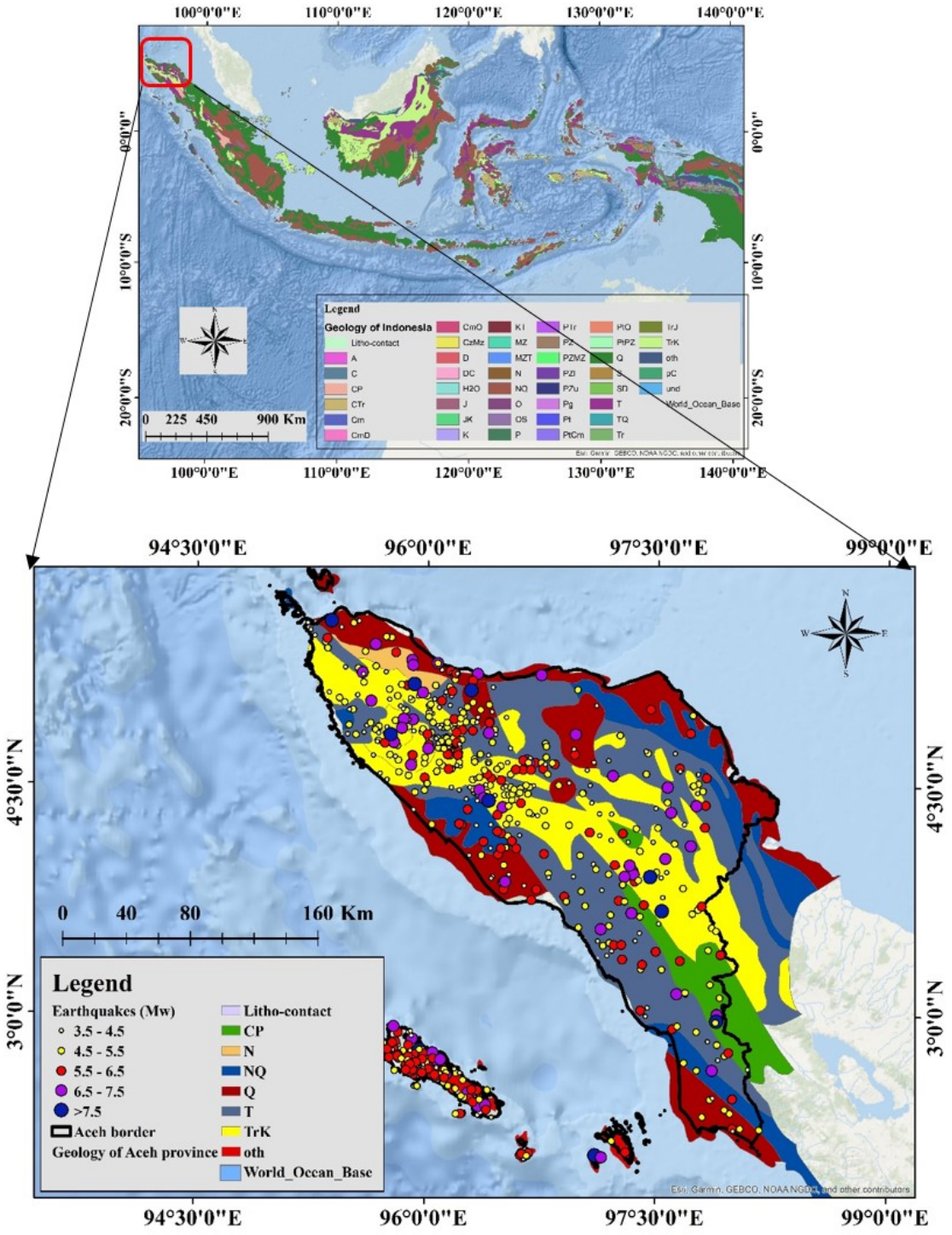

Figure 3.8: Geology map of the study area.

These deposits show a shallow-water marine environment, thereby serving as evidence of a rise in elevation up to 90 m m.s.l. due to the tectonic upliftment (Johar et al. 2013).

On the western side of the Krueng Aceh valley, the unconformable Quaternary sedimentary deposits can be found. Banda Aceh is characterized by a quaternary sedimentary deposit along with some patches of peridotitic rocks. Therefore, The Krueng Aceh valley forms a graben-type structure between the Semangko fault and the splay main fault system (Wang et al. 2006; Culshaw, Duncan & Sutarto 1979).

3.11. Palu city as a case study (for evaluating the transferability of the developed models)

Sulawesi Island is situated at the convergence zone of three major plates such as; the Indian-Australian Plate, the Pacific Plate, and the Eurasian Plate (Rusydi & Efendi 2018). Palu is a city in Sulawesi Island in Indonesia (Figure 3.9). It is located at 0◦53042" S, 119◦51034" E as the capital of the Central Sulawesi Province. Various geological rocks and tectonic conditions from the surrounding areas distinguish the city. Sulawesi island is K-shaped, which is characterized by 14 geomorphic units (Cipta et al. 2017). Matsuoka et al. (2006) described and classified the geomorphological units such as tertiary mountains, pre-tertiary mountains, hills, volcanic foot slopes, mountain foot slopes, volcano, and dunes. Volcanoes in Sulawesi covers approximately 75% of the island's area. Several active faults could be found on the island, containing the active Palu-Koro fault found in the northwest part of the Palu city. The Makassar Basin is divided by the Palu-Koro fault zone and the separation produced into the North and South Makassar Basins (Katili 1978). The Palu-Koro fault is a transform fault in nature that is responsible for the movement of some part of western Sulawesi towards the south–southeasterly direction. However, this affects the island's locality and generated two dormant spreading centers in the Makassar Strait (Katili 1978). The northward movement of Sulawesi

happened due to further spreading put up by the left-lateral Palu-Koro fault. Therefore, as a result, Sulawesi moved away from Kalimantan in a direction with a north-northwest–south-southeast axis (Tjia & Zakaria 1974). The main tectonic assemblages found in Sulawesi such as eastern and southern arm ophiolite complexes and northern and southern arms tertiary granites, volcanic deposits (Katili 1978). Palu is unique because of its unique geological structure having five main structures. Palu-Koro strike-slip fault covers approximately an area of 50 km in width near Palu where fault slip range is 30–40 mm/year according to Socquet et al. (2006). Alluvial deposits, granite fragments, beach sediments, molasses sediment, and metamorphic rocks could be found in a different part of the city within the valley.

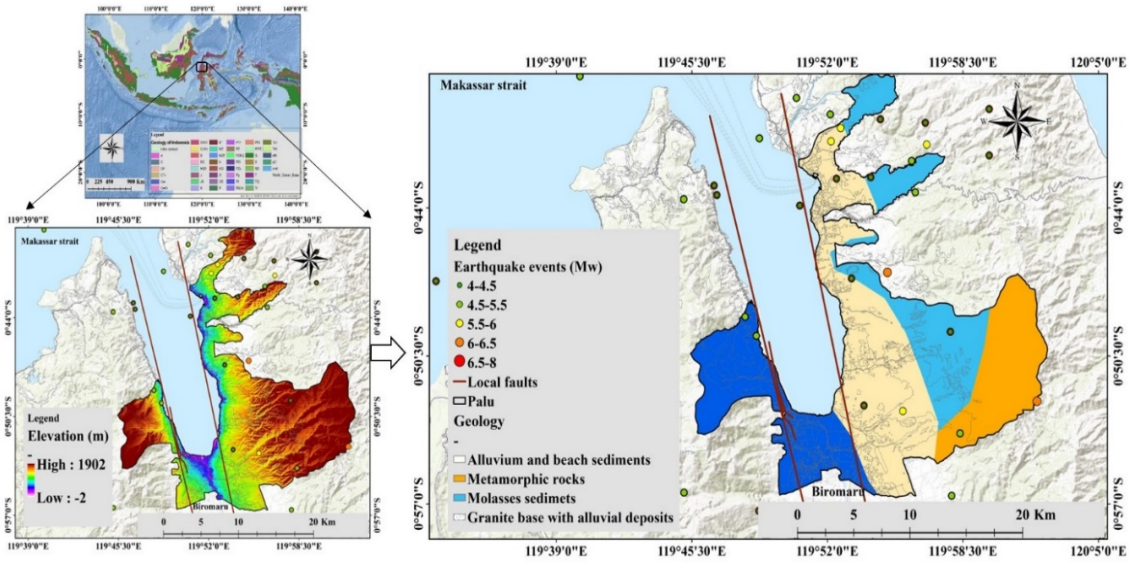

Figure 3.9: Location of Palu city.

3.12. Data acquisition

Various sets of data were collected from the several official websites of Statistics Indonesia as the main source (Figure 3.10). However, for ERA, data are generally used from single or multiple sources. Freely available earthquake data can be collected from

both public and private agencies. These sources are accessible from the internet and include the Advanced National Seismic System, United States Geological Survey (USGS), National Earthquake Information Center (NEIC), and the Northern California Earthquake Data Center. We have collected the complete earthquake catalog from USGS and NEIC of various magnitudes with coordinates of lat. 2^{O} 30'00''N and 5^{O}00'00''N and long. between 94^{O}30'00''E and 99^{O}00'00''E. Data for the probability, hazard, and vulnerability assessment were collected from various national and international agencies such as Statistics Indonesia (www.bps.go.id/eng), GeoNetwork (http://www.fao.org/geonetwork), and the USGS (https://earthquake.usgs.gov). Digital elevation model (DEM) with 7.5 m resolution and administrative shapefiles in Banda Aceh and Aceh province were collected from the Laboratory of Geographic Information Systems and Spatial Data of Syiah Kuala University.

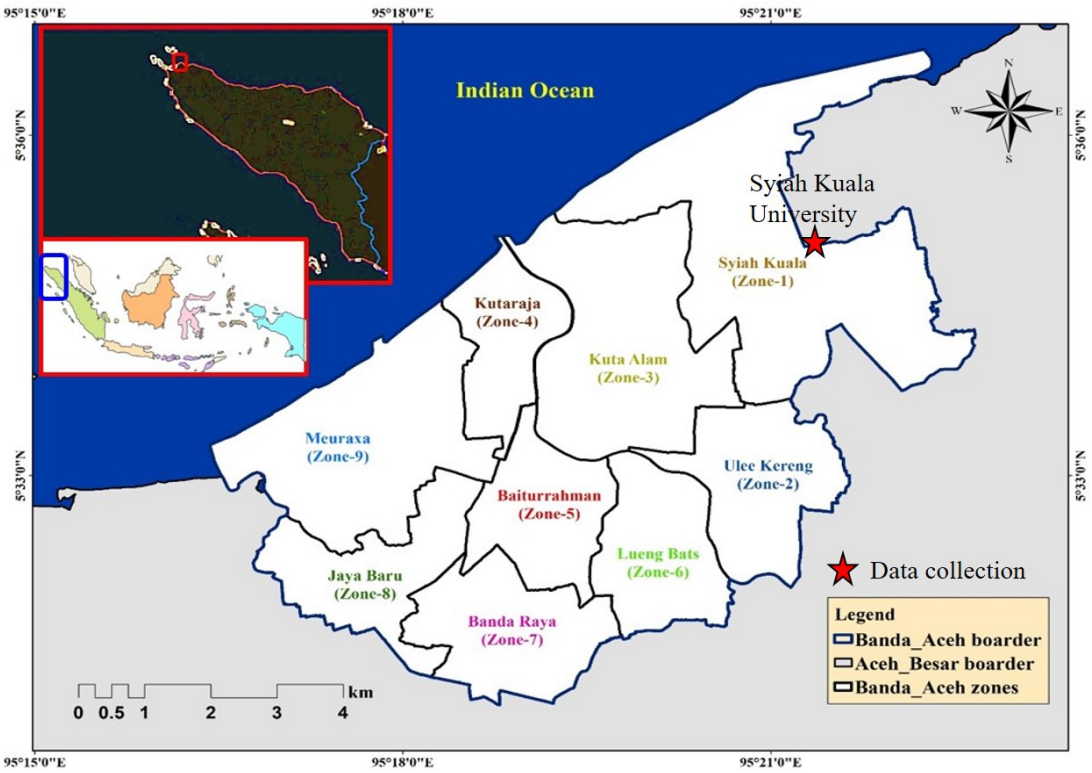

Figure 3.10: Location of Banda Aceh city distributing the sub-districts and the data collection zone.

Inventory data, published maps, geological maps, and seismic tectonic conditions were obtained from the USGS world maps based on the coordinates of Aceh and its surrounding areas from 1800 to 2019 and were applied for the probability assessment and validation purposes.

3.12.1. Data and thematic layers used for objective 1

Vulnerability maps cannot be produced without analyzing criteria individually. The most important part of the approach is the selection of indicators that are adequate to reflect the total vulnerability of Banda Aceh City. Chosen factors and alternatives have been described for the vulnerability assessment (see Table 3.3). However, besides these factors, some were generated from the raw data of segment, polygon type as vector dataset, and DEM as raster dataset. The thematic layers were obtained using ArcGIS. Classification of the criteria is not straightforward because of lacking statistical rules that can automatically classify continuous data (Rozenstein & Karnieli 2011). The major mathematical methods for data classification are equal intervals, natural breaks, manual and statistical consideration, which are GIS default processes (Naghibi, Pourghasemi & Dixon 2016). Many academic scientists and researchers have used their individual discretion to identify class boundaries in continuous data layers. The natural breaks method was applied to classify the values into five classes for the EVA map (Mohammady, Pourghasemi & Pradhan 2012; Pourghasemi, Mohammady & Pradhan 2012). For the density calculation, the function of kernel density was applied. A Euclidean function was implemented for distance calculation, which was characterized by a cell size of 5 m (pixel size 5×5 m) applied in the GIS software (Xie & Yan 2008).

Table 3.3: Data used for vulnerability assessment in objective 1.

Goal	Criteria	Selected layers	Scale	Type	Resolution (m)
Vulnerability	Geotechnical (DEM and Segment types)	Slope Curvature Lithology Distance from fault	1:30000	Raster layers	5
	Structural (Segment and polygon types)	Building Characteristics Major offices Transport nodes Educational institutions Service centres Stadium, museum and historical places			
	Social (Segment and polygon types)	Population characteristics Household Characteristics Village chiefs Educated people Popular places Visiting places Parks and others			

In this study, the Kernel density estimation (KDE) model was used to achieve the density of the layers of the building's size, area, floors, and quality (Botev, Grotowski & Kroese 2010). Thereafter, to achieve a value between 1 and 5, reclassification of layers was needed. Table 3.3 presents the details of the data and indicators.

3.12.2. Data and thematic layers used for objective 2

The probability and vulnerability assessment is extremely challenging without considering the significant criteria and the important indicators that depend on the

heterogeneity of the study location (Table 3.4).

Table 3.4: Selected input data layers from literature and data types used in objective 2.

Criteria	Selected layers	Scale	Type	Resolution (m)
Susceptibility Hazard	Slope Curvature Elevation Aspect Epicenter density Epicenter distance Depth density Magnitude distribution PGA density Lithology Amplification factor Fault density Distance from fault Earthquake Intensity	1:30000	Raster layers	5
Vulnerability	Building density District office Educated people Environmental infrastructure Stadium University Chiefs Service centers Offices Population Transport nodes			

The most vital and useful part of the approach is to select the criteria and indicators adequately to obtain an accurate risk map for Banda Aceh. Probability layers were obtained from the DEM and historical events using excel and ArcGIS (Figure 3.11). However, vulnerability layers were obtained from the polygon and segment types of

vector datasets (Figure 3.12). A geodatabase was created and applied individually for probability, hazard, vulnerability, and risk assessment. The details of the criteria and indicators used for this research are presented below.

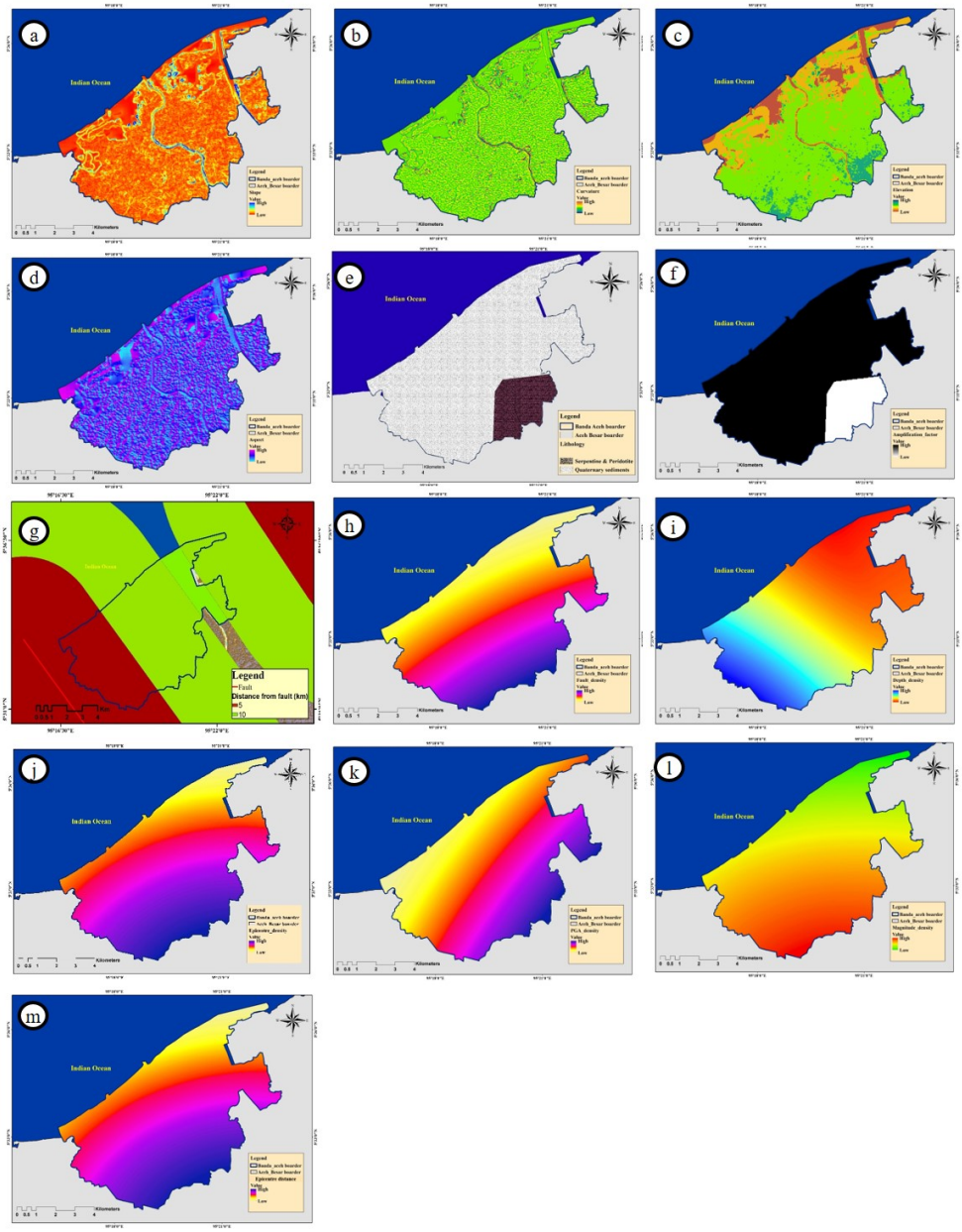

Figure 3.11: Criteria for probability mapping using ANN. (a) Slope, b) curvature, c) elevation, d) aspect, e) lithology, f) amplification factor, g) distance from faults, h) fault density, i) depth density, j) epicenter density, k) PGA density, l) magnitude density, and m) distance from epicentre.

On the basis of the objective and purpose of the study, collected data were used to prepare several layers that were identified and selected after the extensive literature review. Several steps implemented in ArcGIS such as create or modify a thematic layer, filtering of values in a thematic layer, organisation unit search and implementation, navigation between organisation hierarchies, and production of the maps. Thematic map development and management were done based on the requirement of the objective.

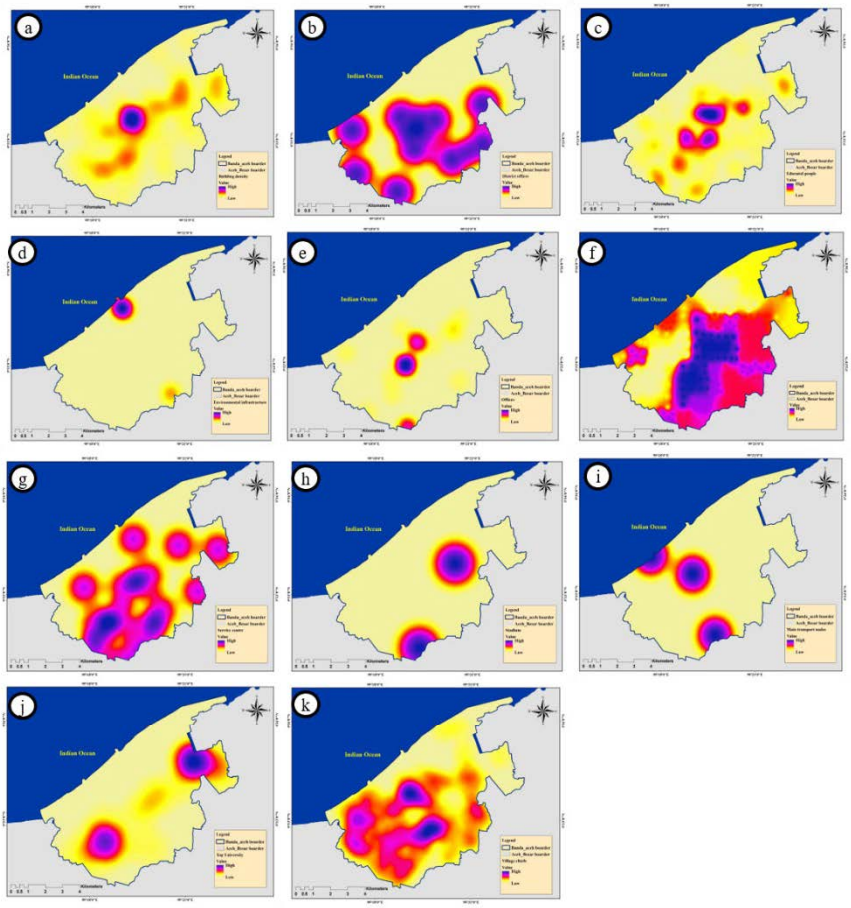

Figure 3.12 Criteria for vulnerability mapping using AHP. (a) Building density, b) district offices density, c) density of educated people, d) environmental infrastructure, e) major offices, f) population density, g) distance from service centers, h) stadium, i) transportation nodes, j) distribution universities and k) distribution of village chiefs.

3.12.3. Data and thematic layers used for objective 3

Nonspatial and spatial data were used in the current research (Figure 3.14). Nonspatial data, such as event time, magnitude, and magnitude error, were collected from the USGS data source (Figure 3.13). Events were filtered based on magnitude larger than 5 Mw because low magnitudes have a small capacity for damage. Accessing a very high-resolution DEM is a challenging factor during data collection and database creation (Ghasemi, Pradhan & Jena 2018). Appropriate attribute selection is a crucial part of this study. The selected attributes for the probability index indicators were obtained based on the exact longitude, latitude, day, month, year, depth, and magnitude.

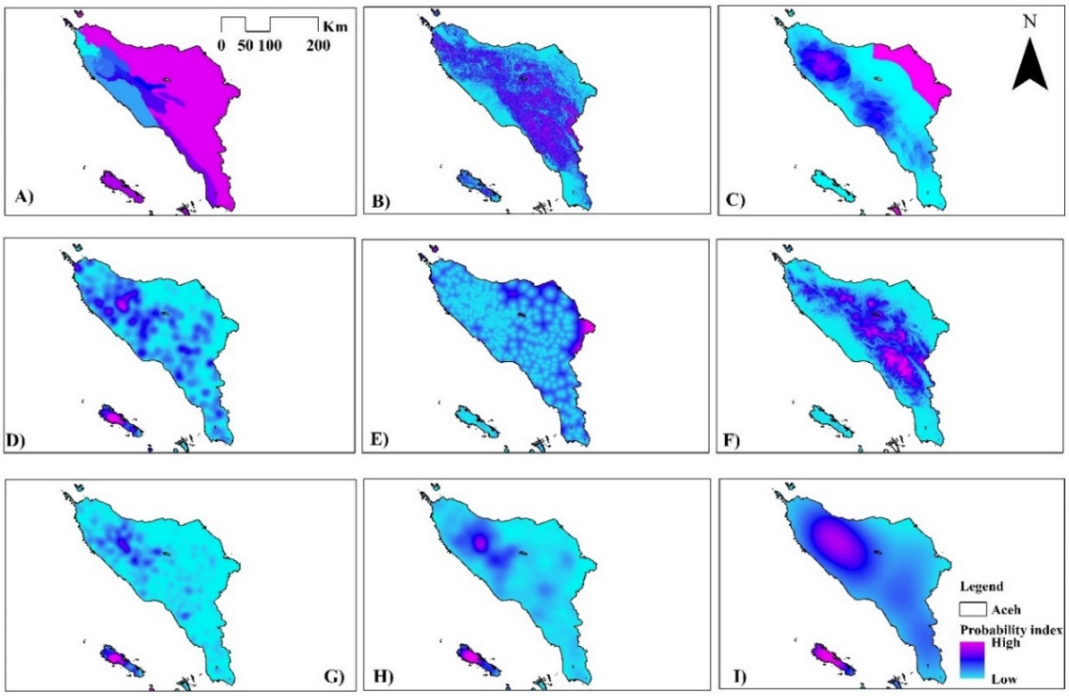

Figure 3.13: Input layers for probability index estimation. (a) lithology with an amplification factor, (b) slope angle, (c) fault density, (d) depth density, (e) proximity to epicenter, (f) elevation, (g) epicenter density, (h) magnitude density, and (i) PGA (Peak ground acceleration) density.

Table 3.5: Probability and vulnerability indicators for ERA used in objective 3.

Data	Types	Factors	Impacts	References
DEM, Earthquake events Geological map,	Probability indicators	Slope	Slope affects the landscape processes such as subsurface flow, runoff rates, erosion potential, and velocity of overland flow. Slopes are associated with crustal faults.	(Bathrellos et al. 2017; Sakellariou et al. 2017)
		Elevation	High elevation projects complicated tectonics. Probability is high with higher elevation.	(Alizadeh et al. 2018)
		Fault density	Areas with high fault density are highly susceptible to earthquakes. If the faults are active then the chance is very high.	(Dimri, Lakhera & Sati 2007)
		Lithology and Amplification factor	Composition of the rocks and their amplification factors helps to identify the areas that could have high ground shaking capacity.	(Jena et al. 2019)
		Epicentre density	Areas with earthquake clustering and epicentre of pairs of large events are highly probable zone.	(Martínez-Garzón et al. 2019; Rashed & Weeks 2003; Soe et al. 2009)

		Magnitude density	Likelihood of occurrence of a particular magnitude at a particular place.	(Zebardast 2013)
		Proximity to epicentre	Avoiding the source location of earthquakes is important because epicentre zones are highly probable.	(Jena et al. 2020)
		Depth density	It gives information on the fault depth and capacity of producing a particular event.	(Soe et al. 2009)
		PGA density	It provides ground acceleration information.	(Morales-Esteban, Martínez-Álvarez & Reyes 2013)
Administrative areas, Buildings shapefile, Population raster file from DIVA-GIS, Shapefile of all other vulnerable layers	Vulnerability indicators	Population density	Higher the population density near the seismic gap of GSF, higher the vulnerability.	(Tate 2012)
		Building density	Expansion of buildings and increase in building density could increase the earthquake risk.	(Vicente et al. 2011)
		Building surface area density	Bigger the surface area of buildings floor lesser the vulnerability.	(Binita, Shepherd & Gaither 2015)
		Building quality	Buildings quality is reliant on material quality, design standards, income of the owner. Therefore, low	(Moradi, Delavar & Moshiri 2015)

			quality buildings area highly vulnerable.	
		Building heights	Buildings vulnerability increases with height and quantity of floors.	(Ebert, Kerle & Stein 2009)
		Building types	Shape and geometric size of the land structure are vital. Large yet consistent shapes or sizes are less vulnerable.	(Tavakoli & Favakoli 1993)
		Proximity to road	Roads provides access to move to the safe place in highly populated and junction areas.	(Vicente et al. 2011; Sarris et al. 2010)
		Proximity to buildings	Be away from high-rise buildings during earthquake is safe.	(Debnath 2013)
		Household density	It is crucial to assess the household population density to vulnerability. Household vulnerability particularly focused by scientists and policy makers.	(Binita, Shepherd & Gaither 2015; Shepard et al. 2012)

Risk assessment is challenging without considering the essential criteria and the significant indicators based on the study area heterogeneity. The selection of relevant

criteria is a vital part of the ANN K-fold cross-validation model to obtain an accurate result for the city. The detailed characteristics of the indicators used in this study area and the raw data were described in Table 3.5. USGS data and data from Statistics Indonesia (www.bps.go.id/eng) were used for probability index estimation and hazard mapping. For the vulnerability assessment, the collected administrative, structural, and social information were used.

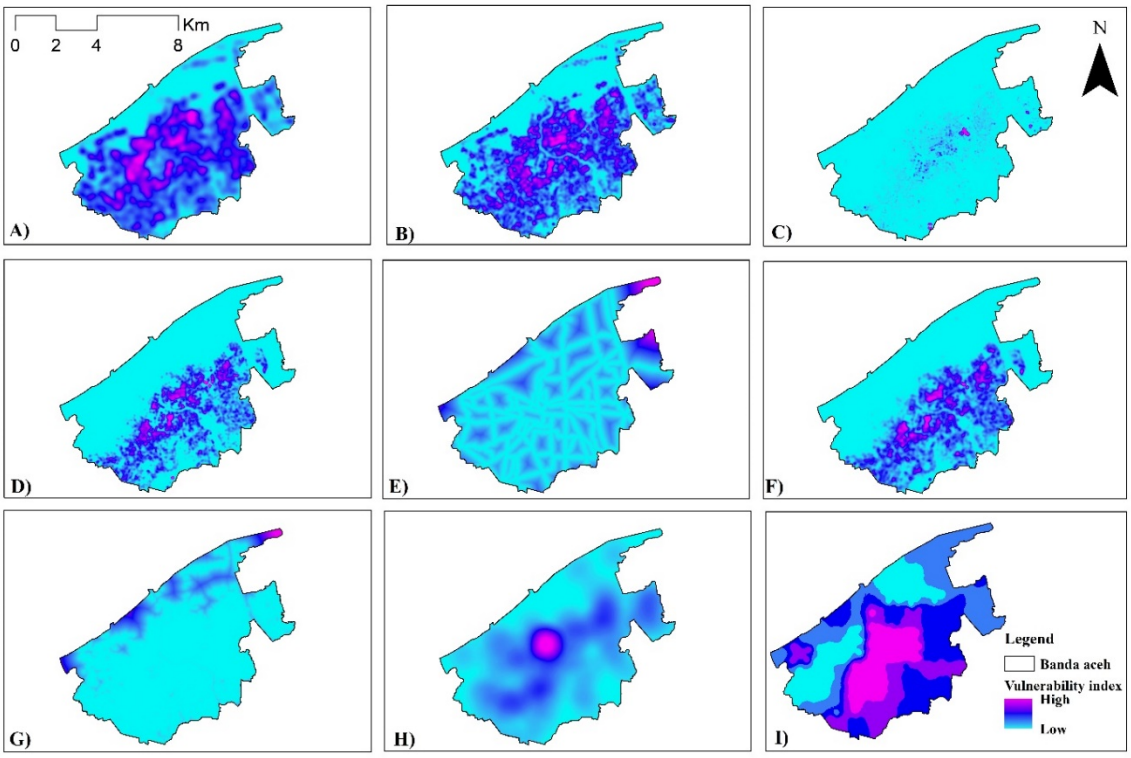

Figure 3.14: Input layers for vulnerability index estimation. (a) household density, (b) building surface area, (c) building quality, (d) building heights, (e) proximity to road, (f) building types, (g) proximity to buildings, (h) building density, and (i) population density. (Building density and population density maps were reproduced after (Jena et al., 2019).

3.13. Factors used in this study and the importance

3.13.1. Probability and hazard indicators

The development of a probability map using the catalogue of historical events of moderate to large earthquakes (M ≥ 5.5) was considered. Therefore, to characterize the spatiotemporal distribution of earthquakes this research generated several thematic indicators for the earthquake probability mapping. The applied method/model accounts for several tectonics parameters along with the spatial and nonspatial datasets, which could potentially influence the spatiotemporal variability. As a fundamental component of risk, this study also calculated the PGA and Intensity variation for earthquake hazard assessment. The whole process required various components, such as active geological faults, historical earthquake catalogues, estimation of geodetic crustal deformation, paleoseismic data, and seismotectonic features. However, hazard analysis could be in two different ways: a particular scenario deterministically identified and used for hazard, while probabilistically, all-potential earthquake scenarios were considered along with the probability to estimate hazard. The detailed parameters used for probability and hazard assessment were presented below.

3.13.1.1. Environmental indicators

Lithology: Banda Aceh is characterized by quaternary sediments with patches of peridotite. Therefore, this provides an indicator of seismic amplification (Alizadeh et al. 2018; Dimri, Lakhera & Sati 2007).

Slope: Slope is one of the key factors for earthquake and landslide analysis. However, slopes are associated with the faults and provide the information of fault slip (Alizadeh et al. 2018).

Elevation: This indicator is important because hilly regions are highly seismic relative to

the plane lands given the complicated tectonics and structure (Alizadeh, Alizadeh, et al. 2018).

Curvature: It gives the positive and negative values of the surface because we can recognize the sediment deposits more in the basin than the dome part of a region, which is important for the seismic study (Consultant 2009)

Aspect: Generally, faults are not characterized by straight lines, plain surfaces, and those vertical to the surface. The dipping direction of faults is associated with the direction of slopes, thereby making it important for the study.

Distance to fault: It is an important factor because the earthquake potential zones are extremely near to faults, and they decrease with distance (Alizadeh, Alizadeh, et al. 2018).

Fault density: Fault density is important because the high density of faults indicates the complex tectonics and are more prone to areas for earthquakes (Alizadeh et al. 2018, Dimri, Lakhera & Sati (2007).

3.13.1.2. Seismic indicators

Magnitude density: Magnitude density provides the chances of occurrence of a particular magnitude of the earthquake at the highly experienced zone (Zebardast 2013; Soe et al. 2009).

PGA density: It is an important indicator because it provides ground acceleration information that is related to the lithology, magnitude, and distance from the earthquake source zone (Soe et al. 2009).

Depth density: It provides information about the fault zone if the earthquake focuses are at the same depth (Soe et al. 2009).

Epicenter density: Epicenter density provides the zone of earthquake clustering that indicates the earthquake probable zones (Soe et al. 2009).

Proximity to epicenter: Avoiding the source location of earthquakes is important because epicentre zones are highly probable (Jena et al. 2020).

Amplification factor: It is one of the important key indicators because the amplification value of each lithotype must be analyzed in an earthquake study (Soe et al. 2009).

3.13.2. Vulnerability indicators

For vulnerability mapping, several layers were selected according to the requirement of objectives (Alizadeh et al., 2018). The layers were building density, building surface area density, building quality, building heights, building types, proximity to the road, Proximity to buildings, household density, district office, educated people density, environmental infrastructure, stadium, distribution of universities, distribution of village chiefs, distance from service centers, major offices, district offices density, population density, and transport nodes, as presented in Figure 3.12. For pairwise comparison, the relative importance of the layers was estimated using VIKOR, AHP and TOPSIS approaches. Then, by applying the normalization technique, the weight and rank of all the layers were evaluated. In the next step, the weighted sum tool in the GIS is used to make the vulnerability map.

3.13.2.1. Social indicators

Population density: The population density is increasing every year, as indicated by the 2000–2017 census data. Unfortunately, the increased population density is towards the seismic gap of the GSF fault in Banda Aceh, thereby resulting in high vulnerability (Rygel, O'sullivan & Yarnal 2006; Alizadeh, Hashim, et al. 2018).

Educated people density: A higher level of literacy can increase more about the awareness of hazards among people than uneducated people. Education can enhance

responsibilities during disasters (Rygel, O'sullivan & Yarnal 2006; Alizadeh et al., 2018). University distribution: Universities are the main source of education that can raise crisis alarms hazards. Therefore, the good distribution of universities in a large city is significant (Alizadeh, Hashim, et al. 2018).

Village chief distribution: "Chiefs" are the highly respected persons in village areas. Through chiefs, the government can provide information on disasters to the people (Alizadeh et al., 2018).

3.13.2.2. Physical indicators

Building density: Land allocation, lowering building construction, and equal distribution of buildings, along with a perfect development plan, can decrease vulnerability to disasters (Alizadeh et al., 2018).

Building surface area density: Bigger the surface area of buildings floor lesser the vulnerability (Binita, Shepherd & Gaither 2015).

Building quality: Buildings quality is reliant on material quality, design standards, the income of the owner. Therefore, low-quality buildings area highly vulnerable (Moradi, Delavar & Moshiri 2015).

Building heights: Buildings' vulnerability increases with height and quantity of floors. However, current innovations and technologies failed while high height buildings are highly vulnerable (Ebert, Kerle & Stein 2009).

Building types: Shape and geometric size of the land structure are vital (Figure A5). Large yet consistent shapes or sizes are less vulnerable (Tavakoli & Favakoli 1993).

Proximity to roads: Roads provide access to move to a safe place in highly populated and junction areas. (Vicente et al. 2011; Sarris et al. 2010)

Proximity to buildings: Be away from high-rise buildings during an earthquake is safe.

(Debnath 2013)

Household density: It is crucial to assess the household population density to vulnerability. Household vulnerability particularly focused by scientists and policymakers. (Binita, Shepherd & Gaither 2015; Shepard et al. 2012)

Service centers and offices: The main offices and the service center distribution is extremely important for a well-planned city in lowering vulnerability (Alizadeh et al., 2018).

Transportation nodes: Transportation nodes are a key factor in disaster management. Street classification is more important than system performance (Alizadeh, Hashim, et al. 2018).

Environmental infrastructure: It is one of the major factors that must be considered for earthquake vulnerability assessment (Blaikie et al. 2014; Alizadeh et al., 2018).

Stadiums: Stadiums full of people are more vulnerable than empty stadiums (Rygel, O'sullivan & Yarnal 2006).

3.14. Software for modeling implementation

In this research, the main data was DEM, which was obtained from Statistics Indonesia. ArcMap software was used to pre, processing, and post-processing, interpolation, and raster to vector, point raster calculation, index estimation, and map preparation (Table 3.6). Python was used to develop ANN, ANN-CV models of earthquake probability mapping required for earthquake risk estimation. It was also used to generate algorithms (individual and ensemble) for the hyperparameters optimization. In addition, these models were integrated with some MCDM models for risk estimation. The MCDM models were implemented using Excel and TOPSIS calculator software. PAST software was used to determine several relationships such as PGA VS INTENSITY using

Silhouette clustering characterized by a 3point average with 95% ellipses, Matrix plotting was conducted to understand the relationship between Mw, PGA, and Intensity variation. Pure Locational Clustering (PLC) approach was also conducted using the PAST to generate a clustered graph for all the major events and to generate a dendrogram. Therefore, GIS (ArcGIS, QGIS) were used to develop the final probability maps of earthquakes and then used for hazard, vulnerability, and risk estimation accordingly. AHP, VIKOR, AHP-TOPSIS methods were employed in association with artificial intelligence and machine learning techniques to carry out the research and to produce a risk map. Several other processing was also done using AHP, TOPSIS, SAW, and linear assignment calculators to confirm the excel-based calculations.

Table 3.6: Detailed software and their characteristics used for the risk assessment.

Software	Characteristics	Uses
Microsoft Excel	Data sorting and Filtering Handle a huge amount of data points Built-in formulae Produce table reports and chart Automatically edit results	Used for the calculation of Intensity, PGA, Amplification factor values and source to site distance. AHP, VIKOR and TOPSIS values calculation.
PAST	Statistic software Manipulation, plotting, Time-series and spatial analysis	Silhouette clustering, Matrix plotting, Pure Locational Clustering (PLC) and dendrogram plotting.
Faultkin (version 7.5) and Georose 5.0	Accepts only data in text format and used for fault slip analysis	Structural geological analysis
Python 3.7	General-purpose programming Statistics software Useful for modeling and algorithm development Code readability	Neural network modeling and accuracy assessment for probability mapping

ArcGIS 10.4.1	Create layered maps and perform basic spatial analysis	Used for database creation, data analysis, mapping, modeling and map production
Expert's Choice	Decision making	To apply experts opinion for validation purposes

3.15. Several mitigation processes

3.15.1. Structural

Earthquake forces are strong enough that buildings cannot be 100% safe. Buildings' earthquake resistance mostly depends on stiffness, strength, and inelastic deformation capacity. The earthquake-generated force could be controlled to a certain extent depending upon structural, geotechnical, and social characteristics. Shaking performance should be checked through the earthquake-shaking table to test the response of structures. These models used to check to shake of building components against seismic waves.

3.15.2. Non-structural

Policies guidelines and training should be provided to implement the structural measures. Specified authorities such as policymakers, decision-makers, planners should approve a proper construction of structures. Suitable building codes formulation and legal implications required. Retrofitting needs to be well formulated for earthquake-resistant constructions as well as old structures keeping the focus on foundation, site selection, construction, materials, and workmanship. Monitoring of developmental and construction work, settlements, and land use planning should be formulated through guidelines in hazard-prone areas to avoid fatalities and loss of property.

3.15.3. Seismic retrofitting

Modification of existing infrastructures, buildings or constructions and converting them to more resistant to earthquake, liquefaction, or ground motion due to seismic activity is called seismic retrofitting. Understanding of seismic behavior on structures and the current knowledge on experienced earthquakes in urban areas seismic retrofitting could be well acknowledged (Alizadeh et al. 2018).

3.15.4. Long-term measures for mitigation

Re-framing of old building codes, implementation, guidelines is quite important. Strong rules should be developed for high seismic areas. Identifying high vulnerable, risky areas and legal corporation of earthquake-resistant features is required. Earthquake proof public utilities construction and substitutes for infrastructures to reduce risk. Earthquake-resistant community buildings should be constructed in seismic zones of moderate to higher intensities. The requirement of R&D for disaster mitigation, preparedness, prevention is quite important (Schilderman 2004). Evolving educational curriculum and practical training is needed for disaster-related topics.

3.16. Summary

The summaries attained from the developed models were delineated in this chapter for earthquake probability, hazard, vulnerability, and risk assessment as follows:

1. Banda Aceh/ Aceh province and Palu/ Sulewasi province were selected as two case studies to perform the ERA.
2. The chosen study areas were seismically active with very frequently occurred earthquakes. Moreover, these locations contribute to the economic and tourism sectors in Indonesia.

3. High-resolution 7.5m DEM, historical earthquakes catalog, and social, structural information were used in this study for several thematic indicators preparation.
4. Several conditioning factors were prepared using several data layers in a GIS database and then with the modification of model the importance of factors was identified to be used for earthquake probability mapping. Similarly, vulnerability layers were chosen to perform mapping using several MCDM approaches.
5. ANN, ANN-CV models were developed and optimized and then integrated with various MCDM techniques to produce an earthquake risk assessment map on a city scale.
6. Using the developed integrated techniques, vulnerability areas, risk areas, and populations at risk were derived.
7. Risk results revealed that the ANN-CV-AHP-TOPSIS model performs better than the ANN-AHP model. The risk areas and population at risk vary in both the models.
8. All the developed maps were performed through pre-post processings using Python and GIS environment.
9. To reduce earthquake risk various mitigation processes were suggested in this chapter.

CHAPTER 4

RESULTS AND DISCUSSION

4.1. Introduction

This chapter demonstrates the results of case studies obtained using the developed integrated model for earthquake risk assessment in the city scale. The probability, hazard, vulnerability, and risk results using several conditioning factors, and triggering factors are also presented in this section. Moreover, the improvement of the developed model was also demonstrated in this chapter. In addition, vulnerable and risk areas were estimated along with the total population under risk were also calculated and illustrated in this chapter including the mitigation suggestions for Banda Aceh and Palu city. The produced high-resolution maps were presented in this chapter to understand the risk prone areas.

4.2. Objective 1

4.2.1. Social vulnerability

For the Social Vulnerability (SV) map (Figure 4.1), the ranking is done on the degree of vulnerable areas based on natural break classification represented by a color scale from dark green (less vulnerable areas) to red (very high vulnerable areas) (Chakraborty, Tobin & Montz 2005). The geospatial unit is used for the indicator representation and the social vulnerability index (SVI) corresponded to administrative zones within the city (Figure A3). The results of the decision matrix, priority and rank of all the vulnerable layers are presented in Table 4.1.

Table 4.1 Decision matrix, priority and rank evaluation for the criteria of social vulnerability.

	1	2	3	4	5	6	7	8
1	1	2.00	2.00	3.00	3.00	4.00	5.00	7.00
2	0.50	1	2.00	3.00	4.00	4.00	5.00	7.00
3	0.50	0.50	1	3.00	2.00	4.00	4.00	6.00
4	0.33	0.33	0.33	1	0.50	2.00	3.00	4.00
5	0.33	0.25	0.50	2.00	1	3.00	5.00	7.00
6	0.25	0.25	0.25	0.50	0.33	1	2.00	4.00
7	0.20	0.20	0.25	0.33	0.20	0.50	1	3.00
8	0.14	0.14	0.17	0.25	0.14	0.25	0.33	1

No	Category	Priority	Rank
1	Household density	26.9%	1
2	Household surface area	24.0%	2
3	Educated people	16.9%	3
4	Village chiefs	8.1%	5
5	Highly popular place	12.3%	4
6	Religious sites	5.6%	6
7	Visiting places	3.9%	7
8	Parks	2.2%	8

Number of comparisons = 28
Consistency Ratio CR = 4.6%
Principal Eigenvalue = 8.448
Eigenvector solution: 6 iterations, delta = 2.2E-8

1. The very-low social vulnerability (characterized by 26.93% area and 62,190 population) index included four neighborhood villages, namely, zones 1, 3, 4, and 9 that are located along the coastal part of the city. These areas are supposed to be less sheltered and characterized by a better recovery capacity than the other areas.
2. Low social vulnerability (characterized by 33.62% area and 85,155 population) can be observed in zones 1, 2, 6, and 8. These areas are found to be less exposed to low residential building density. The design and planning of buildings in these areas are better than in other areas. Moreover, these areas have less population.
3. Medium social vulnerability (characterized by 20.41% area and 48,554 population) is

visible in zones 2, 3, 5, 6, 7, and 8 in a non-homogeneous manner. The medium category includes villages with a medium exposure of buildings. However, this can consequently confirm that household density and size are at the medium level in locations with medium population density and educated people, which falls within this category.

4. High social vulnerability (characterized by 13.66% area and 31,473 population) is detected from the northeast central region toward the southwest central neighborhoods, where zones 1, 3, 5, and 8 score high in the vulnerability index. This category is characterized by high household density with less size and surface areas along with low-quality infrastructures.

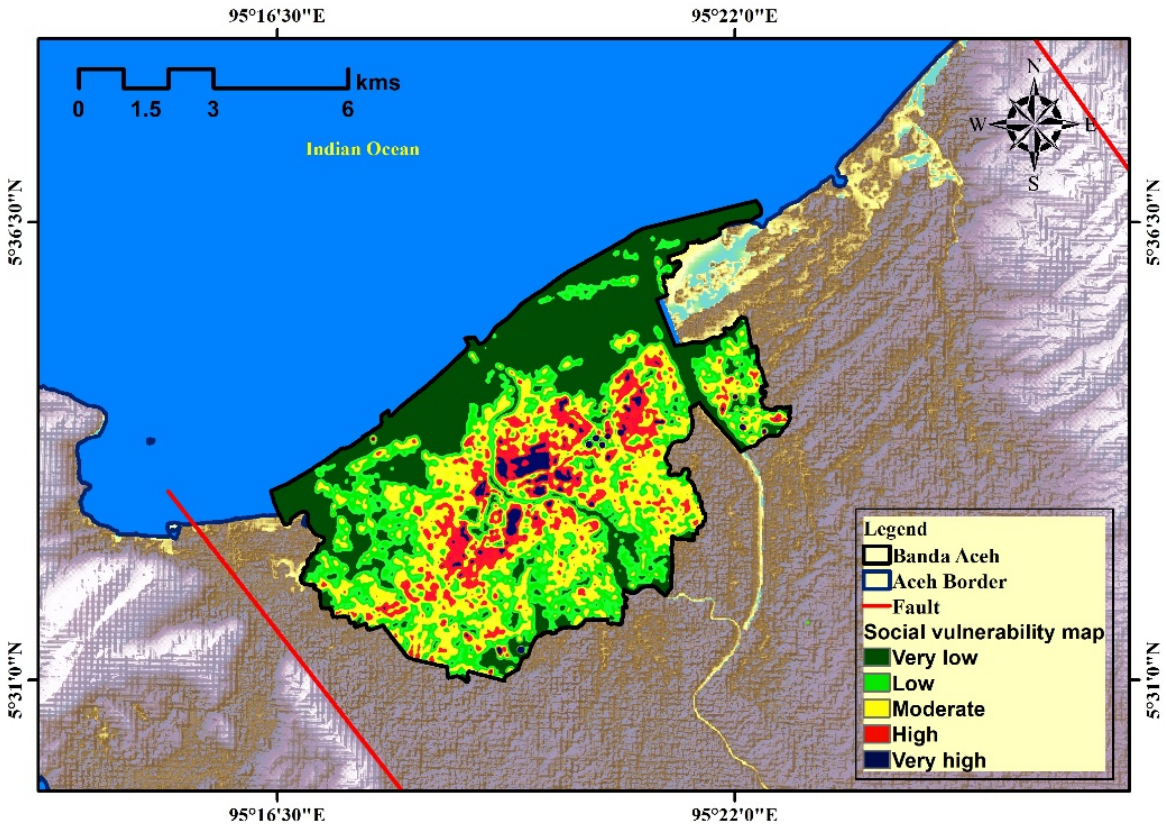

Figure 4.1: Social vulnerability map.

5. The very-high social vulnerability index (characterized by 5.35% area and 10,975 population) describes the central part of the city, which covers zones 3 and 5 that are highly exposed, but may have the capacity to recover soon. Therefore, the focus should be on the high- and medium-vulnerability areas in the city.

4.2.2. Structural vulnerability

The vulnerability of structures was calculated and classified into the five categories of very high, high, medium, low, and very low, as shown in Figure 4.2 and A4. Decision matrix, priority, and rank of all the structural vulnerability criteria were presented in Table 4.2. According to the geographical distribution, infrastructure development and very high vulnerability of residential, commercial, and educational buildings can be found in zones 3 and 5, whereas safe buildings are located in zones 1, 3, 4, and 9.

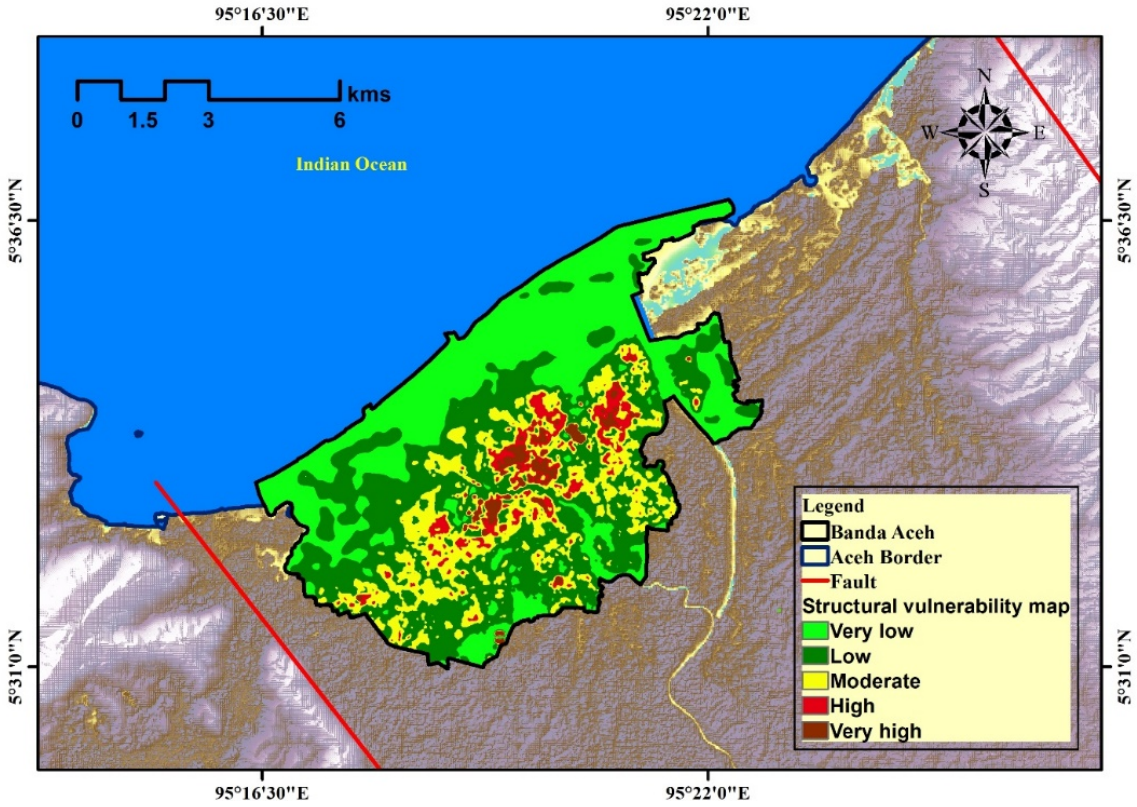

Figure 4.2: Structural vulnerability map.

From a statistical viewpoint, 3.71%, 10.03%, 22.35%, 31.71%, and 32.20% of buildings have very high, high, medium, low, and very low structural vulnerability, respectively. Moreover, the zones where these buildings are located account for 7,173; 24,070; 52,144; 79,370; and 75,590 of the population, respectively (Table 4.5).

Historical research about the city indicates that the main cause of vulnerability or the low vulnerability condition is the existing traditional buildings. Zones 3 and 5, which are considered the center of Banda Aceh City, were not well constructed and some buildings have not been renovated because of their cultural heritage status. Zones 2, 5, 6, and 8 are among the oldest settlements and the structures were not developed on the basis of standards. Furthermore, city boundary expansion in zones 1, 4, and 3 have increased the structural vulnerability of the structures in these locations. Nevertheless, some newly constructed and reinforced buildings in zones 21 and 22 are the major reasons for safe buildings in these locations.

Table 4.2: Decision matrix, priority, and rank evaluation for the criteria of structural vulnerability.

	1	2	3	4	5	6	7	8	9	10	11
1	1	2.00	3.00	3.00	4.00	3.00	3.00	5.00	7.00	6.00	7.00
2	0.50	1	3.00	3.00	4.00	3.00	3.00	5.00	6.00	4.00	6.00
3	0.33	0.33	1	1.00	3.00	3.00	3.00	5.00	7.00	4.00	6.00
4	0.33	0.33	1.00	1	2.00	0.50	0.50	5.00	6.00	4.00	6.00
5	0.25	0.25	0.33	0.50	1	0.33	0.33	3.00	4.00	3.00	4.00
6	0.33	0.33	0.33	2.00	3.00	1	1.00	4.00	6.00	4.00	6.00
7	0.33	0.33	0.33	2.00	3.00	1.00	1	4.00	5.00	4.00	5.00
8	0.20	0.20	0.20	0.20	0.33	0.25	0.25	1	2.00	0.50	2.00
9	0.14	0.17	0.14	0.17	0.25	0.17	0.20	0.50	1	0.33	2.00
10	0.17	0.25	0.25	0.25	0.33	0.25	0.25	2.00	3.00	1	2.00

11	0.14	0.17	0.17	0.17	0.25	0.17	0.20	0.50	0.50	0.50	1

No	Category	Priority	Rank
1	Building density	22.9%	1
2	Building surface area	19.4%	2
3	Offices	13.8%	3
4	Sub district offices	9.0%	6
5	Transportation nodes	5.5%	7
6	Educational institutes	10.1%	4
7	School density	9.7%	5
8	Stadium	2.7%	9
9	Museum	1.9%	10
10	Service centres	3.3%	8
11	Historical places	1.8%	11

Number of comparisons = 55
Consistency Ratio CR = 5.5%
Principal Eigen value = 11.830
Eigenvector solution: 6 iterations, delta = 3.1E-8

4.2.3. Geotechnical vulnerability

The geotechnical vulnerability map was constructed by using the susceptibility of city buildings on the basis of geotechnical factors in Banda Aceh City. Decision matrix, priority, and rank of all the factors were presented in the Table 4.4. This susceptibility is classified into five categories, namely, very high, high, medium, low, and very low (Figure 4.3). The results of the geotechnical vulnerability showed that 11.71% of the entire area with 11,970 population is characterized by very high vulnerability. However, high, moderate, low, and very low vulnerable zones can be found in 15.05%, 40.57%, 25.96%, and 6.69% of the area, respectively (Table 4.6).

Table 4.3: Decision matrix, priority, and rank evaluation for the criteria of geo-technical vulnerability.

No	Category	Priority	Rank
1	Slope	16.9%	3
2	distance from fault	44.3%	1
3	geology	38.7%	2
	Number of comparisons = 3 Consistency Ratio CR = 1.9% Principal Eigen value = 3.018 Eigenvector solution: 4 iterations, delta = 1.9E-10	1 2 3 1 1 0.3 0.50 2 3.00 1 1.00 3 2.00 1.00 1	

Zones 1, 3, 4, 6, and 9 in the northwest areas of the city fall within the low or very low vulnerability. Despite the high slopes in zones 1, 3, 5, and 8, these areas are classified under medium geotechnical vulnerability because of the minimum low PGA values and the low liquefaction probability than the coastal areas.

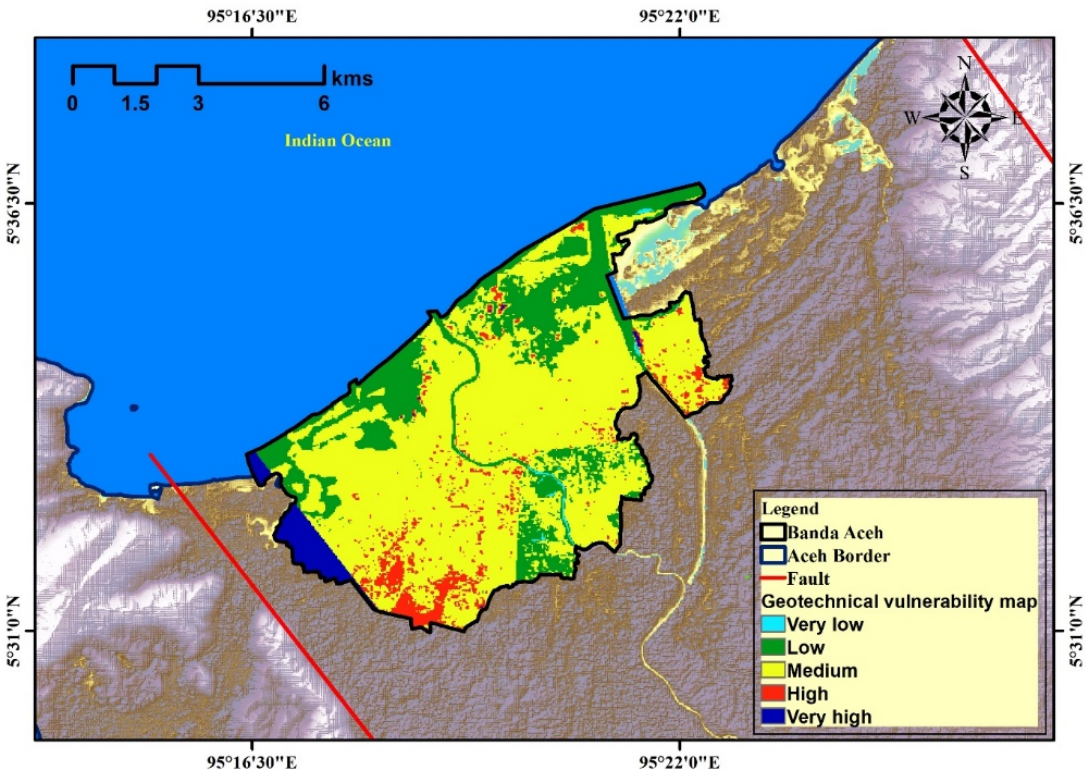

Figure 4.3: Geotechnical vulnerability map.

However, in the southern and some parts of the northeast regions, zones 1, 3, and 7 are considered high vulnerability areas, whereas the southwest regions are considered very high vulnerability because of the fault system, high slope, and high liquefaction susceptibility.

4.2.4. Final vulnerability map

Earthquake vulnerability map was produced using three vulnerable layers explained above. Alternatives were chosen to produce a decision matrix based on the criteria. Three selected alternatives, such as social (population density only), structural (building density only), and geotechnical (distance from active faults only) achieve ranks 1, 2, and 3, respectively. The ranks were calculated by using the normalized decision matrix based on the VIKOR approach. The Si and Ri values obtained are 1, 0.84, 0 and 0.625, 0.558, 0, respectively (Table 4.5). The chosen alternatives were used to understand the importance of alternatives. Decision matrix for ranking the alternatives were presented in Table 4.4**.**

Figure 4.4 presents the final map. The results showed that 3.4% of Banda Aceh City has very high vulnerability, 11.9% has high vulnerability, 23.73% has medium vulnerability, 28.82% has low vulnerability, and 32.20% has very low vulnerability, which constitutes safe areas (Figure 4.4). The central parts of the city and some parts of the north include zones 1, 3, 4, and 9, which are considered locations with very low or no vulnerability. These areas are not affected by steep slopes in the northern parts due to the low PGA amplitude.

Table 4.4: Decision matrix for ranking the alternatives by using the VIKOR method.

Criteria/Alternatives	Social Vulnerability	Structural vulnerability	Geotechnical vulnerability
Social characteristics	0.25	0.5	1
Structural characteristics	0.33	1	2
Geo-technical characteristics	1	3	4
Calculated weights based on AHP approach	0.625	0.238	0.137

Table 4.5: Normalized decision matrix and ranking of alternatives by using the VIKOR method.

				Sj	Rj	Qj	Rank
Social characteristics	0.231	0.156	0.218	1.000	0.625	1.000	1
Structural characteristics	0.305	0.312	0.436	0.840	0.558	0.867	2
Geo-technical characteristics	0.924	0.937	0.873	0.000	0.000	0.000	3
Max	0.924	0.937	0.873	1.000	0.625		
Min	0.231	0.156	0.218	0.000	0.000		

Zone 5 and the north part of the city can be considered the first and oldest settlements of Banda Aceh City. Hence, the buildings here are non-adaptable to the necessary criteria. This limitation is generally attributed to a lack of funding, cultural heritage, and low awareness among residents.

The primary aim of the current study is to describe the earthquake vulnerability of buildings and the population in Banda Aceh City. Conducting an overlay analysis through GIS is important for all the derived vulnerability layers, as depicted in Figure 28, 29, and 30. The results showed that numerous residential buildings situated in zones 1, 2, 3, 5, and 6 exhibited high earthquake vulnerability. Moreover, only a few residential buildings located in zones 9, 7, and 8 are considered very safe.

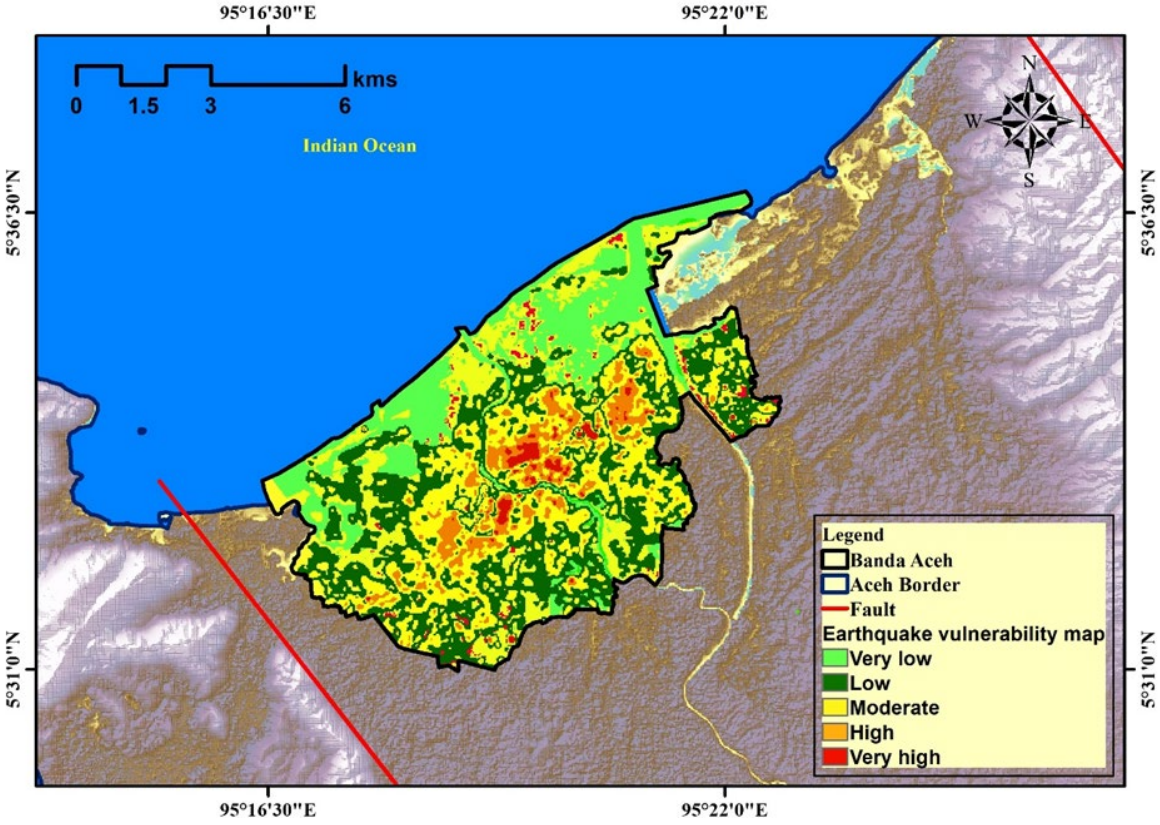

Figure 4.4: Earthquake vulnerability map (EVM) by using the AHP and VIKOR method.

Results show that out of the 59 km^2 of the city, 2 km^2 and 7 km^2 fall under very high and high vulnerability zones, respectively. Moreover, 14, 17, and 19 km^2 of land area fall under medium, low, and very low vulnerability zones, respectively. As the area in very

high vulnerability zones is small, the population in the very high vulnerability zone is approximately 6,573. Figure 4.4 shows a very high vulnerability zone located in the city center. In addition, 25, 070 residents are in the highly vulnerable zone, whereas the rest reside in medium, low, and very low vulnerability areas (Table 4.6).

Table 4.6: Estimation of population and area under vulnerable zones in Banda Aceh City.

	ID	Vulnerability	Area (Sq. Km)	Area (Hect are)	Percentage	Population
Social Vulnerability	1	Very low	16	1610	26.93	62,190
	2	Low	20	2010	33.62	85,155
	3	Medium	12	1220	20.41	48,554
	4	High	8	817	13.66	31,473
	5	Very high	3	320	5.35	10,975
	Total		**59**	**5977**	**100**	**238,347**
Structural Vulnerability	1	Very low	19	1919	32.20	75,590
	2	Low	19	1900	31.71	79,370
	3	Medium	13	1336	22.35	52,144
	4	High	6	600	10.03	24,070
	5	Very high	2	222	3.71	7173
	Total		**59**	**5977**	**100**	**238,347**
Geotechnical Vulnerability	1	Very low	4	400	6.69	2,333
	2	Low	15	1552	25.96	75,544
	3	Medium	24	2425	40.57	109,500
	4	High	9	900	15.05	39,000
	5	Very high	7	700	11.71	11,970

	Total		**59**	**5977**	**100**	**238,347**
Final Vulnerability	1	Very low	19	1919	32.20	75,699
	2	Low	17	1692	28.82	76,587
	3	Medium	14	1446	23.73	54,244
	4	High	7	691	11.86	25,070
	5	Very high	2	229	3.39	6573
	Total		**59**	**5977**	**100**	**238,347**

4.2.5. Discussion

Brooks (2003) stated that labelling communities are not appropriate because some are naturally more vulnerable than other communities. Hahn, Riederer & Foster (2009) further added that vulnerability estimation should be a part of a scheme to empower and engage communities. Alizadeh, Hashim, et al. (2018) applied MCDM tools to predict earthquake vulnerability. They described the performance of the method as well as the quality of the resulting map. They mentioned that communities should make key decisions during disasters to avoid losses. Major building structures in Banda Aceh are old and constructed by using traditional methods, whereas newly developed infrastructures have not been following the construction standards; hence, these buildings are vulnerable to earthquakes. This vulnerability was evident from the 2004 earthquake that hit Banda Aceh City with a magnitude of Mw 9.2. By realizing the importance of building characteristics and data limitations, the developed structural vulnerability map could play an important role in earthquake risk assessment. The demographic context is vital during and after such events. Therefore, social characteristics have a direct interrelation with death, damage toll, and relief facilities.

During the last decade, experts have not paid enough attention to the issue associated with social characteristics, and not much work has been performed on this viewpoint in the aftermath of the 2004 earthquake. However, geotechnical features are influential in increasing the scope of vulnerability during an event. Geotechnical specifications, such as strong ground motion specifically controlled by the complex combination duration, frequency, distance from hypocenter, magnitude, slope, lithology, distance from the fault, and curvature, can be used to understand the history of Banda Aceh. Thus, consideration of PGA while designing structures, which is the major reason for building damages, is vital (Panahi, Rezaie & Meshkani 2014). Sometimes, an unstable steep slope as the foundation of a structure can cause a landslide, earthquakes, and liquefaction in alluvial and sandy lithotypes (Sarvar, Amini & Laleh-Poor 2011). Therefore, these vulnerable layers are important to be noticed, which can lead to destruction and an increase in damages.

The key weakness of analyzing vulnerabilities is the assessment of people's weaknesses without focusing on their capabilities. For example, we can consider a disabled female more highly vulnerable than a disabled male. This assumption and ignorance will affect vulnerability results. Figure 4.5 shows the results of the population and areas under vulnerable zones. However, the figure shows that the population increases with the decrease in vulnerability, whereas the area increases while a decrease in vulnerability occurs. In Figure 4.6, the total injury and fatalities in Indonesia and Banda Aceh were plotted. Compared with the vulnerability results obtained in this study, more fatalities and injuries were recorded during the intensity 9 and magnitude Mw 7.0 earthquake in Aceh in Sumatra and Java. Three zones of fatalities were identified on the basis of earthquake magnitudes and depths in Figure 4.6d. Fatalities are high if the focus of earthquakes is

found at a depth of 0 to 50 km.

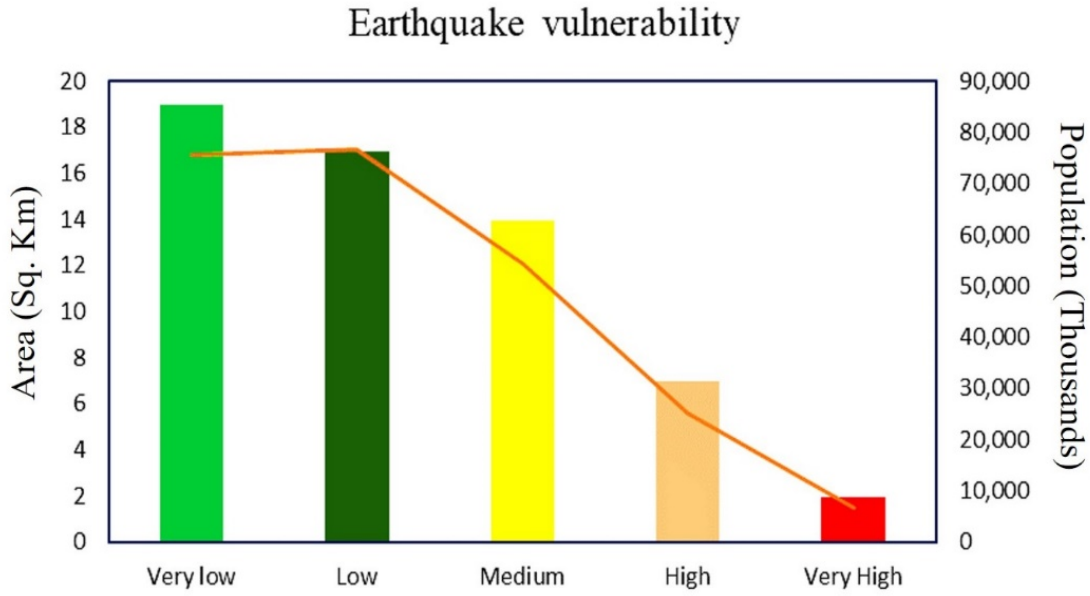

Figure 4.5: Graphical presentation of earthquake vulnerability with area and population.

Therefore, the focus should be on high and medium vulnerability zones with high fatalities, because the population is minimal in very high vulnerable zones, which are located in the city center. In addition, the central region has the capacity to mitigate and recover before and after an earthquake. Each property and life need to be considered in analyzing vulnerabilities. Understanding these vulnerabilities will help mitigate earthquake disasters in the near future. Vulnerability should be compounded, or consider more than one indicator of vulnerability, such as level of education, a person with a disability, building characteristics, and geological factors.

Implications on integration programs: Integration of earthquake risk reduction programs with various development programs are needed to reduce the social, environmental, and economic impact of disasters (Iemura et al. 2006). The current study has revealed three

main contributing factors responsible for very high vulnerability, namely, “building

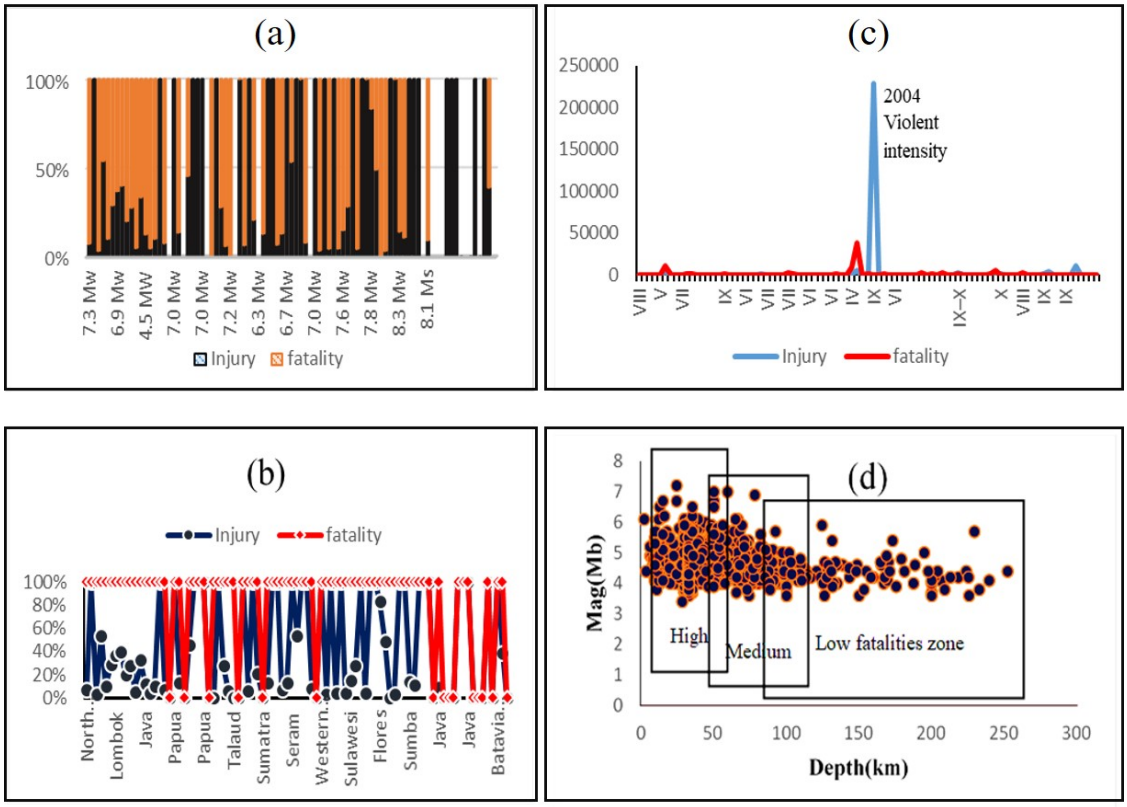

Figure 4.6: Injury and fatalities in Indonesia due to earthquakes on the basis of; a) Magnitude, b) Location, c) Intensity, and d) Depth.

characteristics,” “population growth,” and “household characteristics.” Therefore, focusing on mitigation, preparedness, and response and recovery programs is important.

4.2.6. Validation

Validation of the current developed EVA map reveals that by applying the building inventory and zonation hazard data with implementing spatial analysis, building hazard in Banda Aceh has been assessed by Irwansyah & Hartati (2014) during the 2004 earthquake. According to their result, 95% of the total number of buildings, includes 36,312 of units that fall under the low hazard zone, whereas less than 3% includes 1,051

units under the high hazard zones. Jena et al. (2019) described in their recent study on earthquake risk assessment in Banda Aceh that very high and high-risk areas account for 7.23% and 15.31% to the total city area, respectively, and the central part is more vulnerable than coastal areas.

Therefore, the results are compared with the previous studies that show that approximately 3.4% of area including educational facilities, residential houses, religious facilities, and commercial buildings fall under the very high vulnerability zone. Moreover, 11.9% of area under the high vulnerability zone surrounds the very high vulnerability zones. Irwansyah & Hartati (2014) showed that residential and commercial buildings occupy the largest area in the city center and obtained as a high-risk zone of approximately 9.885 km^2 of the total area, which is located in the city center. Therefore, our method is more effective because the study implemented a complete set of data by using a robust technique to assess vulnerability.

4.3. Objective 2

4.3.1. Probability estimation using MLP

MLP calculates the information based on the training data. MLP executes the analysis of a non-parametric regression between the input and dependent variables finally in the system that were recognized by an output neuron. MLP was applied to map the earthquake probability in Banda Aceh. The probability results indicate that the training accuracy was reasonably good with a total prediction of 616 earthquake points out of 624. The approach was unable to predict the other eight earthquakes because of the noise in the probability indicators.

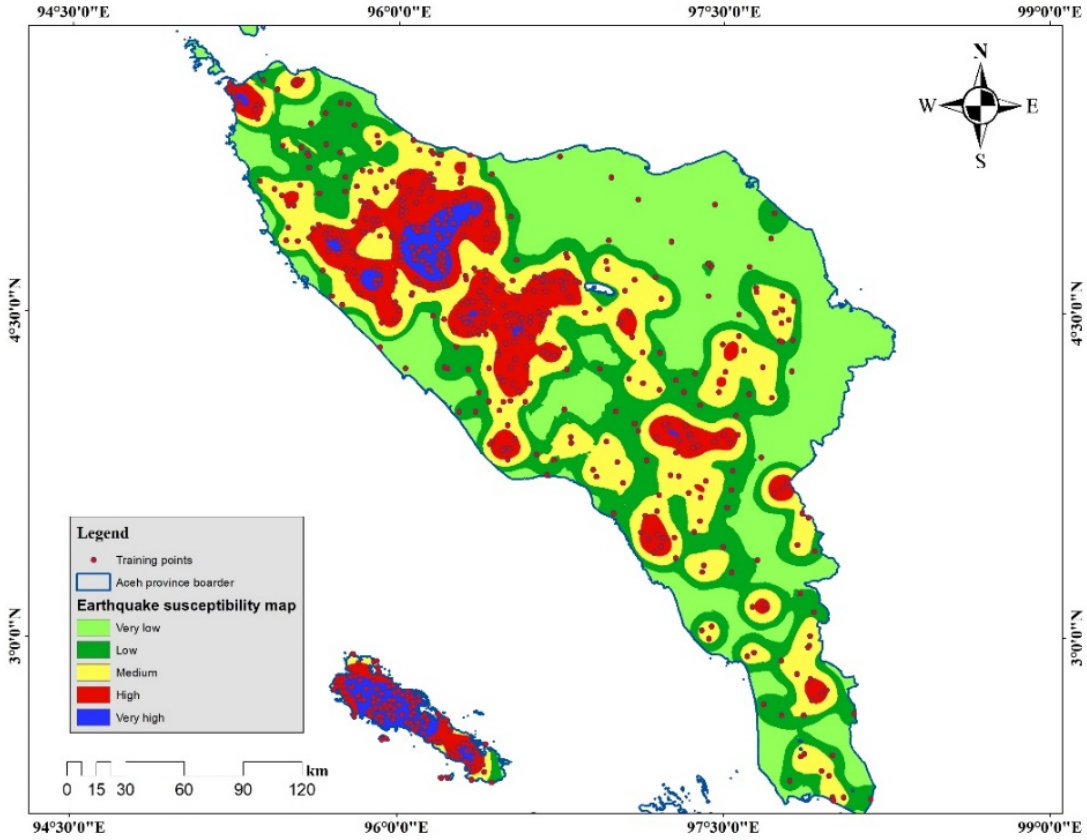

Figure 4.7: Training data used for earthquake probability mapping.

The total prediction was out of 1546 training points characterized by both earthquake and non-earthquake points in Aceh province, as presented in Figure 4.7. The total area predicted from the network under risk is approximately 608400 m^2 in Aceh province. Then, the model tested for the study area of Banda Aceh as the capital of Aceh province. The true positive rate (TPR) and false positive rate (FPR) that was obtained the Banda Aceh were 0.84 and 0.13, respectively. The rate of 0.13 shows that each time we call for a positive, we obtain this specific probability of being wrong. Therefore, this value is called the false positive rate. Likewise, a true negative rate can be analyzed. The graphical representation of accuracy is presented in Figure 4.8.

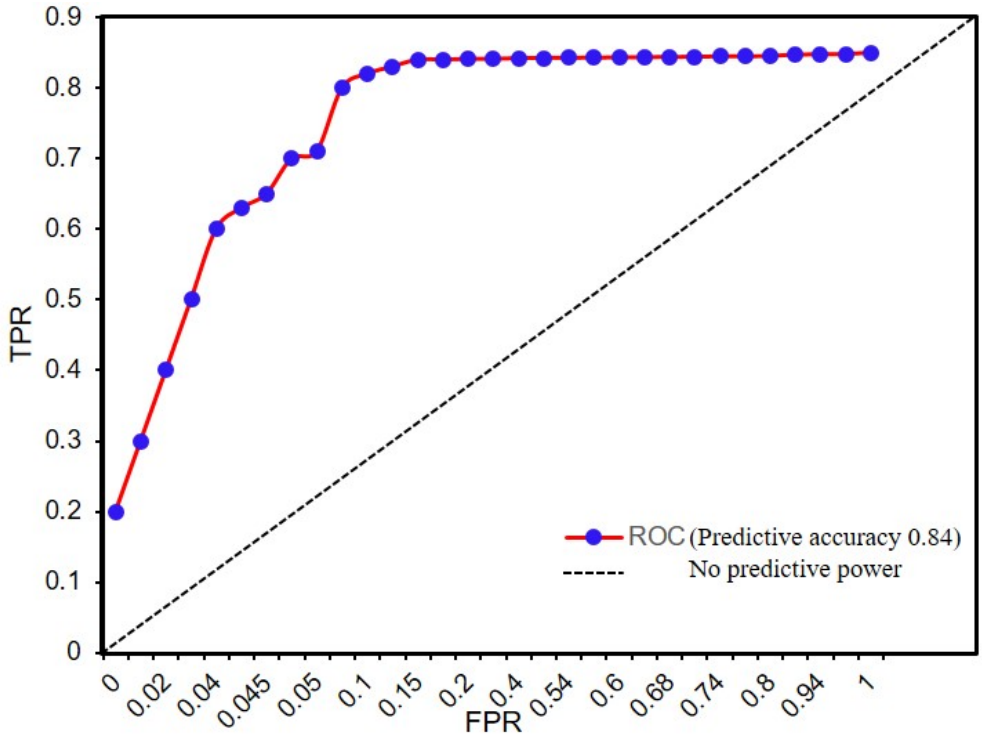

Figure 4.8: Accuracy assessment curve for the earthquake probability map.

The details of TPR, FPR, 1-FPR, TF, threshold, and crossover are listed in Table 4.7. The accuracy of the prediction was 0.84 with RMSE 0.3. Given that the city is very small and is located near the GSF with no evidence of historical earthquakes, the seismic gap in Aceh province may experience future earthquakes. However, the high probability areas can be found in the SE corner of the city, and low probability can be found towards the NW corner of the city as per the resultant probability map. The map explains the potential zone for earthquakes within the city, as presented in Figure 4.9. The SE region of the city found to have a very high probability, whereas the NW part of the city falls under very low probability. The reason behind the high probability in this region is the high fault density, epicenter density, magnitude density, and low distance from the active fault along with high height and amplification value as the city is mostly covered with quaternary sedimentary rocks. The low probability of the NW part of the city is because of low

epicenter, magnitude, and active fault density, along with low height and slope.

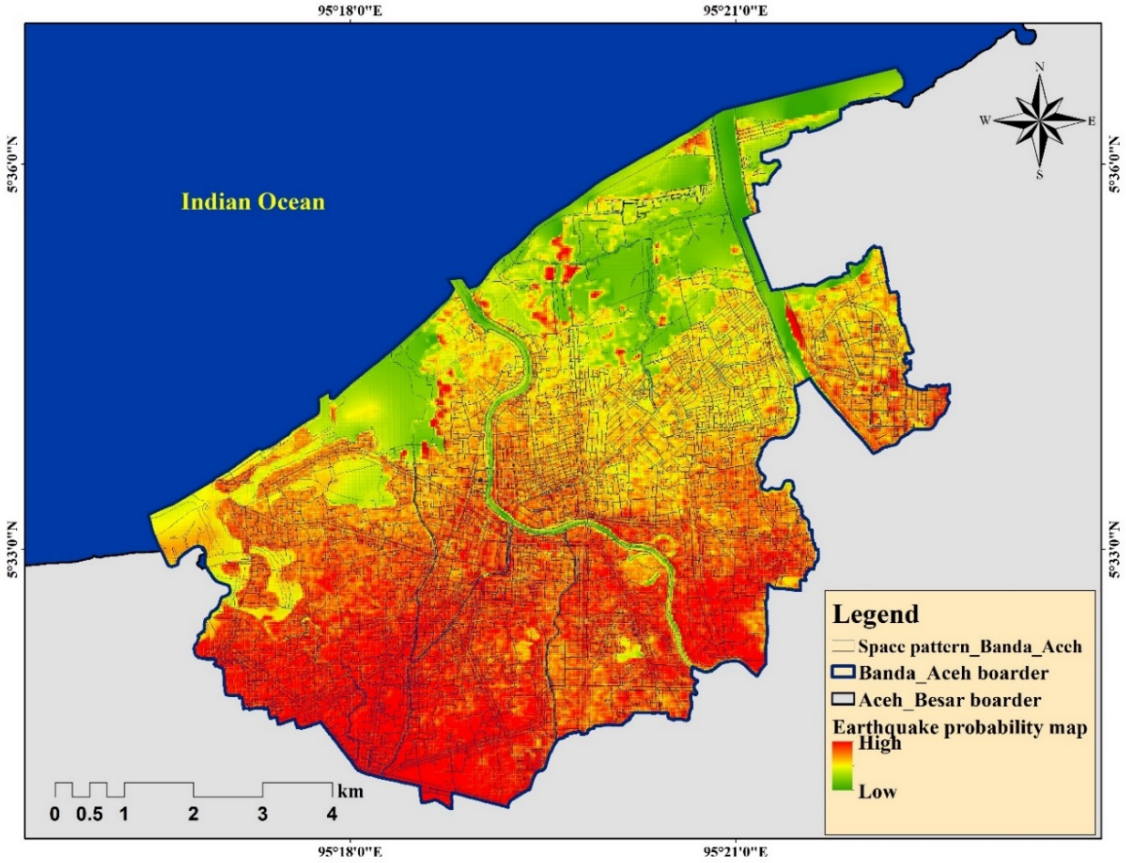

Figure 4.9: Earthquake probability map.

Table 4.7: Prediction results using ANN.

False positive rate (FPR)	True positive rate (TPR)	1-FPR	TF	Thresholds	Crossover
0.132982	0.848876	0.867018	-0.048142	1	1
Total Pixels belong to Earthquake Predicted: 616 earthquakes out of 1546 training points of Aceh province The Total Area Under Risk: 608400 m2 in the Aceh province					

4.3.2. Hazard estimation

A hazard map was developed using the probability map and presented in Figure 4.10. The main objective of the hazard map is to provide information on the extent of possible damage and the activities of disaster prevention. The most important point is to provide residents with comprehensible information through hazard maps. The level of danger of an earthquake can be understood by its intensity. The intensity pattern in the study area can be defined on the basis of the historical records of destructive earthquakes and statistical calculations. Near Banda Aceh along the GSF, high-intensity earthquakes may occur occasionally.

This study calculated how high the level of destruction can be in case of such high-intensity earthquakes. Therefore, it is assumed that when the earthquake intensity becomes more than 9, the hazard will be very high, whereas the intensity 8–9 will be considered high hazard areas, 8–7 is considered medium, 7–5 is low, and below 5 is very low. The hazard map was classified into five different classes based on the quantile classification technique. The results indicate that very high hazard can be found in the SE part of the city and very low hazard in the NW part because of high magnitude earthquakes near the SE part of the city. This type of hazard map is the basic map for the administrative agencies that can be used for disaster prevention services. These maps are used to develop an evacuation and warning system, as well as available facts for land use regulations. These maps can also be used in inhibitory works.

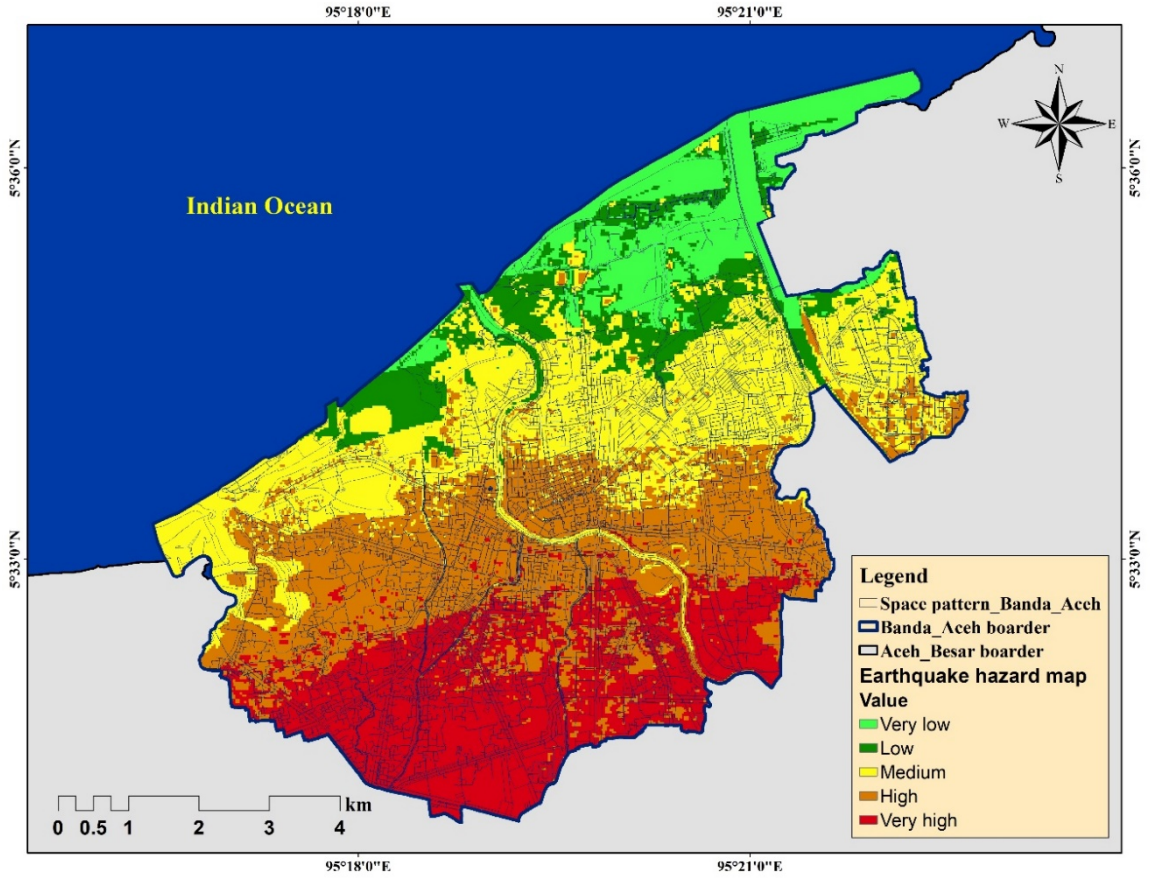

Figure 4.10: Earthquake hazard map.

For the results described in this section, it can be recognized that the better capabilities of a neural network for earthquake prediction and probability modeling characterized by nonlinear and complex relationships among the variables is a developed model to handle variable interactions. Neural networks are not an easily understandable model, but they become complicated with a large number of variables. The performance results explained in this study indicate that the potential of a neural network can be useful for earthquake probability mapping in other study areas and is worthy of further investigation.

4.3.3. Vulnerability index estimation

Integration and aggregation of the various significant indicators described in the data table are included in the tree of the AHP approach. Table 4.8 shows the process and the criteria weights in the hierarchical tree. The calculated rank of criteria, as well as the eigenvalues and consistency ratios, are presented in Table 4.9. The experts can understand the resulted weights and ranks for various criteria by the preliminary investigations, and they can monitor the AHP approach adaptation and review the obtained vulnerability map and the associated uncertainties, thereby approving the resulting map. The vulnerability assessment considered all the layers, analyzed the significance of all the layers using the AHP ranking approach, and applied them to GIS for the vulnerability mapping.

Table 4.8: Decision matrix for vulnerability assessment

Category name	1	2	3	4	5	6	7	8	9	10	11
Building density	1	3	0.33	3	4	2	3	5	3	0.25	2
District office	0.33	1	0.25	2	3	1	0.5	1	1	0.25	1
Educated people density	3	4	1	5	5	3	3	4	3	0.5	4
Environmental infrastructure	0.33	0.5	0.2	1	1	0.33	0.33	0.5	0.25	0.2	0.5
Stadium	0.25	0.33	0.2	1	1	0.33	0.33	0.5	0.33	0.2	0.33
Distribution of universities	0.5	1	0.33	3	3	1	3	3	2	0.33	2
Distribution of Chiefs	0.33	2	0.33	3	3	0.33	1	3	2	0.25	2
Distance from service centers	0.2	1	0.25	2	2	0.33	0.33	1	1	0.2	0.33
Major offices	0.33	1	0.33	4	3	0.5	0.5	1	1	0.25	2
Population density	4	4	2	5	5	3	4	5	4	1	5
Transport nodes	0.5	1	0.25	2	3	0.5	0.5	3	0.5	0.2	1

Table 4.9: Evaluation of weights and rank of layers.

Category	Name	Priority	Rank
1	Building density	12.8%	3
2	District office	5.3%	8
3	Educated people density	19.2%	2
4	Environmental infrastructure	2.8%	10
5	Stadium	2.6%	11
6	Distribution of universities	9.3%	4
7	Distribution of Chiefs	7.6%	5
8	Distance from service centers	3.9%	9
9	Major offices	6.0%	6
10	Population density	24.9%	1
11	Transport nodes	5.4%	7
	Number of comparisons = 55 Consistency Ratio CR = 0.04 Principal Eigenvalue = 11.728 Eigenvector solution: 5 iterations delta = 3.3E-8		

The resultant vulnerability map (Figure 4.11) was acquired by the processing of several vulnerable indicators. In total, 55 comparisons were made with the resultant CR of 0.04. The principal eigenvalue was 11.728 based on the analysis, and the eigenvector solution was five iterations. Mathematically, an eigenvalue that should be non-zero, which corresponds to an eigenvector, points in a direction that is stretched by the transformation. The eigenvalue is the factor by which it is stretched. A negative eigenvalue represents a reverse direction. However, the CR shows that the importance of all the layers is evaluated carefully and accurately. The delta value of 3.3E-8 was obtained from AHP in this analysis. Population density, educated people, and building density were ranked as 1, 2, and 3, with weights of 24.9%, 19.2%, and 12.2%, respectively. The lowest rank was

obtained by environmental infrastructure and stadium, whereas the remainder were ranked medium. The resultant map was classified into five different categories according to experience: very low, low, medium, high, and very high. The results indicate that the mapped areas can be calculated using the option of geometry. Very high vulnerability can be found in the south-central part of the study area because of the high building and population density, along with the government offices and educated people density. Very low vulnerability was observed in the NW part because of the reverse conditions in the region. Therefore, our map is good and useful for national and local government organizations in their vulnerability mapping.

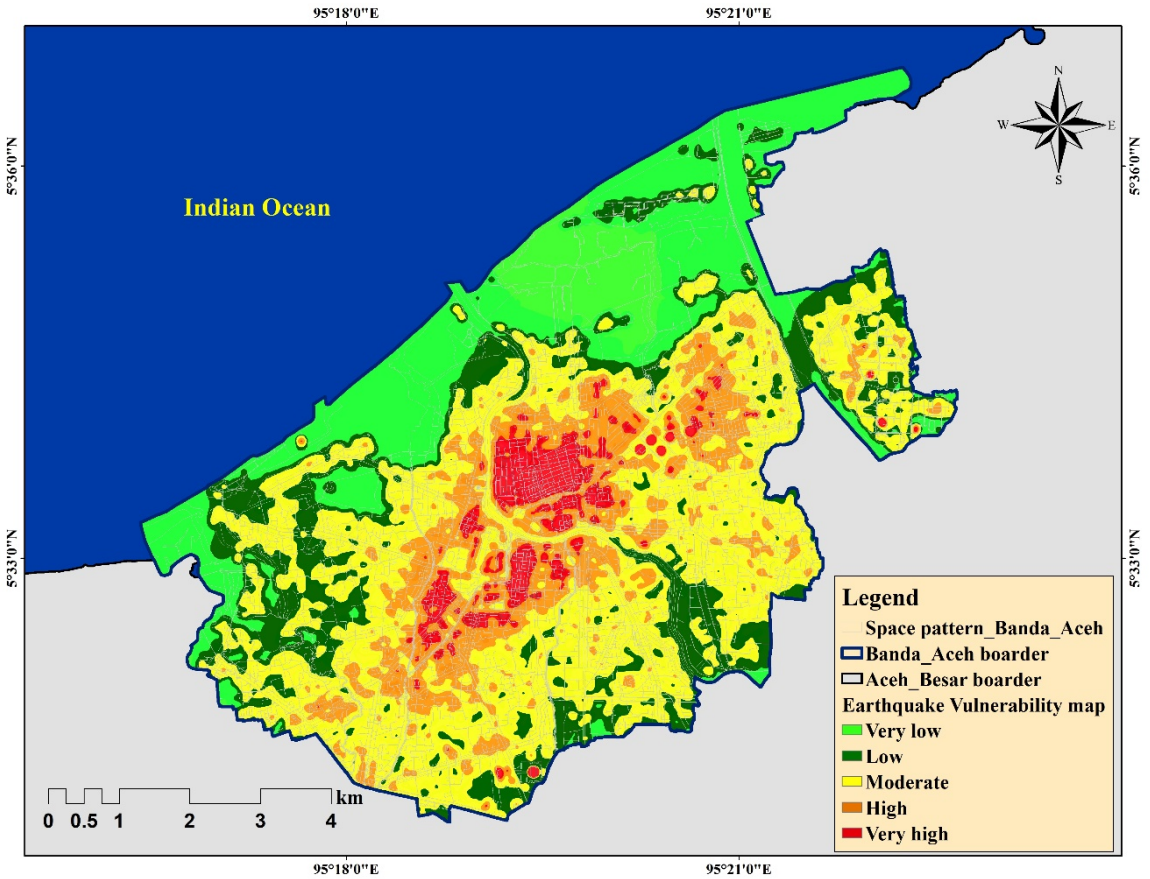

Figure 4.11: Earthquake vulnerability map.

4.3.4. Risk estimation

An earthquake risk map was prepared for Banda Aceh by multiplying the hazard and vulnerability map. The resultant map was classified into five classes by using the quantile classification technique (Birkmann & Welle 2015). Therefore, the areas of all the classes were calculated for the city and for different zones within the city. The geometry showed that 7.23% of the entire area was under extreme risk. High, moderate, low, and very low-risk zones represent 15.31%, 20.99%, 28.70%, and 27.72% of the total area, respectively (Table 4.10). On the basis of the geographic position, the east-southern part of the city, comprising zones 2, 3, 5, 6, and 7, represent the regions with moderate risk. Given the few people and low infrastructure in the zones, 1, 4, 9, and some parts of 3 and 8, the risk chances are low.

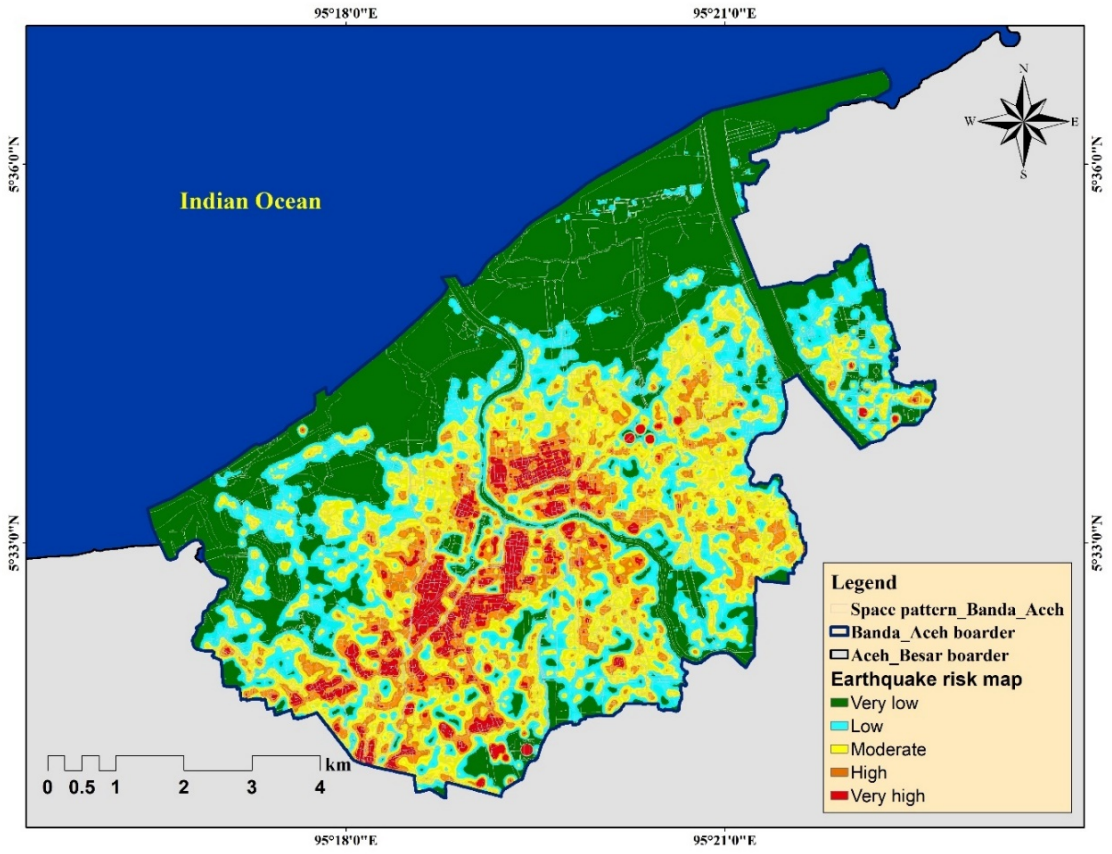

Figure 4.12: Earthquake risk map.

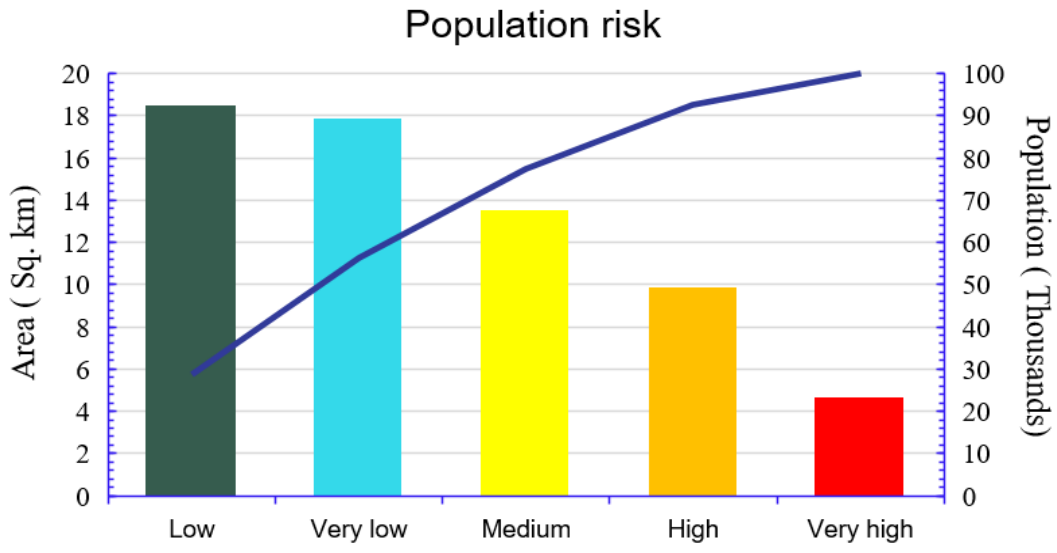

Figure 4.13: Estimated number of population and area within the risk zones.

However, in the south to central regions of the city, zones 3, 5, 7, 8, and some parts of 6 are considered high-risk areas because of the high population density, building density, educated people, government offices, and proximity to the seismic gap of GSF. By simply understanding the vulnerable and hazard zone size and area, one can obtain the impact level of the probable future earthquakes. Therefore, population data of Banda Aceh were used for estimation of the population risk. Thus, risk mapping was conducted in all nine zones of Banda Aceh, as illustrated in Figure 4.12 and graphically presented in Figure 4.13.

The most clustered risk zones are identified. Overall, three zones are considered highly risky areas; the main reason is their geographical location and high population. The detailed calculations of earthquake population risk and area risk for nine different zones and for the entire area are presented in Tables 4.11 and 4.12, respectively.

The issues can be understood by the following five main situations.

1. Areas with very high population, structural, and geotechnical vulnerability comprise 7.23% risk area of the total area. The most at-risk zones are located, as per the results, in zones 3, 5, and 7; either demolition or reconstruction of poor quality buildings are required.
2. The highest number of buildings can be found in the central part of Banda Aceh. However, buildings are situated in zones 2, 3, 5, 7 and 8, and their risk can be reduced by retrofitting and modification based on seismic ground shaking.
3. Moderate risk from geotechnical, structural, and social indicators is found in nearly 20.99% of the city area. Populations in zones 1, 2, 6 and some parts of zones 3, 5, 7 are under moderate risk. Retrofitting or, occasionally, destruction or renovation of the buildings can reduce risk.
4. Populations with low risk can be found in 28.70% of the city. The buildings in zones 1, 2, 6, 8, and 9 are safe and not particularly vulnerable.
5. An extremely low density of residential buildings with low population, which showed very low risk, comprise approximately 27.72% of the total area. By considering the circumstances of structural and geotechnical data, the buildings in this area are under less risk than those in other classes.

Table 4.10: Estimated earthquake population risk and area.

ID	Risk	Area (Sq. km.)	Hectare	Percentage	Population in risk
1	Very low	17.894	1789.46	27.72	65167
2	Low	17.524	1752.40	28.70	76268
3	Medium	12.55	1255.80	20.99	47981
4	High	9.885	988.56	15.31	32363
5	Very high	4.669	466.92	7.23	14018
Total		62.53	6253.14	100	235,797

Table 4.11: Estimation of earthquake risk area of Banda Aceh.

ID	Risk	Area(Km^2)	Hectre	Percentage	Zone	Name
2	Low	4.764	476.4	32.89		
1	Very low	8.962	896.2	61.88		Syiah Kuala
3	Medium	0.735	73.5	5.075	1	
4	High	0.022	2.2	0.15		
			1448.3	**100**		
3	Medium	2.73	281.9	55.6		
2	Low	2.2	220	43.4	2	Ulee Kereng
4	High	0.05	5	0.99		
			506.9	**100**		
1	Low	1.981	198.1	21.2		
2	Very low	3.365	336.5	36.024		
3	Medium	1.923	192.3	20.586	3	Kuta Alam
4	High	1.092	109.2	11.69		
5	Very high	0.98	98	10.49		
			934.1	**100**		
1	Very low	1.347	134.7	37.89		
2	Low	1.436	143.6	40.39		
3	Medium	0.582	58.2	16.37	4	Kutaraja
4	High	0.179	17.9	5.035		
5	Very high	0.011	1.1	0.309		
			355.5	**100**		
4	High	2.5	250	22.32		
5	Very high	2.53	253	22.7		
3	Medium	1.53	153	8.27	5	Baiturrahman
2	Low	1.1	110	45.8		
			766	**100**		
2	Low	1.771	177.1	27.75		
3	Medium	1.939	193.9	30.38		
4	High	2.487	248.3	38.906	6	Lueng Bats
5	Very High	0.189	18.9	2.96		
			638.2	**100**		
2	Low	0.592	59.2	12.82		
4	High	2.145	214.5	46.63		
3	Medium	1.599	159.9	34.76	7	Banda Raya
5	Very high	0.264	26.4	5.74		
			460	**100**		
3	Medium	1.24	124.83	26.71		

4	High	1.26	126.27	27.024		
5	Very high	0.66	66.95	14.32	8	Jaya Baru
2	Low	1.30	130.94	28.023		
1	Very low	0.18	18.26	3.907		
			467.25	**100**		
1	Low	3.38	338.42	38.06		
2	Very low	4.04	404.14	45.45		
3	Medium	1.27	127.57	14.34	9	Meuraxa
4	High	0.15	15.46	1.74		
5	Very high	0.035	3.525	0.40		
			889.115	**100**		

Table 4.12: Estimation of population under risk in nine zones of Banda Aceh.

ID	Risk	Area (Sq.km)	Population in risk	Percentage	Zone	Name
2	Low	3.38	12309	39		
1	Very low	4.04	14713	45.5		
3	Medium	1.27	4625	14.44	9	Meuraxa
4	High	0.15	546	1.754		
5	Very high	0.035	127	0.45		
			32322	**100**		
3	Medium	1.24	5837	37.41		
4	High	1.26	4588	27.024		
5	Very high	0.66	1082	3.627	8	Jaya Baru
2	Low	1.3	4734	28.023		
1	Very low	0.18	655	3.907		
			16898	**100**		
5	Very high	0.592	2156	11.843		
4	High	2.645	9633	52.91		
3	Medium	1.499	5459	29.97	7	Banda Raya
2	Low	0.264	961	5.27		
			18210	**100**		
2	Low	1.771	7449	32.14		
3	Medium	1.939	8061	34.79		
4	High	2.487	6966	30.06	6	Lueng Bats

5	Very high		0.189	694	2.99		
				23170	**100**		
4	High		2.53	6292	22.75		
5	Very high		2.50	6351	22.96		
3	Medium		1.53	2295	8.30	5	Baiturrahman
2	Low		1.1	12710	45.97		
				27648	**100**		
1	Very low		1.347	4906	37.89		
2	Low		1.436	5230	40.39		
3	Medium		0.582	2119	16.37	4	Kutaraja
4	High		0.179	652	5.035		
5	Very high		0.011	40	0.309		
				12947	**100**		
1	Low		1.981	7214	21.2		
2	Very low		3.365	12255	36.024		
3	Medium		1.923	7003	20.586	3	Kuta Alam
4	High		1.092	3977	11.69		
5	Very high		0.98	3569	10.49		
				34019	**100**		
3	Medium		2.72	9906	53.66		
2	Low		2.2	8312	45.02	2	Ulee Kereng
4	High		0.05	242	1.31		
				18460	**100**		
2	Low		4.764	17350	32.89		
1	Very low		8.962	32639	61.88	1	Syiah Kuala
3	Medium		0.735	2676	5.075		
4	High		0.022	80	0.15		
				52747	**100**		

4.3.5. Validation

Validation of the resulted probability map was implemented in sequence to examine the accuracy in Figure 4.14. The trained model of Aceh province was obtained and converted to a probability map of Aceh using GIS. The trained earthquake probability map was presented with five different classes to recognize various zones of probability, as previously shown in Figure 4.7. A well-constructed map accurately shows the domain of interest. If we consider the location of Banda Aceh in the trained map of probability, then we can understand that the result of Banda Aceh matched with the trained map. Not achieving such accuracy may occur when using standardized/classified data.

The total number of training points of earthquakes and the surrounding earthquakes of Aceh province were also used to validate the result. Mostly, the earthquakes were focused on the east, west, and southern regions of Banda Aceh. Therefore, it can be observed that the resultant probability map has a high probability of earthquake occurrence towards the east, west, and southern regions. The histogram of earthquake probability was also presented to understand the flow of probability from one part of a city to the other parts. Hence, the domain mentioned here in this study can be notably seen in the output that represents compatibility and flexibility, proven with a human perspective. To validate the model results of integrated ANN–AHP following the literature review, historical earthquake probability mapping results, historical events, and earthquake impacts must be considered. However, on the basis of the model accuracy of ANN and the CR of AHP, our proposed result is significantly good.

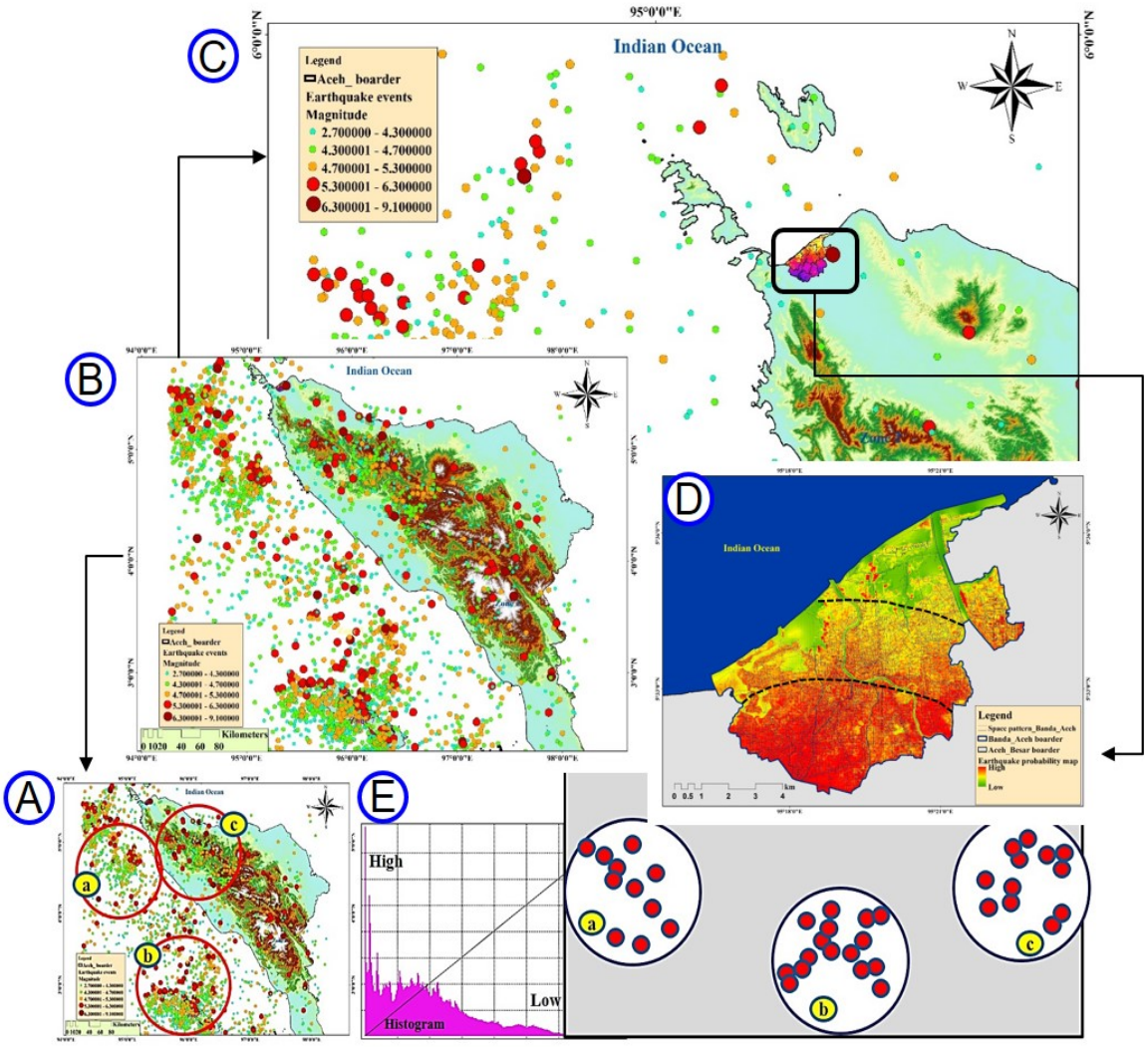

Figure 4.14: Validation of earthquake mapping result: A. Earthquake events in Aceh province (set of earthquakes in different zones of a, b, c); B. Zoomed image of Aceh with earthquakes; C. Position of Banda Aceh and events in Aceh province; D. Earthquake probability map and presented as low to high with the set of earthquakes to validate the Probability result; E. Histogram of probability map that shows the high and low probabilities.

4.4. Objective 3

4.4.1. Crustal fault and subduction zone characteristics

Two main sources of active faults are found in Indonesia, which generate high magnitude earthquakes of more than 7 Mw (Table 4.13). A conservative probabilistic approach was used to reveal the slip rate, fault length, dip angle, and expected magnitude. Magnitude (Mmax) was used to plot versus slip rate (Blaser et al. 2010). The results showed that the slip rate varies from 5 to 55 mm/year, and all the slip rate of faults can generate events with more than 8 Mw (Figure 4.15a). A correlation was observed between the dip angles and length of faults. The dip angle is high when the fault length is small and vice versa, as presented in Figure 4.15b.

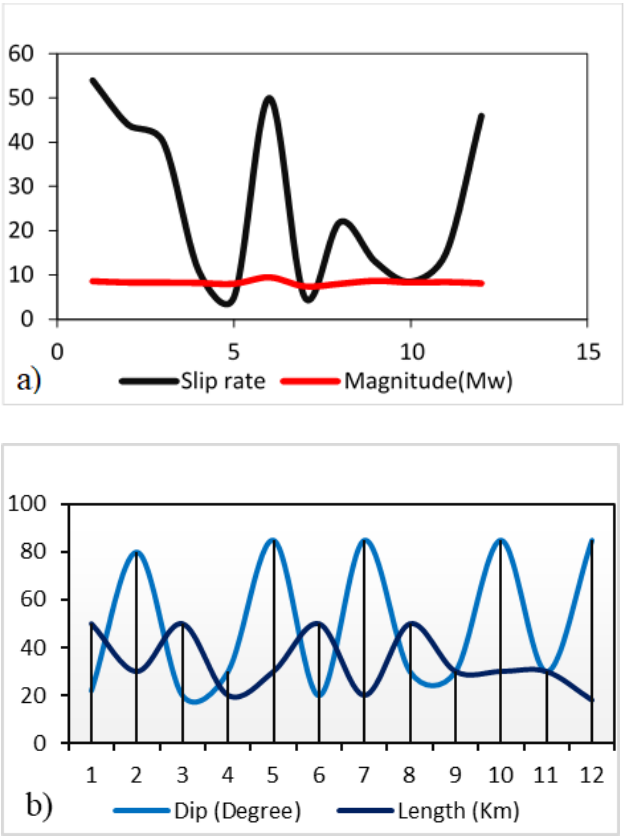

Figure 4.15: (a) Average slip rate and maximum magnitude earthquake observed in crustal and subduction area faults. (b) Average fault dip and length below the ground surface.

Table 4.13: Types of fault and magnitude generating capacity with slip rates in Indonesia.

No	location	source	Fault type	Dip(Km)	Top (Km)	Bottom	Slip rate	Mw	Sources
1	North Sulawesi	Subduction	Thrust	22	3	50	20, 54	8.2, 8.4, 8.6	Irsyam et al. (2008, 2010); Burbidge et al. (2008); USGS; NGDC
2	Palu	Crustal	Strike-slip	80	3	30	30,35,44	7.9, 8.1, 8.3	
3	Seram	Subduction	Thrust	20	3	50	40	7.9, 8.1, 8.3	
4	South Seram	Crustal	Normal	30	3	20	11	7.8, 8.0, 8.2	
5	Semangko	Crustal	Strike-slip	85	3	30	5	7.6, 7.8, 8.0	
6	Sunda Arc	Subduction	Thrust	12-20	3	50	30-50	9.5 (8.3-9.5)	
7	Sunda strait	Crustal	Strike-slip	85	3	20	5	7.0, 7.2, 7.4	
8	Timor	Crustal	Thrust	30	3	50	8,15,22	7.6, 7.8, 8.0	
9	West Molluccca	Crustal	Thrust	30	3	30	13	8.3, 8.5, 8.7	
10	West Sorong	Crustal	Strike-slip	85	3	30	8.5	7.9, 8.1, 8.3	
11	Wetar	Crustal	Thrust	30	3	30	15	8.0, 8.2, 8.4	
12	Yapen	Crustal	Strike-slip	85	3	18	46	7.7, 7.9, 8.1	

4.4.2. Predictive performance, probability, and hazard mapping

The ML algorithm of the implemented ANN model was used for earthquake probability mapping in Banda Aceh. The probability maps were derived using the trained ANN model with experienced earthquake points, which included the locations and medium to high magnitude events with different depths. These maps represent the likelihood of

occurrence of continuous events and the probability of exceeding a specific magnitude based on organized conditioning factors. The results showed that the training accuracy is acceptable, where 1210 points are successfully predicted out of 1248 events on average, and the total training points are 1810. The model did not predict the extra 38 points because of noise and data heterogeneity in probability input layers. The model approximately predicted 567 100 m^2 of area as probable for events in Aceh. Masking of the likely classes of Banda Aceh was obtained and reclassified to five different categories based on quantile classification (Pradhan, Moneir & Jena 2018). Banda Aceh was tested based on the ANN CV fold two. The true positive rate was 0.85, and RMSE was 0.18 for Banda Aceh. The accuracy curves for all the four folds were obtained as 81%, 85.4%, 81.3%, and 83%, respectively, as shown in Table 3.2. Jena et al. (2019) achieved an 84% accuracy in earthquake probabilistic assessment using ANN. The ROC curve is plotted and presented in Figure 4.19a.

For the probable spatial distribution of predicted classes, the probability of earthquake occurrence is high in the northwest and southeast areas, as shown in Figure 4.16. Quantile classification was applied in this analysis to generate five different classes of the nearest values divided through breakpoints (Tehrany, Pradhan & Jebur 2013). Although this method is not the standard for classifying the probability map, still it can be observed that the values are close to each other for earthquake probability mapping. Banda Aceh is a small city with a seismic gap in Aceh Province that may be struck by future events. The high probable areas observed in the city are located in the SE to the NE corner. Medium probability is observed by surrounding the probable high zone toward the west direction. The resultant probability map suggests that the probability decreases toward the coastal areas. The leading cause of high probability toward the eastern part of the city is

associated with high fault density, epicenter, and magnitude density, and the proximity to the active fault is low. Highest amplification can be observed toward the coastal part. The entire city is characterized by quaternary sedimentary rocks, making the city probable toward the east. Opposite conditions for the low likely areas can be recognized. For hazard assessment, hazard increases, and intensity crosses 9 at the intensity scale. Intensities of 8–9, 8–7, 7–5, and less than 5 can be considered as high, moderate, low, and very low. Intensity depends on magnitude and is associated with vulnerable factors. The observed potential zones in Aceh Province could provide necessary information about the occurrence of high magnitude events (Figure 4.16).

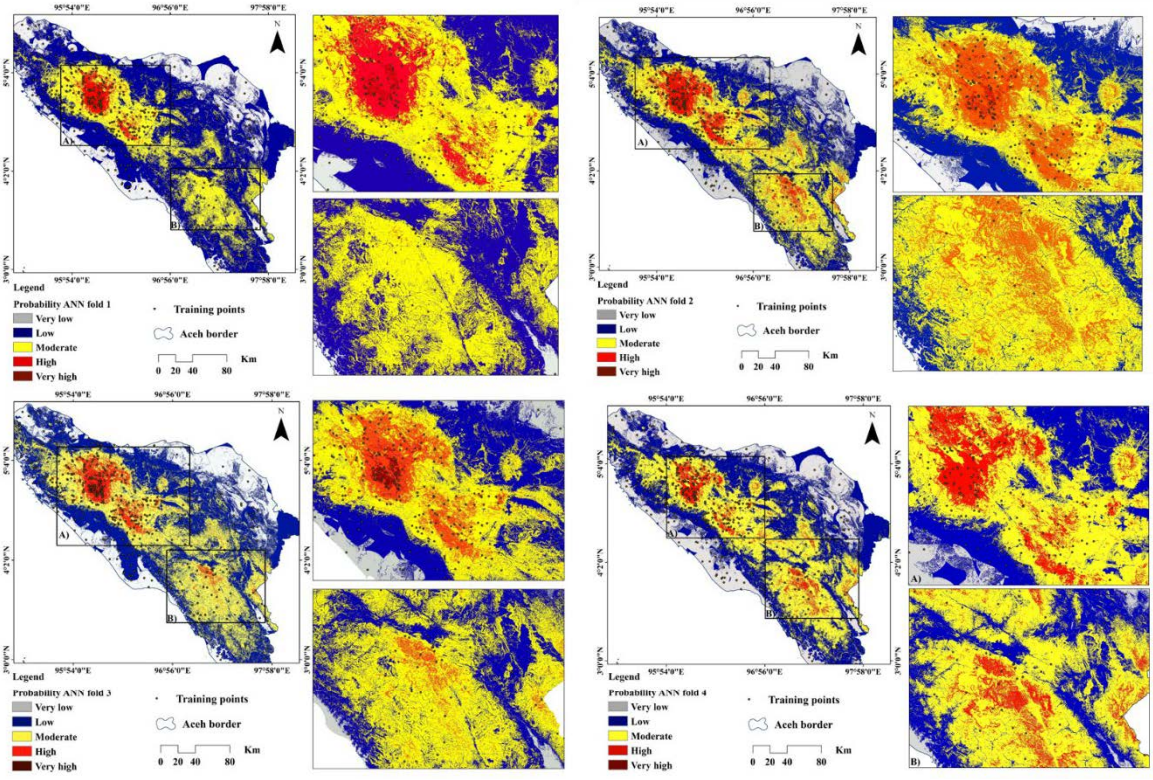

Figure 4.16: Probability index estimation in Aceh province using a fourfold ANN-CV model.

4.4.3. Vulnerability mapping

A vulnerability map was generated based on exposure and vulnerability factors (Figure 4.17). Thirty-six comparisons were conducted, where the CR achieved 0.06 in scoring the factors. The principal eigenvalue originated during the priority analysis was 9.737, and the eigenvector solution achieved six iterations. An eigenvalue must be nonzero that corresponds to an eigenvector. The principal eigenvalues are the points stretched by the transformation. Consequently, a negative eigenvalue directs oppositely. Therefore, the CR manifested that the priority of criteria was accurately and deliberately assessed. The decision-making approach achieved a delta value of 8.7E−9. Population density, building density, and household density achieved priority scores of 1, 2, and 3, with their estimated weights of 39.90%, 24.50%, and 10.70%, respectively (Table 4.14). The remaining criteria achieved medium to a low-rank CR, which was accurate. The priorities of all criteria were plotted based on maximum and minimum values. The obtained results are shown in Figure 4.19(b).

In this research, the whole process evaluated nine factors for the vulnerability assessment that provides acceptable CR. According to the Saaty's article, the magic number of 7(+ or – 2) criteria is acceptable to evaluate CR. Therefore, nine factors reached the highest limit of (7+2) criteria selection. No criteria was removed during the AHP analysis, the last two criteria in accordance with the AHP ranking were removed, while the TOPSIS approach was applied, where seven criteria were selected at the end of the entire process. Although all the criteria are important to achieve a good vulnerability map, last two criteria may provide a biased result.

Table 4.14: Priority estimation and ranking of vulnerability factors.

ID	Criteria	Priority	Rank	(+)	(-)
1	Building density	24.50%	2	8.80%	8.80%
2	Building length	2.00%	9	1.10%	1.10%
3	Shape of buildings	5.50%	5	2.60%	2.60%
4	Surface area density	4.90%	6	1.50%	1.50%
5	Proximity to road	4.20%	7	1.90%	1.90%
6	Perimeter density	2.10%	8	0.90%	0.90%
7	Proximity to buildings	6.10%	4	2.00%	2.00%
8	Household density	10.70%	3	5.40%	5.40%
9	population density	39.90%	1	19.00%	19.00%
Number of comparisons= 36 Consistency Ratio CR = 6.4% Principal Eigenvalue = 9.737 Eigenvector solution: 6 iterations, delta = 8.7E-9					

Seven alternatives that are closely similar to buildings and social characteristics were chosen and decision matrix was calculated (Table 4.15). The best and worst distances from the best and worst vectors were estimated for all alternatives, as presented in Table 4.16. The closeness coefficient score was calculated using the AHP-TOPSIS algorithm, which contributed to a similar rank of criteria, as shown in Table 4.17.

The map shows that approximately 24% (14.16 km^2) of the city is exposed with high to very high vulnerability. The city center and southwestern parts of the study region, including Kuta Alam, Baiturrahman, Banda Raya, Jaya Baru, parts of Siyah Kuala, and Uli Kereng, dominantly belong in this category.

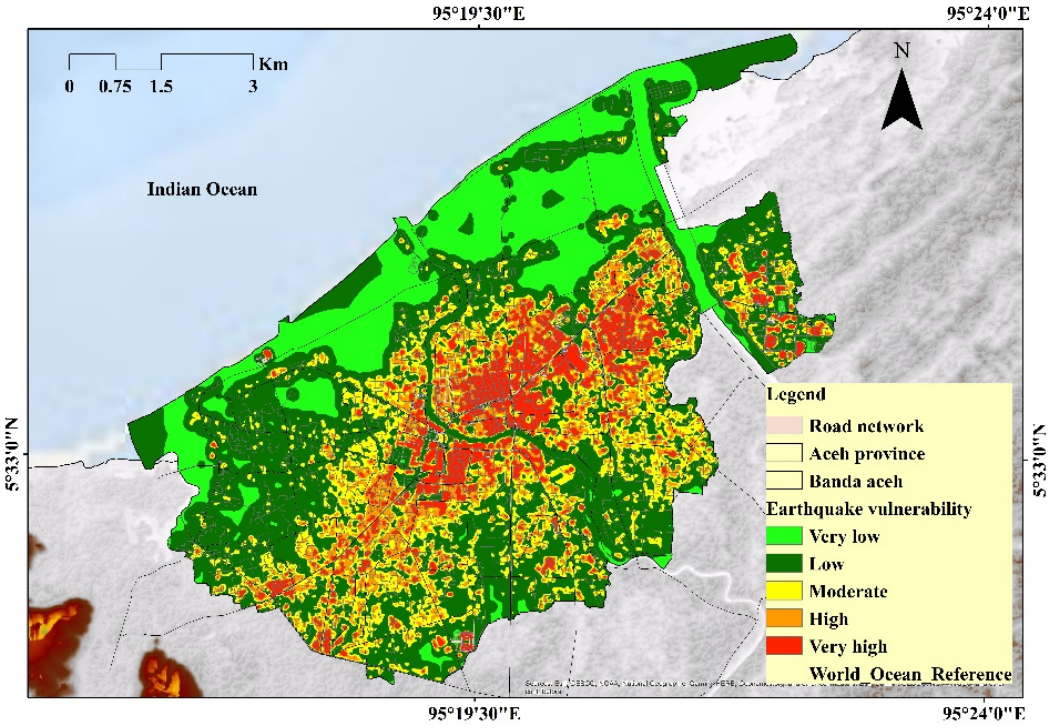

Figure 4.17: Earthquake vulnerability map derived using the hybrid AHP-TOPSIS model.

The main factors that are close to assessing earthquake vulnerability, such as buildings and social characteristics, are accountable for this condition. The results showed that approximately 28% (16.52 km^2) of the city was classified as moderately vulnerable. Moderate vulnerable areas covered the highly sensitive areas surrounding the city center. Low to very low vulnerable areas accounted for 48% (28.32 km^2). Low to very low areas covered the northwestern and southwestern regions, including the coastal part of the city and the hilly regions close to Aceh Besar District. This finding could be due to the small population and building density in these areas that indicate a very low vulnerability. The resulting map shows the spatial variation and degree of vulnerability in the city. Vulnerability mapping illustrates that around 14% (33,368) of the population lives in a very high vulnerable zone, 17% (40,518) of the population can be found in a high

vulnerable zone, followed by 45% (107,256) as a moderately vulnerable, and 24% (57,203) falls under low to very low zone. The vulnerability level is notably high in central areas because of the influences of buildings and population density. Geometry could help in estimating the total number of populations and areas under vulnerable zones for all the nine sub-districts in the city. Therefore, the obtained vulnerability map is useful for Indonesia's government organizations, private, and government agencies in future earthquake risk mapping.

Table 4.15: Normalized Decision Matrix for alternatives ranking using TOPSIS.

Criteria/alternatives	Social characteristics	Total buildings	Household density	Distance from main buildings	C and L type buildings	Large buildings	Distance from road junctions
Population density	[[0.408,	0.26,	0.099,	0.053,	0.045,	0.01,	0.01],
Building density	[0.135,	0.087,	0.075,	0.035,	0.027,	0.005,	0.003],
Household density	[0.103,	0.029,	0.025,	0.026,	0.02,	0.003,	0.002],
Proximity to buildings	[0.06,	0.02,	0.008,	0.009,	0.02,	0.002,	0.001],
Shape of buildings	[0.04,	0.013,	0.006,	0.003,	0.005,	0.002,	0.0005],
Surface area density	[0.02,	0.009,	0.004,	0.002,	0.002,	0.001,	0.0004],
Proximity to road	[0.005,	0.005,	0.003,	0.002,	0.001,	0.0002,	0.0002]]

Table 4.16: Vectors analysis and matrix creation using TOPSIS.

Analysis	Matrix
Best Answer Vector	[[0.408, 0.26, 0.099, 0.053, 0.045, 0.01, 0.01],
Worst answer Vector	[0.005, 0.005, 0.003, 0.002, 0.001, 0.0002, 0.0002]]
Choices Distance From Best Vector	[0, 0.326, 0.393, 0.434, 0.457, 0.476, 0.492]
Choices Distance From Worst Vector	[0.493, 0.176, 0.108, 0.062, 0.038, 0.017, 0]
Closeness Vector of Each Choices	[1, 0.35, 0.22, 0.13, 0.078, 0.035, 0]

Table 4.17: Closeness coefficient and rank estimation of alternatives.

Alternatives	Closeness coefficient	Rank
Social characteristics	1	1
Total buildings	0.35	2
Household density	0.22	3
Distance from main buildings	0.13	4
C and L type buildings	0.077	5
Large buildings	0.034	6
Distance from road junctions	0	7

4.4.4. Risk mapping

A risk map was developed for the city by considering hazard situations and vulnerability results. A quantile classification technique was implemented to classify the map into five different classes, starting from very high to very low (Birkmann & Welle 2015). Risk areas and the total population in each zone were estimated accordingly. Estimated geometry manifested that 4.81 km^2 of a very high-risk zone can be observed in the entire city. Approximately 10.02, 14.7, 14.8, and 20 km^2 areas inside the city were considered high, moderate, low, and very low zones, respectively (Table 4.18). The southwestern parts surrounding the city center constituting the subdistricts, such as Jaya Baru, Banda Raya, Syiah Kuala, Baiturrahman, Kuta Alam, and Jaya Baru, projected a moderate to

high risk, whereas the central, southwestern, and northeastern parts, including the subdistricts of Syiah Kuala, Baiturrahman, Kuta Alam, and Jaya Baru comprised a very high-risk zone. Low population stability and low building density in areas, such as Kuta Raja, Meuraxa, Lueng Bats, parts of Syiah Kuala, and Kuta Alam, manifested low to shallow risk.

The high risk could be due to high building density and building characteristics along with population density, proximity to GSF, and the seismic gap that comes within the city. The overall risk map is spatially depicted in Figure 4.18. Risk uncontrolled loss may occur in the future. Therefore, the risk map illustrated that around 3.7% (10,252) of people were observed as very high risk in the city, whereas the high-risk zone covered approximately 18% (44,443).

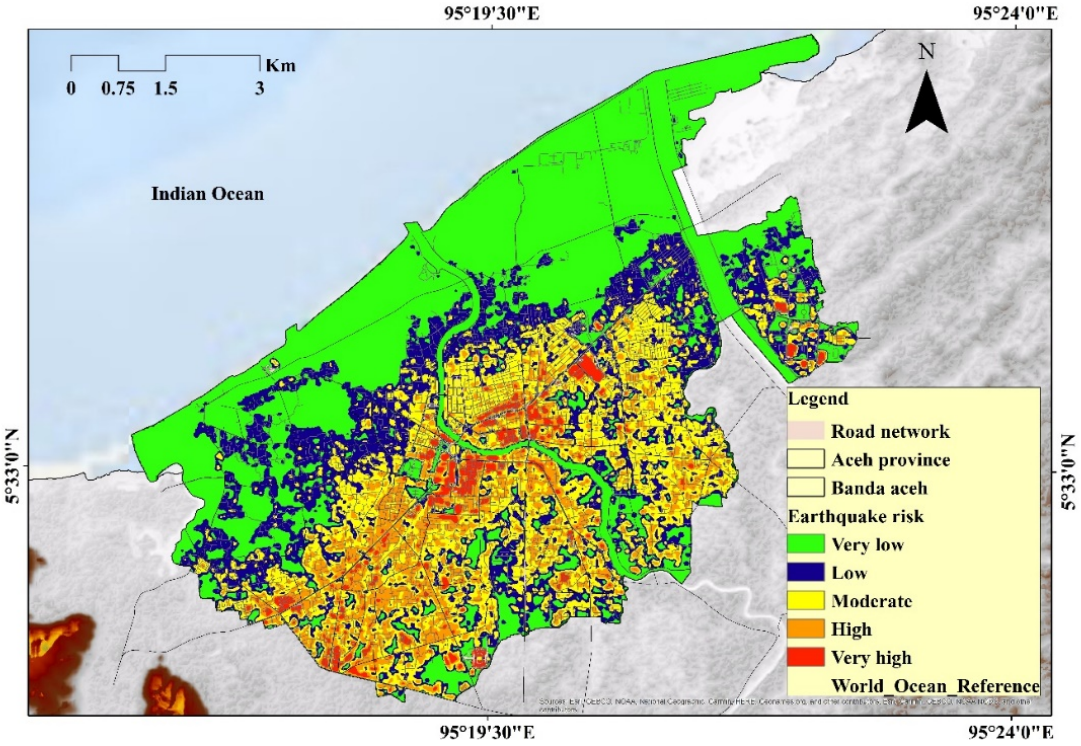

Figure 4.18: Risk map obtained from fourfold ANN-CV and hybrid AHP-TOPSIS model.

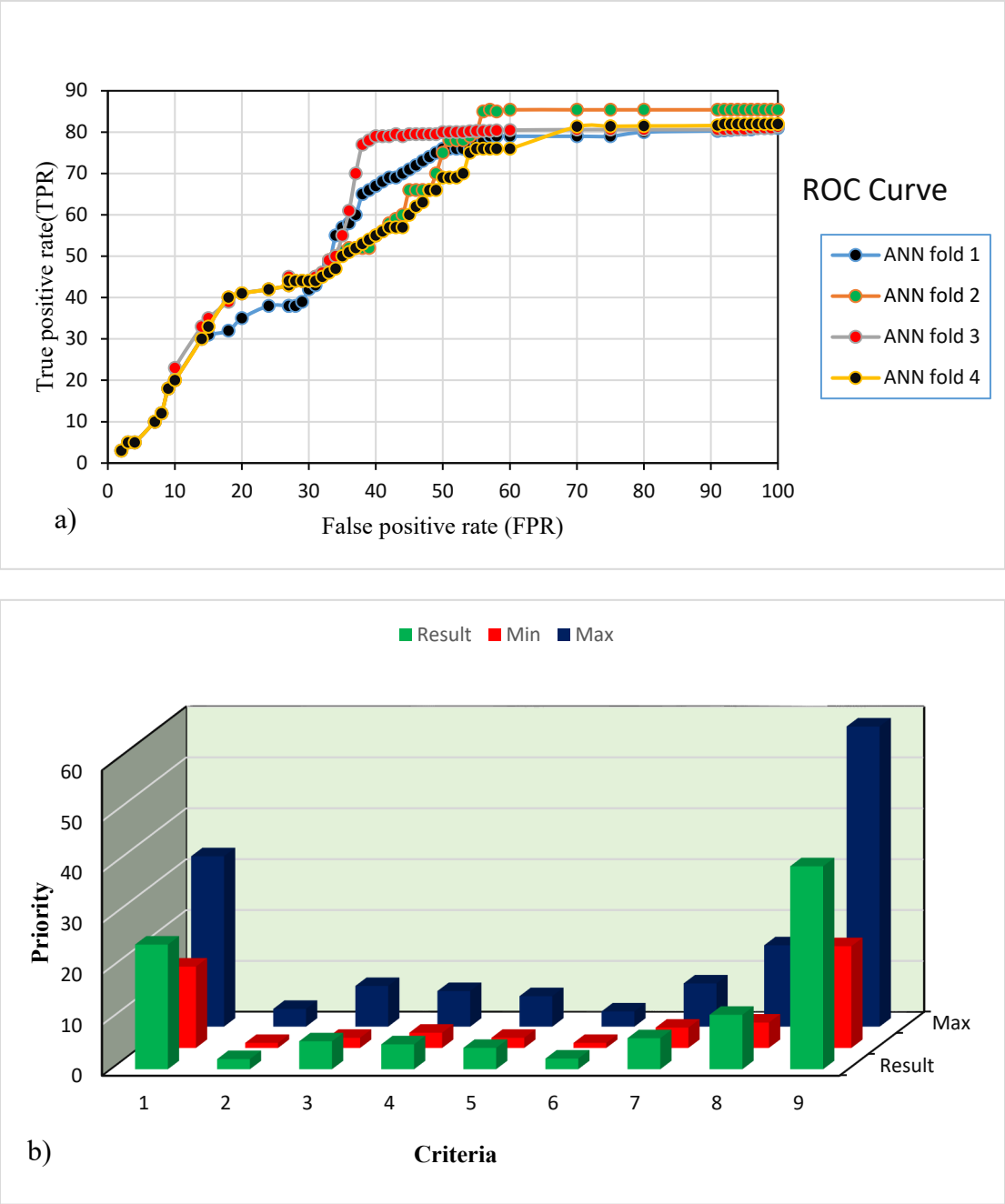

Figure 4.19: (a) Accuracy curve for probability index estimation, and (b) Maximum, minimum and resulted priority of vulnerability criteria.

Moderate to very low-risk impacts were explicitly observed in 47% (106,824), 25% (58,949), and 7.3% (17,213), respectively (Table 4.18). These areas were located close to the coastlines with a small population and planned the tsunami-based land use planning

and several adequate mitigation measures. Consistency was observed in the spatial risk assessment by comparing the vulnerability index and degree of hazard results particularly in the areas near the coast with low elevation, low slope, loose sedimentary rocks, low population, and building characteristics. The risk levels changed after the 2004 tsunami because of adequate mitigation planning. Mohsen et al. 2019 achieved 90.01% ANN accuracy in earthquake vulnerability assessment and estimated the total population in a vulnerable zone. Mohsen et al. (2018) achieved 95.66% accuracy in social vulnerability assessment using ANN for Tabriz City in Iran.

The risk in Banda Aceh can be perceived by focusing on some conditions.

(1) Very high-risk areas of approximately 4.81% should be the focus of the government with the reconstruction or demolition of low-quality buildings.

(2) A dense building density could be observed in the city center of Banda Aceh. The high-risk area, which is 10.02% of the total area, could be lessened by considering ground shaking-based retrofitting and modification.

(3) Moderate risk generated caused by social, economic, structural, and geotechnical factors could be observed in 23.3% of the city. Therefore, retrofitting, reconstruction and renovation of buildings are some options to reduce the risk.

(4) Low risk could be found in 23.73% of areas with (58,949) population. Buildings and residents are safe in these areas.

A low density (17,213 population) of residential buildings covers the coastal parts of the city. This study explored the areas with the nearest tectonic condition and coastal ground shaking. Therefore, these areas could be more vulnerable to a tsunami than earthquake risk.

Table 4.18: Estimation of area and population under earthquake risk

Area name	Very high		High		Moderate		Low		Very low	
Risk zones	Area (Km^2)	population	Area (Km^2)	population	Area (Km^2)	population	Area (Km^2)	population	Area (Km^2)	population
Syiah Kuala	0.03	64	0.03	183	1.1	7994	2.8	11,152	4.1	3529
Ulee Kereng	0.02	43	0.07	369	2.9	21,074	0.8	3,187	1.7	1463
Kuta Alam	1.1	2,345	1.4	6220	2.7	19,621	1.9	7,568	2.9	2,496
Kutaraja	0.01	22	0.22	976	0.5	3,634	2	7,966	2.3	1980
Baiturrahman	2.6	5,545	2.6	11,542	1.6	11,627	1.1	4,381	0.7	603
Lueng Bats	0.3	640	1.9	8,278	2.3	16, 713	1.3	5,178	1.4	1204
Banda Raya	0.43	916	2.3	10,222	1.8	13,081	0.5	1992	1.7	1463
Jaya Baru	0.5	1065	1.5	6,653	1.6	11,627	1.2	4780	1.6	1377
Meuraxa	0	0	0	0	0.2	1453	3.2	12,745	3.6	3,099
Total	**4.81**	**10,252**	**10.02**	**44,443**	**14.7**	**106,824**	**14.8**	**58,949**	**20**	**17,213**

4.4.5. Validation

The results of risk mapping were validated using the previously published work (Jena et al. 2019). The results were validated based on the earthquake inventory data, results of decision-making approach, feedback gained from some local people, and accuracy explained by experts and researchers. ANN CV obtained 85.4% accuracy in the twofold probability assessment. The hybrid AHP-TOPSIS decision-making model obtained a CR of 0.06. Therefore, all the earthquake events experienced in Aceh were used to cross-check with our earthquake risk map, which was satisfactory. Ten experts were invited to provide their feedback on our risk results (Table 4.20). Some 2004 earthquake and tsunami images on Google Earth were crosschecked to find some damage buildings. Therefore, the results are good and can be useful for the city residents by considering the output obtained from the above-described objectives. The experts profile and their specialization were presented in Table 4.19.

Table 4.19 Table of experts' profiles for the AHP-TOPSIS approach

Category	No. of Experts	Profession	Specialisation	Recruitment process	Evaluation process for pair-wise comparison	Validation process
Experts	2	Seismologist	Experts in the seismic study, vulnerability, hazard, risk assessment, monitoring, mapping,	MCDM application in their study. Mapping in Physical, structural, geotechnical vulnerability Expert in local and regional	Objective of the research requirements Application of method evaluation	Vulnerability determinants Representation of spatial maps

			GIS, Artificial intelligence, Multi-criteria decision making	vulnerability assessment Data analysis expertise	Requirement of spatial analysis Vulnerability determinants Satty's Intensity scale	Expected uncertainties Map validation Results Communicability How useful to land use planning Benefit to local people
Researchers	6	Geologist, hydrologist, GIS analyst, soil physicist, geotechnical researcher	Researcher on natural hazards using GIS and remote sensing	Multi-criteria mapping using AHP, ANP, TOPSIS, VIKOR etc. Qualitative assessment with sensitivity Published good articles in high impact journals		
General people	2	Banda Aceh residents	Two local people having a general knowledge of earthquake	Local geographical knowledge Experienced audience		

Table 4.20: Feedback summary on earthquake vulnerability and risk map obtained from opinions of different categories of people

Category	Total Number of Respondents	Feedback		
		Highly Satisfied	Satisfied	Not Satisfied
Experts	2	2	0	0
Researchers	6	4	1	1
General people	2	2	0	0
Total	10 (100%)	8 (80%)	1 (10%)	1 (10%)

4.5. Results of case study (Palu city)

4.5.1. Relationship between Mw, PGA and intensity variation

Matrix plot is generally used to obtain the relationship between several variables. Therefore, in this study, earthquake magnitude, PGA values obtained for the location and the possible intensity for each scenario were calculated and correlated to understand the relationship among them. The three variables obtained from the calculation using the inventory data of earthquake events from USGS were applied using the Matlab tools. However, the results obtained from the plotting is presented in Figure 4.20. The interpolation method was also implemented to join the three variables smoothly. The total number of variables was 200. The variable values vary between -3.19 to 8.09. Many negative values could be observed in the intensity section while positive values could be found in the magnitude section. However, PGA values vary at a level of 0.571 while magnitude varies within 4 to 8 Mw.

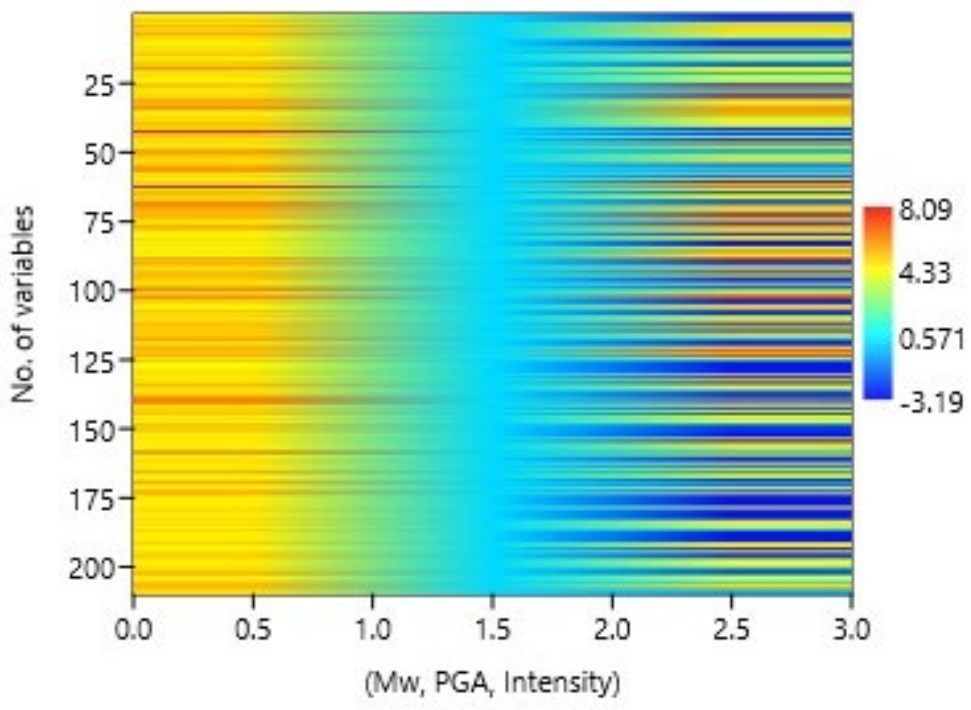

Figure 4.20: Relationship between Mw, PGA and intensity variation.

Therefore, this analysis shows that earthquakes intensity on a particular site depends on the site to source distance and does not directly depend on the magnitude.

4.5.2. Silhouette clustering analysis

Silhouette clustering analysis is an interpretation and validation method to clarify the consistency within the data cluster. Therefore, in this study, the obtained PGA and intensity values for all the earthquakes were applied to check the consistency between them. Succinct representation of data points was plotted graphically to show their object classification.

The four cross-correlation obtained in figure 4.21 varies with the lag values of -105 to 105. However, in the case of the correlation between epicentral distance and source-to-site distance, when the lag value is zero the correlation is one and the p-value reaches zero. The p-values vary in a range from 0.028 to 0.919 in the crosscorrelation portraying a positive correlation, where source-to-site distance leads in the correlation. The second crosscorrelation reveals that the p-values vary in a range from 0.00012 to 0.974. In this case, the lag value is zero the correlation is -0.266 and the p-value reaches 0.00009 with positive correlation where depth leads. The third and fourth crosscorrelation projects that the p-values varies in a range from 0.014 till 0.99 and 0.0003 till 0.973, respectively. In these cases, the lag value is zero the correlation is 0.073 and 0.246 while the p-value reaches 0.287 and 0.0003, respectively. The results show that Mw versus intensity shows positive correlation and intensity leads and Mw versus PGA shows positive correlation and PGA leads. There is a strong correlation between epicentral distance with source-to-site distance and Mw with PGA are strongly correlated. However, the other two

correlations performed in figure 4.21 are moderately correlated. The possible reasons could be calculations of variables were performed through several attenuation laws.

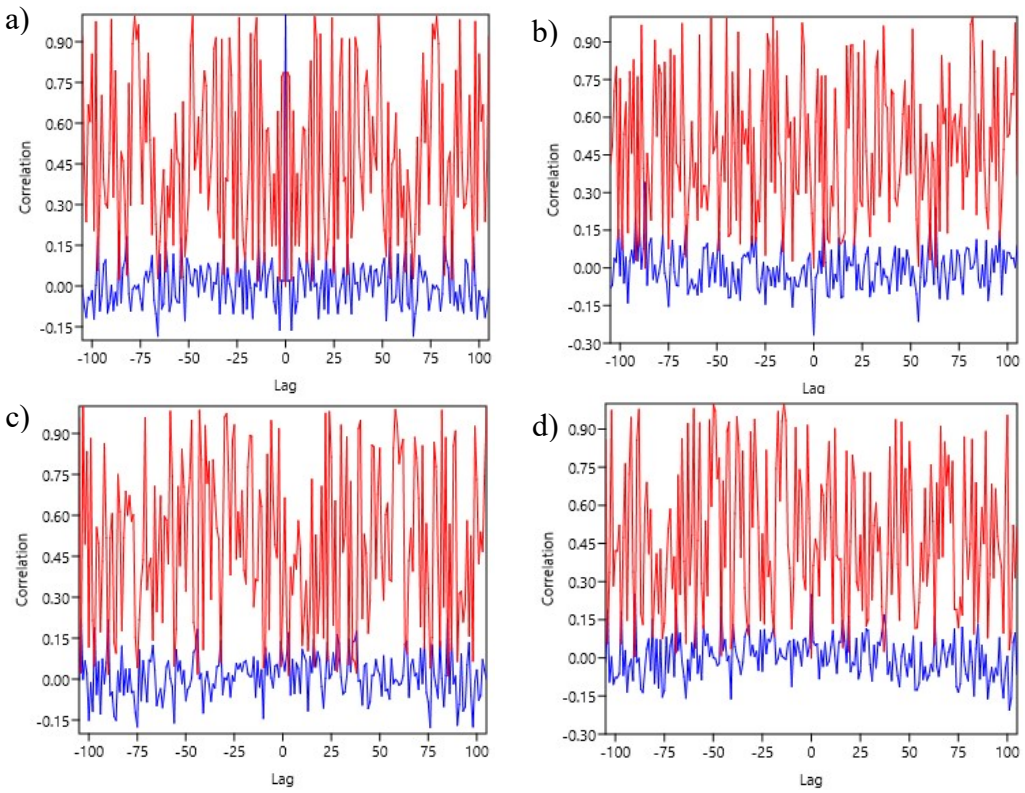

Figure 4.21. cross-correlation shows (red signal portray p-values while the blue signal is the correlation spectrum) a) epicentral distance vs source-to-site distance, b) PGA vs depth, c) Mw vs intensity, d) Mw vs PGA.

In general, silhouette value is a value that shows the similarity of an object to its cluster as compared to other clusters. Figure 4.22a plotted with Silhouette clustering, log y and 3point average. Silhouette clustering was included to plot all the indicators in a single graph. Log y will provide the plot for negative values while 3-point average could provide the graph in a signal form. Figure 4.22a shows that the values of Intensity (E) and PGA (D) vary in a similar way while the relative values for A, B and F vary in a similar way.

This graph shows that if the signal varies smoothly then the values are almost close to each other having a large cluster which could be seen in case of magnitude (C) as the magnitude varies from 4 to 8 with very minor changes.

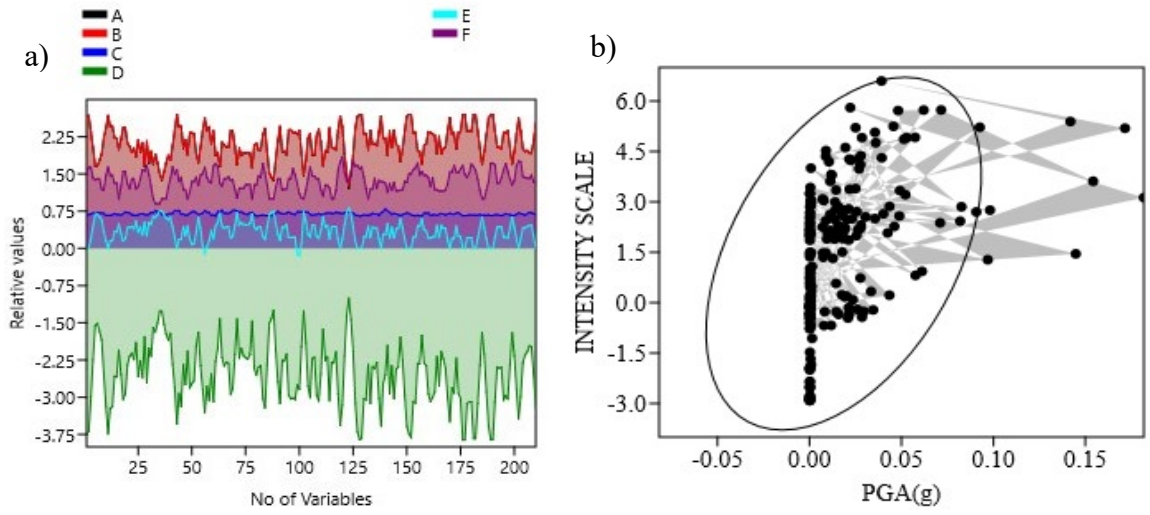

Figure 4.22. Silhouette clustering analysis: a) Relative change of values for five indicators (A) epicentral distance, (B) source to site distance, (C) magnitude (Mw), (D) PGA, (E) intensity, (F) depth of earthquake focus, b) PGA vs Intensity.

Figure 4.22b shows the plot of the Silhouette clustering of intensity against PGA. This study analyzed the data with a 3-point average and 95% confidence. However, as the silhouette values range from −1 to +1. Therefore, the object will be considered as poorly matched to neighboring clusters and well-matched to its own cluster if the high value observes. From this graph, it is clear that most objects have a high value that shows an appropriate clustering configuration (Figure 4.22b). Ellipse in this graph considers the objects as a single cluster. There are no negative values, therefore no clustering configuration observed in a negative value. Euclidean distance was applied to calculate the silhouette values as the distance metric.

4.5.3. Pure Locational Clustering (PLC) approach

In this research, Pure Locational Clustering (PLC) approach was applied using the classical clustering technique for defining and evaluating the number of clusters.

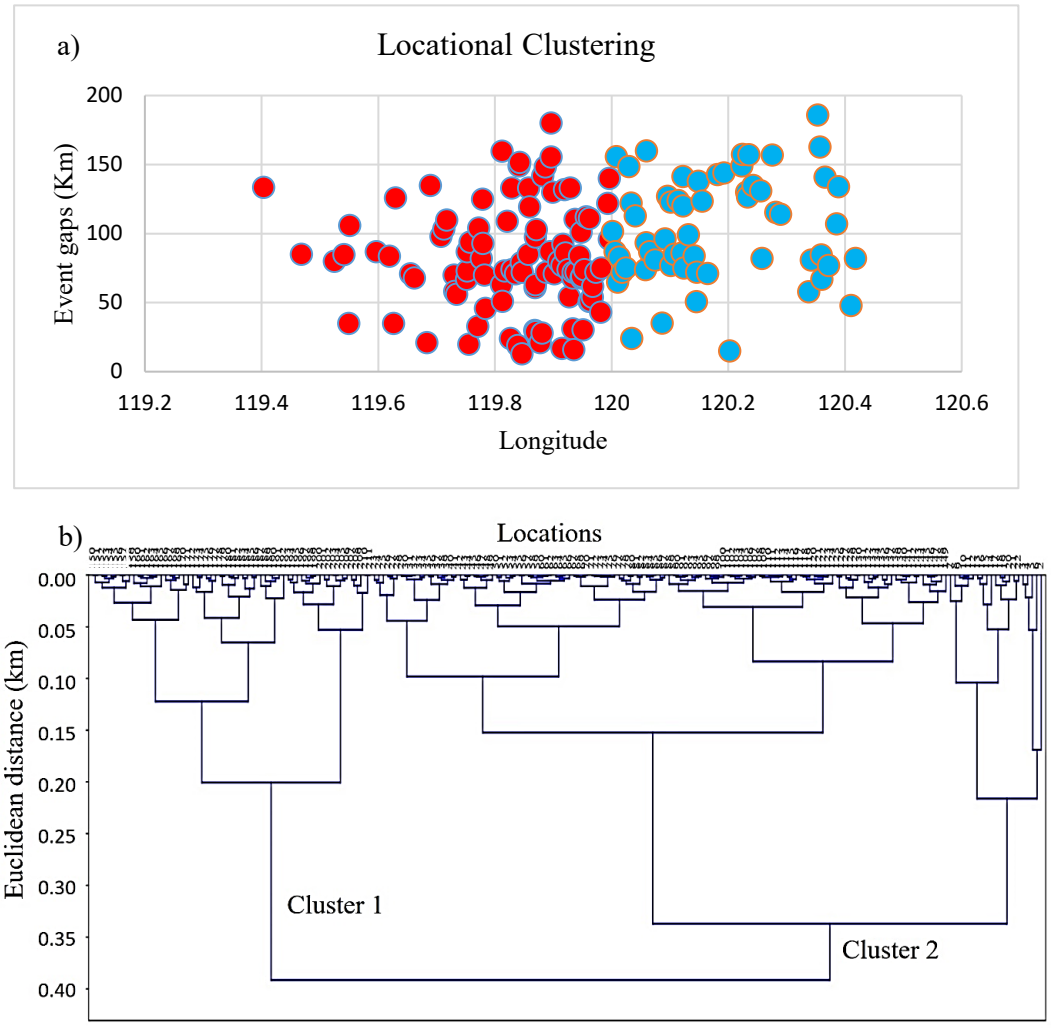

Figure 4.23 a) Locational clustering analysis using earthquake longitude and event gap, b) Dendrogram shows between Euclidean distance and clusters.

PLC is an approach implemented in the current study that is defined on the basis of geographic coordinates of a set of earthquake locations. The figure 4.23a presented below shows the results of the classical clustering performed using the earthquake locations. However, the elbow method was applied to figure out the optimum clusters by

investigating the obtained critical points on the plotted graph. However, in total two optimum numbers of clusters were obtained in this study. It could be observed that the distance generated between the clusters was less in classical clustering than any other clustering such as the K-means algorithm. Thus, classical hierarchical clustering is implemented as a countermeasure in the current research. The dendrogram presented in figure 4.23b shows the Euclidean distance between the groups they based on and the clusters on the least distance between the points. The clustering method is applied to figure out the centroid of the longitudes and then the locations prone to earthquakes were observed, which depends on the distance of the events, the clusters could be mapped.

4.5.4. Probability assessment

Fewer studies have been conducted for Palu on earthquake probabilistic assessment however; SSA is one of them (Aucelli et al. 2018; Dhar, Rai & Nayak 2017; Monahan et al. 2018). The seismic zone map of Palu (SNI 03-1726-2002) shows that the region comes under a high to very high hazard zone trending northeast–southwest direction across the central part of the city characterized by metamorphic rocks, unconsolidated deposits and fewer granitic patches. Probabilistic estimation in Palu gives PGA of approximately 0.5 to 0.6g for 10% exceedance in 50 years. From this study, the highest PGA obtained is 0.2 for Palu, which comes under the very strong category. However, the SSA depends on the amplification factor of rock types. Therefore, the PGA observed in Palu used for the hazard assessment. During the probability mapping, training and testing was performed using all the factors as input and events as target (Figure 4.24). The proposed ANN-CV model was not able to predict 14 data points. However, the reason could be noise and data heterogeneity in the thematic layers. However, during the data processing some unusual data points were removed for better accuracy. The proposed model predicted

approximately 205 m^2 as the most probable area. As the study is a probability assessment,

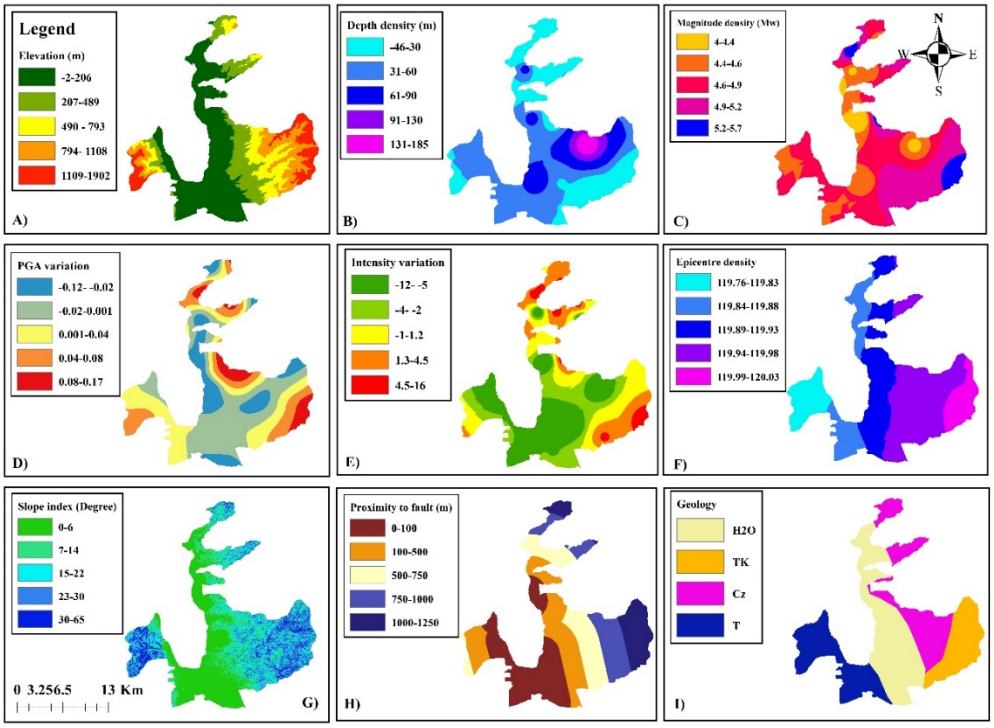

Figure 4.24 factors for probability assessment.

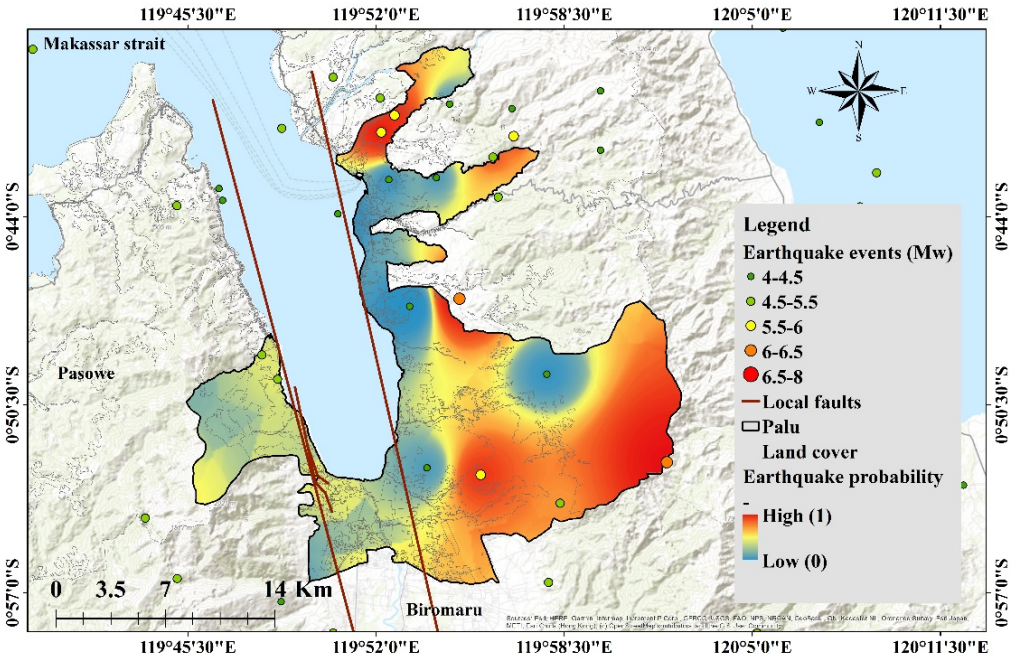

Figure 4.25. Probability results from ANN-CV approach.

therefore no classification technique was applied for probable classes in Palu city. Nevertheless, the probability must vary between 0 and 1. Palu city was tested using the fold 2 of ANN CV. The true positive rate for the city was estimated as 0.88 and RMSE was 0.16. The spatial distribution of the probability of occurrence is higher in the eastern and northern parts of the eastern limb of Palu city as presented in figure 4.25. However, Palu is a small city that is located close to the Palu-Koro active fault system has the capacity to strike strong future earthquakes. Therefore, high probability in the city located at eastern limb in north-south direction. Medium probability is surrounding the high and low probability could be found in the east and west direction. The leading cause of high probability could be the major active fault system, a huge number of events in the eastern part and the high magnitude events. Seismic amplification is higher in the coastal part than other areas in the city; however, loose sedimentary rocks making the city more probable towards the east and northern regions. The reasons could be reverse for the low probability.

Intensity distribution was obtained and multiplied with the probability to generate the earthquake hazard map for events more than the 4Mw. With high intensity of more than 9 can be considered as a very high hazard, while as high, moderate, low and very low hazard can be classified with intensity variation such as 8–9, 8–7, 7–5 and <5, respectively (Jena et al. 2019; Bayrak et al. 2009).

4.5.6. Vulnerability mapping

The vulnerability assessment was conducted and a map was produced using several vulnerable factors for Palu (Figure 4.26). Vulnerable areas geometry and the buildings within could help in calculating the number of vulnerable populations and areas in the

city.

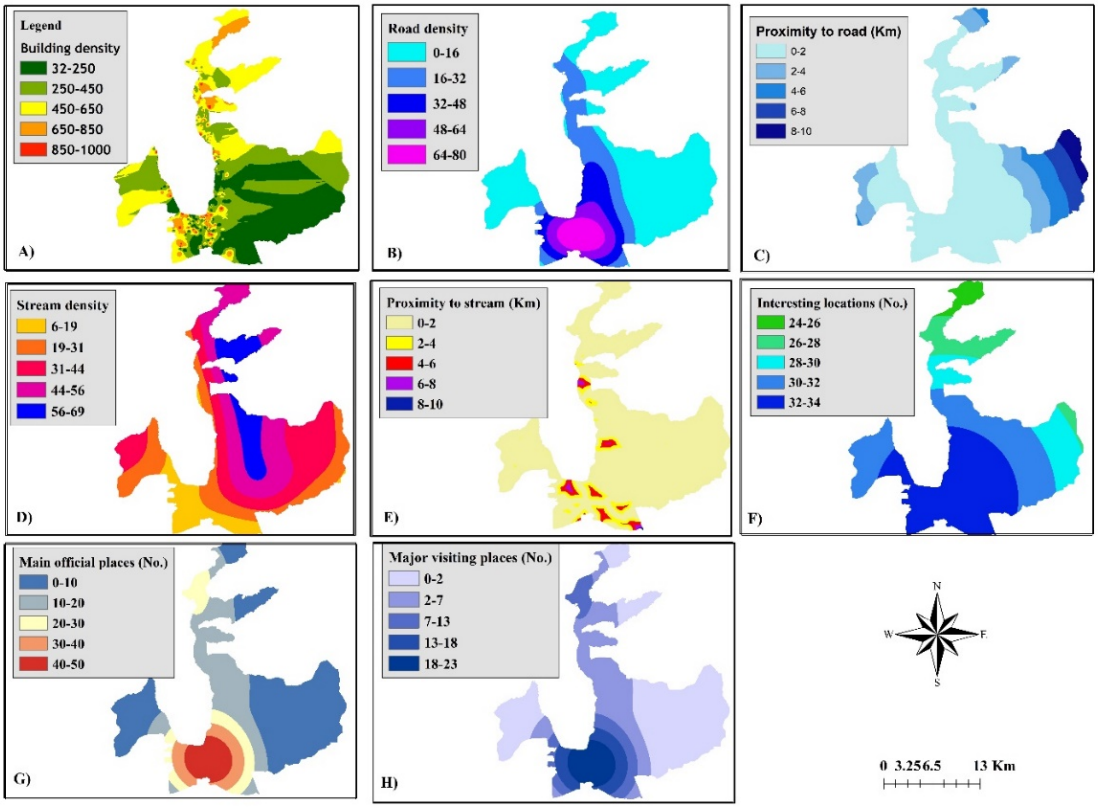

Figure 4.26. Factors influencing EVA.

Seven vulnerable factors were applied in the AHP approach for pairwise comparison and weight calculation (Jena, Pradhan & Beydoun 2020). Twenty-one number of comparisons were carried out with an achieved consistency ratio (CR) of 0.07. The priority analysis evaluated the principal eigenvalue as 7.586; however, the eigenvector solution achieved six iterations. An eigenvalue must be nonzero and a negative eigenvalue directs inappropriate evaluation. However, CR value less than 0.1 demonstrated that the criteria were deliberately assessed. Delta value observed as 2.9E-8 during the MCDM processing. Priority scores for all the 8 layers were achieved. However, building density, road density and major offices achieved the weights of 43.1%, 20.8% and 12.5% and ranked as 1, 2, and 3, respectively (Table 4.21). CR obtained from the process shows that pairwise

comparison was accurate. The remaining criteria achieved medium to a low rank as per the results presented in Table 2. A maximum and minimum of all the weights were also obtained. Seven alternatives were chosen out of 8 against all the seven major criteria from which the criteria interesting locations were removed. The details of factors, weights and ranks were presented in Table 4.21. Then using the TOPSIS approach, it was concluded that there is no need of the factor interesting locations which was removed from the study.

Approximately 20% (78.80 km^2) area of Palu is estimated as high to very high vulnerability. The city center dominant to a very high and northsouth limb of the city belongs to the high vulnerability category. Factors that could account for this condition of very high to high vulnerability are social characteristics that are high in the city center. Moderate conditions covered both the sensitive and remote areas around the city with a huge areal characteristic. The vulnerable map showed that 40% (157.60 km^2) area came under a moderately vulnerable category (Figure 4.27)**.** An estimated area of 40% (157.60 km^2) covered by low to very vulnerability. Low areas covered the southestern close to the hilly regions and some parts of western coastal regions of the city.

The reason for the indication of low vulnerability could be low social characteristics. Spatially the vulnerability variation could be observed from the resulting map for the Palu city. Approximately, 80% of the population lives in a very high, high and moderately vulnerable zone, whereas 20% situated in the low vulnerable zone. Notably, very high to high vulnerability mostly influenced by high population and building density. Therefore, the produced vulnerability map could be implemented as a source map for future risk mapping in Indonesia.

Table 4.21. Priority and rank of criteria for vulnerability assessment.

Category		Priority	Rank	(+)	(-)	
1	Building density	43.1%	1	20.7%	20.7%	Number of comparisons = 21 Consistency Ratio CR = 7.3% Principal eigenvalue = 7.586 Eigenvector solution: 6 iterations, delta = 2.9E-8
2	Road density	20.8%	2	8.0%	8.0%	
3	Proximity to road (in m)	9.7%	4	4.5%	4.5%	
4	Stream density	4.5%	6	2.0%	2.0%	
5	Proximity to stream (in m)	2.8%	7	1.4%	1.4%	
6	Major official places	12.5%	3	6.7%	6.7%	
7	Major visiting places	6.7%	5	1.4%	1.4%	

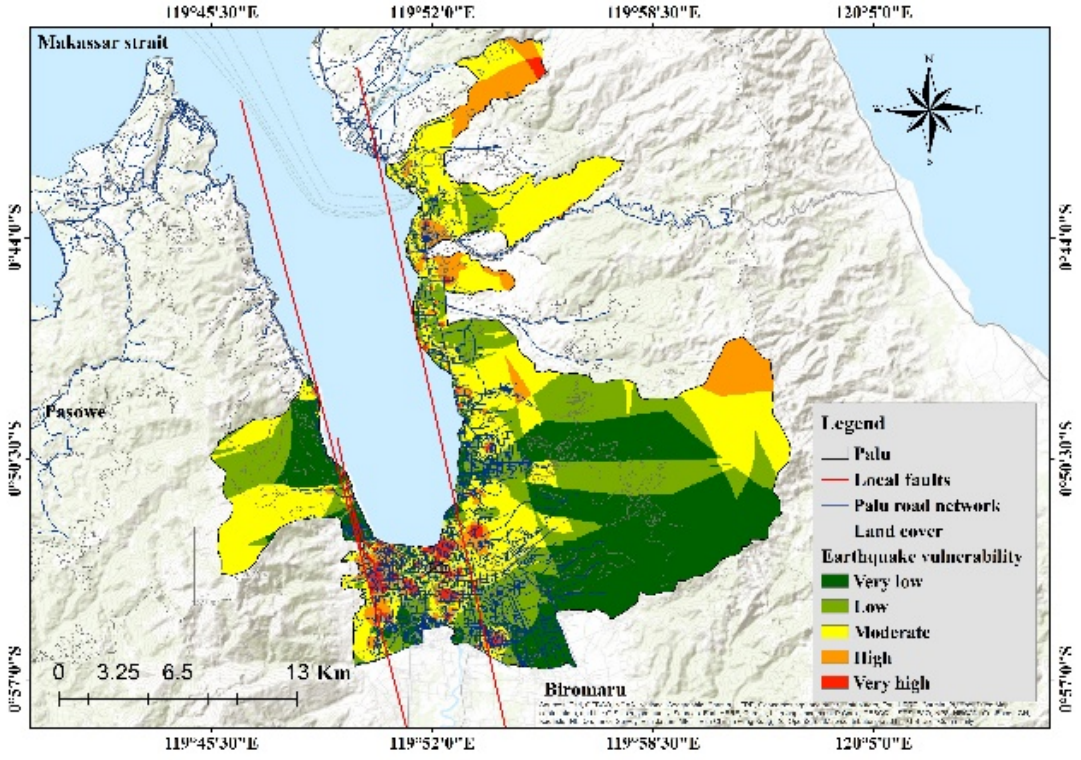

Figure 4.27. Vulnerability map resulted from AHP approach.

4.5.7. Risk estimation

Finally, the earthquake risk was mapped spatially and presented in figure 4.28. Several

classification techniques used for classifying the developed maps. In this study, the quantile technique was employed to classify the risk into five classes such as very high, high, moderate, low, and very low. Based on the obtained results 67 km^2 (17 %), 87 km^2 (22.08 %) of the city was regarded as a very high-to high risk zone. while 240 km^2 (60.91 %) of the city comprised of moderate to very low risk. The high to very high risk areas are observed in the city center and some parts in the northern limb of the city. Medium to very low risk could be expected towards the eastern part of the city having hilly areas. The detailed assessment of building types, quality of materials and number of floors could be conducted for the Palu city that was not performed in this study. Very high and high risk areas of the city should be the focus of the Indonesian Govt. for earthquake mitigation planning.

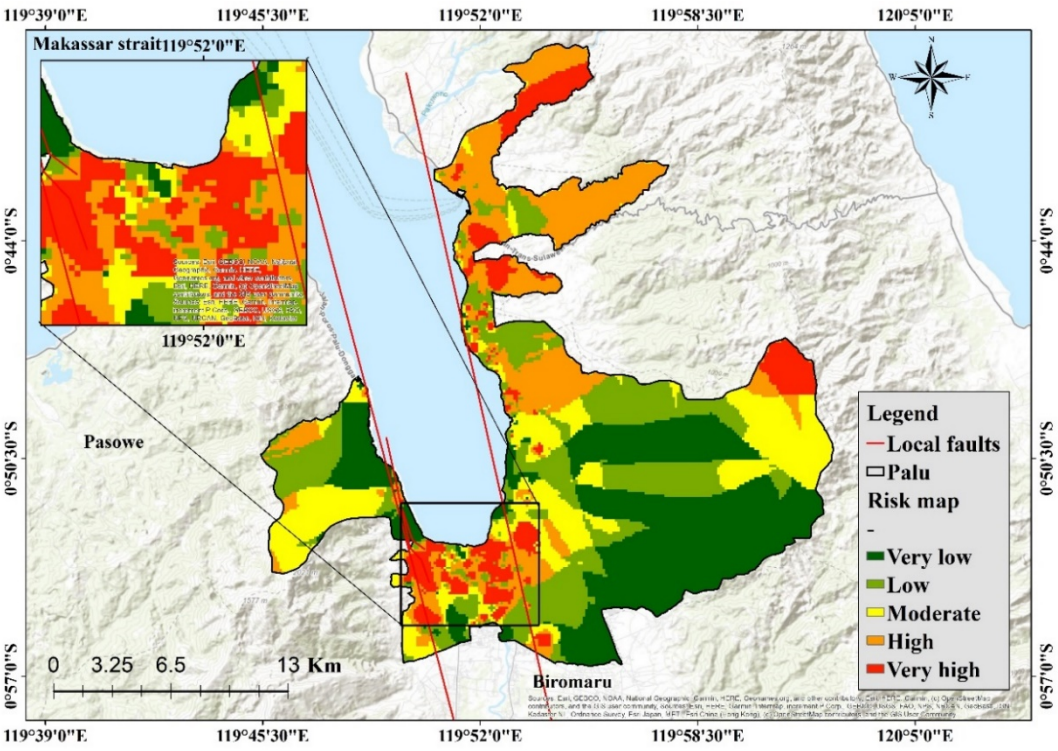

Figure 4.28. Risk map resulted from integrated ANN-CV and AHP-TOPSIS approach.

4.6. Summary

In chapter 4, the application of developed integrated models for probability, hazard, vulnerability and risk assessment modeling leads to the following results:

1. The suggested models explicitly extracted the important factors and added some new factors in the earthquake risk assessment and demonstrated. In addition, the assessment was conducted on Banda Aceh and Palu city in Indonesia was presented. Different software and their uses in this research were described and specifically the datasets and their origin were also pinpointed.
2. Several attenuation equations and the historical earthquake events were used to calculate some important layers such as PGA, Intensity variation, Lithology with amplification factors map. The results show that the earthquake risk is highly affected by local seismotectonic condition, lithology, building quality and density and population density, respectively.
3. In the first objective, using the administrative data, social, structural and geotechnical characteristics of the study location earthquake vulnerability assessment was conducted. Risk assessment in the two study areas were obtained in multi-scenario based study. Both the study areas are prone to high magnitude earthquakes and the mega thrust earthquake of 9.3Mw was experienced in Banda Aceh in Banda sea, therefore chosen for the implementation of the model.
4. In the second objective, using the high-resolution DEM, historical earthquake events several thematic layers originated and earthquake probability assessment was conducted with an accuracy of (84%) and then hazard assessment was conducted using the all the earthquake intensity scenarios.
5. Finally, the risk assessment was conducted using the vulnerability and hazard data,

using the integrated ANN-AHP model and total population is under the risk areas were calculated as very low (65167), low (76268), moderate (47981), high (32363), very high (14018).

6. In the third objective, ANN was again modified to ANN-CV and then AHP was modified to AHP-TOPSIS and finally an integrated ANN-CV and hybrid AHP-TOPSIS model was designed to map the earthquake risk, which provides better result than the previous model with an accuracy of (85.4%)
7. The difference in the last two developed models were observed in terms of accuracy, limitations, obtained results and validation. Different mitigation strategies for very high and high-risk areas assessed and discussed.

CHAPTER 5

CONCLUSIONS AND FUTURE WORK RECOMMENDATIONS

5.1. General

This research deployed high-resolution DEM with detailed social, structural, geotechnical characteristics and complete inventory data. Consequently, this work produced earthquake probability, hazard, vulnerability, and risk in a tropical country like Indonesia. The research is intended on the development of integrated models, and estimation of the population under earthquake risk on a city scale. This research implemented a novel combination of the AHP-VIKOR model, integrated ANN-AHP model, and ANN-CV with AHP-TOPSIS model using the machine-learning algorithms in python and ArcGIS. Earthquakes are the only natural geo-hazards, which is almost impossible to be forecasted or predicted. However, mapping, monitoring, and mitigation planning could assist in estimating the probability, hazard, and risk for such catastrophes through several artificial intelligence-based geospatial methods. The recurrent megathrust and some major events experienced in Banda Aceh and Palu city, Indonesia. Therefore, earthquake risk assessment is indispensable to map the risk areas and population that could assist in the appropriate planning and mitigation processes. Even though numerous methods, models, approaches, and techniques are already developed for earthquake risk mapping, however, mostly these methods are quite complex, traditional, and time-consuming. Therefore, GIS-based integrated machine learning-MCDM models simplify the risk assessment processes and provide good accuracy.

Earthquake is a physical-based active tectonics phenomenon. Therefore, hazard and risk should be assessed when striking a pose as a threat to properties and lives. Therefore, substantial analysis must be conducted systematically in a city-scale area, such as Banda Aceh and Palu area. Earthquake mechanisms and active tectonics phenomenon are varied temporally and spatially. Elimination of such a phenomenon from the research could trigger exponential natural hazards. Therefore, ERA in terms of mapping and estimating risk could aid in providing a full insight of earthquake risk that could assist in mitigation planning, development of protective barriers, and monitoring.

5.2. Conclusions of objective 1

In this study, an integrated MCDM model was developed for EVA to produce a vulnerability map and quantify the population in vulnerable zones. For the first time, VIKOR and AHP were integrated and applied for a city-scale assessment. The following conclusions can be drawn from the current study. In EVA, data from several sources were collected and applied to estimate the vulnerability out of which past earthquake events, building and population characteristics were vital. In the city, 17% of buildings fall under high vulnerability, where 7% of buildings fall under severe vulnerability. This result may be due to the age of surveyed buildings and their characteristics. However, 48% of the buildings were moderately vulnerable to an earthquake. These buildings are found along the northeast central toward the southwest of the city. The EVA map illustrates high vulnerability to earthquake impacts for Syiah Kuala, Kuta Alam, Baiturrahman, and Jaya Baru. The EVA map validation was successfully performed by applying the current research results quantitatively. Infrastructure, communities, and environments within these zones are the primary impacts of earthquakes. Authorities could use the results for mitigation strategies to protect humans and resources from violent earthquakes in the

identified vulnerable zones.

The focus of the study is the potential use of MCDM in Banda Aceh City in Indonesia for an accurate assessment. The integrated vulnerability assessment approaches show that the developed MCDM model outranks the other MCDM models from various perspectives. However, the scale of vulnerability was developed in the current study by applying natural break and expert's opinion, which is important for experts to translate the significance of vulnerability properly. The assessment techniques used, namely the AHP approach and the VIKOR method, produced an acceptable vulnerability assessment result. The proposed method has good variances in vulnerability mapping that can be a good state for decision-makers while applying for future risk assessment.

5.3. Conclusions of objective 2

In this study, a model for the earthquake risk estimation in an urban area using an integrated technique of ANN–AHP was developed. The model is a GIS-based spatial analysis useful for the city scale. The adopting information about the selection of the indicators from the literature with combined techniques was advantageous and effective for ERA that was applied for Banda Aceh. However, the incorporation of knowledge about geomorphology, geology, and structural information, as well as the data of historical earthquake events, are important and will aid in generating an earthquake risk map for the city. Nine zones of Banda Aceh were used in the investigation as two groups of analysis characterized by several sub-parameters.

The ANN model is extremely useful for earthquake probability measurement, and the AHP method is useful for the weight calculation of the parameters for earthquake vulnerability assessment. The ranks and weights were decided on the basis of the

judgments and preferences of the authors. Given that the RMSE is very low, the ANN model has a low chance of misinterpretation of the earthquake probable areas, and the CR in AHP shows the quality of vulnerability results. The developed method found that an urban area might have several risk patterns if all factors are considered. Findings indicate that the geological factors have contributed the highest impact to earthquake probability assessment, whereas social factors contribute highest for vulnerability assessment in Banda Aceh. However, factors vary in different zones of Banda Aceh. The results reveal that the highest risk zones were possibly 3, 5, 7, and 8 in the central-southern part of the city. Comparatively, the other parts have low-to-moderate earthquake risk. Developmental infrastructure and master plans of the city show that it is expanding towards the southern direction towards the GSF fault. Thus, at present, parts of the city with various schools, universities, and informal settlements are situated near the fault. Settlements, construction, and a developmental city plan near the fault may cause a serious problem in the future if the city grows towards the fault without attention being placed on dangers posed by faults and many other concerns.

Population density and building density are high in the very high-risk zones. Government offices and the main transportation junctions can critically exacerbate the conditions. The city deserves outstanding consideration of support from the local and the national government to reassess the managing strategies of natural disasters because the city already was exposed to the 2004 tsunami and its consequences. Therefore, appropriate guides are needed to manage the city and aid decision-makers to recognize the influence of various factors and to understand the deficiencies in each zone. The critical condition of buildings and the populated risk zone area should be included in government observations, and programs of risk reduction must be improved. Lack of proper space

distribution within the city and poor developmental city planning can be considered the future factors for risk. Therefore, the ANN–AHP model in this study provides an effective and practical estimation of earthquake risk and provides urban planning information.

5.4. Conclusions of objective 3

This study showed that 10,252 and 44,443 people belonged to a very high and high-risk zone in Banda Aceh, which should be the focus of the national government. Five main situations described in the risk assessment should be analyzed, and adequate measures should be taken. Regulatory, institutional, political, and environmental factors participating in the earthquake hazard indirectly associated with ERA. Some human-induced earthquakes were experienced by considering the specific locations of human activity. Constructing recreational areas, dams, and tunnels could trigger large magnitude events. Population concentration was high in the city, and human activity was not considered because it is away from the GSF. Therefore, settlements and massive infrastructures close to GSF could indicate a highly probable zone for earthquakes. Thus, social and structural data collected from several census data sources were used. The reason for collecting the opinion of experts was because of their field background regarding GIS-based risk assessment, geographical knowledge, and leading expertise in criteria-based vulnerability and risk assessment. The obtained vulnerability factors may have some limitations. This study did not consider all factors that determine total vulnerability. This study aimed to localize the minimum vulnerability factors that define the vulnerability of Banda Aceh. The risk map for Banda Aceh indicated that the result is significantly accurate using the proposed model.

Special guidance by experienced decision makers is necessary to manage the Banda Aceh City for understanding the influence of several indicators and identifying the deficiencies. The government should observe the critical condition of infrastructures and populated areas in which risk reduction could be improved. Spatial distribution and poor city planning could be extended as vulnerable factors in future research. Therefore, the K fold ANN-hybrid AHP-TOPSIS model is useful and provides practical information on earthquake risk estimation. Our future studies will focus on biodiversity and its prominent roles in earthquake probability and risk assessment. Convolutional neural networks could be applied for predictive-based probability assessment. ML techniques are intelligence-based models with accurate predictions and require massive training data and many probability factors. ML methods, such as random forest and support vector machines, could be useful for earthquake probability, hazard, vulnerability, and risk assessment.

5.5. Conclusions of Palu case study

According to the risk results, very high and high risk areas could be observed in 67 km^2 (17 %), 87 km^2 (22.08 %) of the city while 240 km^2 (60.91 %) of the city comprised of moderate to very low risk. The results obtained from both risk maps are quite helpful for future studies. A detailed risk assessment could be conducted using complete inventory, seismic indicators, active tectonics and geospatial data. Necessary criteria were reasonably chosen based on previous research and experience in the field. In this study, AHP and TOPSIS techniques were applied for vulnerability assessment, while ANN-CV was applied for probability assessment. The details of limitations were described in conclusions for objective 3 in section “5.4 Conclusions of objective 3”.

5.6. Research drawbacks and limitations

The proposed models for earthquake probability, hazard, vulnerability and risk assessment have been applied in Banda Aceh in Indonesia and the study achieved the research objectives. Therefore, lack of proper spatial distribution within the city and poor developmental city planning can be considered as the future factors for risk, which was not included in the first objective. The drawback of this study is that much time is needed for the model's implementation on a wider-scale because the pairwise comparision is challenging and the process is time-consuming, and it requires a large amount of experts opinion.

Several drawbacks were encountered in the second and third objective that could influence the results. Firstly, the ANN model design and training required considerable time and a sufficient amount of training data. Second, the multicriteria approach was applied for risk assessment in this study. Managing the data quality and processing of criteria was challenging to achieve acceptable results. There are several limitations associated with this research. This research used the freely available LULC data for vulnerability mapping rather than high-resolution LULC data. For instance, LIDAR data can improve risk assessment rather than applying the DEM with a 7.5 m resolution, that can result in generating best conditioning factors and maps. Population data were recent, including the monthly deaths, although born individuals were not considered. These limitations will be the focus of future studies. The limitation also includes several criteria that have been considered in previous research on the estimation of an earthquake vulnerability index, such as soil liquefaction, seismic resonance, and building categories. These criteria were not considered in this study because of the lack of data. This study also provides limited vulnerability results without consideration of health, education, and

day and night vulnerability. Moreover, this work was limited to the pre-earthquake spatial probability, vulnerability and risk assessment. There is no post-earthquake study was conducted in this research.

However, the city should be the focus of earthquake risk reduction by the national and state government in Indonesia. The availability of good vulnerability, hazard and risk assessment approaches raises concerns to achieve a simplistic tool on a global scale. The authors assume that the developed multi-criteria decision making (MCDM) models provide a robust basis for the current risk estimation. This study recommends developing new MCDM models for future studies that include more consistent and detailed analysis that can be implemented globally.

5.7. Recommendations for future work

In this research, the proposed models were implemented and all the three objectives were achieved. Moreover, further work can be done on earthquake risk assessment by applying a detailed dataset using the latest models of artificial intelligence. The recommendation for future work are:

1. Indonesia is a seismically active region that experienced a huge number of earthquakes therefore, it still requires further intense research using paleo seismic factors (identified paleoseismic faults), geodetic factors (dimensional changes in crustal motion), and geophysical factors (fluid-related earthquake precursors).
2. To improve the accuracy while dealing with uncertainties can be another future research to achieve good results in earthquake hazard and risk assessment as well as prediction.
3. The employed methods and the developed models in this research should be exercised

in other seismic prone areas in India, Japan, or America for the derivation of comprehensive information.

4. This research concentrates on the earthquake hazard, vulnerability, and risk assessment using the 7.5m resolution DEM, inventory, and several other rasters and vector layers. Many qualitative and quantitative elements that control the earthquake phenomenon is complicated tectonics and stress accumulation and release. Interferometric Synthetic Aperture RADAR (InSAR) and Unmanned Aerial Vehicle (UAV) could be engaged in the risk assessment. Several sensors are accessible to be tested for that reason.
5. The current research can be enhanced further by utilizing a completed inventory dataset including detailed seismic factors. In addition, an earthquake early warning and monitoring system should be developed in association with a public agency, decision-makers, individual researchers for constructing and evaluating alternative earthquake risk models.
6. The future study could emphasize organizing city-scale pre- and post-EVA in developed and developing countries to produce a valid EVA tool.
7. Seismic probability mapping should be the main research as the earthquake prediction is challenging that could be done by developing novel machine learning and advanced artificial intelligence algorithms.

REFERENCES

Abdollahi, A., Pradhan, B., Shukla, N., Chakraborty, S. & Alamri, A. 2020, 'Deep Learning Approaches Applied to Remote Sensing Datasets for Road Extraction: A State-Of-The-Art Review', *Remote Sensing*, vol. 12, no. 9, p. 1444.

Abdollahzadeh, G. & Faghihmaleki, H. 2017, 'Probabilistic two-hazard risk assessment of near-fault and far-fault earthquakes in a structure subjected to earthquake-induced gas explosion', *Journal of Building Engineering*, vol. 13, pp. 298-304.

Abraham, A. 2005, 'Artificial neural networks. In p. H. Sydenham & r. Thorn (eds.), handbook of measuring system design', New York: John Wiley & Sons.

Adger, W.N., Brooks, N., Bentham, G., Agnew, M. & Eriksen, S. 2005, *New indicators of vulnerability and adaptive capacity*, Tyndall Centre for Climate Change Research Norwich.

Adger, W.N. & Kelly, P.M. 1999, 'Social vulnerability to climate change and the architecture of entitlements', *Mitigation and Adaptation Strategies for Global Change*, vol. 4, no. 3-4, pp. 253-66.

Aghataher, R., Delavar, M., Nami, M. & Samnay, N. 2008, 'A fuzzy-AHP decision support system for evaluation of cities vulnerability against earthquakes', *World Applied Sciences Journal*, vol. 3, no. 1, pp. 66-72.

Aghdam, I.N., Varzandeh, M.H.M. & Pradhan, B. 2016, 'Landslide susceptibility mapping using an ensemble statistical index (Wi) and adaptive neuro-fuzzy inference system (ANFIS) model at Alborz Mountains (Iran)', *Environmental Earth Sciences*, vol. 75, no. 7, p. 553.

Ahmad, R.A., Singh, R.P. & Adris, A. 2017, 'Seismic hazard assessment of Syria using seismicity, DEM, slope, active faults and GIS', *Remote Sensing Applications: Society and Environment*, vol. 6, pp. 59-70.

Akhoondzadeh, M., De Santis, A., Marchetti, D., Piscini, A. & Cianchini, G. 2018, 'Multi precursors analysis associated with the powerful Ecuador (MW= 7.8) earthquake of 16 April 2016 using Swarm satellites data in conjunction with other multi-platform satellite and ground data', *Advances in Space Research*, vol. 61, no. 1, pp. 248-63.

Al-Arifi, N.S., Fat-Helbary, R., Khalil, A.R. & Lashin, A.A. 2013, 'A new evaluation of seismic hazard for the northwestern part of Saudi Arabia', *Natural Hazards*, vol. 69, no. 3, pp. 1435-57.

Alarifi, A.S., Alarifi, N.S. & Al-Humidan, S. 2012, 'Earthquakes magnitude predication using artificial neural network in northern Red Sea area', *Journal of King Saud University-Science*, vol. 24, no. 4, pp. 301-13.

Alizadeh, M., Alizadeh, E., Asadollahpour Kotenaee, S., Shahabi, H., Beiranvand Pour, A., Panahi, M., Bin Ahmad, B. & Saro, L. 2018, 'Social vulnerability assessment using artificial neural network (ANN) model for earthquake hazard in Tabriz city, Iran', *Sustainability*, vol. 10, no. 10, p. 3376.

Alizadeh, M., Hashim, M., Alizadeh, E., Shahabi, H., Karami, M.R., Beiranvand Pour, A., Pradhan, B. & Zabihi, H. 2018, 'Multi-criteria decision making (MCDM) model for seismic vulnerability assessment (SVA) of urban residential buildings', *ISPRS International Journal of Geo-Information*, vol. 7, no. 11, p. 444.

Alizadeh, M., Ngah, I., Hashim, M., Pradhan, B. & Pour, A.B. 2018, 'A hybrid analytic network process and artificial neural network (ANP-ANN) model for urban earthquake vulnerability assessment', *Remote Sensing*, vol. 10, no. 6, p. 975.

Ambraseys, N.N. & Melville, C.P. 1995, 'Historical evidence of faulting in Eastern Anatolia and Northern Syria', *Annals of Geophysics*, vol. 38, no. 3-4.

Armaş, I. 2012, 'Multi-criteria vulnerability analysis to earthquake hazard of Bucharest, Romania', *Natural Hazards*, vol. 63, no. 2, pp. 1129-56.

Asencio-Cortés, G., Martínez-Álvarez, F., Morales-Esteban, A. & Reyes, J. 2016, 'A sensitivity study of seismicity indicators in supervised learning to improve earthquake prediction', *Knowledge-Based Systems*, vol. 101, pp. 15-30.

Asim, K., Martínez-Álvarez, F., Basit, A. & Iqbal, T. 2017, 'Earthquake magnitude prediction in Hindukush region using machine learning techniques', *Natural Hazards*, vol. 85, no. 1, pp. 471-86.

Atkinson, G.M. 2009, 'Earthquake time histories compatible with the 2005 National building code of Canada uniform hazard spectrum', *Canadian Journal of Civil Engineering*, vol. 36, no. 6, pp. 991-1000.

Atkinson, P.M. & Tatnall, A.R. 1997, 'Introduction neural networks in remote sensing', *International Journal of Remote Sensing*, vol. 18, no. 4, pp. 699-709.

Aucelli, P.P.C., Di Paola, G., Valente, E., Amato, V., Bracone, V., Cesarano, M., Di Capua, G., Scorpio, V., Capalbo, A. & Pappone, G. 2018, 'First assessment of the local seismic amplification susceptibility of the Isernia Province (Molise Region, Southern Italy) by the integration of geological and geomorphological studies related to the first level seismic microzonation project', *Environmental Earth Sciences*, vol. 77, no. 4, p. 118.

Azeez, O.S., Pradhan, B., Jena, R., Jung, H.-S. & Ahmed, A.A. 2019, 'Traffic emission modelling using LiDAR derived parameters and integrated geospatial model', *Korean Journal of Remote Sensing*, vol. 35, no. 1, pp. 137-49.

Bahadori, H., Hasheminezhad, A. & Karimi, A. 2017, 'Development of an integrated model for seismic vulnerability assessment of residential buildings: application to Mahabad City, Iran', *Journal of Building Engineering*, vol. 12, pp. 118-31.

Bai, S., Wang, J., Zhang, Z. & Cheng, C. 2012, 'Combined landslide susceptibility mapping after Wenchuan earthquake at the Zhouqu segment in the Bailongjiang Basin, China', *Catena*, vol. 99, pp. 18-25.

Baja, S., Chapman, D.M. & Dragovich, D. 2007, 'Spatial based compromise programming for multiple criteria decision making in land use planning', *Environmental Modeling & Assessment*, vol. 12, no. 3, pp. 171-84.

Bappenas & Community, t.h.I.D. 2005, 'Indonesia: Preliminary damage and loss assessment—The December 26, 2004 natural disaster', National Development Planning Agency Jakarta, Indonesia.

Barber, A.J., Crow, M.J. & Milsom, J. 2005, 'Sumatra: Geology, resources and tectonic evolution', Geological Society of London.

Barreca, G., Bonforte, A. & Neri, M. 2013, 'A pilot GIS database of active faults of Mt. Etna (Sicily): A tool for integrated hazard evaluation', *Journal of volcanology and geothermal research*, vol. 251, pp. 170-86.

Bathrellos, G.D., Skilodimou, H.D., Chousianitis, K., Youssef, A.M. & Pradhan, B. 2017, 'Suitability estimation for urban development using multi-hazard assessment map', *Science of the Total Environment*, vol. 575, pp. 119-34.

Battarra, M., Balcik, B. & Xu, H. 2018, 'Disaster preparedness using risk-assessment methods from earthquake engineering', *European Journal of Operational Research*, vol. 269, no. 2, pp. 423-35.

Bayrak, Y., Öztürk, S., Çınar, H., Kalafat, D., Tsapanos, T.M., Koravos, G.C. & Leventakis, G.-A. 2009, 'Estimating earthquake hazard parameters from instrumental data for different regions in and around Turkey', *Engineering Geology*, vol. 105, no. 3-4, pp. 200-10.

Beale, H.D., Demuth, H.B. & Hagan, M. 1996, 'Neural network design', *Pws, Boston*.

Beccari, B. 2016, 'A comparative analysis of disaster risk, vulnerability and resilience composite indicators', *PLoS Currents*, vol. 8.

Bellier, O., Sebrier, M., Pramumijoyo, S., Beaudouin, T., Harjono, H., Bahar, I. & Forni, O. 1997, 'Paleoseismicity and seismic hazard along the Great Sumatran Fault (Indonesia)', *Journal of Geodynamics*, vol. 24, no. 1-4, pp. 169-83.

Bender, B. & Perkins, D.M. 1987, *SEISRISK III: a computer program for seismic hazard estimation*, US Government Printing Office.

Benedetti, L., Finkel, R., King, G., Armijo, R., Papanastassiou, D., Ryerson, F., Flerit, F., Farber, D. & Stavrakakis, G. 2003, 'Motion on the Kaparelli fault (Greece) prior to the 1981 earthquake sequence determined from 36Cl cosmogenic dating', *Terra Nova*, vol. 15, no. 2, pp. 118-24.

Bilham, R. & Ambraseys, N. 2005, 'Apparent Himalayan slip deficit from the summation of seismic moments for Himalayan earthquakes, 1500–2000', *Current Science*, pp. 1658-63.

Binita, K., Shepherd, J.M. & Gaither, C.J. 2015, 'Climate change vulnerability assessment in Georgia', *Applied Geography*, vol. 62, pp. 62-74.

Brinkman, B.A., LeBlanc, M., Ben-Zion, Y., Uhl, J.T. & Dahmen, K.A. 2015, 'Probing failure susceptibilities of earthquake faults using small-quake tidal correlations', *Nature Communications*, vol. 6, no. 1, pp. 1-7.

Birkmann, J. 2007, 'Risk and vulnerability indicators at different scales: Applicability, usefulness and policy implications', *Environmental Hazards*, vol. 7, no. 1, pp. 20-31.

Birkmann, J. & Welle, T. 2015, 'Assessing the risk of loss and damage: exposure, vulnerability and risk to climate-related hazards for different country classifications', *International Journal of Global Warming*, vol. 8, no. 2, pp. 191-212.

Blaikie, P., Cannon, T., Davis, I. & Wisner, B. 2014, *At risk: natural hazards, people's vulnerability and disasters*, Routledge.

Blaser, L., Krüger, F., Ohrnberger, M. & Scherbaum, F. 2010, 'Scaling relations of earthquake source parameter estimates with special focus on subduction environment', *Bulletin of the Seismological Society of America*, vol. 100, no. 6, pp. 2914-26.

Bletery, Q., Thomas, A.M., Rempel, A.W., Karlstrom, L., Sladen, A. & De Barros, L. 2016, 'Mega-earthquakes rupture flat megathrusts', *Science*, vol. 354, no. 6315, pp. 1027-31.

Bommer, J.J. & Abrahamson, N.A. 2006, 'Why do modern probabilistic seismic-hazard analyses often lead to increased hazard estimates?', *Bulletin of the Seismological Society of America*, vol. 96, no. 6, pp. 1967-77.

Bommer, J.J., Scherbaum, F., Bungum, H., Cotton, F., Sabetta, F. & Abrahamson, N.A. 2005, 'On the use of logic trees for ground-motion prediction equations in seismic-hazard analysis', *Bulletin of the Seismological Society of America*, vol. 95, no. 2, pp. 377-89.

Botev, Z.I., Grotowski, J.F. & Kroese, D.P. 2010, 'Kernel density estimation via diffusion', *The annals of Statistics*, vol. 38, no. 5, pp. 2916-57.

Bray, J.D., Seed, R.B., Cluff, L.S. & Seed, H.B. 1994, 'Earthquake fault rupture propagation through soil', *Journal of Geotechnical Engineering*, vol. 120, no. 3, pp. 543-61.

Brebbia, C.A. 1996, *The Kobe earthquake: geodynamical aspects*.

Brooks, N. 2003, 'Vulnerability, risk and adaptation: A conceptual framework', *Tyndall Centre for Climate Change Research Working Paper*, vol. 38, no. 38, pp. 1-16.

Bui, D.T., Ho, T.-C., Pradhan, B., Pham, B.-T., Nhu, V.-H. & Revhaug, I. 2016, 'GIS-based modeling of rainfall-induced landslides using data mining-based functional trees classifier with AdaBoost, Bagging, and MultiBoost ensemble frameworks', *Environmental Earth Sciences*, vol. 75, no. 14, p. 1101.

Bui, D.T., Tuan, T.A., Klempe, H., Pradhan, B. & Revhaug, I. 2016, 'Spatial prediction models for shallow landslide hazards: a comparative assessment of the efficacy of support vector machines, artificial neural networks, kernel logistic regression, and logistic model tree', *Landslides*, vol. 13, no. 2, pp. 361-78.

Cannon, T. 1994, 'Vulnerability analysis and the explanation of 'natural'disasters', *Disasters, development and environment*, vol. 1, pp. 13-30.

Campbell, K. & Bozorgnia, Y. 1994, 'Empirical analysis of strong ground motion from the 1992 Landers, California, earthquake', *Bulletin of the Seismological Society of America*, vol. 84, no. 3, pp. 573-88.

Campbell, K.W. & Bozorgnia, Y. 2003, 'Updated near-source ground-motion (attenuation) relations for the horizontal and vertical components of peak ground acceleration and acceleration response spectra', *Bulletin of the Seismological Society of America*, vol. 93, no. 1, pp. 314-31.

Cao, J., Zhang, Z., Wang, C., Liu, J. & Zhang, L. 2019, 'Susceptibility assessment of landslides triggered by earthquakes in the Western Sichuan Plateau', *Catena*, vol. 175, pp. 63-76.

Chai, T. & Draxler, R.R. 2014, 'Root mean square error (RMSE) or mean absolute error (MAE)?–Arguments against avoiding RMSE in the literature', *Geoscientific Model Development*, vol. 7, no. 3, pp. 1247-50.

Chakraborty, J., Tobin, G.A. & Montz, B.E. 2005, 'Population evacuation: assessing spatial variability in geophysical risk and social vulnerability to natural hazards', *Natural Hazards Review*, vol. 6, no. 1, pp. 23-33.

Chang, J.C.-J. & King, W.R. 2005, 'Measuring the performance of information systems: A functional scorecard', *Journal of Management Information Systems*, vol. 22, no. 1, pp. 85-115.

Chaulagain, H., Rodrigues, H., Silva, V., Spacone, E. & Varum, H. 2015, 'Seismic risk assessment and hazard mapping in Nepal', *Natural Hazards*, vol. 78, no. 1, pp. 583-602.

Cheng, C.-T., Zhao, M.-Y., Chau, K. & Wu, X.-Y. 2006, 'Using genetic algorithm and TOPSIS for Xinanjiang model calibration with a single procedure', *Journal of Hydrology*, vol. 316, no. 1-4, pp. 129-40.

Choi, J.-Y., Engel, B.A. & Farnsworth, R.L. 2005, 'Web-based GIS and spatial decision support system for watershed management', *Journal of Hydroinformatics*, vol. 7, no. 3, pp. 165-74.

Cipta, A., Robiana, R., Griffin, J., Horspool, N., Hidayati, S. & Cummins, P.R. 2017, 'A probabilistic seismic hazard assessment for Sulawesi, Indonesia', *Geological Society, London, Special Publications*, vol. 441, no. 1, pp. 133-52.

Clinton, W. 2005, 'Tsunami recovery: Taking stock after 12 months', *Retrieved July*, vol. 27, p. 2007.

Collobert, R., Weston, J., Bottou, L., Karlen, M., Kavukcuoglu, K. & Kuksa, P. 2011, 'Natural language processing (almost) from scratch', *Journal of Machine Learning Research*, vol. 12, p. 2493− 537.

Comprehensive Approach for probabilistic risk assessment, *viewed 10 feb 2018, https://ecapra.org/.*

Consultant, G. 2009, 'Final report: identification of seismic source's zone and tsunami hazard probability as considerations in development policy of Banda Aceh city', *Nanggroe Aceh Darussalam Province (Package-1), Banda Aceh*.

Cornell, C.A. 1968, 'Engineering seismic risk analysis', *Bulletin of the seismological society of America*, vol. 58, no. 5, pp. 1583-606.

Cornell, C.A. & Vanmarcke, E.H. 1969, 'The major influences on seismic risk', *Proceedings of the fourth world conference on earthquake engineering*, vol. 1, pp. 69-83.

Corral, A. 2004, 'Long-term clustering, scaling, and universality in the temporal occurrence of earthquakes', *Physical Review Letters*, vol. 92, no. 10, p. 108501.

Cox, B.R., Bachhuber, J., Rathje, E., Wood, C.M., Dulberg, R., Kottke, A., Green, R.A. & Olson, S.M. 2011, 'Shear wave velocity-and geology-based seismic microzonation of Port-au-Prince, Haiti', *Earthquake Spectra*, vol. 27, no. 1_suppl1, pp. 67-92.

Crowley, H., Pinho, R., Pagani, M. & Keller, N. 2013, 'Assessing global earthquake risks: the Global Earthquake Model (GEM) initiative', *Handbook of seismic risk analysis and management of civil infrastructure systems*, Elsevier, pp. 815-38.

Culshaw, M., Duncan, S. & Sutarto, N. 1979, 'Engineering geological mapping of the Banda Aceh alluvial basin, Northern Sumatra, Indonesia', *Bulletin of the International Association of Engineering Geology-Bulletin de l'Association Internationale de Géologie de l'Ingénieur*, vol. 19, no. 1, pp. 40-7.

Cutter, S.L. 1996, 'Vulnerability to environmental hazards', *Progress in Human Geography*, vol. 20, no. 4, pp. 529-39.

Cutter, S.L., Mitchell, J.T. & Scott, M.S. 2000, 'Revealing the vulnerability of people and places: A case study of Georgetown County, South Carolina', *Annals of the Association of American Geographers*, vol. 90, no. 4, pp. 713-37.

Dalkey, N. & Helmer, O. 1963, 'An experimental application of the Delphi method to the use of experts', *Management Science*, vol. 9, no. 3, pp. 458-67.

Danciu, L., Kale, Ö. & Akkar, S. 2018, 'The 2014 Earthquake Model of the Middle East: ground motion model and uncertainties', *Bulletin of Earthquake Engineering*, vol. 16, no. 8, pp. 3497-533.

Davidson, D.J. & Freudenburg, W.R. 1996, 'Gender and environmental risk concerns: A review and analysis of available research', *Environment and Behavior*, vol. 28, no. 3, pp. 302-39.

Davidson, R.A. & Shah, H.C. 1997, *An urban earthquake disaster risk index*, John A. Blume Earthquake Engineering Center Standford University.

Debnath, R. 2013, 'An assessment of spatio-temporal pattern of urban earthquake vulnerability using GIS: a study on Dhaka City', *Annals of GIS*, vol. 19, no. 2, pp. 63-78.

Deif, A., El-Hussain, I., Al-Jabri, K., Toksoz, N., El-Hady, S., Al-Hashmi, S., Al-Toubi, K., Al-Shijbi, Y. & Al-Saifi, M. 2013, 'Deterministic seismic hazard assessment for Sultanate of Oman', *Arabian Journal of Geosciences*, vol. 6, no. 12, pp. 4947-60.

Delavaud, E., Cotton, F., Akkar, S., Scherbaum, F., Danciu, L., Beauval, C., Drouet, S., Douglas, J., Basili, R. & Sandikkaya, M.A. 2012, 'Toward a ground-motion logic tree for probabilistic seismic hazard assessment in Europe', *Journal of Seismology*, vol. 16, no. 3, pp. 451-73.

Delescluse, M., Chamot-Rooke, N., Cattin, R., Fleitout, L., Trubienko, O. & Vigny, C. 2012, 'April 2012 intra-oceanic seismicity off Sumatra boosted by the Banda-Aceh megathrust', *Nature*, vol. 490, no. 7419, pp. 240-4.

Deligiannakis, G., Papanikolaou, I. & Roberts, G. 2018, 'Fault specific GIS based seismic hazard maps for the Attica region, Greece', *Geomorphology*, vol. 306, pp. 264-82.

Dhar, S., Rai, A. & Nayak, P. 2017, 'Estimation of seismic hazard in Odisha by remote sensing and GIS techniques', *Natural Hazards*, vol. 86, no. 2, pp. 695-709.

Dias, V.H., Papa, A.R. & Ferreira, D.S. 2019, 'Analysis of temporal and spatial distributions between earthquakes in the region of California through Non-Extensive Statistical Mechanics and its limits of validity', *Physica A: Statistical Mechanics and its Applications*, vol. 529, p. 121471.

Dilley, M., Chen, R.S., Deichmann, U., Lerner-Lam, A.L. & Arnold, M. 2005, *Natural disaster hotspots: a global risk analysis*, The World Bank.

Dimri, S., Lakhera, R. & Sati, S. 2007, 'Fuzzy-based method for landslide hazard assessment in active seismic zone of Himalaya', *Landslides*, vol. 4, no. 2, p. 101.

Dou, J., Yunus, A.P., Tien Bui, D., Sahana, M., Chen, C.-W., Zhu, Z., Wang, W. & Thai Pham, B. 2019, 'Evaluating GIS-based multiple statistical models and data mining for earthquake and rainfall-induced landslide susceptibility using the LiDAR DEM', *Remote Sensing*, vol. 11, no. 6, p. 638.

Dutta, S.C., Nayak, S., Acharjee, G., Panda, S.K. & Das, P.K. 2016, 'Gorkha (Nepal) earthquake of April 25, 2015: Actual damage, retrofitting measures and prediction by RVS for a few typical structures', *Soil Dynamics and Earthquake Engineering*, vol. 89, pp. 171-84.

Ebert, A., Kerle, N. & Stein, A. 2009, 'Urban social vulnerability assessment with physical proxies and spatial metrics derived from air-and spaceborne imagery and GIS data', *Natural Hazards*, vol. 48, no. 2, pp. 275-94.

Erden, T. & Karaman, H. 2012, 'Analysis of earthquake parameters to generate hazard maps by integrating AHP and GIS for Küçükçekmece region', *Natural Hazards and Earth System Sciences*, vol. 12, no. 2, pp. 475-83.

Estoque, R.C. 2012, 'Analytic hierarchy process in geospatial analysis', *Progress in Geospatial Analysis*, Springer, pp. 157-81.

Fanos, A.M. & Pradhan, B. 2019, 'A spatial ensemble model for rockfall source identification from high resolution LiDAR data and GIS', *IEEE Access*, vol. 7, pp. 74570-85.

Farabet, C., Couprie, C., Najman, L. & LeCun, Y. 2012, 'Learning hierarchical features for scene labeling', *IEEE Transactions on Pattern Analysis and Machine Intelligence*, vol. 35, no. 8, pp. 1915-29.

Fayyad, U.M., Piatetsky-Shapiro, G. & Smyth, P. 1996, 'Knowledge Discovery and Data Mining: Towards a Unifying Framework', *KDD*, vol. 96, pp. 82-8.

Federal Emergency Management Agency 1979, *viewed 13 June 2017, https://www.fema.gov/hazus.*

Florido, E., Martínez-Álvarez, F., Morales-Esteban, A., Reyes, J. & Aznarte-Mellado, J.L. 2015, 'Detecting precursory patterns to enhance earthquake prediction in Chile', *Computers & Geosciences*, vol. 76, pp. 112-20.

Frankel, A. 1995, 'Mapping seismic hazard in the central and eastern United States', *Seismological Research Letters*, vol. 66, no. 4, pp. 8-21.

Frigerio, I., Ventura, S., Strigaro, D., Mattavelli, M., De Amicis, M., Mugnano, S. & Boffi, M. 2016, 'A GIS-based approach to identify the spatial variability of social vulnerability to seismic hazard in Italy', *Applied Geography*, vol. 74, pp. 12-22.

Ganas, A., Pavlides, S. & Karastathis, V. 2005, 'DEM-based morphometry of range-front escarpments in Attica, central Greece, and its relation to fault slip rates', *Geomorphology*, vol. 65, no. 3-4, pp. 301-19.

García-Cascales, M.S. & Lamata, M.T. 2012, 'On rank reversal and TOPSIS method', *Mathematical and Computer Modelling*, vol. 56, no. 5-6, pp. 123-32.

Gentile, R., Galasso, C., Idris, Y., Rusydy, I. & Meilianda, E. 2019, 'From rapid visual survey to multi-hazard risk prioritisation and numerical fragility of school buildings', *Natural Hazards and Earth System Sciences Discussions*, vol. 19, no. 7, pp. 1365-86.

Geoscience australaia, *viewed 13 June 2018, http://www.ga.gov.au/.*

Global earthquake model, *viewed 13 June 2017, https://www.globalquakemodel.org/.*

Ghasemi, K., Pradhan, B. & Jena, R. 2018, 'Spatial identification of key alteration minerals using ASTER and Landsat 8 data in a heavily vegetated tropical area', *Journal of the Indian Society of Remote Sensing*, vol. 46, no. 7, pp. 1061-73.

Ghorbanzadeh, O., Blaschke, T., Aryal, J. & Gholaminia, K. 2018, 'A new GIS-based technique using an adaptive neuro-fuzzy inference system for land subsidence susceptibility mapping', *Journal of Spatial Science*, pp. 1-17.

Ghorbanzadeh, O., Valizadeh Kamran, K., Blaschke, T., Aryal, J., Naboureh, A., Einali, J. & Bian, J. 2019, 'Spatial prediction of wildfire susceptibility using field survey gps data and machine learning approaches', *Fire*, vol. 2, no. 3, p. 43.

Giardini, D., Danciu, L., Erdik, M., Şeşetyan, K., Tümsa, M.B.D., Akkar, S., Gülen, L. & Zare, M. 2018, 'Seismic hazard map of the Middle East', *Bulletin of Earthquake Engineering*, vol. 16, no. 8, pp. 3567-70.

Gong, P. 1996, 'Geological mapping', *Photogrammetric Engnineering and Remote Sensing*, vol. 62, no. 5, pp. 513-23.

Granger, K., Jones, T., Leiba, M. & Scott, G. 1999, 'Community risk in Cairns', *A multi-hazard risk assessment. Canberra, AGSO*, vol. 130.

Graves, A., Mohamed, A.-r. & Hinton, G. 2013, 'Speech recognition with deep recurrent neural networks', *2013 IEEE international conference on acoustics, speech and signal processing*, IEEE, pp. 6645-9.

Greiving, S., Fleischhauer, M. & Lückenkötter, J. 2006, 'A methodology for an integrated risk assessment of spatially relevant hazards', *Journal of Environmental Planning and Management*, vol. 49, no. 1, pp. 1-19.

Grützner, C., Barba, S., Papanikolaou, I. & Pérez-López, R. 2014, 'Earthquake geology: science, society and critical facilities', *Annals of Geophysics*, vol. 56, no. 6.

Grützner, C., Schneiderwind, S., Papanikolaou, I., Deligiannakis, G., Pallikarakis, A. & Reicherter, K. 2016, 'New constraints on extensional tectonics and seismic hazard in northern Attica, Greece: the case of the Milesi Fault', *Geophysical Journal International*, vol. 204, no. 1, pp. 180-99.

Gulkan, P. & Sozen, M.A. 1999, 'Procedure for determining seismic vulnerability of building structures', *Structural Journal*, vol. 96, no. 3, pp. 336-42.

Gutenberg, B. & Richter, C.F. 1944, 'Frequency of earthquakes in California', *Bulletin of the Seismological Society of America*, vol. 34, no. 4, pp. 185-8.

Hagiwara, Y. 1974, 'Probability of earthquake occurrence as obtained from a Weibull distribution analysis of crustal strain', *Tectonophysics*, vol. 23, no. 3, pp. 313-8.

Hahn, M.B., Riederer, A.M. & Foster, S.O. 2009, 'The Livelihood Vulnerability Index: A pragmatic approach to assessing risks from climate variability and change—A case study in Mozambique', *Global Environmental Change*, vol. 19, no. 1, pp. 74-88.

Halchuk, S. & Adams, J. 2004, 'Deaggregation of seismic hazard for selected Canadian cities', *Proceedings of the 13th World Conference on Earthquake Engineering, Vancouver, Canada. Paper*, vol. 2470.

Hall, R. 2002, 'Cenozoic geological and plate tectonic evolution of SE Asia and the SW Pacific: computer-based reconstructions, model and animations', *Journal of Asian Earth Sciences*, vol. 20, no. 4, pp. 353-431.

Hanks, T.C., Abrahamson, N.A., Boore, D.M., Coppersmith, K.J. & Knepprath, N.E. 2009, 'Implementation of the SSHAC Guidelines for Level 3 and 4 PSHAs—Experience gained from actual applications', *US Geological Survey Open-File Report*, vol. 1093, p. 66.

Hannich, D., Hötzl, H. & Cudmani, R. 2006, 'The influence of groundwater on damage caused by earthquakes–an overview'.

Hardebeck, J.L. 2004, 'Stress triggering and earthquake probability estimates', *Journal of Geophysical Research: Solid Earth*, vol. 109, no. B4.

Harmsen, S., Perkins, D. & Frankel, A. 1999, 'Deaggregation of probabilistic ground motions in the central and eastern United States', *Bulletin of the Seismological Society of America*, vol. 89, no. 1, pp. 1-13.

Haykin, S.S. 2009, 'Neural networks and learning machines/Simon Haykin', New York: Prentice Hall.

Helmstaedter, M., Briggman, K.L., Turaga, S.C., Jain, V., Seung, H.S. & Denk, W. 2013, 'Connectomic reconstruction of the inner plexiform layer in the mouse retina', *Nature*, vol. 500, no. 7461, pp. 168-74.

Hinton, G., Deng, L., Yu, D., Dahl, G.E., Mohamed, A.-r., Jaitly, N., Senior, A., Vanhoucke, V., Nguyen, P. & Sainath, T.N. 2012, 'Deep neural networks for acoustic modeling in speech recognition: The shared views of four research groups', *IEEE Signal Processing Magazine*, vol. 29, no. 6, pp. 82-97.

Hosseini, A., GHasemi, Z., Ahadnejad, M. & Alimoradi, T. 2014, 'Evaluation of qualitative and quantitative indicators of social housing in the Tabriz metropolitan', *International Journal of Behavioral Sciences,* vol. 4, pp. 19-30.

Idowu, S., Saguna, S., Åhlund, C. & Schelén, O. 2016, 'Applied machine learning: Forecasting heat load in district heating system', *Energy and Buildings*, vol. 133, pp. 478-88.

Iemura, H., Igarashi, A., Pradono, M.H. & Kalantari, A. 2006, 'Negative stiffness friction damping for seismically isolated structures', *Structural Control and Health Monitoring: The Official Journal of the International Association for Structural Control and Monitoring and of the European Association for the Control of Structures*, vol. 13, no. 2-3, pp. 775-91.

Ikram, A. & Qamar, U. 2015, 'Developing an expert system based on association rules and predicate logic for earthquake prediction', *Knowledge-Based Systems*, vol. 75, pp. 87-103.

Ilanlu, M., Ardakani, A., Paknezhad, H., Ebrahimi, M. & Gelsefid, Y.A.S. 2013, 'Identifying the urban vulnerable areas against the earthquake with GIS case study radio darya st. chalous', *International Journal of Advanced Studies in Humanities and Social Science*, vol. 1, no. 4, pp. 264-73.

INFORM Risk Index, *viewed 13 july 2018, http://www.inform-index.org.*

Irwansyah, E. 2010, 'Building damage assessment using remote sensing, aerial photograph and GIS data-case study in Banda Aceh after Sumatera Earthquake 2004', *Proceeding of Seminar on Intelligent Technology and Its Application (SITIA 2010)*, vol. 11, pp. 57-65.

Irwansyah, E. & Hartati, S. 2014, 'Assessment of building damage hazard caused by earthquake: integration of FNN and GIS', *Ieri Procedia*, vol. 10, pp. 196-202.

Jaffe, B.E. & Gelfenbuam, G. 2007, 'A simple model for calculating tsunami flow speed from tsunami deposits', *Sedimentary Geology*, vol. 200, no. 3-4, pp. 347-61.

Jahan, I., Ansary, M., Ara, S. & Islam, I. 2011, 'Assessing social vulnerability to earthquake hazard in Old Dhaka, Bangladesh', *Asian Journal of Environment and Disaster Management (AJEDM)*, vol. 3, no. 3, pp. 285-300.

Jankowski, P. & Nyerges, T. 2001, 'GIS-supported collaborative decision making: results of an experiment', *Annals of the Association of American Geographers*, vol. 91, no. 1, pp. 48-70.

Jefferies, M. & Been, K. 2015, *Soil liquefaction: a critical state approach*, CRC press.

Jena, R., Pradhan, B. & Beydoun, G. 2020, 'Earthquake vulnerability assessment in Northern Sumatra province by using a multi-criteria decision-making model', *International Journal of Disaster Risk Reduction*, vol. 46, p. 101518.

Jena, R., Pradhan, B., Beydoun, G., Al-Amri, A. & Sofyan, H. 2020, 'Seismic hazard and risk assessment: a review of state-of-the-art traditional and GIS models', *Arabian Journal of Geosciences*, vol. 13, no. 2, p. 50.

Jena, R., Pradhan, B., Beydoun, G., Sofyan, H. & Affan, M. 2019, 'Integrated model for earthquake risk assessment using neural network and analytic hierarchy process: Aceh province, Indonesia', *Geoscience Frontiers*, vol. 11, no.2, pp. 613-634.

Johar, F., Majid, M.R., Jaffar, A.R. & Yahya, A.S. 2013, 'Seismic microzonation for Banda Aceh city planning', *Planning Malaysia*, vol. 11, no. 2.

Kafle, S.K. 2006, 'Rapid disaster risk assessment of coastal communities: a case study of mutiara village, Banda Aceh, Indonesia', *Proceedings of the International Conference on Environment and Disaster Management held in Jakarta, Indonesia on December*, pp. 5-8.

Kaliraj, S., Chandrasekar, N. & Magesh, N. 2015, 'Evaluation of multiple environmental factors for site-specific groundwater recharge structures in the Vaigai River upper basin, Tamil Nadu, India, using GIS-based weighted overlay analysis', *Environmental Earth Sciences*, vol. 74, no. 5, pp. 4355-80.

Kanai, K. 1961, 'An empirical formula for the spectrum of strong earthquake motions', *Bulletin of Earthquake Research*, vol. 39, pp. 85-95.

Kaplan, M., Renaud, F. & Lüchters, G. 2009, 'Vulnerability assessment and protective effects of coastal vegetation during the 2004 Tsunami in Sri Lanka', *Natural Hazards and Earth System Science*, vol. 9, no. 4, pp. 1479-94.

Karaman, H. & Erden, T. 2014, 'Net earthquake hazard and elements at risk (NEaR) map creation for city of Istanbul via spatial multi-criteria decision analysis', *Natural Hazards*, vol. 73, no. 2, pp. 685-709.

Karimzadeh, S., Cakir, Z., Osmanoğlu, B., Schmalzle, G., Miyajima, M., Amiraslanzadeh, R. & Djamour, Y. 2013, 'Interseismic strain accumulation across the North Tabriz Fault (NW Iran) deduced from InSAR time series', *Journal of Geodynamics*, vol. 66, pp. 53-8.

Karimzadeh, S., Kadaş, K., Askan, A., Erberik, M.A. & Yakut, A. 2017, 'A study on fragility analyses of masonry buildings in Erzincan (Turkey) utilizing simulated and real ground motion records', *Procedia Engineering*, vol. 199, pp. 188-93.

Karimzadeh, S., Miyajima, M., Hassanzadeh, R., Amiraslanzadeh, R. & Kamel, B. 2014, 'A GIS-based seismic hazard, building vulnerability and human loss assessment for the earthquake scenario in Tabriz', *Soil Dynamics and Earthquake Engineering*, vol. 66, pp. 263-80.

Karunanithi, N., Grenney, W.J., Whitley, D. & Bovee, K. 1994, 'Neural networks for river flow prediction', *Journal of Computing in Civil Engineering*, vol. 8, no. 2, pp. 201-20.

Katili, J.A. 1978, 'Past and present geotectonic position of Sulawesi, Indonesia', *Tectonophysics*, vol. 45, no. 4, pp. 289-322.

Khan, S. 2012, 'Vulnerability assessments and their planning implications: a case study of the Hutt Valley, New Zealand', *Natural Hazards*, vol. 64, no. 2, pp. 1587-607.

Khan, S.A., Pilakoutas, K., Hajirasouliha, I., Garcia, R. & Guadagnini, M. 2018, 'Seismic risk assessment for developing countries: Pakistan as a case study', *Earthquake Engineering and Engineering Vibration*, vol. 17, no. 4, pp. 787-804.

Klügel, J.-U. 2008, 'Seismic hazard analysis—Quo vadis?', *Earth-Science Reviews*, vol. 88, no. 1-2, pp. 1-32.

Koh, H.L., Teh, S.Y., Liu, P.L.F., Ismail, A.I.M. & Lee, H.L. 2009, 'Simulation of Andaman 2004 tsunami for assessing impact on Malaysia', *Journal of Asian Earth Sciences*, vol. 36, no. 1, pp. 74-83.

Kramer, S.L. 1996, *Geotechnical Earthquake Engineering*, Pearson Education India.

Krizhevsky, A., Sutskever, I. & Hinton, G.E. 2012, 'Imagenet classification with deep convolutional neural networks', *Advances in Neural Information Processing Systems*, pp. 1097-105.

Krinitzsky, E.L. 1993, 'Earthquake probability in engineering—Part 2: Earthquake recurrence and limitations of Gutenberg-Richter b-values for the engineering of critical structures: The third Richard H. Jahns distinguished lecture in engineering geology', *Engineering Geology*, vol. 36, no. 1-2, pp. 1-52.

Kussul, N., Shelestov, A. & Skakun, S. 2008, 'Grid system for flood extent extraction from satellite images', *Earth Science Informatics*, vol. 1, no. 3-4, p. 105.

Lee, W. & Brillinger, D. 1979, 'On Chinese earthquake history—An attempt to model an incomplete data set by point process analysis', *Earthquake Prediction and Seismicity Patterns*, Springer, pp. 1229-57.

Leung, M.K., Xiong, H.Y., Lee, L.J. & Frey, B.J. 2014, 'Deep learning of the tissue-regulated splicing code', *Bioinformatics*, vol. 30, no. 12, pp. i121-i9.

Lin, P.-S. & Lee, C.-T. 2008, 'Ground-motion attenuation relationships for subduction-zone earthquakes in northeastern Taiwan', *Bulletin of the Seismological Society of America*, vol. 98, no. 1, pp. 220-40.

Lindell, M.K. & Perry, R.W. 2000, 'Household adjustment to earthquake hazard: A review of research', *Environment and Behavior*, vol. 32, no. 4, pp. 461-501.

Liu, L.B., Berger, P., Zeng, A. & Gerstenfeld, A. 2008, 'Applying the analytic hierarchy process to the offshore outsourcing location decision', *Supply Chain Management: An International Journal*.

Louie, J.N. 2001, 'Faster, better: shear-wave velocity to 100 meters depth from refraction microtremor arrays', *Bulletin of the Seismological Society of America*, vol. 91, no. 2, pp. 347-64.

Løvholt, F., Setiadi, N.J., Birkmann, J., Harbitz, C.B., Bach, C., Fernando, N., Kaiser, G. & Nadim, F. 2014, 'Tsunami risk reduction–are we better prepared today than in 2004?', *International Journal of Disaster Risk Reduction*, vol. 10, pp. 127-42.

Malczewski, J. 1999, *GIS and multicriteria decision analysis*, John Wiley & Sons.

Malczewski, J. & Liu, X. 2014, 'Local ordered weighted averaging in GIS-based multicriteria analysis', *Annals of GIS*, vol. 20, no. 2, pp. 117-29.
Mardani, A., Zavadskas, E.K., Govindan, K., Amat Senin, A. & Jusoh, A. 2016, 'VIKOR technique: A systematic review of the state of the art literature on methodologies and applications', *Sustainability*, vol. 8, no. 1, p. 37.
Martínez-Garzón, P., Ben-Zion, Y., Zaliapin, I. & Bohnhoff, M. 2019, 'Seismic clustering in the Sea of Marmara: Implications for monitoring earthquake processes', *Tectonophysics*, vol. 768, p. 228176.
Martins, V.N., e Silva, D.S. & Cabral, P. 2012, 'Social vulnerability assessment to seismic risk using multicriteria analysis: the case study of Vila Franca do Campo (São Miguel Island, Azores, Portugal)', *Natural Hazards*, vol. 62, no. 2, pp. 385-404.
Matsuoka, M., Wakamatsu, K., Fujimoto, K. & Midorikawa, S. 2006, 'Average shear-wave velocity mapping using Japan engineering geomorphologic classification map', *Structural Engineering/Earthquake Engineering*, vol. 23, no. 1, pp. 57s-68s.
McCloskey, J., Nalbant, S.S. & Steacy, S. 2005, 'Earthquake risk from co-seismic stress', *Nature*, vol. 434, no. 7031, pp. 291-
McGuire, R. 1976, 'FORTRAN computer program for seismic risk analysis (No. 76-67)', *US Geological Survey*, vol. 25.
McGuire, R.K. 1978, *FRISK: computer program for seismic risk analysis using faults as earthquake sources*, 2331-1258, US Geological Survey.
McGuire, R.K. 1995, 'Probabilistic seismic hazard analysis and design earthquakes: closing the loop', *Bulletin of the Seismological Society of America*, vol. 85, no. 5, pp. 1275-84.
McIlraith, A.L. & Card, H.C. 1997, 'Birdsong recognition using backpropagation and multivariate statistics', *IEEE Transactions on Signal Processing*, vol. 45, no. 11, pp. 2740-8.
Mehta, P.K. & Burrows, R.W. 2001, 'Building durable structures in the 21 st century', *Indian Concrete Journal*, vol. 75, no. 7, pp. 437-43.
Meng, Y. & Malczewski, J. 2015, 'A GIS-based multicriteria decision making approach for evaluating accessibility to public parks in Calgary, Alberta', *Human Geographies*, vol. 9, no. 1, p. 29.
Megawati, K., Pan, T.-C. & Koketsu, K. 2005, 'Response spectral attenuation relationships for Sumatran-subduction earthquakes and the seismic hazard implications to Singapore and Kuala Lumpur', *Soil Dynamics and Earthquake Engineering*, vol. 25, no. 1, pp. 11-25.
Mhaske, S.Y. & Choudhury, D. 2010, 'GIS-based soil liquefaction susceptibility map of Mumbai city for earthquake events', *Journal of Applied Geophysics*, vol. 70, no. 3, pp. 216-25.
Michetti, A.M. & Marco, S. 2005, 'Future trends in paleoseismology: Integrated study of the seismic landscape as a vital tool in seismic hazard analyses', *Tectonophysics*, vol. 408, no. 1-4, pp. 3-21.
Mikolov, T., Deoras, A., Povey, D., Burget, L. & Černocký, J. 2011, 'Strategies for training large scale neural network language models', *2011 IEEE Workshop on Automatic Speech Recognition & Understanding*, IEEE, pp. 196-201.
Mili, R.R., Hosseini, K.A. & Izadkhah, Y.O. 2018, 'Developing a holistic model for earthquake risk assessment and disaster management interventions in urban fabrics', *International Journal of Disaster Risk Reduction*, vol. 27, pp. 355-65.

Mohammady, M., Pourghasemi, H.R. & Pradhan, B. 2012, 'Landslide susceptibility mapping at Golestan Province, Iran: a comparison between frequency ratio, Dempster–Shafer, and weights-of-evidence models', *Journal of Asian Earth Sciences*, vol. 61, pp. 221-36.

Mohanty, W.K. & Walling, M.Y. 2008, 'First order seismic microzonation of Haldia, Bengal Basin (India) using a GIS platform', *Pure and Applied Geophysics*, vol. 165, no. 7, pp. 1325-50.

Monahan, P., Levson, V., Hayes, B., Dorey, K., Mykula, Y., Brenner, R., Clarke, J., Galambos, B., Candy, C. & Krumbiegel, C. 2018, 'Mapping the Susceptibility to Amplification of Seismic Ground Motions in the Montney Play Area, Northeast British Columbia'.

Moradi, M., Delavar, M.R. & Moshiri, B. 2015, 'A GIS-based multi-criteria decision-making approach for seismic vulnerability assessment using quantifier-guided OWA operator: a case study of Tehran, Iran', *Annals of GIS*, vol. 21, no. 3, pp. 209-22.

Morales-Esteban, A., Martínez-Álvarez, F. & Reyes, J. 2013, 'Earthquake prediction in seismogenic areas of the Iberian Peninsula based on computational intelligence', *Tectonophysics*, vol. 593, pp. 121-34.

Moustafa, S.S. 2015, 'Application of the analytic hierarchy process for evaluating geo-hazards in the Greater Cairo area, Egypt', *Electronic Journal of Geotechnical Engineering*, vol. 20, no. 6, pp. 1921-38.

Mulargia, F., Stark, P.B. & Geller, R.J. 2017, 'Why is probabilistic seismic hazard analysis (PSHA) still used?', *Physics of the Earth and Planetary Interiors*, vol. 264, pp. 63-75.

Muñoz, M.A., Sun, Y., Kirley, M. & Halgamuge, S.K. 2015, 'Algorithm selection for black-box continuous optimization problems: A survey on methods and challenges', *Information Sciences*, vol. 317, pp. 224-45.

Murthy, V. 2007, 'Textbook of Soil Mechanics and Foundation Engineering-Geotechnical Engineering Series', Statish Kumar Jain: New Delhi, Pvt.

Naghibi, S.A., Pourghasemi, H.R. & Dixon, B. 2016, 'GIS-based groundwater potential mapping using boosted regression tree, classification and regression tree, and random forest machine learning models in Iran', *Environmental Monitoring and Assessment*, vol. 188, no. 1, p. 44.

Natawidjaja, D.H. & Triyoso, W. 2007, 'The Sumatran fault zone—From source to hazard', *Journal of Earthquake and Tsunami*, vol. 1, no. 01, pp. 21-47.

Nazzal, J.M., El-Emary, I.M. & Najim, S.A. 2008, 'Multilayer perceptron neural network (MLPs) for analyzing the properties of Jordan Oil Shale 1'.

Nedic, V., Despotovic, D., Cvetanovic, S., Despotovic, M. & Babic, S. 2014, 'Comparison of classical statistical methods and artificial neural network in traffic noise prediction', *Environmental Impact Assessment Review*, vol. 49, pp. 24-30.

Norwegian Seismic Array, *viewed 13 feb 2018, https://www.norsar.no/r-d/safe-society/earthquake-hazard risk/the-selena-open-risk-software/.*

Nyimbili, P.H., Erden, T. & Karaman, H. 2018, 'Integration of GIS, AHP and TOPSIS for earthquake hazard analysis', *Natural Hazards*, vol. 92, no. 3, pp. 1523-46.

Oliveira, C.S. 2003, 'Seismic vulnerability of historical constructions: a contribution', *Bulletin of Earthquake Engineering*, vol. 1, no. 1, pp. 37-82.

Ordaz, M., Aguilar, A. & Arboleda, J. 2001, 'CRISIS 99-18. Ver. 1.018. Program for Computing Seismic Risk', *Instituto de Ingeniería Universidad Nacional Autónoma de México*.

Ouma, Y.O. & Tateishi, R. 2014, 'Urban flood vulnerability and risk mapping using integrated multi-parametric AHP and GIS: methodological overview and case study assessment', *Water*, vol. 6, no. 6, pp. 1515-45.

Pachakis, D. & Kiremidjian, A.S. 2004, 'Estimation of downtime-related revenue losses in seaports following scenario earthquakes', *Earthquake Spectra*, vol. 20, no. 2, pp. 427-49.

Panahi, M., Rezaie, F. & Meshkani, S. 2014, 'Seismic vulnerability assessment of school buildings in Tehran city based on AHP and GIS', *Natural Hazards and Earth System Sciences*, vol. 14, no. 4, p. 969.

Panakkat, A. & Adeli, H. 2007, 'Neural network models for earthquake magnitude prediction using multiple seismicity indicators', *International Journal of Neural Systems*, vol. 17, no. 01, pp. 13-33.

Panakkat, A. & Adeli, H. 2009, 'Recurrent neural network for approximate earthquake time and location prediction using multiple seismicity indicators', *Computer-Aided Civil and Infrastructure Engineering*, vol. 24, no. 4, pp. 280-92.

Paola, J.D. & Schowengerdt, R. 1995, 'A review and analysis of backpropagation neural networks for classification of remotely-sensed multi-spectral imagery', *International Journal of Remote Sensing*, vol. 16, no. 16, pp. 3033-58.

Papanikolaou, D.J. & Royden, L.H. 2007, 'Disruption of the Hellenic arc: Late Miocene extensional detachment faults and steep Pliocene-Quaternary normal faults—Or what happened at Corinth?', *Tectonics*, vol. 26, no. 5.

Papanikolaou, I. 2003, 'Generation of high resolution seismic hazard maps in extensional tectonic settings through integration of earthquake geology, fault mechanics theory and GIS techniques', *Unpublished PhD thesis, University of London*, p. 437.

Papanikolaou, I.D., Van Balen, R., Silva, P.G. & Reicherter, K. 2015, 'Geomorphology of active faulting and seismic hazard assessment: New tools and future challenges', *Geomorphology*, vol. 237, pp. 1-13.

Papoulia, J., Stavrakakis, G. & Papanikolaou, D. 2001, 'Bayesian estimation of strong earthquakes in the Inner Messiniakos fault zone, southern Greece, based on seismological and geological data', *Journal of Seismology*, vol. 5, no. 2, pp. 233-42.

Paris, R., Lavigne, F., Wassmer, P. & Sartohadi, J. 2007, 'Coastal sedimentation associated with the december 26, 2004 tsunami in lhok nga, west banda aceh (sumatra, indonesia)', *Marine Geology*, vol. 238, no. 1-4, pp. 93-106.

Paris, R., Wassmer, P., Sartohadi, J., Lavigne, F., Barthomeuf, B., Desgages, E., Grancher, D., Baumert, P., Vautier, F. & Brunstein, D. 2009, 'Tsunamis as geomorphic crises: lessons from the December 26, 2004 tsunami in Lhok Nga, west Banda Aceh (Sumatra, Indonesia)', *Geomorphology*, vol. 104, no. 1-2, pp. 59-72.

Park, S., Choi, C., Kim, B. & Kim, J. 2013, 'Landslide susceptibility mapping using frequency ratio, analytic hierarchy process, logistic regression, and artificial neural network methods at the Inje area, Korea', *Environmental Earth Sciences*, vol. 68, no. 5, pp. 1443-64.

Park, Y., Kim, J., Jo, D.J. & Kim, S. 2015, 'Urban mud and debris flow disaster vulnerability assessment associated with landslide hazard map: application to Busan, Korea', *Journal of Korean Society of Hazard Mitigation*, vol. 15, no. 5, pp. 283-9.

Parsons, T. 2005, 'Significance of stress transfer in time-dependent earthquake probability calculations', *Journal of Geophysical Research: Solid Earth*, vol. 110, no. B5.

Pay, A.C. 2001, 'A new methodology for the seismic vulnerability assessment of existing buildings in Turkey'.

Peduzzi, P., Dao, H., Herold, C. & Mouton, F. 2009, 'Assessing global exposure and vulnerability towards natural hazards: the Disaster Risk Index', *Natural Hazards and Earth System Sciences*, vol. 9, no. 4, pp. 1149-59.

Perol, T., Gharbi, M. & Denolle, M. 2018, 'Convolutional neural network for earthquake detection and location', *Science Advances*, vol. 4, no. 2, p. e1700578.

Petersen, M.D., Dewey, J., Hartzell, S., Mueller, C., Harmsen, S., Frankel, A. & Rukstales, K. 2004, 'Probabilistic seismic hazard analysis for Sumatra, Indonesia and across the Southern Malaysian Peninsula', *Tectonophysics*, vol. 390, no. 1-4, pp. 141-58.

Pitilakis, K., Alexoudi, A., Argyroudis, S., Monge, O. & Martin, C. 2005, 'Chapter 9: Vulnerability assessment of lifelines', *Assessing and Managing Earthquake Risk. Geo-Scientific and Engineering Knowledge for Earthquake Risk mitigation: Developments, Tools and Techniques", Springer Publ*.

Pitilakis, K., Alexoudi, M., Argyroudis, S., Monge, O. & Martin, C. 2006, 'Earthquake risk assessment of lifelines', *Bulletin of Earthquake Engineering*, vol. 4, no. 4, pp. 365-90.

Pourghasemi, H.R., Mohammady, M. & Pradhan, B. 2012, 'Landslide susceptibility mapping using index of entropy and conditional probability models in GIS: Safarood Basin, Iran', *Catena*, vol. 97, pp. 71-84.

Pradhan, B., Abokharima, M.H., Jebur, M.N. & Tehrany, M.S. 2014, 'Land subsidence susceptibility mapping at Kinta Valley (Malaysia) using the evidential belief function model in GIS', *Natural Hazards*, vol. 73, no. 2, pp. 1019-42.

Pradhan, B. & Jena, R. 2016, 'Spatial relationship between earthquakes, hot-springs and faults in Odisha, India', *IOP Conference Series: Earth and Environmental Science*, vol. 37, IOP Publishing, p. 012070.

Pradhan, B. & Lee, S. 2009, 'Landslide risk analysis using artificial neural network model focusing on different training sites', *International Journal of Physical Sciences*, vol. 3, no. 11, pp. 1-15.

Pradhan, B. & Lee, S. 2010, 'Regional landslide susceptibility analysis using back-propagation neural network model at Cameron Highland, Malaysia', *Landslides*, vol. 7, no. 1, pp. 13-30.

Pradhan, B., Moneir, A.A.A. & Jena, R. 2018, 'Sand dune risk assessment in Sabha region, Libya using Landsat 8, MODIS, and Google Earth Engine images', *Geomatics, Natural Hazards and Risk*, vol. 9, no. 1, pp. 1280-305.

Rahman, N., Ansary, M.A. & Islam, I. 2015, 'GIS based mapping of vulnerability to earthquake and fire hazard in Dhaka city, Bangladesh', *International journal of disaster risk reduction*, vol. 13, pp. 291-300.

Ram, T.D. & Wang, G. 2013, 'Probabilistic seismic hazard analysis in Nepal', *Earthquake Engineering and Engineering Vibration*, vol. 12, no. 4, pp. 577-86.

Rashed, T. & Weeks, J. 2003, 'Assessing vulnerability to earthquake hazards through spatial multicriteria analysis of urban areas', *International Journal of Geographical Information Science*, vol. 17, no. 6, pp. 547-76.

Risk Quantification & Engineering, *viewed 13 July 2018, https://www.corelogic.com/products/rqe.aspx*.

Roberts, G., Houghton, S., Underwood, C., Papanikolaou, I., Cowie, P., van Calsteren, P., Wigley, T., Cooper, F. & McArthur, J. 2009, 'Localization of Quaternary slip rates in an active rift in 105 years: An example from central Greece constrained by 234U-230Th coral dates from uplifted paleoshorelines', *Journal of Geophysical Research: Solid Earth*, vol. 114, no. B10.

Roberts, G.P., Cowie, P., Papanikolaou, I. & Michetti, A.M. 2004, 'Fault scaling relationships, deformation rates and seismic hazards: an example from the Lazio–Abruzzo Apennines, central Italy', *Journal of Structural Geology*, vol. 26, no. 2, pp. 377-98.

Rouet-Leduc, B., Hulbert, C., Lubbers, N., Barros, K., Humphreys, C.J. & Johnson, P.A. 2017, 'Machine learning predicts laboratory earthquakes', *Geophysical Research Letters*, vol. 44, no. 18, pp. 9276-82.

Roy, G.D., Karim, M.F. & Ismail, A.I.M. 2007, 'A nonlinear polar coordinate shallow water model for tsunami computation along North Sumatra and Penang Island', *Continental Shelf Research*, vol. 27, no. 2, pp. 245-57.

Rozenstein, O. & Karnieli, A. 2011, 'Comparison of methods for land-use classification incorporating remote sensing and GIS inputs', *Applied Geography*, vol. 31, no. 2, pp. 533-44.

Ruano, A.E., Madureira, G., Barros, O., Khosravani, H.R., Ruano, M.G. & Ferreira, P.M. 2014, 'Seismic detection using support vector machines', *Neurocomputing*, vol. 135, pp. 273-83.

Ruddock, A. 2007, '‘Hers and His’: A Gendered Perspective on Disaster', *Human Rights in Global Light*, p. 77.

Rusydi, M. & Efendi, R. 2018, 'Earthquake hazard analysis use Vs30 data in Palu', *Journal of Physics: Conference Series*, vol. 979, IOP Publishing, p. 012054.

Rusydy, I., Idris, Y., Muksin, U., Cummins, P. & Akram, M.N. 2020, 'Shallow crustal earthquake models, damage, and loss predictions in Banda Aceh, Indonesia', *Geoenvironmental Disasters*, vol. 7, no. 1, p. 8.

Rydelek, P.A. & Sacks, I.S. 1989, 'Testing the completeness of earthquake catalogues and the hypothesis of self-similarity', *Nature*, vol. 337, no. 6204, pp. 251-3.

Rygel, L., O’sullivan, D. & Yarnal, B. 2006, 'A method for constructing a social vulnerability index: an application to hurricane storm surges in a developed country', *Mitigation and Adaptation Strategies for Global Change*, vol. 11, no. 3, pp. 741-64.

Saaty, T.L. 1988, 'What is the analytic hierarchy process?', *Mathematical Models for Decision Support*, Springer, pp. 109-21.

Saaty, T.L. 1990a, 'An exposition of the AHP in reply to the paper “remarks on the analytic hierarchy process”', *Management Science*, vol. 36, no. 3, pp. 259-68.

Saaty, T.L. 1990b, 'How to make a decision: the analytic hierarchy process', *European Journal of Operational Research*, vol. 48, no. 1, pp. 9-26.

Saaty, T.L. 2008, 'Decision making with the analytic hierarchy process', *International Journal of Services Sciences*, vol. 1, no. 1, pp. 83-98.

Safi, Y. & Bouroumi, A. 2013, 'Prediction of forest fires using artificial neural networks', *Applied Mathematical Sciences*, vol. 7, no. 6, pp. 271-86.

Sekac, T., Jana, S.K., Pal, I. & Pal, D.K. 2016, 'GIS based evaluation in earthquake hazard micro-zonation-a case study of Madang and Morobe Province, Papua New Guinea', *International Journal of Advanced Engineering Research and Science*, vol. 3, no. 8, p. 236817.

Sakellariou, D., Lykousis, V., Alexandri, S., Kaberi, H., Rousakis, G., Nomikou, P., Georgiou, P. & Ballas, D. 2007, 'Faulting, seismic-stratigraphic architecture and Late Quaternary evolution of the Gulf of Alkyonides Basin–East Gulf of Corinth, Central Greece', *Basin Research*, vol. 19, no. 2, pp. 273-95.

Sakellariou, S., Tampekis, S., Samara, F., Sfougaris, A. & Christopoulou, O. 2017, 'Review of state-of-the-art decision support systems (DSSs) for prevention and suppression of forest fires', *Journal of Forestry Research*, vol. 28, no. 6, pp. 1107-17.

San Cristóbal, J. 2011, 'Multi-criteria decision-making in the selection of a renewable energy project in spain: The Vikor method', *Renewable Energy*, vol. 36, no. 2, pp. 498-502.

Sánchez-Lozano, J.M., Teruel-Solano, J., Soto-Elvira, P.L. & García-Cascales, M.S. 2013, 'Geographical Information Systems (GIS) and Multi-Criteria Decision Making (MCDM) methods for the evaluation of solar farms locations: Case study in south-eastern Spain', *Renewable and Sustainable Energy Reviews*, vol. 24, pp. 544-56.

Sarker, J.K. 2011, 'GIS based methodologies of seismic Hazard and risk analysis for Bangladesh'.

Sarmah, T. & Das, S. 2018, 'Earthquake Vulnerability Assessment for RCC Buildings of Guwahati City using Rapid Visual Screening', *Procedia Engineering*, vol. 212, pp. 214-21.

Sarris, A., Loupasakis, C., Soupios, P., Trigkas, V. & Vallianatos, F. 2010, 'Earthquake vulnerability and seismic risk assessment of urban areas in high seismic regions: application to Chania City, Crete Island, Greece', *Natural Hazards*, vol. 54, no. 2, pp. 395-412.

Sarvar, H., Amini, J. & Laleh-Poor, M. 2011, 'Assessment of risk caused by earthquake in region 1 of Tehran using the combination of RADIUS, TOPSIS and AHP models', *Journal of Civil Engineering and Urbanism*, vol. 1, no. 1, pp. 39-48.

Scawthorn, C. & Chen, W.-F. 2002, *Earthquake Engineering Handbook*, CRC press.

Scherbaum, F., Delavaud, E. & Riggelsen, C. 2009, 'Model selection in seismic hazard analysis: An information-theoretic perspective', *Bulletin of the Seismological Society of America*, vol. 99, no. 6, pp. 3234-47.

Schnebele, E., Jaiswal, K., Luco, N. & Nassar, N.T. 2019, 'Natural hazards and mineral commodity supply: Quantifying risk of earthquake disruption to South American copper supply', *Resources Policy*, vol. 63, p. 101430.

Schilderman, T. 2004, 'Adapting traditional shelter for disaster mitigation and reconstruction: experiences with community-based approaches', *Building Research & Information*, vol. 32, no. 5, pp. 414-26.

Sekac, T., Jana, S.K., Pal, I. & Pal, D.K. 2016, 'A GIS based approach into delineating liquefaction susceptible zones through assessment of site-soil-geology—a case study of Madang and Morobe Province in Papua New Guinea (PNG)', *International Journal of Innovative Research in Science, Engineering and Technology, ISSN (Online)*, pp. 2319-8753.

Sen, T. 2006, 'Construction of uniform hazard response spectra using Monte Carlo simulation', *Proc. First*.

Setiawan, B. 2017, 'Site specific ground response analysis for quantifying site amplification at A regolith site', *Indonesian Journal on Geoscience*, vol. 4, no. 3, pp. 159-67.

Setiawan, B., Jaksa, M., Griffith, M. & Love, D. 2018, 'Seismic site classification based on constrained modeling of measured HVSR curve in regolith sites', *Soil Dynamics and Earthquake Engineering*, vol. 110, pp. 244-61.

Setiawan, B., Saidi, T., Yuliannur, A., Polom, U., Ramadhansyah, P. & Ali, M. 2020, 'Ambient noise analysis for characterizing sub-surface dynamic parameters', *IOP Conference Series: Materials Science and Engineering*, vol. 712, IOP Publishing, p. 012012.

Shah, M., Qaisar, M., Iqbal, J. & Ahmed, S. 2012, 'Deterministic Seismic Hazard Assessment of Quetta, Pakistan', *15th World Conference on Earthquake Engineering, Lisbon Portugal*.

Shapiro, S.A., Dinske, C. & Kummerow, J. 2007, 'Probability of a given-magnitude earthquake induced by a fluid injection', *Geophysical Research Letters*, vol. 34, no. 22.

Shaw, R., Iemura, H., Takahashi, Y., Pradono, M.H., Sukamdo, P. & Kurniawan, R. 2006, 'Earthquake and tsunami questionnaires in Banda Aceh and surrounding areas', *Disaster Prevention and Management: An International Journal*.

Shcherbakov, R., Zhuang, J., Zöller, G. & Ogata, Y. 2019, 'Forecasting the magnitude of the largest expected earthquake', *Nature Communications*, vol. 10, no. 1, pp. 1-11

Shen, K.-w. & Wang, J.-q. 2018, 'Z-VIKOR method based on a new comprehensive weighted distance measure of Z-number and its application', *IEEE Transactions on Fuzzy Systems*, vol. 26, no. 6, pp. 3232-45.

Shepard, C.C., Agostini, V.N., Gilmer, B., Allen, T., Stone, J., Brooks, W. & Beck, M.W. 2012, 'Assessing future risk: quantifying the effects of sea level rise on storm surge risk for the southern shores of Long Island, New York', *Natural Hazards*, vol. 60, no. 2, pp. 727-45.

Shimizu, S., Sugisaki, K. & Ohmori, H. 2008, 'Recursive Sample-Entropy method and its application for complexity observation of earth current', *2008 International Conference on Control, Automation and Systems*, IEEE, pp. 1250-3.

Siemon, B., Ploethner, D. & Pielawa, J. 2006, 'Hydrogeological Reconnaissance Survei in the Province Nanggroe Aceh Darussalam Northern Sumatra, Indonesia Survei Area: Banda Aceh/Aceh Besar 2005, Report Vol', *C-1, BGR/Bundesanstalt für Geowissenschaften und Rohstoffe (Federal Institute for Geosciences and Natural Resources)*.

Sietsma, J. & Dow, R.J. 1991, 'Creating artificial neural networks that generalize', *Neural Networks*, vol. 4, no. 1, pp. 67-79.

Smith, K. 2003, *Environmental hazards: assessing risk and reducing disaster*, Routledge.

Socquet, A., Simons, W., Vigny, C., McCaffrey, R., Subarya, C., Sarsito, D., Ambrosius, B. & Spakman, W. 2006, 'Microblock rotations and fault coupling in SE Asia triple junction (Sulawesi, Indonesia) from GPS and earthquake slip vector data', *Journal of Geophysical Research: Solid Earth*, vol. 111, no. B8.

Socquet, A., Vigny, C., Chamot-Rooke, N., Simons, W., Rangin, C. & Ambrosius, B. 2006, 'India and Sunda plates motion and deformation along their boundary in Myanmar determined by GPS', *Journal of Geophysical Research: Solid Earth*, vol. 111, no. B5.

Soe, M., Ryutaro, T., Ishiyama, D., Takashima, I. & Charusiri, K.W.-I.a.P. 2009, 'Remote sensing and GIS based approach for earthquake probability map: a case study of the northern sagaing fault area, Myanmar', p. 29.

Solomos, G., Pinto, A. & Dimova, S. 2008, 'A review of the seismic hazard zonation in national building codes in the context of eurocode 8', *European Commission Joint Research Centre, Luxembourg*, vol. 72.

Sørensen, M.B. & Atakan, K. 2008, 'Continued earthquake hazard in northern Sumatra', *Eos, Transactions American Geophysical Union*, vol. 89, no. 14, pp. 133-4.

Spence, R. & So, E. 2009, 'Estimating shaking-induced casualties and building damage for global earthquake events', *Cambridge, UK.: Cambridge Architectural Research Ltd*.

Srinivasalu, S., Thangadurai, N., Switzer, A.D., Mohan, V.R. & Ayyamperumal, T. 2007, 'Erosion and sedimentation in Kalpakkam (N Tamil Nadu, India) from the 26th December 2004 tsunami', *Marine Geology*, vol. 240, no. 1-4, pp. 65-75.

Stead, D., Eberhardt, E. & Coggan, J. 2006, 'Developments in the characterization of complex rock slope deformation and failure using numerical modelling techniques', *Engineering Geology*, vol. 83, no. 1-3, pp. 217-35.

Stefánsson, R. 2020, 'Useful predictions ahead of large earthquakes and lessons learned for future progress', *Geodesy and Geodynamics*, vol. 11, no. 1, pp. 1-17.

Stein, S., Geller, R.J. & Liu, M. 2012, 'Why earthquake hazard maps often fail and what to do about it', *Tectonophysics*, vol. 562, pp. 1-25.

Stein, S. & Liu, M. 2009, 'Long aftershock sequences within continents and implications for earthquake hazard assessment', *Nature*, vol. 462, no. 7269, pp. 87-9.

Stein, S. & Okal, E.A. 2007, 'Ultralong period seismic study of the December 2004 Indian Ocean earthquake and implications for regional tectonics and the subduction process', *Bulletin of the Seismological Society of America*, vol. 97, no. 1A, pp. S279-S95.

Stein, S. & Okal, E.A. 2011, 'The size of the 2011 Tohoku earthquake need not have been a surprise', *Eos, Transactions American Geophysical Union*, vol. 92, no. 27, pp. 227-8.

Stirling, M. & Petersen, M. 2006, 'Comparison of the historical record of earthquake hazard with seismic-hazard models for New Zealand and the continental United States', *Bulletin of the Seismological Society of America*, vol. 96, no. 6, pp. 1978-94.

Stokoe, K. 2001, 'Liquefaction resistance of soils summary report from 1996 NCEE and 1998 NCEER/NSF workshops on evaluation of resistance of soil', *Journal of Geotechnical and Geoenvironmental Engineering*, vol. 127, pp. 817-33.

Subrahmanyan, V. 2001, 'Seismic signatures in the Kalu river basin, Thane district and Mumbai', *Research highlights in earth system science, Indian Geological Congress*, pp. 201-4.

Switzer, A.D., Srinivasalu, S., Thangadurai, N. & Mohan, V.R. 2012, 'Bedding structures in Indian tsunami deposits that provide clues to the dynamics of tsunami inundation', *Geological Society, London, Special Publications*, vol. 361, no. 1, pp. 61-77.

Synolakis, C.E. & Kong, L. 2006, 'Runup measurements of the December 2004 Indian Ocean tsunami', *Earthquake Spectra*, vol. 22, no. 3_suppl, pp. 67-91.

Szegedy, C., Liu, W., Jia, Y., Sermanet, P., Reed, S., Anguelov, D., Erhan, D., Vanhoucke, V. & Rabinovich, A. 2015, 'Going deeper with convolutions', *Proceedings of the IEEE Conference on Computer vision and Pattern Recognition*, pp. 1-9.

Tang, A. & Wen, A. 2009, 'An intelligent simulation system for earthquake disaster assessment', *Computers & Geosciences*, vol. 35, no. 5, pp. 871-9.

Tao, X., Zhen, G., Zuo, H. & Zhang, M. 1996, 'Application of an AI and GIS based seismic hazard assessment procedure to seismic zonation of Taiyuan-Linfen region', *Earthquake Research in China*, vol. 12, no. Suppl., pp. 18-24.

Tas, N., Cosgun, N. & Tas, M. 2007, 'A qualitative evaluation of the after earthquake permanent housings in Turkey in terms of user satisfaction—Kocaeli, Gundogdu Permanent Housing model', *Building and Environment*, vol. 42, no. 9, pp. 3418-31.

Tate, E. 2012, 'Social vulnerability indices: a comparative assessment using uncertainty and sensitivity analysis', *Natural Hazards*, vol. 63, no. 2, pp. 325-47.

Tavakoli, B. & Favakoli, A. 1993, 'Estimating the vulnerability and loss functions of residential buildings', *Natural Hazards*, vol. 7, no. 2, pp. 155-71.

Tehrany, M.S., Pradhan, B. & Jebur, M.N. 2014, 'Flood susceptibility mapping using a novel ensemble weights-of-evidence and support vector machine models in GIS', *Journal of Hydrology*, vol. 512, pp. 332-43.

Telford, J. & Cosgrave, J. 2006, *Joint evaluation of the international response to the Indian Ocean tsunami: Synthesis report*, Tsunami Evaluation Coalition (TEC).

Theilen-Willige, B. 2010, 'Detection of local site conditions influencing earthquake shaking and secondary effects in Southwest-Haiti using remote sensing and GIS-methods', *Natural Hazards & Earth System Sciences*, vol. 10, no. 6.

Thiri, M.A. 2017, 'Social vulnerability and environmental migration: The case of Miyagi Prefecture after the Great East Japan Earthquake', *International Journal of Disaster Risk Reduction*, vol. 25, pp. 212-26.

Tierney, K. 2006, 'Social inequality: Humans and disasters', *On risk and disaster: Lessons From Hurricane Katrina, np, Philadelphia, University of Pennsylvania Press. http://dx.doi. org/10.9783/9780812205473.109*.

Tinti, S. & Mulargia, F. 1985, 'Effects of magnitude uncertainties on estimating the parameters in the Gutenberg-Richter frequency-magnitude law', *Bulletin of the Seismological Society of America*, vol. 75, no. 6, pp. 1681-97.

Tjia, H. & Zakaria, T. 1974, 'Palu-Koro strike-slip fault zone, Central Sulawesi, Indonesia', *Sains Malaysiana*, vol. 3, no. 1, pp. 65-86.

Tompson, J.J., Jain, A., LeCun, Y. & Bregler, C. 2014, 'Joint training of a convolutional network and a graphical model for human pose estimation', *Advances in Neural Information Processing Systems*, pp. 1799-807.

Torres, Y., Arranz, J.J., Gaspar-Escribano, J.M., Haghi, A., Martínez-Cuevas, S., Benito, B. & Ojeda, J.C. 2019, 'Integration of LiDAR and multispectral images for rapid exposure and earthquake vulnerability estimation. Application in Lorca, Spain', *International Journal of Applied Earth Observation and Geoinformation*, vol. 81, pp. 161-75.

Tsai, C.-H. & Chen, C.-W. 2010, 'An earthquake disaster management mechanism based on risk assessment information for the tourism industry-a case study from the island of Taiwan', *Tourism Management*, vol. 31, no. 4, pp. 470-81.

Turmov, G., Korochentsev, V., Gorodetskaya, E., Mironenko, A., Kislitsin, D. & Starodubtsev, O. 2000, 'Forecast of underwater earthquakes with a great degree of probability', *Proceedings of the 2000 International Symposium on Underwater Technology (Cat. No. 00EX418)*, IEEE, pp. 110-5.

Turner, B.L., Kasperson, R.E., Matson, P.A., McCarthy, J.J., Corell, R.W., Christensen, L., Eckley, N., Kasperson, J.X., Luers, A. & Martello, M.L. 2003, 'A framework for vulnerability analysis in sustainability science', *Proceedings of the National Academy of Sciences*, vol. 100, no. 14, pp. 8074-9.

Uchida, N., Kalafat, D., Pinar, A. & Yamamoto, Y. 2019, 'Repeating earthquakes and interplate coupling along the western part of the North Anatolian Fault', *Tectonophysics*, vol. 769, p. 228185.

Umar, Z., Pradhan, B., Ahmad, A., Jebur, M.N. & Tehrany, M.S. 2014, 'Earthquake induced landslide susceptibility mapping using an integrated ensemble frequency ratio and logistic regression models in West Sumatera Province, Indonesia', *Catena*, vol. 118, pp. 124-35.

United states Geological Survey, *viewed 15 June 2017, https://earthquake.usgs.gov/data/pager/.*

United Nations system for disaster risk reduction, *https://www.unisdr.org/we/inform/publications/2752, viewed 20 July 2017.*

Utsu, T. 1984, 'Estimation of parameters for recurrence models of earthquakes', *Bulletin of the Earthquake Research Institute, University of Tokyo*, vol. 59, pp. 53-66.

Uyeda, S. 2015, 'Current affairs in earthquake prediction in Japan', *Journal of Asian Earth Sciences*, vol. 114, pp. 431-4.

Varazanashvili, O., Tsereteli, N., Amiranashvili, A., Tsereteli, E., Elizbarashvili, E., Dolidze, J., Qaldani, L., Saluqvadze, M., Adamia, S. & Arevadze, N. 2012, 'Vulnerability, hazards and multiple risk assessment for Georgia', *Natural Hazards*, vol. 64, no. 3, pp. 2021-56.

Vicente, R., Parodi, S., Lagomarsino, S., Varum, H. & Silva, J.M. 2011, 'Seismic vulnerability and risk assessment: case study of the historic city centre of Coimbra, Portugal', *Bulletin of Earthquake Engineering*, vol. 9, no. 4, pp. 1067-96.

Violette, S., Boulicot, G. & Gorelick, S.M. 2009, 'Tsunami-induced groundwater salinization in southeastern India', *Comptes Rendus Geoscience*, vol. 341, no. 4, pp. 339-46.

Wang, K., Chen, Q.-F., Sun, S. & Wang, A. 2006, 'Predicting the 1975 Haicheng earthquake', *Bulletin of the Seismological Society of America*, vol. 96, no. 3, pp. 757-95.

Wang, L., Peng, J.-j. & Wang, J.-q. 2018, 'A multi-criteria decision-making framework for risk ranking of energy performance contracting project under picture fuzzy environment', *Journal of Cleaner Production*, vol. 191, pp. 105-18.

Wang, L., Wang, X.-k., Peng, J.-j. & Wang, J.-q. 2020, 'The differences in hotel selection among various types of travellers: A comparative analysis with a useful bounded rationality behavioural decision support model', *Tourism Management*, vol. 76, p. 103961.

Wang, L., Zhang, H.-y., Wang, J.-q. & Li, L. 2018, 'Picture fuzzy normalized projection-based VIKOR method for the risk evaluation of construction project', *Applied Soft Computing*, vol. 64, pp. 216-26.

Weichert, D.H. 1980, 'Estimation of the earthquake recurrence parameters for unequal observation periods for different magnitudes', *Bulletin of the Seismological Society of America*, vol. 70, no. 4, pp. 1337-46.

Werner, S.D., Taylor, C., Moore, J. & Walton, J. 2000, 'A risk-based methodology for assessing the seismic performance of highway systems'.

Wijetunge, J. 2009, 'Field measurements and numerical simulations of the 2004 tsunami impact on the east coast of Sri Lanka', *Pure and Applied Geophysics*, vol. 166, no. 4, pp. 593-622.

Williams, T., Szary, P., Thomann, T., Konnerth, C. & Nemeth, E. 2002, *GIS applications in geotechnical engineering*.

Wilson, R. 1985, 'Predicting Areal Limit of Earthquake-Induced Landsliding, Evaluating Eathquake Hazards in the Los Angeles Region-An Earth-Science Perspective', *US Geological Survery Professional Paper 1360*, pp. 317-45.

Wistuba, M., Malik, I., Krzemień, K., Gorczyca, E., Sobucki, M., Wrońska-Wałach, D. & Gawior, D. 2018, 'Can low-magnitude earthquakes act as a triggering factor for landslide activity? Examples from the Western Carpathian Mts, Poland', *Catena*, vol. 171, pp. 359-75.

Woessner, J., Laurentiu, D., Giardini, D., Crowley, H., Cotton, F., Grünthal, G., Valensise, G., Arvidsson, R., Basili, R. & Demircioglu, M.B. 2015, 'The 2013 European seismic hazard model: key components and results', *Bulletin of Earthquake Engineering*, vol. 13, no. 12, pp. 3553-96.

Xie, Z. & Yan, J. 2008, 'Kernel density estimation of traffic accidents in a network space', *Computers, Environment and Urban Systems*, vol. 32, no. 5, pp. 396-406.

Xu, C., Dai, F. & Xu, X. 2010, 'Wenchuan earthquake-induced landslides: an overview', *Ore Geology Reviews*, vol. 56, no. 6, pp. 860-74.

Xu, Y., Ren, T., Liu, Y. & Li, Z. 2018, 'Earthquake prediction based on community division', *Physica A: Statistical Mechanics and its Applications*, vol. 506, pp. 969-74.

Yakut, A., Aydogan, V., Ozcebe, G. & Yucemen, M. 2003, 'Preliminary seismic vulnerability assessment of existing reinforced concrete buildings in Turkey', *Seismic Assessment and Rehabilitation of Existing Buildings*, Springer, pp. 43-58.

Yeats, R.S. & Prentice, C.S. 1996, 'Introduction to special section: Paleoseismology', *Journal of Geophysical Research: Solid Earth*, vol. 101, no. B3, pp. 5847-53.

Yohe, G. & Tol, R.S. 2002, 'Indicators for social and economic coping capacity—moving toward a working definition of adaptive capacity', *Global Environmental Change*, vol. 12, no. 1, pp. 25-40.

Youd, T.L. 1995, 'Liquefaction-induced lateral ground displacement'.

Youngs, R.R. & Coppersmith, K.J. 1985, 'Implications of fault slip rates and earthquake recurrence models to probabilistic seismic hazard estimates', *Bulletin of the Seismological Society of America*, vol. 75, no. 4, pp. 939-64.

Youssef, A.M., Al-Kathery, M. & Pradhan, B. 2015, 'Landslide susceptibility mapping at Al-Hasher area, Jizan (Saudi Arabia) using GIS-based frequency ratio and index of entropy models', *Geosciences Journal*, vol. 19, no. 1, pp. 113-34.

Yücemen, M., Özcebe, G. & Pay, A. 2004, 'Prediction of potential damage due to severe earthquakes', *Structural Safety*, vol. 26, no. 3, pp. 349-66.

Yunita, H., Setiawan, B., Saidi, T. & Abdullah, N. 2018, 'Site response analysis for estimating seismic site amplification in the case of Banda Aceh-Indonesia', *MATEC Web of Conferences*, vol. 197, EDP Sciences, p. 10002.

Yuzal, H., Kim, K., Pant, P. & Yamashita, E. 2017, 'Tsunami evacuation buildings and evacuation planning in Banda Aceh, Indonesia', *Journal of Emergency Management (Weston, Mass.)*, vol. 15, no. 1, pp. 49-61.

Zahran, S., Brody, S.D., Peacock, W.G., Vedlitz, A. & Grover, H. 2008, 'Social vulnerability and the natural and built environment: a model of flood casualties in Texas', *Disasters*, vol. 32, no. 4, pp. 537-60.

Zare, M., Pourghasemi, H.R., Vafakhah, M. & Pradhan, B. 2013, 'Landslide susceptibility mapping at Vaz Watershed (Iran) using an artificial neural network model: a comparison between multilayer perceptron (MLP) and radial basic

function (RBF) algorithms', *Arabian Journal of Geosciences*, vol. 6, no. 8, pp. 2873-88.
Zebardast, E. 2013, 'Constructing a social vulnerability index to earthquake hazards using a hybrid factor analysis and analytic network process (F'ANP) model', *Natural Hazards*, vol. 65, no. 3, pp. 1331-59.
Zhang, J. & Jia, Z. 2010, 'The study on assessment index of urban social vulnerability to the earthquake disaster', *Technolology Guide*, vol. 36, pp. 12-4.
Zhang, W., Xu, X. & Chen, X. 2017, 'Social vulnerability assessment of earthquake disaster based on the catastrophe progression method: A Sichuan Province case study', *International Journal of Disaster Risk Reduction*, vol. 24, pp. 361-72.
Zhang, Y., Van den Berg, A.E., Van Dijk, T. & Weitkamp, G. 2017, 'Quality over quantity: Contribution of urban green space to neighborhood satisfaction', *International Journal of Environmental Research and Public Health*, vol. 14, no. 5, p. 535.
Zhao, Y. & Takano, K. 1999, 'An artificial neural network approach for broadband seismic phase picking', *Bulletin of the Seismological Society of America*, vol. 89, no. 3, pp. 670-80.
Zhihuan, Z. & Junjing, Y. 1990, 'Prediction of earthquake damages and reliability analysis using fuzzy sets', *[1990] Proceedings of First International Symposium on Uncertainty Modeling and Analysis*, IEEE, pp. 173-6.
Zhou, G., Esaki, T., Mitani, Y., Xie, M. & Mori, J. 2003, 'Spatial probabilistic modeling of slope failure using an integrated GIS Monte Carlo simulation approach', *Engineering Geology*, vol. 68, no. 3-4, pp. 373-86.

.

APPENDIX I

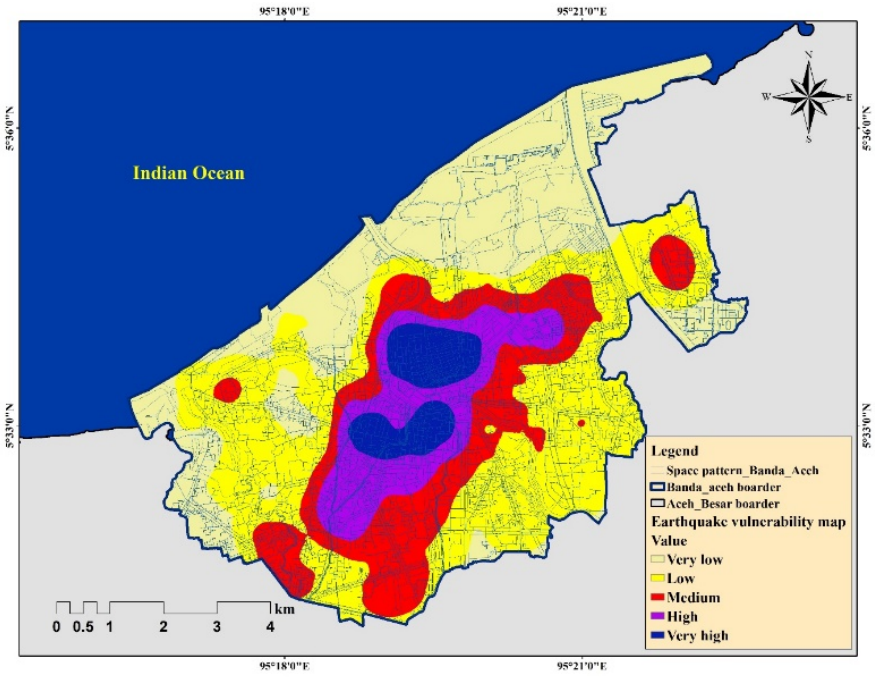

Figure A1. Earthquake vulnerability map.

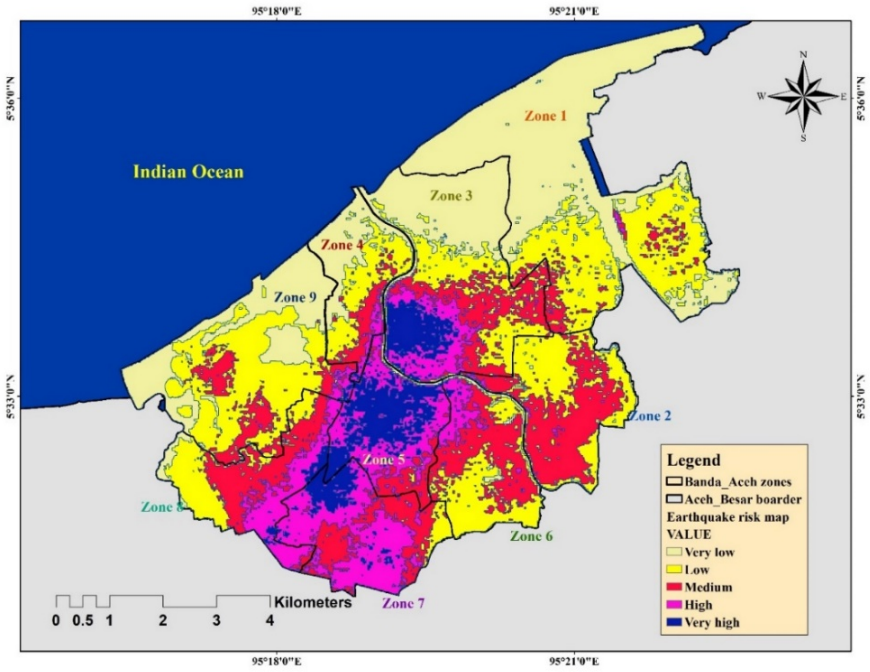

Figure A2. Earthquake risk map developed using the integrated ID–AHP approach.

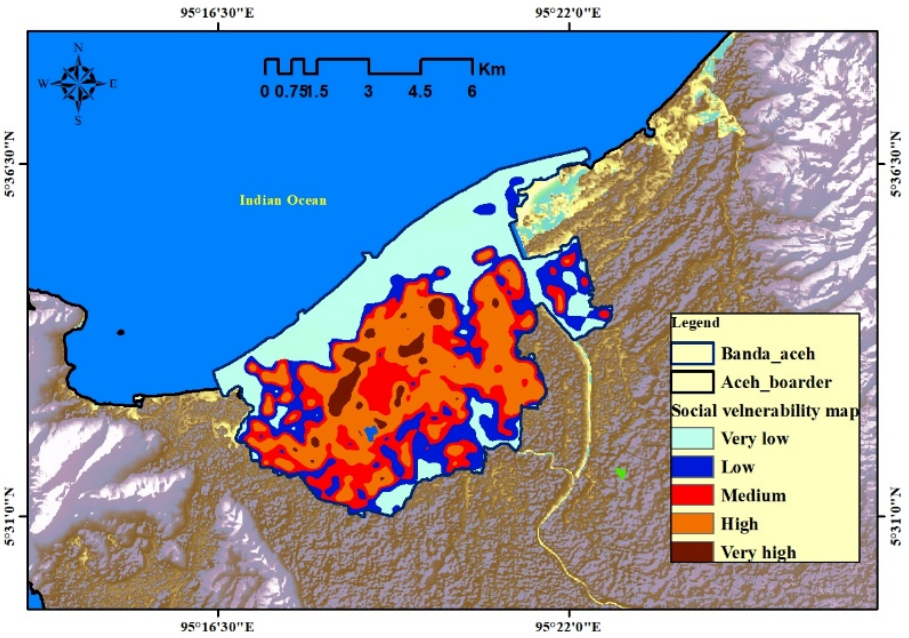

Figure A3. Social vulnerability map created using the entropy method.

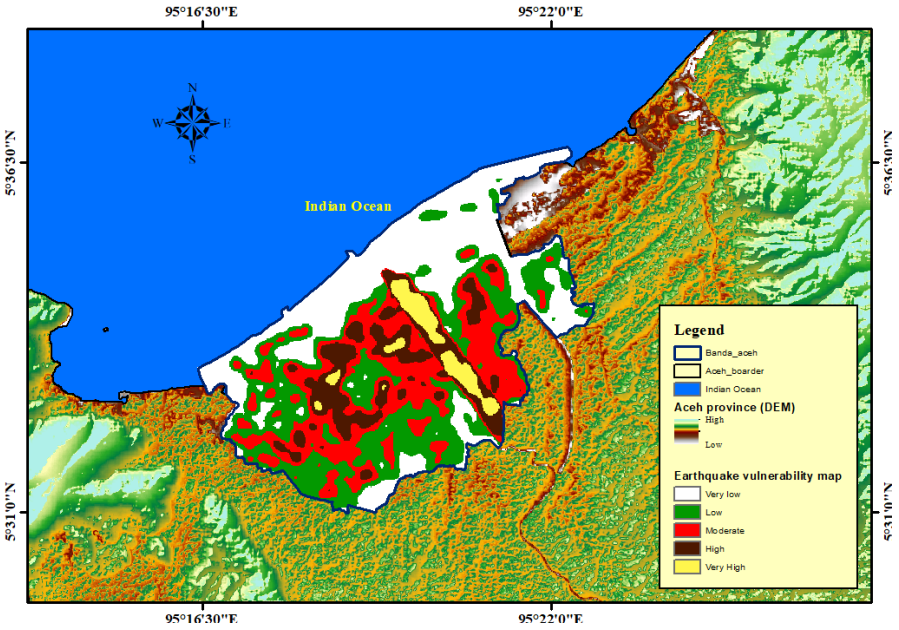

Figure A4. Structural vulnerability based on building density and building size and age.

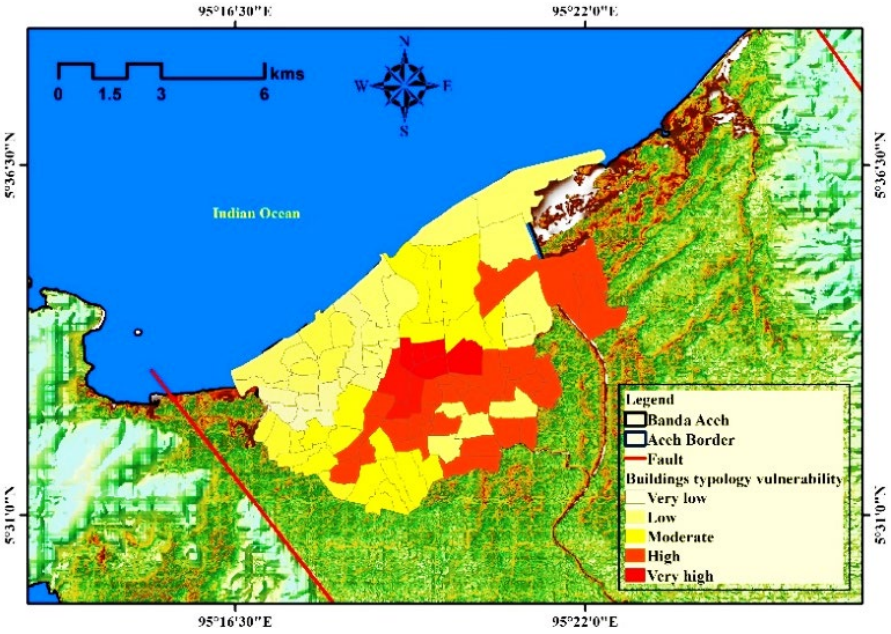

Figure A5. Mapping of buildings typology vulnerability in villages in the city.